Influence of formulation and microstructure on the final properties of filled high performance polymers

Carine El Khoury

N°d'ordre NNT: **2022LYSES003**

THESE de DOCTORAT DE L'UNIVERSITE DE LYON
Opérée au sein de
L'université Jean-Monnet

Ecole Doctorale ED SIS 488
Sciences, Ingénierie, Santé

Spécialité de doctorat : Chimie et sciences des matériaux

Soutenue publiquement le 12/01/2022, par :
Carine EL KHOURY

Influence of formulation and microstructure on the final properties of filled high performance polymers

---

Devant le jury composé de :

BISTAC	Sophie	Professeure	Université de Haute Alsace	Rapporteure
REIGNER	Gilles	Professeur	ENSAM	Rapporteur
BAHLOULI	Nadia	Professeure	Université de Strasbourg	Examinatrice
DESSE	Melinda	Docteure	Université Jean-Monnet	Examinatrice Co-encadrante
MAJESTE	Jean-Charles	Professeur	Université Jean-Monnet	Examinateur Directeur de Thèse
SCHLIPF	Mickael	Docteur	FPS Gmbh	Invité
VINCENT	Frederic	Docteur	SBM France	Superviseur industriel
FRANCOIS	Severin	Responsable R&D	SBM France	Invité

To my mom,
To my Dad,
To Biso,
To Thomas.

Acknowledgement

Je tiens à remercier de nombreuses personnes qui m'auront accompagné tout au long de mes quatre années de thèse passées à enquêter sur les polymères haute performance.

Pour commencer, je tiens à remercier les membres du jury pour avoir accepté d'évaluer ce travail. Merci à Sophie BISSAC et Gilles REGNIER, rapporteurs de cette thèse ainsi qu'a Nadia BAHLOULI membre du jury.

Je tiens ensuite à remercier bien évidemment Jean-Charles Majesté aka JCM et Melinda DESSE pour avoir encadrer et diriger cette thèse. Merci pour votre confiance, support et accompagnement depuis le master ! Grace à vous j'ai pu apprendre énormément et évoluer dans mes compétences scientifiques. Merci pour les réunions, et les discussions scientifiques même à l'autre bout de la France. Melinda, merci pour le support moral, les conseils et les encouragements tout le long de ces quatre dernières années. Je n'aurais pas pu demander un meilleur encadrement.

Je remercie également SBM France d'avoir financé ce projet et surtout Frederic Vincent et Severin François d'avoir accepté de le superviser. Je les remercie pour l'attrait qu'ils ont montré pour ces travaux lors de nos réunions et leur intérêt continu tout au long. Je les remercie pour l'apport de leurs connaissances sur le polymère et les idées qui ont émergé grâce à nos discussions scientifiques ainsi que pour leur disponibilité et leur réactivité. Cette collaboration fut un réel plaisir. Une mention spéciale à Brigitte pour son aide et les discussions partagées pendant mes déplacements sur site.

J'adresse mes remerciements à Nora Mallouk pour m'avoir accueillie au sein du CMES et accompagner dans la formation et l'utilisation du MEB. Merci d'être aussi arrangeante et à l'écoute.

Je remercie aussi le personnel permanant du laboratoire IMP, pour leur accueil au laboratoire et l'aide technique qu'ils ont pu m'apporter. Merci donc à Gilles, Claude, Caroline, Lucie et Agnès. Merci à Corinne, Benoit B et Frederic B. Merci à Nathalie pour sa joie de vivre et les pauses café-clopes. Merci Frederic P. pour toutes les fois où tu nous as fait rire avec tes blagues. Merci à Fabien, le stagiaire avec la convention de stage la plus longue ! Merci à Christian Carrot directeur de l'IMP pour ses discussions enrichissantes et remarques scientifiques pertinentes. Merci également à Yvan pour les différents échanges ainsi que tous les CST !

Je souhaite évidemment m'adresser à mes collègues doctorants et post-docs, à ceux qui ont déjà fini et ceux qui ont presque terminé. Merci à Ashley et à Guillaume. A Augustin « on perd on gagne » tu vas gagner 😄. Merci à Romain, et Dara vous y êtes presque courage ! Merci à Nanjunda, nous avons passé de super moment en France et en Inde, je te souhaite le meilleur. Merci aux différentes personnes avec qui nous avons partagés le bureau (bâtiment M et C), Kelly, Nadège, Maryam, Manon, Shaobo et Benoit. Bien évidement sans oublier l'ancienne team Alessandro, Teddy, Bastien, Julien et Dr Dreux ! Sans vous l'intégration à l'IMP n'aurait pas eu le même goût. Merci pour l'accueil, les conseils, toutes les soirées, les bières partagées, la coupe

du monde, des champions et toutes les soirées foot et fléchettes du cross road (Fab t'en fais partie de cette team aussi). Enfin et surtout, the one and only Benjamin le grand. Merci pour les discussions du quotidien, les sérieuses et les moins sérieuses, les voyages, les weekends les soirées, les vacances, Mozza, julien, les rencontres. Bref, tu as été là du début jusqu'a la fin comme promis !

Je souhaite également remercier les doctorants que j'ai pu rencontrer à l'UJM et aux différents laboratoires de Saint-Étienne. Merci à la team ASEC, Corentin, Marion, Bastien, Cyriac, Mathilde. Ce fut une belle année remplie d'événements. Merci également à Maude et Joseph pour la passation et le gala inoubliable avec Bastien.

Je tiens ensuite à remercier mes amis en France et au Liban. Je commencerai par Camille LebraS la bretonne, ma première amie en France, merci d'avoir alléger les heures de cours, merci pour la colocation, les weekends, les pseudo-randos. Merci aux stéphanois, à mon parrain François, et à la Millefa : Pich, Yann, Tirabo, Bastien, Anneko, Steph, Moussmouss, Faz, Mamane et Ju. Ces trois ans sont passées plus vite grâce à vous. Merci également à Florie, Markey, Dédé, Quentin et Geoffrey les petits potes sudistes. Merci à la personne qui m'a poussé à venir à Saint-Etienne dès le départ, Elia. Merci aussi à Joe, le meilleur voisin qu'une personne puisse avoir. Merci à Hassan, Maroon, Maria Choufany, Diane, Sacha, Youssra, Nohra.

Un énorme merci à mes amies d'enfance **Perla** et **Nadine** toujours là malgré la distance et les contraintes de la vie.

Une mention spéciale, et un très grand merci à mes amies qui sont là depuis la licence, les deux docteures Helene et Mackrine. We did it ! 8 ans d'étude et 8 ans d'amitié. Merci pour tous les moments partagés, du Liban jusqu'à Paris.

Un merci du fond du cœur à ma meilleure amie, Christina. Une grande sœur et super copine. Toutes les années ne pourront pas se résumer en deux lignes. En tout cas Merci pour tout.

Merci à ma famille en France, Géraldine et François. Merci pour le soutien et l'accueil.

Merci à ma famille au Liban Papa, Maman et Biso. Merci d'avoir toujours cru en moi. De m'avoir donnée cette liberté. De m'avoir poussé à aller toujours plus loin. Merci pour le soutien quotidien et dans toutes les situations. Un grand merci aussi à Pierre, le tonton mais surtout le grand frère.

Et pour conclure, le meilleur pour la fin, merci à mon ami, mon compagnon et ma famille, Thomas. Sans toi cette thèse n'aurait jamais pu se terminer. Tu as été là pour les moments les plus difficiles, de loin et de près. Ton support était la clé de mon succès. Je ne pourrais jamais te remercier assez.

Merci beaucoup à toutes et à tous.

Table of Contents

I.General introduction

"A polymer is a substance or material consisting of very large molecules, or macromolecules, composed of many repeating subunits"[1]. Polymers are one of the most used materials in every day's life, they can be found in all kind of fields (food, transportation, electronics, medical etc…). They can either be found naturally (silk, rubber, cellulose…) or made synthetically (Polyethylene, polypropylene, polystyrene…). Polymers are divided into families that have the same main characteristics as following:

- Thermoplastics: Polymers that become pliable or moldable after a certain temperature, they solidify upon cooling. Generally, thermoplastics have high molecular weights (e.g., polypropylene, polyethylene, nylon…).
- Thermosets: Polymers that are irreversibly hardened when cured from a soft solid or a resin. (E.g., Epoxy resin, Silicone, Polyurethane)
- Elastomers: Viscoelastic polymers with low intermolecular forces. Their main applications are for tires, soles of shoes and damping elements. (E.g., polybutadiene, styrene-butadiene, polyacrylic rubber)

In modern industry, performance is essential. Some applications require specific properties, as chemical and thermal resistance. For these applications there are a range of thermoplastic polymers called high performance polymers. This family of polymers have a high mechanical properties, chemical resistance and high thermal stability. Polyether ether ketone, polyimide, polytetrafluoroethylene and polyarletherketone make part of these high-performance thermoplastics.

Despite the interesting properties that a high-performance polymer can present, many of the applications requires high standards in different ways, such as specific optical, electrical and tribological properties… Thus, it was necessary to enhance the formulation by adding fillers and additives. Fillers can also be added to improve the processability of the polymer (lowering the viscosity) or to reduce the cost of the material.

The challenge when filling a polymer is mainly the distribution and dispersion of the filler. It is important to obtain the most homogeneous blend in order to reach the optimum properties.

The family of thermoplastics can be divided into small groups of polymers with different properties.

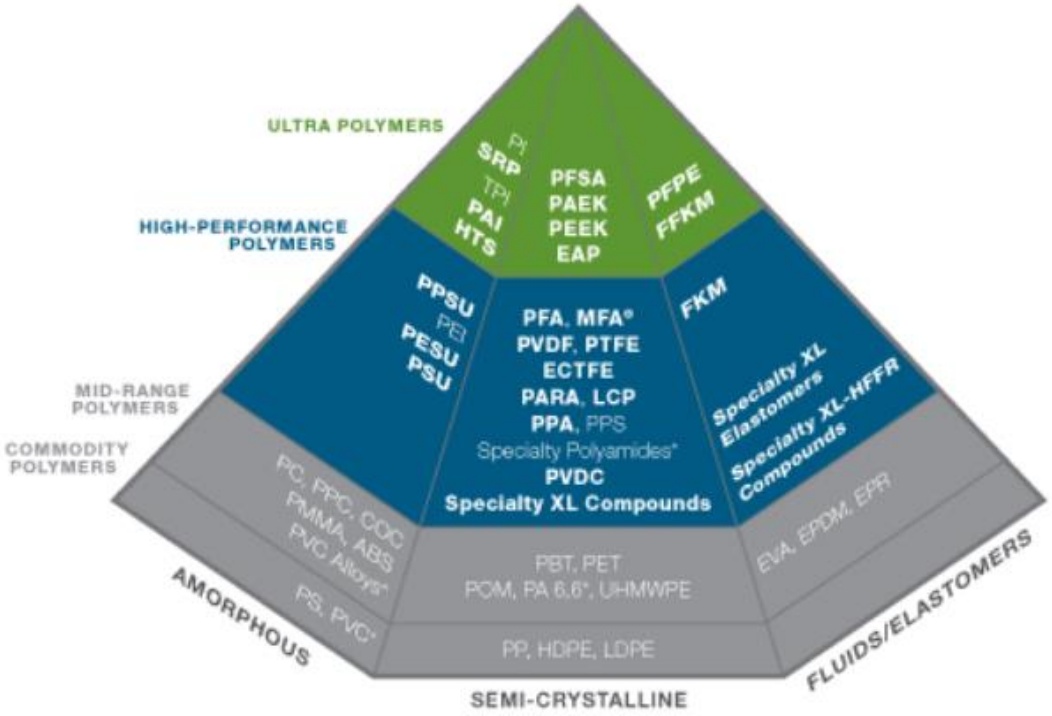

Figure I.1: Pyramid of classifications of polymers[2]

High performance polymers, including PTFE, are applied for specific applications especially when high thermal and chemical resistance is required. Knowing their high cost and little applications compared to commercial polymers, little research studies were conducted on the high-performance polymers. Even though PTFE's microstructure is the center of interest of many studies, filled PTFE and PTFE blends are rarely studied.

For this purpose, this work aims to understand the behavior of high-performance polymers, more specifically PTFE when filled with organic filler such as carbon and Silica. Mechanical properties and microstructure of PTFE blend with PEEK is also a center of interest in this work.

This manuscript is organized as followed:

Chapter I is a literature review on polytetrafluoroethylene (PTFE) and polyether ether ketone (PEEK). The chapter presents the principal studies on the microstructure of PTFE, mechanical properties and process. In addition, it includes filled PTFE and blends of PTFE studies through the time.

Chapter II is a presentation of the applied polymers and organic fillers in this work. It also includes a description of the process parameters: The mixing of the filler in the PTFE, the applied pressure during sintering, the temperature profile. The study of the parameters is presented here and has

led to a choice in optimum processing parameters for each formulation. Finally, this chapter describes the techniques used to characterize the obtained samples.

Chapter III focuses on the influence of the size of the filler and filler content on the properties of PTFE. It presents the results of the microstructure and mechanical characterization.

Chapter IV targets on unfilled and filled blends of PEEK PTFE. The goal is to enhance the properties of filled PTFE by adding PEEK.

Chapter V studies the influence of the grafting of silica particles on the microstructure and mechanical properties of PTFE PEEK blends. This chapter opens for perspectives and possibilities on enhancing filled PTFE PEEK blends.

A general conclusion will summarize the results of those chapters and discuss a global synthesis of the results.

II.Literature review

1 Polytetrafluoroethylene

1.1 Introduction

1.1.1 Discovery

Polytetrafluoroethylene (PTFE) was accidentally discovered by Roy J. Plunkett, a chemist at Du Pont de Nemours, in 1938. Plunkett was working on the cooling of tetrafluoroethylene (a gas) in dry ice when he realized that the gas polymerized and were transformed into a white powder. The trademark was registered in 1945 under the name of "TEFLON". Its first application was in the Manhattan project when used as a sealing joint for uranium production. Nowadays, PTFE is used in various fields, such as utensils for non-stick coating pans and other kitchenware. In the optical fields, it is used to treat anti-reflective glass, in medicine to reinforce stitches or prosthetic valves. It is also well known in the plumbing field for its sealing properties and most of all it is used for lubrication applications because of its low friction coefficient (0.02).

1.1.2 Polymerizations (SPTFE-EPTFE-modified PTFE)

Polytetrafluoroethylene (PTFE) is obtained through polymerization of the monomer Tetrafluoroethylene (TFE) and an addition of a co-monomer to modify the TFE homopolymers. Commercially two polymerization techniques are applied in order to produce PTFE. Suspension polymerization (SPTFE), intended for the production of granular resins, consists of an aqueous polymerization of the TFE monomer in presence or not of a small surfactant amount and an active agitation. Dispersion and fine powder production is made by an emulsion (or dispersion) polymerization, based on a moderate agitation, a generous surfactant amount and a waxy substance (Paraffin wax).

Because of its linear polymerization with no branching, the chains have very low interactions, and leads to a nearly 100% crystalline material. Long polymerized chains lead to high molecular weight and thus, probable entanglement. This high molecular weight leads to high viscosity[3] preventing classical process transformation (injection, extrusion..).

Another drawback of the TFE polymerization is the low ability and difficulty to void closure, i.e., its weldability. These voids affect the mechanical properties and permeability. To eliminate the voids, viscosity must be reduced without extensive recrystallization, therefore, some authors[4,5] proposed to modify the PTFE in dispersion by adding modifiers such as perfluoroalkyl-vinyl-ethers (PPVE) hexafluoropropylene (HFP) or perfluorobutyl ethylene.

No matter the polymerization type, PTFE is produced by batch polymerization with high pressures and in specially designed reactors.

Before obtaining a final usable product, some finishing steps have to be done. In the suspension polymerization case, two finishing steps are considered: washing and drying to remove water

and reduce the particle size. For the emulsion polymerization, cooling and wax decantation are required. Afterwards, dispersion products need coagulation and drying, while fine powders need concentration and formulation.

1.1.3 Types and Applications

After the polymerization, separation and drying of the polymer, suspension polymerization products are then cut according to their application purpose. There are four types of powder obtained from the suspension polymerized PTFE. For compression molding process (1.3.1), smaller powder particles help filling the voids therefore improving the properties[5]. For this function Coarse grinding is applied to have *coarse cut resin* or Fine grinding for *finely divided resin*. For isotactic/automatic molding, fine powder is hard to handle due to its poor flow and low bulk density. Therefore, Fine grinded powder is agglomerated to obtain *pelletized resin* also called *free flow powder.* This process is achieved by dry or wet techniques, and can also be used to add fillers into the pellets making it easier to process afterwards. The last type of suspension PTFE is *pre-sintered resin* made from *free-flow powders* of once melted PTFE. The application of these powders is for tubes and rods production with the ram extrusion process (1.3.2).

As for emulsion polymerization products, as mentioned in the section above, two types of products are obtained: *Fine powders* and *dispersion PTFE*. After the polymerization and finishing steps, *PTFE dispersions* are transformed into coatings. *Fine powders* on the other side are applied in the paste extrusion process (1.3.3).

1.2 Microstructure: Crystalline and amorphous phase

1.2.1 Chain structure

PTFE is a linear polymer, made of a carbon backbone chain. Each carbon has two fluorine attached to it[5].Usually it is compared to polyethylene (PE) where Hydrogen atoms are replaced with Fluor atoms. Although their chemical structure may look exactly the same, PE and PTFE have different properties on all levels. Fluorine is the most electronegative element, larger than hydrogen and its bond with the carbon (C-F) is stronger than the one with Hydrogen (C-H). This polarity difference between C-F and C-H bonding leads to different conformations of PE and PTFE ; the PE crystallization takes place in a planar and trans-conformation and PTFE in an helical conformation[6].

The only way to obtain a planar conformation for the PTFE would be at high pressures (above 0.65GPa)[7].

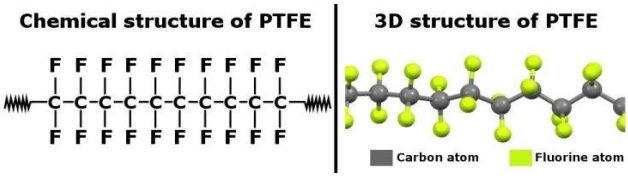

Figure II.1 : PTFE chemical structure[167]

As reported in the literature, the crystalline PTFE conformation is highly dependent on pressure and temperature[3,8,9], as it presents important molecular motion at low temperatures (way below the melting point). Brown[7] reported that the crystalline conformation also depends on the tension and compression. Figure II.2[7] illustrates the different crystalline conformation phases of PTFE for different pressures and temperatures. At atmospheric pressure, PTFE exhibits two different first order crystalline phase transitions at 19°C and 30°C reported and studied by many authors[10,7]. At 19°C a transition occurs from a 13/6 helical chain (Phase II) to a 15/7 helical chain (phase IV). Then at 30°C, a transition from Phase IV to a disordered structure (Phase I).

The last remarkable crystalline transition appears around 340-350°C, and corresponds to the melting temperature where all the crystalline phases disappear and the material becomes completely amorphous. As for the amorphous phase, it also presents two transitions at atmospheric pressure, around -100°C and around 120°C. Those transitions will be discussed in details in the following paragraphs.

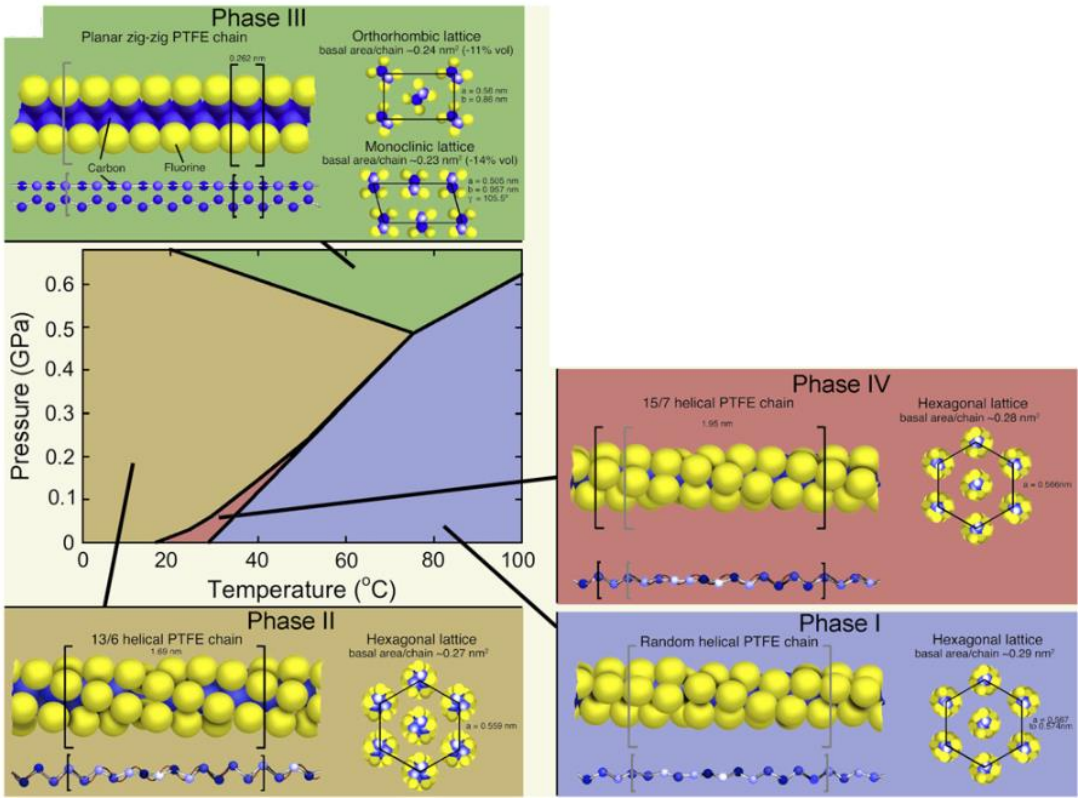

Figure II.2: TEMPERATURE PRESSURE PHASE BEHAVIOR OF CRYSTALLINE PTFE WITH THE INTER- AND INTRA-POLYMER CHAIN[7]

1.2.2 Physical structure

The crystalline structure of PTFE has been the subject of many studies. As a semi-crystalline polymer, PTFE's mechanical and chemical properties are highly dependent on the crystalline rate and structure[8,11,12]. Due to its chain linearity, high molecular weight, and the symmetry of its repetitive unit, PTFE has a high ability to crystallize. In fact, bulk PTFE's crystalline rate can be higher than 90%. Literature studies proved that the crystallization phenomenon of PTFE is unidimentional[13,14]. Furthermore, researchers linked the exceptional properties of the PTFE to its microstructure. For this reason, over the years, authors reported explanations and representations of the amorphous/crystalline structure of PTFE. It was noticed through SEM, WAXS, and DSC tests that PTFE has an uncommon crystalline morphology compared to other polymers (PET, nylon etc…). Bunn et al[10] first analyzed the crystalline morphology using x-ray and electron microscopy on a fractured surface of Polytetrafluoroethylene. The tests revealed a structure formed of long but narrow bands containing fine parallel striations perpendicular to the band length. Later, Speerschneider[15] questioned the morphology of the amorphous phase in order to propose a defined structure of the PTFE. He studied the evolution of the microstructure before and after tensile tests and proposed a model of the morphology (Figure II.3)[15]. This model consists on alternating crystalline platelets and viscous non-crystalline matrix. Hence, Speerchneider[15] confirmed the crystalline lamellae folding microstructure described by Bunn et al[10].

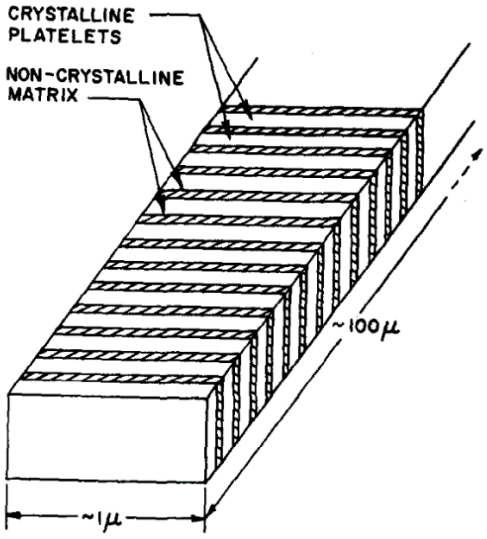

Figure II.3: proposed model of PTFE [15]

It is important to distinguish native PTFE (obtained after synthesis) that has a folded ribbon morphology.[16] Those ribbons are made of single crystals with the chain parallel to the long axis of the ribbons. Linear and folded regions also coexist in each ribbon. As for the melted PTFE, the model proposed is based on thick lamellae with extended crystalline chains.

Bassett et al.[17], were interested in the remarkable thickness of PTFE lamellae reported by Bunn et al[10]. Compared to PE that has the same crystallization from the melt phenomenon, PTFE's lamellae thickness is noted between 1000 to 2500Å and a maximum of 10^5Å while it is 300-400Å for PE with a maximum of 1500Å in extreme cases (long annealing time at melt temperature)[17].

Later, Suwa et al[18] reported the effect of the molecular weight on the crystalline morphology of PTFE. Through measurement of the melt and crystallization temperature, measurement of the heat flow of virgin and sintered PTFE, and microscope observations, Suwa et al[18]. proposed the following morphology, illustrated in Figure II.4.

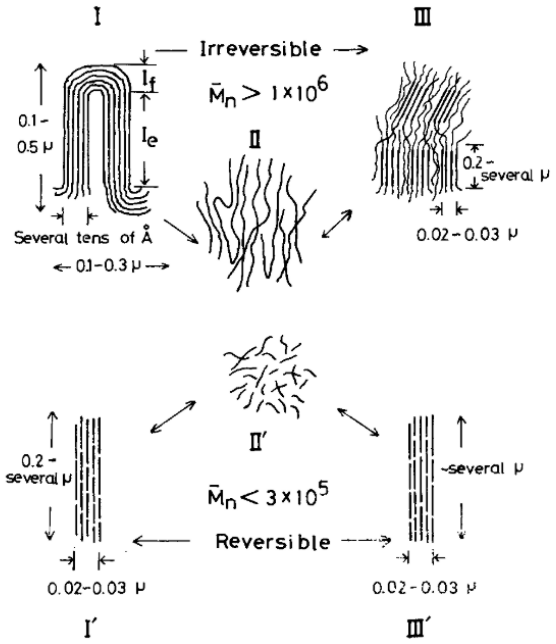

Figure II.4: Model of PTFE chain conformations[18]

I, I': as-polymerized; II, II': molten states; III, III': melt-crystallized states. I, II, III: molecular weight above 1.0 X lo6. I', II', III': molecular weight below 3.10^5.

It was noted that PTFE with a molecular weight lower than 3.10^5 is composed of fibrils with several microns in length, and PTFE with a molecular weight higher than 1.10^6 has a folded ribbons morphology wider than 0.1µ.

Many authors were interested in the influence of the cooling rate and the crystallization temperature of the bulk material on the crystalline rate and the morphology of the crystallites. Ferry[19] reported three facts about bulk sintered PTFE :

- It cannot be obtained in the amorphous phase
- It may be unnecessary to control the cooling rate
- Only isothermal treatments can modify the microstructure. Such treatments need to be properly controlled in order to avoid overshooting when crystallization temperature is reached.

This work also reported two types of microstructures related to the crystallization temperature. High crystallization temperatures induce thicker crystallites and higher melting temperatures. Low crystallization temperatures induce thinner crystallites and lower melting temperatures.

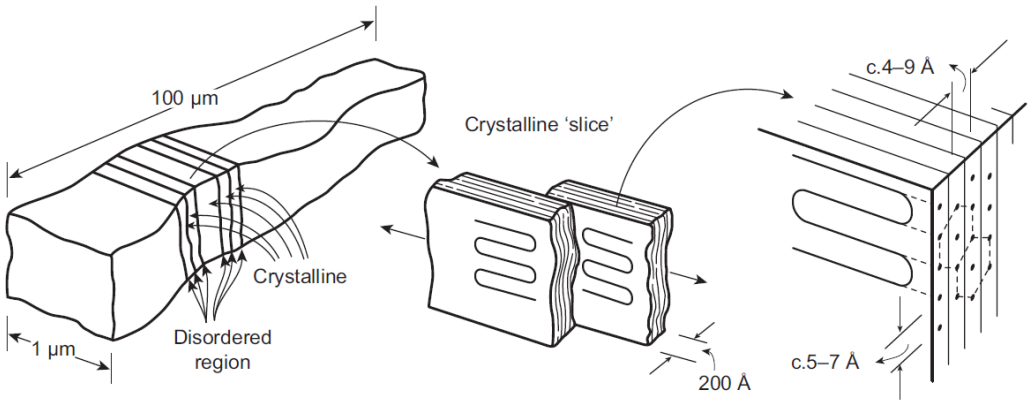

Figure II.5: Crystalline structure of polytetrafluoroethylene [20]

To synthesize, the crystalline structure of polytetrafluoroethylene, as described by Ebnesajjad[6], is a banded structure. The band length varies between 10-100µm, with a bandwidth of 0.2-1µm (Figure II.5[20]). The bandwidth is directly affected by the cooling rate of the polymer: high cooling rates induce thin bands while low cooling rates generate thick bands. The folding over of the crystalline segments produces striations on the bandwidth. Those crystalline segments of 20-30 µm thick are separated by amorphous phases on the bending point.

Concerning the amorphous regions, the presence of two phases was reported in several studies[21–23]: A mobile amorphous phase and a rigid amorphous phase. The mobile amorphous fraction (MAF) is the typical disordered molecular chains randomly arranged in space. The rigid amorphous fraction is the border phase between the crystalline and mobile amorphous phase. This region belongs to the amorphous phase but has a restraint in its chain mobility. A simple

illustration (Figure II.6) of the amorphous phase is proposed by Calleja[21]. Where (1) is the MAF, (2) is the RAF and (3) is the crystalline phase.

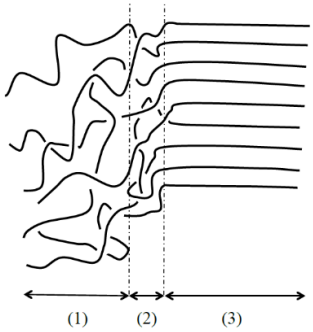

Figure II.6: schematic illustration of PTFE [21]

1.2.3 Transition temperatures

As mentioned before, PTFE shows various temperature transitions. In total, polytetrafluoroethylene counts five well-known transitions (at atmospheric pressure); two of them are first order transitions that occur around 19°C and 30°C. The two other transitions are considered as second order transitions and occur around -100°C and 130°C (120°C to 140°C)[24]. The fifth transition corresponds to the melting temperature of PTFE (around 340°C for virgin PTFE and 327°C for the processed material) also considered as a first order transition.

All three first order transitions affect the crystalline region of the polymer. At 19°C occurs the first crystalline conformation change. Below 19°C, it is a helical chain conformation with a twist of 180° per 13 carbon atoms. The distance between the repetitive units of $13CF_2$ groups is 1.69nm. After 19°C, the molecule untwists slightly and passes to a twist of 180°C per 15 carbon atoms. The distance between the repetitive units of $15CF_2$ groups is 1.95nm.[3]

At 30°C, another change in the conformation occurs where the chain takes a random helical form (Figure II.2). This transition corresponds to the transition from phase IV to phase I. Most authors and literature studies refer to it as the β transition[21,25,26].

Through time, these transitions (first order) have been detected in different testing methods, mostly by dilatometry by Quinn et al.[27] , and Leksina et al.[3] or through calorimetry tests by Furukawa et al. and Marx et al[28]. In addition to dilatometry and calorimetry, WAXS tests helped detect those transitions[3,25,29,30]. In rheological tests, it is hard to differentiate between those two transitions (19°C and 30°C) knowing that they occur in the same temperature region. In rectangular torsion tests, it is showed that the β transition starts way before 19°C.[21] Therefore it is complicated to separate between both transitions.

The most known first order transition of the PTFE is the melting temperature. As first reported by Suwa et al[31], native PTFE has two melting temperatures in a range of 320 - 350°C while melt crystallized samples show one lower melting temperature (around 327°C). Melting temperature also depends on the molecular weight. DSC studies by Suwa[18], show that low molecular weight samples have one single melt peak while high molecular weight samples have a double melt peak. This is related to the morphology of high molecular weight samples discussed in 1.2.2.

At 90°C Araki[32,33], mentioned a first order transition observed as a double transition between 80-100°C for high crystallinity samples, and a simple transition at 90°C for low crystallinity samples. This transition was observed in thermal expansion test, torsion pendulum test and dielectric properties measurements. Despite this study, no further information is given in the literature on the nature of this transition.

Concerning the second order transitions mentioned before, all three of them affect the amorphous phase of the PTFE. After stress relaxation measurements, linear expansion and dielectric properties, Araki[26] mentioned a third second order transition at around -30°C. However, no other author has studied this transition or proved its existence by mechanical tests or thermal tests. The double peak around the β relaxation (in the stress relaxation tests) according to Araki corresponds to the melting temperatures of the folded regions and linear segments in the folded ribbons.

As explained in the section 1.2.2 the amorphous section of the PTFE has at least two phases, the rigid amorphous fraction (RAF) and the mobile amorphous fraction (MAF). Each one of these phases has its own transition temperature. For the MAF it is visible around -100°C and is known as the γ transition. It is associated with the relaxation of small sections of the macromolecule. The rigid amorphous fraction transition can be seen around 130°C and is known as the α transition[21]. It is associated with the relaxation of large sections of the macromolecule. Both transitions have been the center of interest of many authors in order to attribute a glass transition temperature for the PTFE. At this instance, authors do not agree on which transition should be associated to the glass transition.

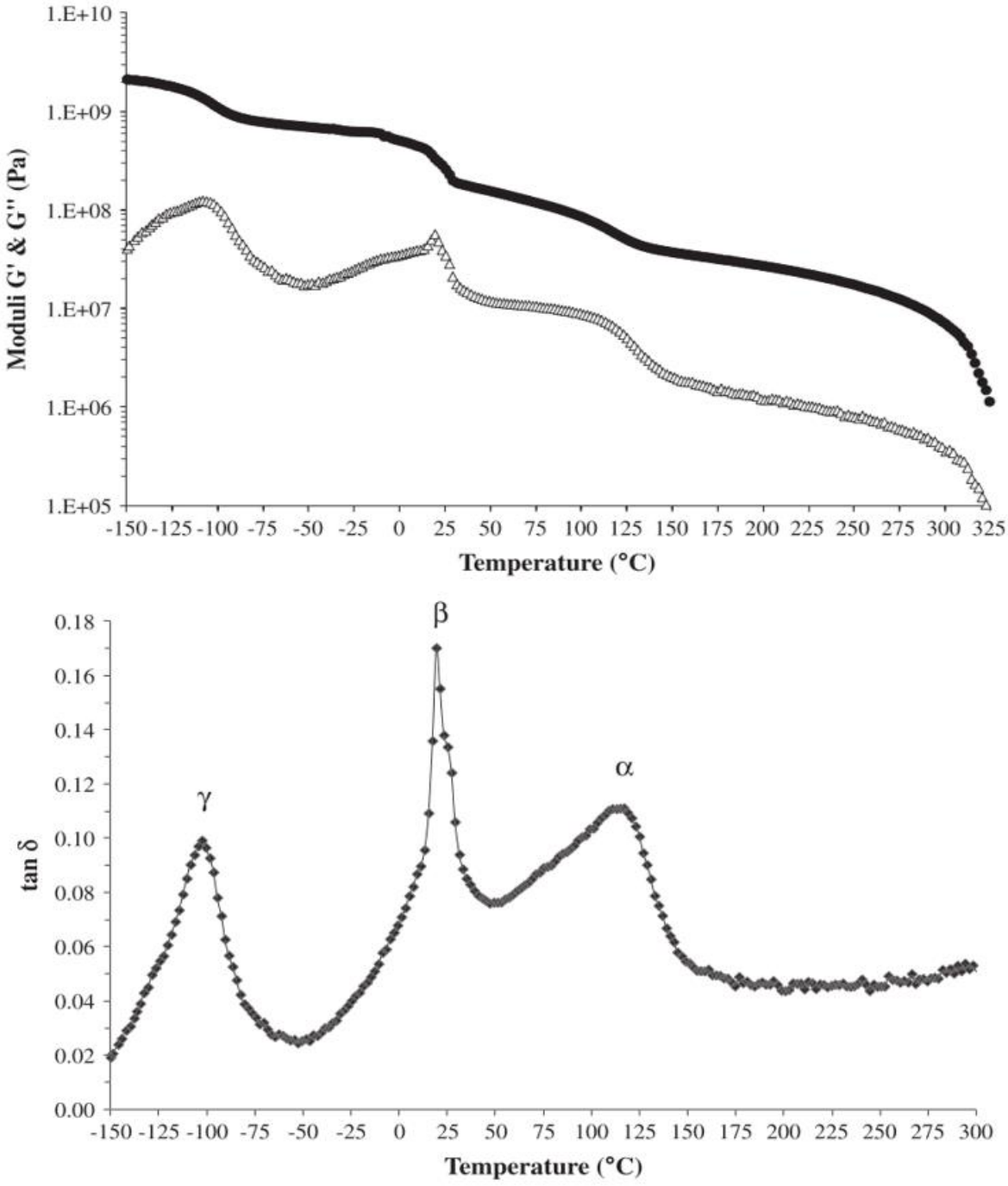

Graph II.1: Thermomechanical analysis of PTFE.

In 2013, Calleja[21], summarized the different opinions of authors with the techniques used in order to determine which transition should be attributed to the glass transition, the summary of which is shown in table below (Table II.1):

Technique	T_g value (°C)	Author
Dynamic mechanical analysis (DMA)	-110	McCrum
	+130	Starkweather Wortmann
Steady or transient rheometry	+110	Tobolsky Araki
Mechanical measurements	-110	Woodward and Sauer Rae and Dattelbaum
Dilatometry (CTE)	+ 123	Araki
Thermally stimulated currents (TSC)	+130	Sauer
Calorimetry and Thermodynamics	-50	Durrell
	-110	Lau
Calculation	-50 -75	Boyer Marchionni
Acoustic	-110	Kvacheva and Perepechko
Permeability measurement	< 20	Fossati

Table II.1: different approaches to assess the Tg of PTFE

Combining dynamical mechanical tests in a large temperature range (-150°C to 200°C) on melted-crystallized PTFE and annealed material, helped improving the fact that each amorphous phase has its own glass transition. More information on the determination of these values is given in the paragraph 1.2.4.

1.2.4 Methods to detect crystallinity rate (WAXS, DSC, Density, spectroscopy)

The crystallinity rate is an important parameter in the properties of PTFE. In fact, most of the properties are influenced by the crystallinity rate[8,9,34,35]. As discussed previously, due to the linearity of its chain and high molecular weight, native PTFE have a high crystallinity rate (93-98%)[3]. Once melted and cooled this crystallinity rate decreases significantly and inversely to the cooling rate and molecular weight of the neat material[22].

In order to determine the crystallinity rate, many authors have used several methods; of course, calorimetry is one of the most used. In addition to calorimetry, x-ray measurements, spectroscopy (infrared, Raman, nuclear magnetic resonance (NMR)) and density measurements were commonly used for crystallinity rate calculation. X-ray measurements, especially wide-angle diffraction (WAXS), is an essential technique in the study of PTFE. Besides identifying the

conformation of the chain structure and the size of the crystalline lamellae[10,25,30,34], this technique also allows to determine the amorphous content, therefore the crystallinity rate of the sample. The method was developed by Ryland[36], described in the Figure II.7 below:

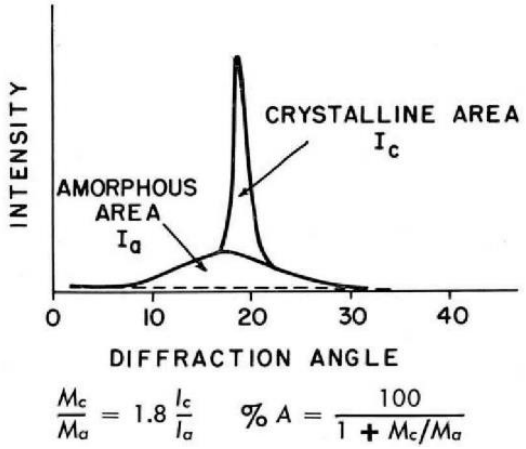

Figure II.7: Amorphous content of PTFE [36]

Where Mc and Ma are respectively the crystalline and amorphous content, 1.8 is a correcting factor, Ia and Ic are the scattering integral intensities of the amorphous and crystalline areas. Although this method seems easy and accurate, yet its results are not very reliable due to the mixture between the pattern of intensities between crystalline and amorphous areas.

Different types of spectroscopies were explored in the literature in order to identify the crystalline rate of PTFE. Infrared spectroscopy technique was first discussed by Moynihan[37], where it was shown that several bands were dependent on the crystallinity rate (700-850 and 384 cm^{-1}) and others insensitive to it (1150-1200 cm^{-1}). The group of band between 700 and 800 cm^{-1} are related to the amorphous phase, as their intensities decrease when the crystallinity rate increases[22]. Therefore, the method described by Moynihan[37] allows to determine the amorphous percentage (%A_m) in the sample by using the ratio of the peaks at 778cm^{-1} and 2367cm^{-1}; and the relation :

$$\%Am = 30.26\frac{A_{778}}{A_{2367}} + 1.73\left(\frac{A_{778}}{A_{2367}}\right)^2 \quad \text{(II.1)}$$

The error on this method was estimated at 1% by Moynihan, while Rae[9] found it to be closer to 10%. Moynihan[37] mentioned that infrared spectroscopy method is much more efficient than that of the X-ray method especially for samples with high crystallinity. Lehnert et al[38] explored and compared the crystalline rate calculation possibility by means of Raman spectroscopy after several contradictory works reported by other authors[39,40]. By using the peak at 1318 cm^{-1}, it is

possible to quantify the band tailing and therefore quantify the crystalline rate of the sample. Results showed a correlation with x-ray, calorimetry and IR spectroscopy. As for the ^{19}F nuclear magnetic resonance, a method explained by Vega[41] shows the possibility to determine the crystallinity rate of the melt-crystallized samples from a linear combination of amorphous and crystalline line shapes. This method is independent from the temperature, and has a correlation with x-ray results as reported by Vega[41,42].

Density measurements on PTFE samples can be carried out through immersion in liquid (ethanol, dihydrogen oxide, dibromomethane) using the sink/swim method or in gas (helium pycnometry). With the density value and the mass of the sample (considered with no voids), it is possible to evaluate the mass fraction of the crystalline phase ($W_{c,d}$) using the following equation[43] :

$$W_{c,d} = \frac{\rho_c(\rho - \rho_a)}{\rho(\rho_c - \rho_a)} \quad \text{(II.2)}$$

ρ represents the sample density, ρ_c ρ_a are the extrapolated densities of the pure crystalline phase (≈2300 kg/m^3) and the pure amorphous phase (≈2040 kg/m^3)[3,44]. Densities of pure and amorphous phases must be extrapolated because PTFE cannot be produced in one exclusive part[9,19].

Authors used the Differential scanning calorimetry (DSC) and modulated DSC (MDSC) in order to study the melt and crystallization behavior of the PTFE[31,45,46], the influence of the molecular weight on the behavior of the crystalline phase[17,18,31], determination of the crystalline rate and nucleation phenomenon[10,46,47]. Considering two perfect phases, one pure amorphous and another pure crystalline, the mass fraction X_c, by means of calorimetry is obtained by the ratio $\frac{\Delta H_f}{\Delta H_f^0}$; ΔH_f is the melt enthalpy and ΔH_f^0 is the melt enthalpy of the crystalline bulk polymer. This value was a subject of discussion and different opinions in the literature. It varies between 57 and 104 J/g[3,36,37,44,48] depending on the author and the extrapolation method. This variation comes from the fact that PTFE cannot be obtained in one pure phase, and the values have to be extrapolated. Therefore, for results analysis some authors specified the value used in their calculations[8,9,30] or others preferred comparing enthalpy of melting (ΔH_f) values that are proportional to the crystallinity rate without interfering with the melt enthalpy of the bulk (ΔH_f^0). It is important to mention, that according to a study done by Sciuti et al[49], DSC measurements on powder granule and simulations of industrial processing by the means of DSC are very discouraging. This technique may induce an overestimation or mislead in the results. This mislead is due to the formation of so called “warts” on the free surface of PTFE. This wart-like structure does not occur in dense material therefore cannot be correlated to industrial simulations.

To sum up the methods, Starkweather[44] divided the estimation of crystallinity degree into two groups: spectroscopy, x-ray and NMR can be used to measure the amorphous content in the sample and show less than 10% of amorphous fraction in native PTFE. The second group consists

of calorimetry and density measurements; they are related to the crystalline content in the sample and show about 80% of crystalline fraction. This discrepancy was also noticed in Rae and al's[9] work where IR and WAXS results gave higher results than DSC and density measurements. Due to all the corrections, uncertainties, discrepancies, errors, results obtained from all these techniques are most of the time different. Lehnert et al[50] made a comparative study about all these methods. It was shown that results from WAXS, density and DSC measurements have the same trends in sample crystallinity but do not exactly have identical values. On the other hand, Starkweather[44] mentioned a correlation between ^{19}F NMR and density measurement, while Lehnert et al[50] did not notice relevant degrees of correlation between ^{19}F NMR and other methods. Lenhert and al added that results from NMR are underestimated comparing to WAXS measurements. This difference may be caused by the estimation of the perfect two-phase model. In addition, results with WAXS are more accurate in estimating the amorphous rather than the crystalline phase. With a comparison with the work of Moynihan[37], raman and IR spectroscopy results were found to be correlated, though some deviations were observed between Raman and DSC measurements at high molecular weights. This deviation comes from the fact that two-phase model cannot be taken into consideration when working with high molecular weight samples.

To conclude on the crystalline rate measuring techniques, each technique has its specific process to measure the crystalline rate. Either by measuring the amorphous phase or by considering two perfectly separated phases, measurement methods cannot be compared to one another.

1.3 Processing methods

1.3.1 Compression molding (Sintering)

As mentioned previously, due to its high viscosity (10^{10} – 10^{12} P^3), PTFE is not melt-processible. Thus, one of the cheapest and most used technique is the compression molding. This process is similar to ceramic and metallic powder technique. Compression molding is divided into two main steps: compaction of PTFE (fine powder or free-flow resin), sintering of the green material[5,24,51,52] presented in the scheme Figure II.8.

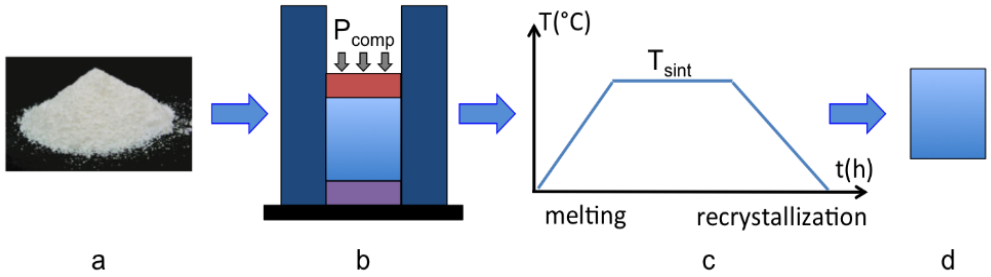

Figure II.8: Schematic representation of the main steps of the manufacturing process of PTFE[53]

The pressing step consists on compacting the powder by applying a defined pressure. In this step, the pressure applied rearranges the powder, reduces pores and releases the air between the

particles. The pressure applied in this step gives the powder a sufficient strength that allows handling afterwards. Generally the pressure applied is between 15 and 70 Mpa[53] depending on the particle shape, the desired thickness and density. The parameters influencing the final properties of the samples are compaction pressure, temperature, surface roughness, dwell time etc… The effect of these parameters are seen on the density, hardness and tensile strength[52–54]. As for the temperature, although the powder has better flow for temperature inferior to 19ºC, it is hard to compress it well below that temperature. Therefore, it is necessary to condition the powder prior to compacting at a temperature between 21 and 25ºC for 24h and maintain a temperature between 21 and 28ºC while compacting[5]. It is necessary to apply a sufficient dwell time in order to obtain an even compaction of the powder; insufficient time will lead to a gradient in the density, micro-cracks, air entrapment… Pressure release must be slow in order to avoid visible micro-cracks due to the rapid expansion of the entrapped air. After the compaction, the obtained material is unloaded; it is usually referred to as *the green part*. The green part is put aside for degassing. In this step, the gas that could not exist during the compaction step is released, and the material is relaxed from the residual stresses. It is important to degas the material before the sintering step; otherwise, cracks will develop during the temperature cycle.

The second step of this process is the sintering. For this step, the green part is free of the mold and the pressure. Temperature is increased above the melting temperature (340ºC[48,55]) but held before the degradation point[56], typically between 360 and 390ºC[5,24]. While the temperature is increasing, the green part first completes its elastic recovery; then it begins the expansion after the melting point. To ensure a homogeneous temperature, slow heating must be applied[5] because of the low thermal conductivity of the PTFE. When the sintering temperature is reached, the particles start fusing, coalescence thus eliminating voids and maximizing the properties of the part. The held time influences the final properties of the material [8,9]. The choice of the held time is made as a function of the dimensions of the part (thickness, diameter[5]. Figure II.9 illustrates examples on sintering cycles according to the dimensions and the weight of the sample.

Preform size		Sintering Cycle		
Size, mm (dia × length) (O.D./I.D.) × (L)	Weight, kg_f	Heating rate	Sintering	Cooling rate
50 × 50*	0.2	50 °C/h	5 h at 370 °C	50 °C/h
100 × 100*	1.7	30 °C/h	10 h at 370 °C	30 °C/h
174/52 × 130*	6.0	30 °C/h	12 h at 370 °C	30 °C/h
420/150 × 600**	150	50 °C/h (25 °C → 150 °C) 3 h at 150 °C	20 h at 365 °C	10 °C/h (365 °C → 315 °C)
		25 °C/h (150 °C → 250 °C) 3 h at 250 °C		10 h at 315 °C 10 °C/h (315 °C → 250 °C)
		15 °C/h (250 –315 °C) 5 h at 315 °C		
		10 °C/h (315 –365 °C)		25 °C/h (250 °C → 100 °C)
420/150 × 1200**	300	50 °C/h (25 °C→ 150 °C) 5 h at 150 °C	30 h at 365 °C	10 °C/h (365 °C→ 315 °C)
		25 °C/h (150 °C→ 250 °C) 5 h at 250 °C		10 h at 315 °C 10 °C/h (315 °C→ 250 °C)
		15 °C/h (250 °C→ 315 °C) 5 h at 315 °C		
		10 °C/h (315 °C→ 365 °C)		25 °C/h (250 °C→ 100 °C)

Notes:
**Preforming pressure: 150 kg/cm² (dual press). * Compression speed: 40–60 mm/min (pressure applied in 4 stages). * Dwell time: 30 min or more.*
***Preforming pressure: 150 kg/cm² (dual press). ** Compression speed: 40–60 mm/min (pressure applied in 4 or 5 stages). ** Dwell time: 45 min or more.*

Figure II.9: Sintering cycles suggestions

A schematic diagram of preforming and sintering sequence of the PTFE[5] is shown in the Figure II.10

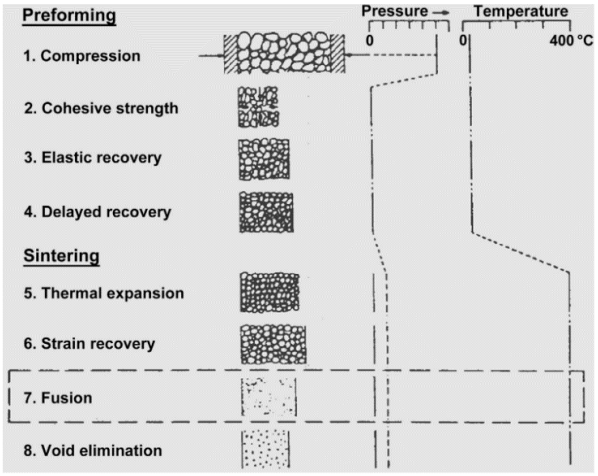

Figure II.10: schematic diagram of preforming and sintering sequence of the PTFE [5]

Finally, the cooling rate is also a key parameter to obtaining a sample with optimized properties. Knowing that the cooling rate determines the crystallinity of the material and the crystallinity rate determines the final properties, therefore the cooling rate controls the final properties of the material. Depending on the wished toughness or roughness properties of the sample, the cooling rate has to be modified. For a maximum toughness low crystalline rate is necessary, which means, a rapid cooling, while for maximum roughness, the material needs a high crystalline rate, so a slow cooling[3]. No matter the desired properties, the cooling rate needs to be carefully controlled to avoid overshooting, cracks and uncontrolled crystalline morphology[3,57,58]. In some

cases, an annealing is performed while cooling or after reaching the ambient temperature. If the annealing temperature is around the crystallization temperature (300 - 325 º C), it allows a control of the crystalline morphology and the thickness of the lamellae. If the annealing temperature is at low temperatures (around 100ºC), it removes the residual stresses in the material[58].

1.3.2 Ram extrusion

Another type of S-PTFE process is the Ram extrusion. This technique is the only possible one for suspension PTFE in order to obtain samples in a continuous production process. The overall principle of ram extrusion is similar to that of the compression molding: preform of a green part, sintering and cooling, but all gathered in one machine (Figure II.11). It allows the production of tubes, rods, L-shapes cross section and other types of ram extrudable profiles. Ram extrusion is mostly used in the industries for tubes, joints, seals etc… in order to gain time in the production and limit the material waste.[5]

Figure II.11: an example of a horizontal ram extrusion[5]

For handling reasons, PTFE poured into the hopper has to be a free-flow resin for a better handling of the material[5]. The first step is to feed the ram extruder with the resin. During a cycle, the feed part provides a uniform weight into the die section. This part is usually cooled at 21ºC to keep the PTFE in good conditions. After the feeding, the compaction step is assured by the advance motion of the ram that retracts afterwards in order to recompress a new batch of resin against the first one. The preform is then pushed into the first heating zone where it gets sufficient heat to reach the melting point. The heating temperature should be chosen well in order to melt the PTFE and sinter it during the residence time in the heating die.[5] Finally, the samples forgoes a cooling step, which determines the crystallinity rate and the shrinkage of the rod. Most of the time the rod is air quenched (the rod leaves the die and is directly exposed to the air). This methods provides the lowest crystallinity and the minimum shrinkage as reported by Ebnesajjad[5].

1.3.3 Paste Extrusion (melt processable PTFE)

Paste extrusion is a process used for wire coating, tubes or PTFE tapes. This is mainly a combination of the compression molding and the ram extrusion; however, this process requires lubricating liquids. The lubrication is the first step of the technique; fine powder resin (coagulated dispersion powder) of PTFE with diameters around 0.2µm is mixed with the lubricating liquid in order to form a paste. A cylindrical billet is then preformed by compacting the paste at low pressure (around 2Mpa)[59]. The preform is extruded in a ram extruder at a temperature slightly higher than 30°C. Afterwards, the lubricant is evaporated using an oven. Finally, the extruded preform is either sintered (wire coating, tubes) or calendared (tapes) and passed through an oven (without sintering). Figure II.12 illustrates a schematic example of a hydraulic tube paste extruder.

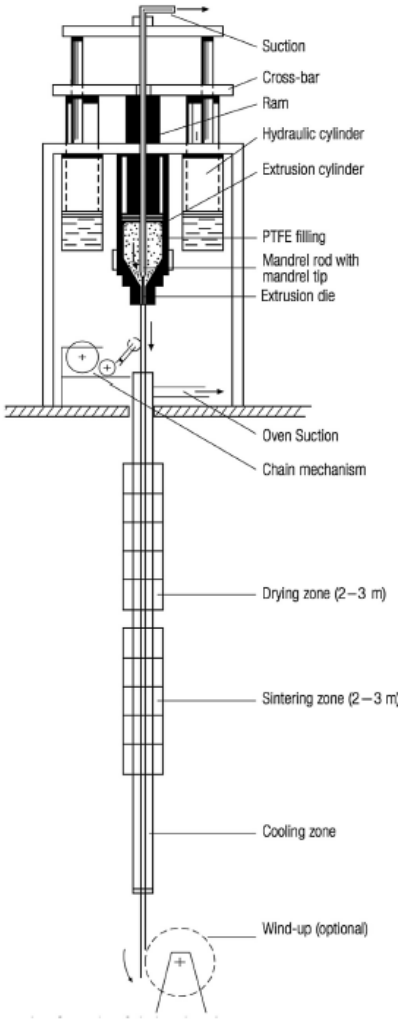

Figure II.12: Hydraulic paste extruder for tube fabrication[5]

The extrusion of lubricated PTFE at low temperature is possible thanks to its transitions at ambient temperature aforementioned (1.2.2). Shearing at a temperature less than 19°C causes sliding of the crystals past each other. However, between 19 and 30°C the particles are loose and shearing causes unwinding of crystals and creates fibrils that then leads to poor orientation of the particles causing leakage in the finale product. Moreover, at temperatures higher than 30°C, the fibrillation of PTFE is easy to achieve leading to a greater risk in product failure. It is therefore important to orient the particles and extrude the paste at low temperature in order to have strong mechanical properties[59]. In addition, the handling of the fine powder must be carried out with care, as it is extremely sensitive to shearing, which can also lead to premature fibrillation. Lubricant quantity and molecular weight are also important parameters because they directly influence the pressure of the extrusion. Last, the extrusion also depends on the geometry of the machine, die cone angle length, extrusion speed and temperature.[5]

1.4 Mechanical properties

1.4.1 Introduction

Through time, mechanical properties of PTFE were not the center of interest of the authors as PTFE was mostly used for coating purposes; therefore, most of the studies focused on the tribological and wear properties. At first tensile tests were performed in order to determine the morphology of the PTFE[11,15], then authors got more and more interested in the mechanical properties of the PTFE and studied its behavior in creep[60,61], tension[8,34], compression[9,61], fracture toughness[35,62–64] and shock response[65,66].

1.4.2 Tension-compression

Studying the tensile properties of PTFE started with Dyment[67] by comparing its behavior to some plastics at low temperature. Compared to Polycaprolactam (PCL), Polytrifluoromonochloroethylene (PTFCLE) and Rigid PolyVinylChloride unplasticized (PVC), PTFE was the only one that retained ductility at the lowest temperature (-196°C). In addition, it showed a remarkable increase in the tensile strength when passing from room temperature to very low temperatures (-196°C). Further studies of the tensile properties were conducted by Speerschneider[11,15] aiming at a better comprehension of the PTFE morphology. Tensile tests were performed at low strain-rate (3 and 6.10^{-4} s^{-1}) combined with microscopic tests to observe the microstructural changes at different crystalline content and testing temperatures. At low temperatures, samples showed kinking and bowing deformation in band striae that resulted in high strength and low ductility, whereas at high temperatures the band striae's deformations were sliding and rotating resulting in low strength and high ductility. Stress-strain relations were only affected by the band size at temperatures below 0°C, where small band size had the highest strength, but above 0°C, there was no difference. Those results proved the proposed model of morphology by Speerschneider et al.[15] (Figure II.3).

Later Fischer et al.[68,69] also studied the influence of the crystalline content and the temperature on the tensile behavior, but in different environments (N_2, CO_2, He, acetone). It was confirmed, in line with Speerschneider's work, that the elastic modulus is not affected by the crystallinity rate at low temperature (-195°C). Knowing that the modulus is an average of the crystalline and amorphous modulus, at low temperatures the amorphous and the crystalline phase have the same modulus.

At 25°C both crystalline (T_β) and amorphous ($T\gamma$) (1.2.3) transitions have occurred and the stress-strain behavior is independent from the grain size or crystallinity. As for the tests at -70°C, Fischer et al.[68] explained the difference of mechanical behavior found by Speerschneider[11] in the samples with different crystallinity rate. Speerschneider performed the tests in a nitrogen atmosphere, which turned out to produce a crazing effect on PTFE, causing yield drops for thick band crystallites. Actually around -70°C gases like N_2, CO_2, Ar and O_2 have the same crazing effect, while helium creates an inert atmosphere. Figure II.13 shows a comparison between the tests performed by Speerschneider, Fischer and Brown.

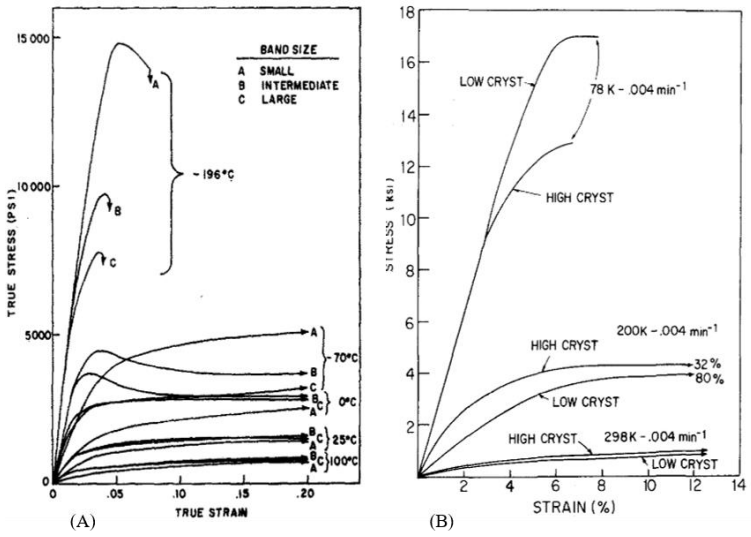

Figure II.13: Tensile behavior at different temperatures and crystalline rate (A): according to Speerschneider[11] (B) according to brown in an inert atomsphere[7]

Several years later (2000's) authors started showing interest in the mechanical properties of PTFE. Tensile properties of PTFE were studied in tension, compression for different strain-rates, temperatures and crystallinity rates[8,9]. In compression, deformation at higher strain rates showed an increase in the yield and flow stresses. It was noticed that low crystallinity samples were able to be loaded at 50% true strain at -198°C without failure, while high crystalline samples

failed at approximatively at 35% true strain. This highlights the fact that at temperatures lower than γ transitions the glassy amorphous domains allow greater ductility than the crystalline regions[9]. Around room temperature (0°C, 25 ° C and 50°C), crystalline regions showed stiffer behavior than the amorphous one's. In a complimentary work on the properties of PTFE in tension, Rae et al.[8] showed that at small strain (<2%) the Poisson ratio for compression is different of the one for tension, while the strain-rate sensitivity was the same for both compression and tension. In addition, tension tests showed a more pronounced yield but a similar work hardening rate. This phenomenon could be explained by the different deformation methods (void formation and micro-fibril growth, crystalline slip, twinning etc…) that can be excited or retarded depending on the local stress state (positive or negative).

The tensile tests study by Rae et al.[8] was compared with the ones by Speerschneider[11,15] and Koo[70]. This comparison showed that at large strains, samples with lower crystallinity rates are stiffer than those with high crystallinity rates, but only for temperatures above room temperature. Around room temperature and at -15°C no significant difference was noticed between samples with different crystallinities.

Rae et al.[8] presented the evolution of Young's modulus and the yield stress as a function of temperature (Figure II.14) as well as the true failure strain and failure stress as a function of temperature. Those parameters showed a strong dependence on the testing temperature: Young's modulus and yield stress both decrease when the temperature increase. While true strain and stress failure showed a dependence on the crystalline phases (Figure II.2) of PTFE.

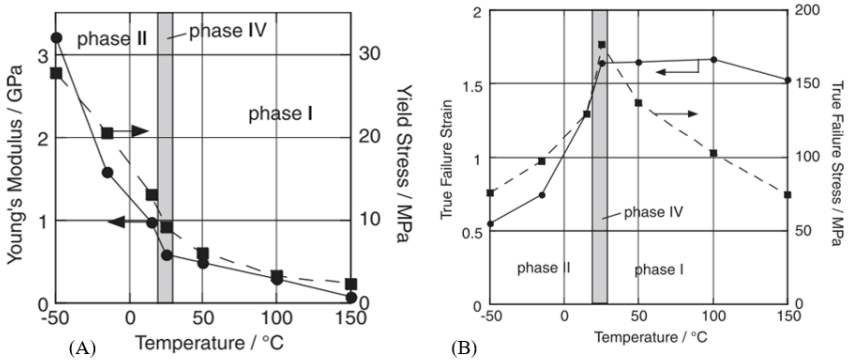

Figure II.14: (A) Young's modulus and 2% offset yield stress as a function of temperature. (B) : True strain and stress failure as a function of temperature[8]

SEM observations illustrated the mechanism of failure in each phase. All three phases (I, II, IV) showed a failure initiated at a corner. Phase II has a brittle failure with a plastic deformation accompanied with microvoids, coalescence and an order of magnitude smaller than the size of a PTFE granule.

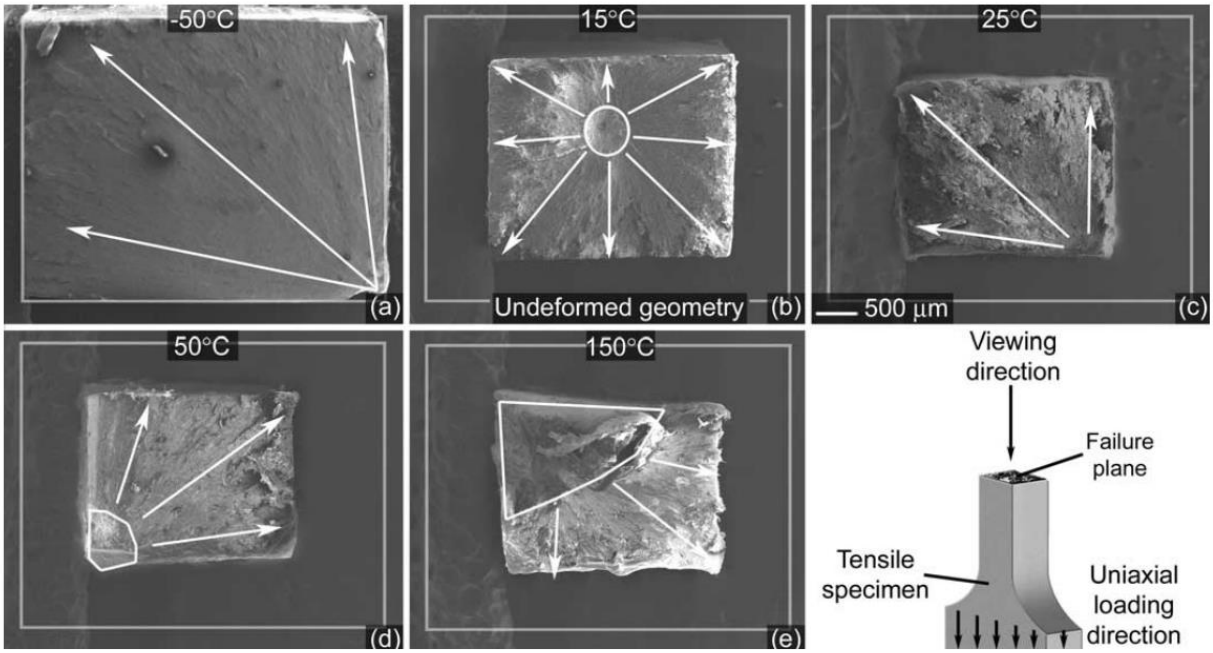

Figure II.15: SEM Photos of material failure at different temperatures. The grey boundaries indicate the initial undeformed geometries. Failure propagation paths are indicated with white arrows. The white boundaries in (b), (d), and (e) highlight regions of fibril formation.

In phase IV, localized plastic deformation induced a stable porous microstructure able to handle high stress and strains. As for the phase I, two types of plastic deformation were observed, one similar to the phase IV in the crack growth region (stable porous structure), and a dense network of fibrils in the crack initiation region. The only temperature with a distinct crack initiation was at 15°C (in the region of the transition from phase II to IV), were the crack started in the center of the sample. Stable fibrils were also noticed and a radial brittle failure. This combination of failure mechanism could be caused by the mix of both crystalline phases. In addition, during loading, temperature may vary in the sample, therefore, different temperatures could be reached in the center than in the rest of the sample which could lead to a different crystalline structure in that particular region.

Brown et al[65] have also investigated the soft recovery of the PTFE shocked in the phase transition II -III. They noticed that when shocked in phase II, Young's modulus, crystallinity and yield stress decreased. While shocked in the phase transition from II to III there is an increase in crystallinity independently of the applied pressure, and an increase in Young's modulus and yield stress with increasing pressure. In 2016, Song[43] compared tensile properties of PTFE samples with different crystallinity rates. Results showed an increase in Young's modulus with increasing crystallinity, while tensile strength and elongation at break had an opposite behavior.

1.4.3 Fracture toughness

PTFE has a remarkable ductile behavior, with a brittle fracture morphology that shows more similarities with metals than polymers. Joyce[62,64] and Brown[34,35] are the authors that were the most interested in the behavior of the PTFE through the fracture toughness test. Joyce[62,64] showed a significant reduction in the toughness when going from 20°C to -18°C, while it did not change or increase while cooling from -18ºC to -73°C. Although temperature has the most impact on the fracture toughness behavior, Joyce[62] mentioned an enhanced decrease in the toughness with increasing load. In a complimentary work, Joyce[64] demonstrated the high toughness and crack tip blunting at temperatures around ambient with slow loading. This work also highlighted the fact that high loading rates result in crack growth via the development of "pop-ins" instabilities that become smaller and more numerous with an increasing load. In addition, rapid loading resulted in rapid ductile crack growth, and lower material fracture resistance. Brown et al[34,35] pushed the investigation of the fracture toughness by studying the effect of the crystalline phase and the crystallinity rate on the toughness. The first study[34] focused on the morphology of the PTFE in the fracture toughness test and the crack propagation. Two main mechanism of fracture were observed: the first one is a "brittle fracture with cleavage fracture surfaces and nominal local deformation representative of micro-voids coalescence" and the second one is "ductile failure with significant localized deformation in the form of fibril"[34]. It was pointed out that fibrils' formation from the point of pre-crack are only observed for PTFE in phase IV. PTFE in phase IV and I have the ability to locally deform around the micro-voids and set up a stable fibril formation. Fibrils act as a bridge in the crack plane; they delay the crack propagation and dissipate energy through localized plastic deformation. In accordance with previously mentioned information (1.4.2), in phase II, fracture occurs in two forms: micro-voids coalescence, or cleavage resulting in a low resistance to fracture. Figure II.16 illustrates the fracture mechanism observed in PTFE.

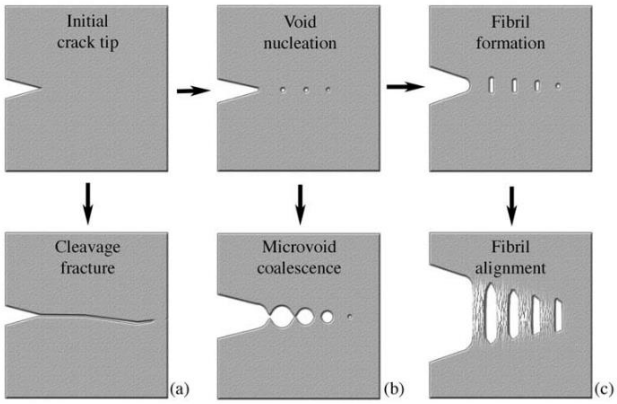

Figure II.16: Schematic of the primary fracture mechanisms observed in PTFE: (a) cleavage, (b) micro-void coalescence, and (c) ductile fibril formation[34].

After understanding the fracture behavior of the PTFE around the β transition; Brown[35] evaluated the crystallinity rate influence on the fracture testing. The study compared two different crystallinity rates (53% and 62%), with samples from Joyce's studies[62,64] and concluded that with increasing crystallinity fibrils formation is restricted; therefore, higher crystalline samples show less toughness and resistance to crack propagation.

1.4.4 Viscoelastic properties (linear DMA-Rheology)

Dynamic mechanical properties and melt rheological aspects of PTFE are the least studied properties. Besides the fact that PTFE is mostly used for coating, PTFE's high viscosity makes it hard to study its mechanical properties above its melting point. Authors mainly used the dynamic mechanical tests to explore the temperature transitions of PTFE[21,26,48,71,72]. Others tried to find a correlation between the dynamic mechanical properties and the crack propagation[35,63,73] or with molecular weight[12,74,75].

McCrum[71,76] studied the internal friction of the PTFE below the melting temperature (-270 to 327°C) by using a pendulum torsion. McCrum's work focused on the influence of the crystalline rate on the temperature transitions. It correlated the crystalline rate with the strength (S) of the torsion moduli G and the intensity of the maximum logarithmic decrement δ_M at each temperature transition. At -100°C and 127°C, S and δ_M decreased with increasing crystallinity and were attributed to amorphous region, while transitions at 27°C and 327°C were attributed to the crystalline region as their G strength and ∂_M increased with increasing crystallinity. Araki[33] applied the same test method as McCrum[71] and compared two samples with different crystallinities; the work agreed with McCrum's conclusions and was compared to other methods of detecting the first and second order transitions. Calleja[21] also investigated the temperature transition of PTFE by means of a stress-controlled dynamic rheometer from -150°C up to its melting point. Results confirmed the four transitions observed by McCrum[71] but reported a different behavior of tan δ at the α transition when crystallinity in the sample varies. Calleja emitted the hypothesis that "the α process is only characteristic of the mechanical relaxation of these constrained amorphous areas and the higher Tα rises is the direct consequence of the inner stresses increase due to the development of crystalline zones". This hypothesis was completed by tensile testing to prove that γ transition is correlated with the glass transition.

Kisbenyi[63] studied the correlation of the viscoelastic properties with fracture toughness. Test were carried out in a wide temperature range (-100°C to 200°C); the comparison between the impact test and viscoelastic test showed a slight difference in the transition temperatures. For the γ transition, the impact test has a higher temperature than of the one seen with tan δ, while for the α and β transition, impact test has a lower value than the one in tan δ with a difference up to 30°C. Brown[35] reported the influence of the crystallinity on the dynamic mechanical properties. The work confirmed the same trends seen in the Young's modulus. Studies by Brown

confirmed McCrum and Kisbenyi's work when considering the tendencies in the tan δ curve. The work also mentioned a similar behavior of the fracture test with the dynamic mechanical properties in the phase II-IV of PTFE.

Starkweather[77] used a capillary rheometer to determine the apparent viscosity of virgin granular, melt-processed granular and virgin coagulated dispersion PTFE before their melting point. All three kinds of granules showed a behavior that differs from a Newtonian fluid as their shear stress increased much more slowly with increasing apparent shear rate. Powders have the same behavior at low shear rates but deviate at higher ranges. The work also pointed out a decrease in the shear stress between 30°C and the melting point. A minimum was noticed at 300°C marking the start of the melting step that occurs after 327°C.

Tobolsky[78,79] determined the maximum relaxation times of PTFE using the stress-relaxation method. It was clear that crystallinity rate did not affect the relaxation times knowing that the test occurs at 380°C (above crystalline melt temperature), but this temperature was not sufficient to reach the degradation of the material. In addition, Tobolsky[78] mentioned a correlation between the temperature and the maximum relaxation times in accordance with the one defined by Williams-Landel-Ferry equation (WLF)[78,79]; this correlation gave a glass transition temperature of 110°C. A later study by Ajroldiet al.[74] measured the melt viscosity at 360°C by means of tensile creep test in the linear viscoelasticity range and found a correlation between the zero strength time (ZST) and the viscosity (ŋ). Ajorldi et al[74]. obtained a molecular weight between entanglement (M_e) points from the pseudo-equilibrium compliance D_e, calculated from the creep curve. This value of the M_e (7500 g/mol) was in accordance with Tobolsky's[78,79] work from the stress relaxation test (6600 g/mol). In addition, Ajordli et al. compared their results with the WLF equation, confirming a glass transition temperature around 127°C (similar to Toblosky's) and determined an activation energy for the viscous flow close the one found by Tobolsky (~ 20 Kcal/mole). Wu's[80] purpose was to determine the molecular weight of PTFE made through dispersion. For this aim, the work consisted on testing in a parallel plate geometry a disc of a pressed PTFE "green" sample sintered in-situ, in the rheometer at 370°C an hour before a step shear-strain application and followed by a stress relaxation. The M_e calculated from the plateau of the moduli gave a value (5490 g/mol) close to the ones reported by Tobolsky and Ajorldi et al. Frick et al[75] also used the plate-plate melt test to determine zero shear viscosity and the molecular weight of a polymerized and modified emulsion and suspension PTFE. The work proved that it is possible to modify the viscosity by modifying the PTFE with a co-monomer while preserving the molecular weight, thus modifying the mechanical properties. In a recent work, Song[43] investigated the effect of the crystallinity on several parameters including viscoelastic properties. Storage modulus in DMA tests from ambient (20°C) to 250°C showed higher values for higher crystallinity rates. Song et al. estimated that higher crystalline rates and larger crystals improve the load bearing capacity and the resistance to deformation.

1.5 Conclusion

PTFE has interesting tribological properties in addition to thermal and chemical resistance. Crystalline properties and the glass transition of PTFE have been the center of interest of many studies[11,15,21]. However, in order to enhance creep and wear properties, PTFE has to be filled with organic fillers such as glass or carbon fiber. In the next section, studies on the properties of filled PTFE will be discussed.

2 Filled PTFE

2.1 Introduction

2.1.1 Effect of the fillers on the PTFE

As seen in a previous section (II.1) polytetrafluoroethylene has interesting qualities regarding its chemical inertness, tribological and mechanical properties. Yet, for some engineering applications such as seals, bearings and gaskets, PTFE has a lack in some properties such as wear and creep (deformation under load) resistance. In order to improve those properties one of the solutions is filling the PTFE matrix.

Through time and depending on the filler type, size and rate, fillers showed remarkable enhancement in different properties such as creep resistance, wear behavior, thermal conductivity, thermal expansion and electrical properties. In order to have a difference in the PTFE behavior it is recommended to have at least 5 vol% of filler in the compound and maximum 40 vol% to preserve the mechanical properties of the final product[5].

2.1.2 Fillers used through time

According to the desired properties, filler type, shape and quantities can differ in the compound. The most commonly used fillers are illustrated in the Figure II.17.

Each filler is responsible for improving one or more properties but as a counterpart, some concessions have to be made for other properties. Glass fibers are known in the enhancement of wear and creep behavior, on the other hand, porosity is higher and some discoloring in the sintered part is observed. Carbon fibers can achieve the same improvements as the glass fiber with lower content. In addition, it increases flex and compressive modulus. Carbon powder can also improve thermal conductivity and, combined with graphite, improves remarkably the wear properties. Bronze in a high filling rate (40-60wt%)[5] raises thermal and electrical conductivity and reduces deformation under load. Filler choice is therefore based on the application of the final part.

Filler	Material Description	Particle Size, μm	Particle Shape	Density, g/cm^3
Glass	E glass, usually size reduced fibers	Diameter 13 mm Length 0.8 mm Aspect ratio >10	Milled fibers	2.5
Carbon	Amorphous petroleum coke	Diameter <75 μm	High purity powdered coke, or natural or synthetic graphite. Irregular shape particles	1.8
Carbon fiber	Pitch or PAN[a] based		Short fibers	
Graphite	>99% C, synthetic or natural	<75 μm	Irregular shape	2.26
Bronze	9/1 copper to tin ratio	<60 μm	Spherical or irregular shape	
Molybdenum disulfide	Mineral (98% pure)	<65 μm		4.9

[a]*PAN is an abbreviation for polyacrylonitrile. PAN fibers are thermally carbonized to obtain carbon fiber.*

Figure II.17: Commonly used fillers and their properties[5]

2.2 Filling techniques

Before choosing the compounding technique, it is necessary to identify the PTFE grade and type needed for the production. The process application for filled compounds is the same applied for unfilled PTFE: low flow resins for compression molding, free flow resins for isotactic/automatic molding, and pre-sintered form for ram extrusion (more information in section 1.1.3). Depending on the PTFE type the compounding technique differs, some types are less difficult than others to mix.

However, filling the PTFE matrix is a challenging process due to many factors. First, PTFE has an extreme charge of particles and functional neutrality in its chains. Secondly, its high viscosity will not allow the polymer to flow upon melting and coat the surface of the filler. PTFE's low friction coefficient reduces the mechanical interactions with the fillers therefore separation between the matrix and the filler can easily occur. As a remedy, one of the solutions is filling the PTFE and pelletizing the mixture in order to trap the filler. In addition to all of this, the process temperatures for PTFE are around 400°C; thus, fillers have to support this temperature for several hours, eliminating many candidates.

2.2.1 Suspension PTFE filling

Suspension polymerized PTFE are the most used grade when filling is required. Fine cut resin is the starting point of compounding due do their small size. The first step of compounding is blending the filler with the PTFE in order to obtain low-flow PTFE compounds. Each company/industry has its own steps/methods in blending the powder, but blending consists of two basic steps: Tumbling and milling. Tumbling with a drum tumbler (or another tumbling

device), makes a rough blend. Then the milling step assures a good blending, dispersion and distribution for a homogeneously mixed powder and filler. Several milling techniques and machines exist. The most used and known ones are the hammer and Rietz mills, their concept is to expose the blend into small rotating hammers in a mesh-screening basket. Another type of mill is the V-shape miller; it is composed of two connected cones rotating around a horizontal axis. This way the blend is transferred from one cone to another during each rotation, mixing the filler and the resin powder[5]. Blending parameters such as time, speed and blending steps are defined by the filler type and rate. The low-flow PTFE product is used to produce billets and sheets, but one of the problems faced is the separation of the PTFE powder from the filler due to their un-existing adhesion or mechanical interaction. Therefore, in some cases, an agglomeration step is required to trap the filler with the PTFE particles. The agglomeration is obtained by mixing the low flow compound produced with water-immiscible organic solvent and/or water and in some cases a surfactant. The mixture is then heated and sheared. The agglomerated granules are separated and dried from the liquid. Several methods and patents found in the literature explain, according the type of filler, detailed parameters and steps for this compounding method[81–84].

2.2.2 Emulsion PTFE filling

Emulsion polymerized PTFE is less likely to be filled because of its large agglomerate size that makes obtaining a homogeneous blend of solid fillers with fine powders complicated. In addition, excessive filling and large fillers generate stresses and shearing that will lead to fibrillation of the PTFE. This point was discussed in the section 1.3.3: fibrillation in the mixing step is harmful for the particles and ineffective for the process. Therefore, filling emulsion polymerized PTFE is limited by a certain filling volume rate and filler shape. Fine powders are mainly compounded in order to color the sample, increase electrical conductivity or increase abrasion resistance.[5,6,59,85]

For low filled fine powder PTFE, compounding steps are more or less similar to the ones of the suspension PTFE. Blending in a V-blender, rolling or tumbling thoroughly after adding the filler, adding a lubricant to the resin, screening the compound, storing for 12h at 35°C to allow the diffusion of the lubricant in the polymer. The key factor of each step remains the handling of the powder that needs to be delicate in order to avoid shearing and fibrillation. Parameters such as milling time, temperature and speed are determined by the quantity of the batch and the compounder's process[5,6,59].

For highly filled systems, co-coagulation compounding is applied so that high amounts of filler can be introduced in the system without harming the particles. Dispersion PTFE is applied for this technique. It consists of mixing the filler with the surfactant present in the PTFE and water. Then adding in one step the dispersion PTFE into the mixture while stirring gently. Finally filtering the material and drying in an oven at 120°C. The final product is generally intended to paste extrusion[5,6].

2.3 Carbon filled PTFE

2.3.1 Introduction on carbon filled systems

Different types of carbon-based fillers exist; the only natural form is graphite that is one of the allotropes of carbon (diamond is the second and only one). Graphite is considered as the most stable natural form of carbon. Due to its particular structure and nature, graphite has interesting properties such as a high thermal stability, electrical and thermal conductivity and self-lubricating properties. Added to molten steel, graphite allows increasing the carbon content in metal alloys, and mixed with clay, graphite constitutes a pencil base.

The other types of carbon-based fillers are synthetic: carbon fibers (or graphite fiber) are obtained from a chemical and mechanical transformation of polymers such as polyacrynitrile (PAN), petroleum pitch or from natural cellulosic fibers like cotton or linen. Carbon fibers have high tensile strength and present high stiffness considering its size (5-10 micron of diameters for 2.5 – 7 GPa of tensile strength)[86]. It is highly used in the textiles field especially in sporting goods, microelectrodes and most of all in composites material. Carbon black (CB) is an amorphous form of carbon. It is another form of synthetic carbon-based fillers, made from the incomplete combustion of heavy petroleum products (coal tar, ethylene cracking tar etc…). The highest consumption of the carbon black production goes to the formulation of tires where carbon black assures the strengthening and reinforcement of the elastomers. Carbon black is also used in high performance coatings for conductivity, UV protection and pigmentation. In addition, it is applied in printing inks and electrostatic discharge compounds (ESD) (international carbon black association, n.d.).

2.3.2 Types of carbon fillers and properties in polymer matrix

Besides electronics, textiles, pencils and metal alloys, carbon-based fillers are highly applied in polymers compounds. Carbon fibers (CF) are employed when strength, stiffness, lower weight and better fatigue properties are needed. They are mostly applied in the automotive industry where the carbon fiber provides the strength and mass reduction while the polymer matrix assures the cohesion and the protection of the fibers[87]. Nguyen-tran et al[88] demonstrated an enhancement in the mechanical properties (tensile, flexural strength) and a decrease in the weight of CF-reinforced nylon-6 (PA6) polypropylene (PP) and carbon nanotube blends. In the aerospace field, carbon fiber reinforced polymers are replacing the metallic alloys in the aircraft's structure. De Rosa et al[89] demonstrated the efficiency of carbon fibers/carbon nanotube composites for aerospace applications.

Carbon black (CB) is the main filler of rubbers, mostly in tires but also for mechanical rubbers goods (automotive belts and hoses for example). Adding carbon black into elastomers provides,

depending on the size, structure, porosity and surface activity, an increase in tensile strength, abrasion resistance, hardness, viscosity, conductivity etc[90]… In addition, CB is used as a filler for conductive materials and pigmentation. Five types of CB are manufactured by the industries : thermal black, lamp black, furnace black, acetylene black, and channel black[91]. Furnace and thermal blacks are used for filling plastics and rubbers. The high degree of porosity and high surface area are important properties for better electrical conductivity. Depending on the type of polymer (amorphous or semi-crystalline) carbon black concentration may vary in order to have the best-desired properties. For amorphous polymers such as PMMA (polymethylmetacrylate) dispersion of carbon black is homogenous and the percolation threshold is higher than that of crystalline polymers where the filler is ejected by the crystalline phase and is concentrated in the amorphous zones. In the tire industries, small CB particle size (thermal process) assure an increase in the tensile strength and abrasion resistance with a decrease in rebound and dispersibility. Higher surface activity, on the other hand, increases rebound and modulus[90]. Aside from reinforcement and pigmentation, CB is a good filler for polymers that are easily affected by ultra-violet lights such as polypropylene (PP). In that case, CB takes the role of a stabilizer that prevents chain scission and consequently the degradation of the mechanical properties[92].

Graphite is considered as a multifunction filler; they are added in polymer matrix for their high modulus (110 GPa), high strength (125 GPa)[93] and reinforcement efficiency. Li and Zhong[94] reported the effect of graphite nano-platelets (GNP's) on polymers such as polystyrene (PS) and polyethylene (PE). It was cleared out that GNPs are not only suitable for enhancing mechanical properties but also for the wear resistance, electrical and thermal conductivity. Graphite/epoxy and graphite/thermoplastics such as Polyetheretherketone (PEEK) or PS are highly useful for airframe production, they allow a reduction in the cost and the weight while preserving the mechanical and electrical properties of the materials as reported by Vodicka[95].

2.3.3 Influence of carbon fillers on PTFE matrix

Just like other polymers, PTFE can be filled with carbon-based fillers. The main aim of filling the PTFE with carbon-based fillers is to enhance its wear and creep properties. Therefore, most of the studies discussed in the literature tested the tribological and wear properties of filled PTFE[96–98]. Carbon powder, carbon fiber and graphite or even sometimes a combination of two or more are used as fillers[99]. Carbon based fillers can withstand PTFE's processing temperatures, and are inert to hydrofluoric acid. Carbon fiber enhances flex and compressive modulus in addition to lowering creep[5]. Bijwe et al.[100] explored the tribological properties of PTFE reinforced with chopped carbon fibers in adhesive and abrasive wear modes. The study showed a lower friction coefficient and a better wear performance at higher loads than for low loads. Bijwe et al[100] demonstrated that the best performances of the composite would be for a slow speed (up to 4m/s) high loads and for applications at temperatures lower than 150°C.

A disadvantage of the carbon fiber is the poor interfacial adhesion and the difficulty to distribute it uniformly in the PTFE matrix. Authors proposed a surface treatment of the carbon fiber in order to improve this drawback[97,101]. Shi et al.[102] tested different types of surface treatment of carbon fiber mixed with PTFE and reported an improvement in the tribological properties. Rare earth (La_2O_3 solution) was noted as the best surface treatment compared to the other methods in the study. Aderikha el al[98] proposed and ultrasound treatment for the expanded graphite (EG) which showed a better dispersion and distribution of the carbon filler.

2.4 Silica filled PTFE

2.4.1 Introduction on silica filled systems

Silicon dioxide known as Silica is an inorganic material found in nature mostly as quartz and sand. It constitutes one of the most abundant families of material and exists as a compound of several minerals or synthetic products.

Silica can be found in a crystalline or amorphous form, and has a wide application range: the main application for silica is in the construction industry for concrete production. It is also the main element for glass production when it is transformed at high temperature (1200°C) and solidifies as a glass without crystallizing. It is also used in optical fibers for telecommunication, an additive in food production, in cosmetics such as toothpaste, in semiconductors production etc…

In the last few decades, research studies have made it possible to control the size, shape, porosity and crystallinity of silica depending on the needed application. In addition, several modifications can allow a precise surface nature, which leads to a control of the hydrophobicity of the silica.

2.4.2 Types of silica and properties in polymer matrix

In 2007, the INRS French institute differentiated silica types between sand, amorphous and crystalline[103]. The Association of Synthetic Amorphous Silica Producers (ASASP) provided a classification of the silica types as shown in the Figure II.18 [104,105].

In the polymer industry, silica is used as a reinforcement filler in thermosetting, thermoplastics and rubbers. Depending on the size and type of silica, properties of polymers are more or less enhanced. A study of Wang et al[106] showed that the addition of silica in epoxy resin has a remarkable influence in enhancing the Young modulus and yield stress of the material. Other studies[107,108] highlighted the improvement of the thermal and mechanical properties of silica filled rubbers. Guneyisi et al[109] showed a compensation effect on the tensile strength modulus of rubberized concrete due to the addition of fumed silica in the blend. In addition to a decrease in the strength loss due to rubber addition. On the other hand, silica filling is also applied in polyolefin thermoplastics such as polyethylene (PE) and low-density PE (LDPE). Kalfuset al[110]

studied the influence of the nano-silica filler in several polyolefin such as LDPE, HDPE and PP. Nano-silica filler decreased the crystallinity rate, influenced the morphology and the viscoelastic properties of the polymers especially after Tg . Zhang et al[111] used a grafted nano-silica in HDPE matrix and noted an improvement in the mechanical properties (strength and elongation at break) even at low filling rates such as 0.75 volume percent of nano-silica.

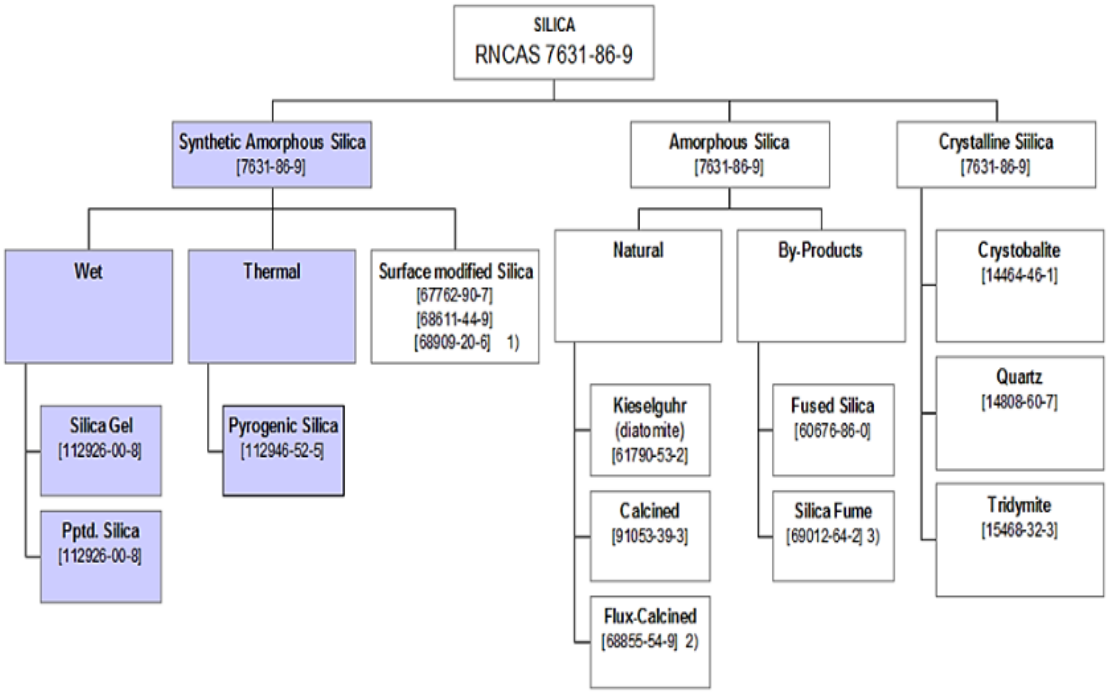

Figure II.18: Overview of silica types by ASAP.

As mentioned above, several types of silica exist of which precipitated and fumed. Precipitated silica is an amorphous porous form of silica made through precipitation from a solution containing silicate salts. Figure II.20 explains the different steps of the precipitated silica process. The precipitation step determines the morphology (porosity, specific surface) of the particles, which is an important characteristic for the final properties. The filtration step controls the purity of the product. In the drying step, silica granules acquire their physico-chemical properties, form, porosity… The final silica obtained is a white powder composed of elementary particles forming aggregates which in turn lead to agglomerates[105] (Figure II.19).

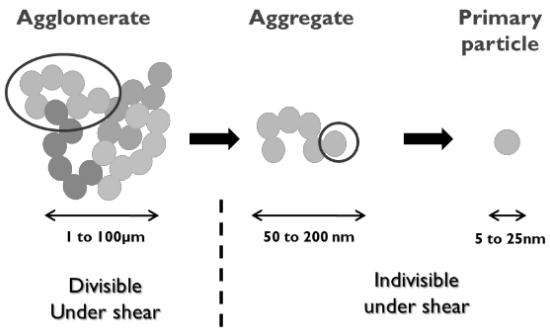

Figure II.19: Structure of the precipitated silica[105]

As shown in the Figure II.19, agglomerates are highly sensitive to shear and are divided into aggregates, while aggregates are indivisible into the primary particle.

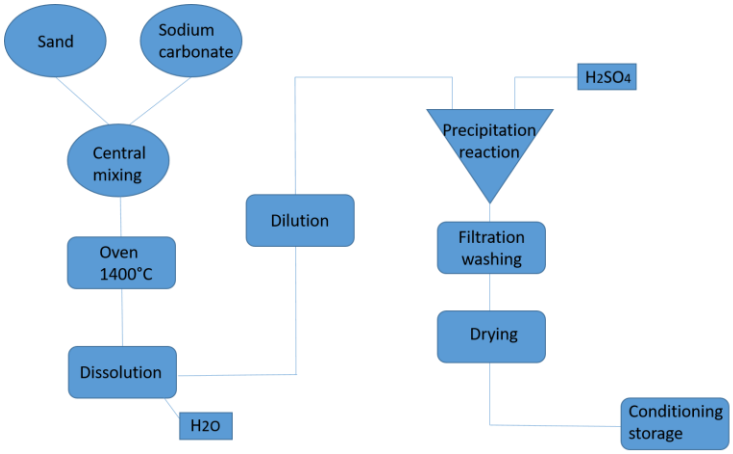

Figure II.20: Precipitated Silica process ref

Precipitated silica's main application is the reinforcement of elastomers in the tire industry. It is also applied in cosmetics such as toothpastes, in shoes soles, in the paper industry etc…

Fumed silica or pyrogenic silica is produced by burning volatile silanes ($SiCl_4$) in an oxygen-hydrogen flame. The preparation of the fumed silica is illustrated in the Figure II.21 below:

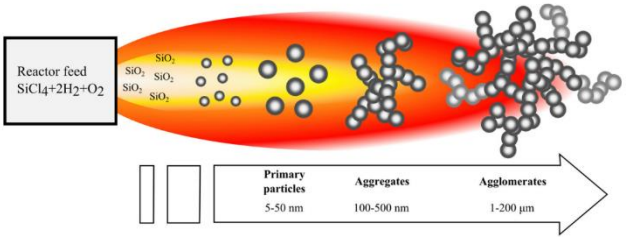

Figure II.21: Fumed silica preparation[112]

After the flame process, the produced silica is an amorphous white powder. Fumed silica is well known for its high specific surface (10–400 m^2/g[113]). It is applied in cosmetics, for its light-diffusing properties as well as in paint, coatings, toothpastes etc…

2.4.3 Influence of the silica on PTFE Matrix

PTFE silica compounds are mainly used for dielectric materials for printed circuit boards (PCB). Few studies on Silica filled PTFE can be found in the literature. Reports on silica filled PTFE started to be seen in the early 2000's. Basu[114] applied an emulsion PTFE filled with hydrophobically modified silica (HMS) in order to create a superhydrophobic material.

Chen et al[115,116] studied the effect of the silica size, content and the use of a coupling agent on the properties of the PTFE such as water absorption, tensile strength and dieletric properties. For these studies, Chen et al. used a suspension PTFE with a particle size around 0.2-0.3 µm and two different sizes of fused amorphous silica (5 and 25 µm). Silica was coated with Phenyltrimetoxysilane at several coating levels. Filling the PTFE was achieved in an aqueous environment and then dried in an oven. Afterwards, the compound was pressed and roll-milled in order to obtain sheets sintered in an oven. The study reported an improvement in the dielectric properties, water absorption, and tensile strength when coating the silica with coupling agent. An optimum of the properties was observed for a 3 wt% coating level. As for the size and the content of Silica, the optimum filling content was noticed for the 25 µm silica at a 60 wt%.

On the other hand, Huang et al[117] compared a nano-sized silica (20 nm) at 2 wt% with a micron-sized silica (5 µm) at 33 wt% filled in a water based dispersion PTFE (average particle size 210 nm). The study reported a decrease in the mechanical modulus of the compound filled nano-sized fillers. This decrease was accompanied with an increase in the dielectric properties. Huang et al. concluded to an increase in the porosities when increasing the nano-sized silica content that induced a degradation in the mechanical modulus.

Yuan et al[58] investigated the effect of the sintering temperature on Silica filled PTFE compounds. The compound was made with an aqueous dispersion PTFE and a fused silica of 14 µm average particle size; moreover, phenyltrimethoxysilane as a coupling agent was used. Different

properties were tested: crystallinity rate showed an increase with increasing sintering temperature between 350°C and 390°C, while the polymerization degree decreased (i.e. the melting temperature). As for the dielectric constant, a maximum was noticed at 370°C before an obvious drop for higher temperatures. For density values, 360°C was the maximum before a drop. The authors concluded that 370°C was an optimum temperature for sintering. Martins et al[118,119] determined the visco-elastic properties of a PTFE filled with silica at 42 vol%. The studies did not mention the type of PTFE or silica used; yet Martins et al. showed an increase in elastic modulus and stiffness when filling the PTFE.

2.5 Conclusion

Through time, several fillers have been added to neat PTFE such as carbon black, silica, fiber glass etc.…These fillers showed an influence on the wear, creep and tensile strength of the PTFE. However, very few studies discussed the influence of the nature or the size of the filler on the properties of PTFE. For this purpose, the work in this thesis will discuss the influence of the fillers on the crystalline structure of the PTFE and on the dynamic mechanical testing in tension compression.

3 PEEK/PTFE blends

3.1 Introduction

Polyether ether ketone (PEEK) is a semi-crystalline thermoplastic that belongs to the Polyaryletherketones (PAEKs) family. PAEKs are linear aromatic polymers, known for their exceptional mechanical and chemical properties in addition to their excellent wear, creep and fatigue performances. They are attributed to high performance polymers and distinguished by their aromatic rings joined by ether or ketone linkage.[120]

PEEK is known for its thermal resistance properties; its melting temperature is around 340°C with a glass transition around 143°C. Although it has remarkable properties, PEEK presents limitations such as its price (~100-150 €/kg) and its high processing temperatures, in addition to its low resistance to UV.

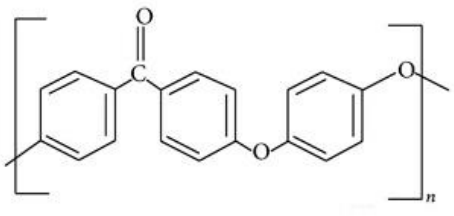

Figure II.22: PEEK molecular structure

3.2 Microstructure

Like the majority of semi-crystalline polymers, mechanical properties are directly related to its microstructure (crystallinity and morphology). Crystallinity and morphology depend on two major parameters that are thermal history and molecular weight. Even the final product color depends on the crystallinity of the PEEK; a high crystalline PEEK has a grey color while products with low crystallinity have a brown color. (Example Figure II.23)

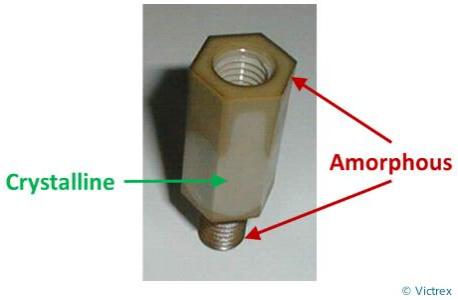

Figure II.23: Color difference between amorphous and crystalline PEEK[121]

Often, studies compare PEEK structure and morphology with Polyethylene terephthalate (PET), where both can be quench cooled from melt in order to have an amorphous material. It has been proven that, when heated up from glassy state or cooled down from the melting state, PEEK has a two-phase crystal/amorphous structure.[122] This structure consists on crystalline lamellae with a size comprised between 20 and 60 Å[122] depending on the melt conditions. These lamellae, if not disrupted, grow into three-dimensional spherulites of about 25-40 µm[120,122]. Later Chu et al.[123] highlighted the influence of the melting temperature on the spherulite size, where it increased with increasing the melting temperature. In addition, Chu et al.[123] pointed out the fact that molecular weight is capable of changing the crystalline morphology. According to Chu et al, PEEK with high molecular weight (~50 000 g/mol) generates higher nucleation densities and therefore shows a densely packed, sheaflike spherulite with small lamellae structure. (Figure II.24)

Figure II.24: Sheaflike strucutre of PEEK Spherulite according to Chu et al[123]

Based on the crystalline characteristics (content, spherulites size…) and molecular weight, PEEK shows different mechanical behavior. According to literature[121,124,125], an increase in the molecular weight increases the impact toughness, fracture toughness (K_{IC}) and the fatigue crack growth toughness (FCG). While an increase in the crystallinity rate decreases the impact toughness and fracture toughness, the FCG increases. Sobieraj et al.[125] summarized (Table II.2) the effect of molecular weight, crystallinity rate, spherulite size and aging on the impact toughness, fracture toughness and fatigue crack growth.

Material characteristics	Effect on impact toughness	K_{IC}	FCG
↑ Molecular weight	↑	↑	↑
↑ Crystallinity rate	↓	↓	↑
↑ Spherulite size		↓	↓
↑ Aging	↓		

Table II.2: Morphology effect on impact toughness KIC and FCG according to Sobierj et al.

For the crack propagation Sobieraj et al[125] as well as Chu et al[123] suggested that PEEK with a low molecular weight has an intraspherulitic fracture process, while high molecular weight PEEK has in interspherulitic fracture process.

3.2 Processing and applications

PEEK is a very versatile material when coming to processing. When in the molten state, the viscosity of the PEEK is equivalent to those of Polycarbonate or Polyvinyl chloride (10^2-10^3 Pa.s) but at much higher temperatures (~400°C). This particularity makes it processable by most of the existing transformations means such as the extrusion, molding injection, compression molding, rotomolding etc…

Depending on the chosen transformation process, parameters such as temperature, cooling rate etc… must be adapted. The common parameter of pre-processing is the handling and the drying. PEEK is a delicate material that can easily be contaminated if not well handled. According to Victrex's processing guide[121,126] it is recommended to dry PEEK products for 3 to 5 hours at 150°-160°C, prior to processing in order to have a moisture content in te sample below 0.02% . Moisture in the PEEK granule can cause defects in the final parts during processing (black spots or entrapped air in the product).

Injection molding is one of the most applied transformation processes for PEEK materials. It is recommended to inject the material into a mold heated to 180/190°C (above T_g) to ensure a

homogeneous crystallization. Thanks to its high thermal stability, it is possible to regrind PEEK materials without causing degradation. This way reworking ground sprues, runners and rejected parts is possible.

Extrusion process is applied for several applications such as wires, cabling coating, tubes, sheets… Standard extrusion processing is required with some specifications such as a temperature around 400-450°C with an ideal residency time inferior to 30min.

Roto-molding, compression molding and sintering are also transformations adapted for PEEK processing.

No matter the process chosen for the production, it is always necessary to regulate the cooling rate and temperature in order to control the crystallinity rate and morphology.

PEEK can be found in all types of industries; it is often an alternative for steels, aluminum or titanium. Figure II.25 summarize the applications of peek products according to the industries. It is the best solution when temperature and chemical resistance are required, in addition to high mechanical properties.

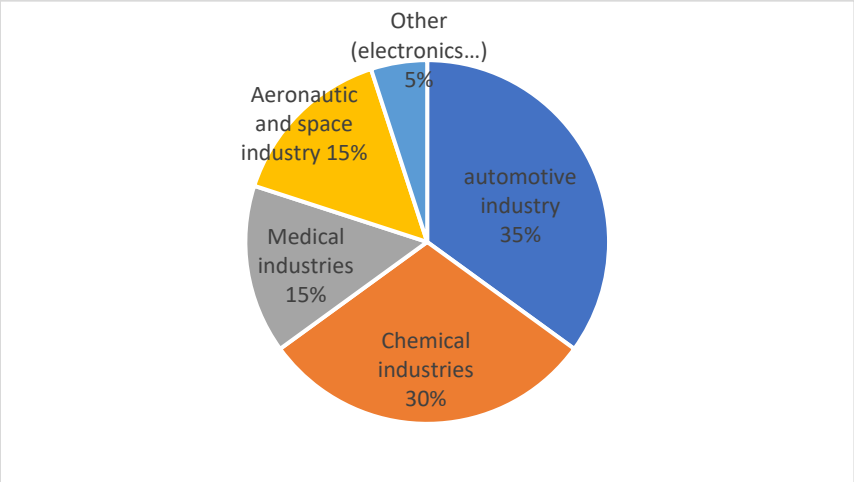

Figure II.25: Industrial Applications FOR PEEK materials[127]

For automotive application PEEK is useful for its high temperature and chemical resistance, therefore it is widely applied “under the hood” in pieces such as bearings, sealing, gaskets etc… the resistance against γ rays allowed PEEK to find applications in the nuclear industry especially in sleeves for electric cables. Being biocompatible allowed peek to be applied in the medical field where sterilization is required.

3.3 Filled PEEK

In order to improve the wear resistance of PEEK materials , several types of reinforcement (inorganic fillers) have been studied[128,129] : Carbon fiber, glass fiber, silica, titanium etc… .

Kuo et al[130–132] studied the influence of the nano-filled PEEK with Silica and alumina on the behavior of the composite. The study showed[131] that reinforcing PEEK with nano-silica or alumina particles improves its hardness, elastic modulus, tensile strength and thermal stability (up to 40 additional degrees). Afterwards Lai et al.[130] tested the same types of fillers while adding a coupling agent and noticed a better dispersion of the particles in the PEEK matrix. Modifying the filler's surface improved the hardness and elastic modulus (by 7%) even more than the unmodified fillers.

Misrha et al[133] reinforced PEEK with Zirconia fillers ; thermal stability, storage modulus, tensile strength, flexural modulus and strength were enhanced. Lai et al. [130] showed that the storage modulus value reached for 3 wt% of zirconia is reached with 10wt% of silica..

3.4 PEEK/ PTFE Blends

Mixing PTFE with PEEK is one of the solutions to compensate the low wear and friction properties of PEEK. Therefore, most of the studies focused on the best combination of PTFE-PEEK in order to improve the wear behavior[134–136]. However, the blend of those two polymers is not sufficient and most studies (although rare) treat PTFE/PEEK/filler composites.

Moreover, rare are the studies that discuss the microstructure and the mechanical properties of PEEK-PTFE blends. Some studies in the literature discussed PEEK-PTFE and fillers in the blends, such as graphite flakes and chopped carbon fibers [137,138]. Qu et al[137] studied a four component material : Graphite/carbonfiber/PTFE/PEEK. They observed an increase in the stiffness of the composite, a decrease in the storage modulus and no change in the thermal expansion coefficient. Gladson et al[138] studied the effect of 5 wt% nano-wire alumina on PEEK-PTFE matrix, where it showed that dynamic mechanical properties (storage modulus) increased significantly compared to PEEK-PTFE composite (12%) and glass transition temperature increased by 32°C. The study concluded that this is an interesting material for high mechanical strength and low electric conductivity applications.

4 Conclusion

In conclusion, this literature review gave a general idea on the PTFE, its properties, transformation methods and limits. PTFE is distinguished by its several temperature transitions marking a first or second order transition. To this day, authors do not agree on the glass transition of the PTFE[21].

In addition to its remarkable transitions, PTFE is very influenced by its crystallinity rate, authors showed different behaviors of mechanical properties depending on the crystalline content of the PTFE[12,25,45].

Even though PTFE has remarkable properties in tribology[139], chemical resistance and temperature resistance[5], it possesses some weaknesses when it comes to creep and wear resistance[100]. Several studies showed an interest in filling PTFE in order to enhance its creep, wear and mechanical properties[46,115,117,140,141]. However, most of the studies focused on the tribological properties, and very few discussed the influence of the filler on the microstructure and visco-elastic properties[46].

For this purpose, this work will study composites of PTFE filled with organic fillers such as silica and carbon black at different content, size and surface nature. The main focus will be on the influence of those fillers on the microstructure, the linear and non-linear visco-elastic properties. In addition, blends of PTFE and PEEK filled with silica will be discussed.

III.Materials and Methods

1 Materials

1.1 Polymers

Polytetrafluoroethylene (PTFE) is the polymer adopted for this study. For welding reasons, we chose a non-free flow (Fine powder) modified grade of PTFE with a PPVE content below 1%. It is a suspension grade of PTFE with an average particle size of 25µm.

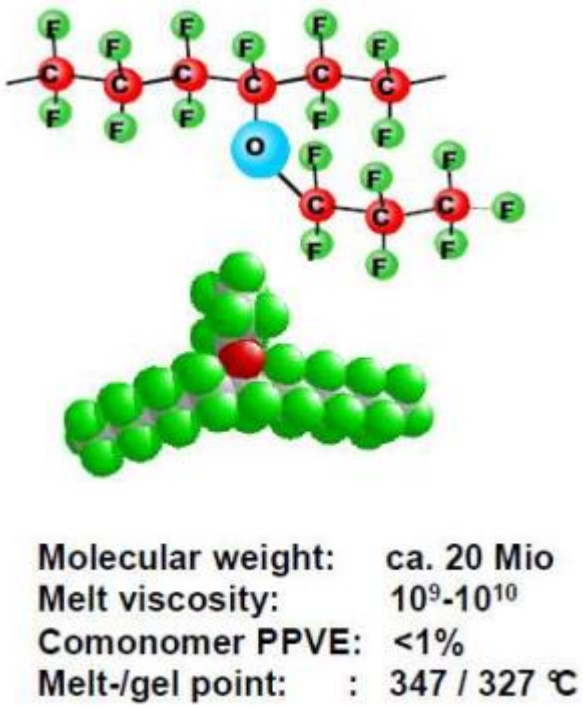

Figure III.1: Modified PTFE chemical structure

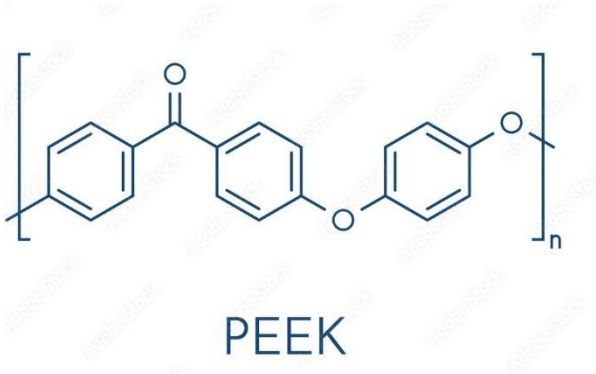

Figure III.2: PEEK Repetitive unit

A second polymer, PEEK (Figure III.2), was chosen to blend with the PTFE, in order to enhance the mechanical properties of the PTFE. PEEK was purchased from Victrex, a fine powder grade with an average particle size of 50µm, a melt viscosity of 350 Pa.s and a melting point of 345°C (supplier's information).

1.2 Fillers

As mentioned previously, the aim of the study is to understand the relationship between the microstructure and the mechanical properties of filled PTFE. Therefore, two fillers of different nature were tested: Carbon Black and Silica.

The carbon black has an average sphere particle size of 25µm.

As for the Silica different sizes were tested:

- Silica 1: Precipitated synthetic amorphous porous Silica. With and average particle size of 4µm; and a specific surface of 100 m^2/g.
- Silica 2: High dispersible precipitated synthetic amorphous Silica micro-pearl. With an average particle size of the considered agglomerates between 200 and 300µm;
- Silica 3: Hydrophilic fumed nano-silica. With an average particle size of 0.2-0.3µm and a specific surface of 200 m^2/g.

1.3 Coupling agents

In order to modify the nature of surface of the Silica and thus improve the PTFE/filler interface, two coupling agents were investigated:

1. Trimethoxyphenylsilane 97% (PTMS)
2. 1H,1H,2H,2H-Perfluorooctyltriethoxysilane (PFTOS)

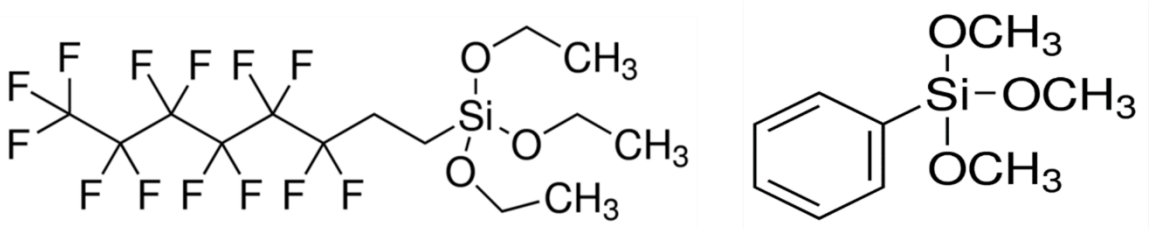

Figure III.3: chemical structure of the coupling agents: PFTOS on the left and PTMS on the right.

2 Characterization Methods

2.1 Microstructure characterization

2.1.1 Differential scanning calorimetry

Out of the several existing methods that determine the crystallinity of the PTFE, differential scanning calorimetry was one of the chosen methods. Tests were carried out on a Q10 DSC from TA instruments. Samples tested were between 5 and 8 mg extracted from the heart of the sample. The tests consisted on a heating and a cooling ramp from 150°C to 360°C and from 360°C to 150°C at 10°C/min. For results analysis, crystallinity rate was calculated as follow:

$$X_c = \frac{\Delta H_f}{\Delta H_f^0} \quad \text{(III.1)}$$

Where X_c is the mass crystalline content, ΔH_f is the mass melt enthalpy and ΔH_f^0 is the mass melt enthalpy of the crystalline bulk polymer. ΔH_f^0 value as mentioned in the literature[5,8,10,15,19] varies from 57 to 104 J/g . In our work the value was fixed at 80 J/g[9] the same as in the studies by Rae et al.[8,9].

In addition to crystalline content determination, the differential scanning calorimetry was used to give an estimation of the lamellae size, by applying the Gibbs-Thomson theory:

$$T_m = T_m^\infty \left[1 - \frac{2\gamma}{\Delta H_m^\infty l}\right] \quad \text{(III.2)}$$

Where T_m is the melt temperature, T_m^∞ is the equilibrium melting temperature of an infinitely large and flat crystal, l the lamellae size and γ the crystal/liquid interfacial energy. Based on the work of Ferry et al.[19], T_m^∞ is a result of an extrapolation to zero heating rate of the melting temperature. DSC test was then carried out by varying the heating rate then measuring the melt enthalpy, extrapolating to zero in order to determine the melt temperature T_m without the superheating phenomenon. This extrapolation led to a value of 334°C for the virgin PTFE. The crystal/liquid interfacial energy (γ) value obtained from the literature[19] is fixed at 0.111 J/m^2.

2.1.2 Microscopic observation

An observation of filled PTFE blends was carried on a Hirox SH 4000 mini scanning electron microscope in order to determine the homogeneity and the morphology of the blends. Samples were freeze fractured in liquid nitrogen for simple observations in a back scattering electron (BSE) signal. Before observation, the sample was gold coated for 60 seconds in order to have a better conductibility of the electrons. The observations were at a 15KV tension.

2.1.3 Density measurement

The density of the sample was determined through two methods: experimental and theoretical, in order to estimate the void content in the samples by comparing the theoretical and experimental results.

Theoretical results are based on the following equation considering a compact sample:

$$\rho_s = \frac{\omega_f * \rho_f + \omega_{PTFE} * \rho_a * (1 - \omega_a) + \omega_{PTFE} * \rho_c * \omega_c}{m_s} \quad \text{(III.3)}$$

Where ρ_s and m_s are respectively the density and weight of the sample, ρ_f and ω_f are the density and weight content of the filler, ρ_a and ω_a are the density and weight content of the amorphous phase of PTFE (ρ_a = 2.04 ± 0.03 g.cm^{-3})[23] and finaly ρ_c and ω_c are the density and weight content of the crystalline phase of PTFE (ρ_c 2.3 ± 0.01 g.cm^{-3}).

Experimental density was measured using a glass pycnometer by weighing the immersion in water or ethanol. Therefore, the density is calculated by the following equation:

$$\rho_s = \frac{m_s}{v_p - \frac{m_l}{\rho_l}} \quad \text{(III.4)}$$

Where v_p, is the volume of the pycnometer, m_l and ρ_l are respectively the weight and the density of the liquid.

2.2 Mechanical characterization

2.2.1 Linear dynamic mechanical analysis (linear DMA)

Torsion oscillations of rectangular specimen tests were performed on an ARES rheometer. Samples of 2 mm of thickness and 10 mm large were cut in the sintered discs. The test consists on a linear temperature ramp from -40°C to 250°C at 3°C/min with a 0.1% strain and a frequency of 1 Hz under a nitrogen atmosphere. It is important to note that the response of the material at 0.1% strain was linear. This test aims to evaluate the storage and loss shear modulus (G', G''), and the damping factor (tan δ) in the linear domain of the material. The temperature ramp allows a comprehension of the viscoelastic properties of the material in the different crystalline states:

- From -40°C to 20°C: The contribution of the filler in the presence of the rigid amorphous phase in an ordered helical chain form and the crystalline phase.
- From 20°C to 120°C: The contribution of the filler in the presence of the rigid amorphous phase with a random helical chain and the crystalline phase.
- From 120°C to 250°C: the contribution of the filler to the matrix with the crystalline phase.

Ideally, in order to complete further the investigation of the reinforcement induced by the presence of fillers, it would have been interesting to study the effect of the filler on the polymer after 250°C and until the fusion temperature, but the torsion test could not be applied because of the creep behavior of the material. In addition, parallel plate geometry was not ideal for the testing because the material slipped on the geometry causing a non-repeatable testing.

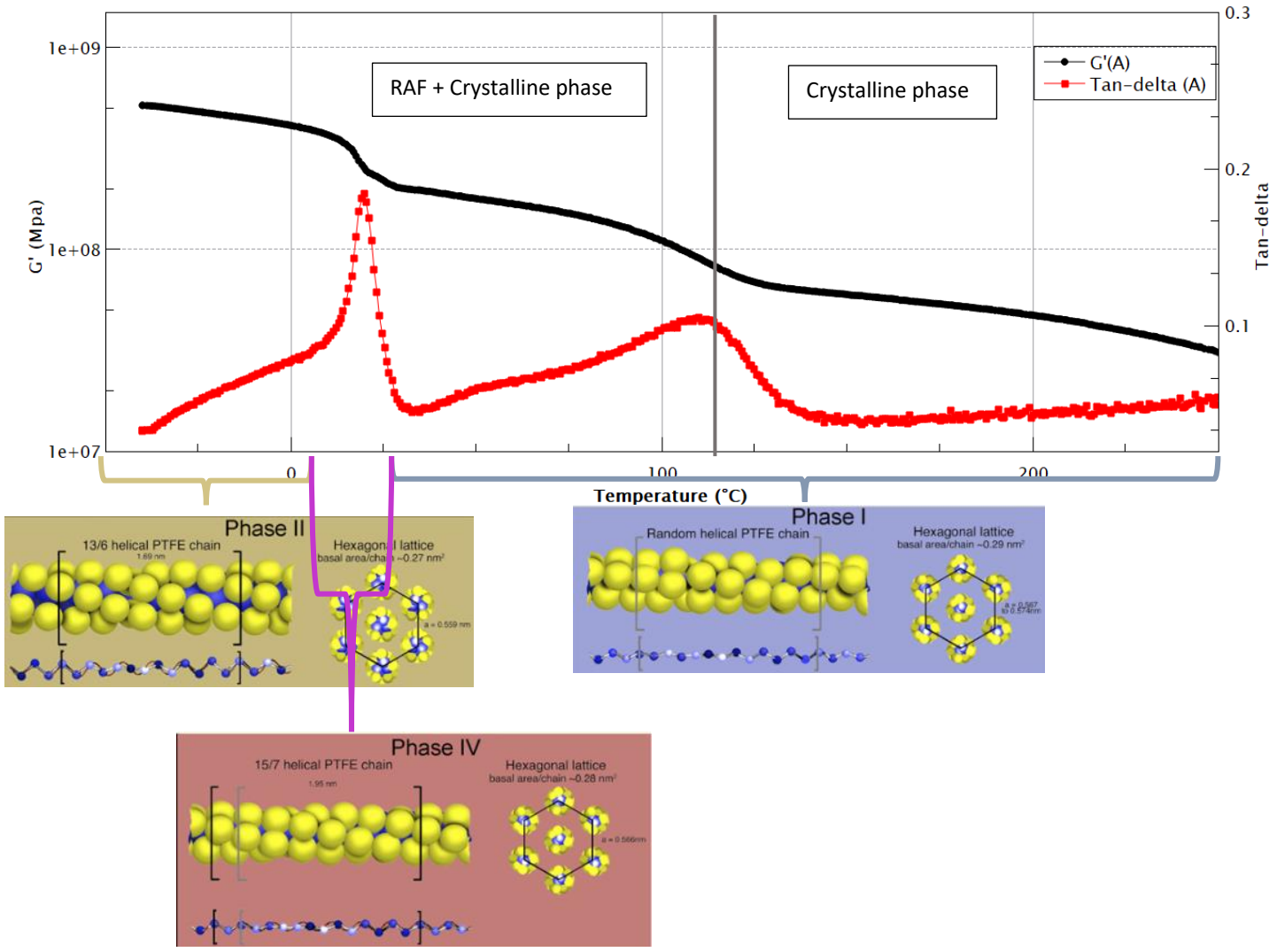

Figure III.4: Example of the Linear DMA result for virgin PTFE sample.

2.2.2 Non-linear dynamic mechanical analysis (non-linear DMA)

Dynamic mechanical analysis tests were performed out of the linear domain of the samples. Tests took place on a Metravib-1000 DMA. Traction compression tests were carried on samples of 4 mm of thickness and 4 mm large cut from sintered discs. The test consists on a temperature ramp from -60°C to 250°C with a 5 Mpa stress oscillations (in traction and compression) and 0.5 Hz of frequency. This test evaluates the storage and loss modulus (E', E''), the damping factor (tan δ) out of the linear domain of the material. The test gave a macroscopic point of view on the material, where the samples undergo a traction compression oscillation out of the linear domain in a way that exposed the influence of the microscopic defaults (such as morphology inhomogeneity, porosity, filling limit content etc…).

3 Process parameters adaptation

3.1 Silica grafting

3.1.1 Introduction

One of the work goals is to evaluate the influence of the surface modification of the silica on the morphology of the PTFE / silica blend and its properties (crystallinity and mechanical). Hence for some samples, grafting of the silica before blending was an additional step to the process.

For this purpose, only silica 1 was modified using two coupling agents, PTMS and PFTOS. Coupling agents were chosen based on literature studies[46,115,142]. Both PTMS and PFTOS applications intended to limit the agglomeration of silica particles in the blending step and assuring a more homogeneous dispersion. Moreover, the intuitive reason for choosing PFTOS is the presence of the fluor chain that could induce a better adhesion with the PTFE particles.

Some studies in the literature have observed the influence of surface modification of silica using different coupling agents. For instance, Chen et al[115]. studied the impact of the phenyltrimetoxysilane quantity added in the process on thermal, dielectric and mechanical properties; it turned out that 3 wt% was the best compromise for having the best properties. Yuan et al.[142] studied the influence of mixture of two coupling agents perfluorooctyltriethoxysilane (F8261) and Z6124 + aminopropyltriethoxysilane (KH550) at different quantities on water absorption, dielectric properties and density. The authors found an optimum quantity of both coupling agents that enhanced the properties of the composite. Both studies described the grafting methods of the silica but did not run any test to detect the presence of the coupling agent on the surface of their silica once mixed in the PTFE matrix.

Bosq et al[143]. on the other hand, studied the influence of grafted nano-silica on the PTFE crystalline properties. In their work, the grafting efficiency was detected via infrared

spectroscopy (IRTF), thermal gravimetry analysis (TGA). Unfortunately, the work did not compare modified and non-modified nano-silica.

In our case, the size of Silica 1 is in the same range of size applied in the study carried out by Yuan et al.[142]; therefore, the silica was modified using the same coupling agent (PFTOS) and applying the same grafting process described in their work. This coupling agent was also inspired by Bosq et al.[143] who applied a fluorinated coupling agent to modify the surface of their silica. The main objective was not only to avoid the formation of agglomerates but also to improve the wettability with PTFE matrix using a fluorinated coupling agent. PTMS on the other hand was used as a comparison with the work from Chen et al.[116].

3.1.2 Grafting detection

As mentioned above, only Bosq et al's work[143] proved the efficiency of its grafting, while other studies just relied on the evolution of the properties. TGA, IRTF and ultraviolet spectroscopy were used to try and observe the grafting of the coupling agent. However, non-of the applied techniques led to a quantitative result. The absence of proper observation of grafting can have two probable causes: either the grafting did not take place, or the amount of modified surface was too small to be detected.

Indeed, taking into consideration the silica size that is used (4µm) the specific surface, and the approximative silanol groups for this type of silica (around 4 to 6 OH/nm^2)[144], the available surface for grafting would not exceed 1% of the total surface. Therefore, even if the surface modification took place, it is very hard to detect this small percentage of grafting by means of TGA or infrared. Therefore, indirect determination of the grafting through improvement of mechanical properties was used.

Thus, the modified silica was mixed with the PTFE using the previously described methods; samples were produced for microstructure and mechanical testing in order to seek any difference between the samples that would indicate a change in the properties.

3.1.3 Influence of the grafting on the microstructure

Table III.1 summarizes the samples produced with modified and non-modified silica and their crystalline content. It also presents the influence of the grafting on the crystalline content, the α and β temperature transitions and their damping factor in rectangular torsion tests.

For PTFE/Silica blends, it is clear that the modification of the silica surface with PFTOS or PTMS increases the crystalline content by around 5% whatever the silica content. This result is in accordance with Yuan et al.[142] where the modification of the silica surface increased the crystalline content according to the content of the coupling agents.

Sample	Filler content (vol%)	Coupling agent	Xc (%)	Tβ (ºC)	Tanδ (β)	Tα (ºC)	Tanδ (α)
1	16	-	42	23	0.186	113	0.096
2	16	PFTOS	44	21	0.190	112	0.107
3	23	-	45	25	0.179	112	0.085
4	23	PTMS	53	24	0.178	113	0.081
5	23	PFTOS	51	24	0.187	113	0.086

Table III.1: comparison of DSC and mechanical results for samples filled with grafted and non-grafted Silica 1

After the crystalline content, the linear response of the samples was tested in torsion oscillation of rectangular specimens. According to the results presented in Table III.3 no significant effect was noticed on the linear response of the samples. Temperature transition in addition to their damping factor strength remained the same with or without grafting the silica.

3.1.4 Grafting influence on mechanical properties

The main aim of the grafting was to avoid the breaking during the non-linear dynamic mechanical testing. This breaking was generally caused by the inhomogeneity of the samples due to improper filler dispersion. As can be seen from the Table III.2, modifying the surface of the silica did not prevent a breaking in the test. For some grafted samples such as sample 2, the breaking occurred at a higher temperature than for sample 1, with no couping agent but the grafting did not prevent it completely.

Sample	Filler content (vol%)	Coupling agent	E' (-50ºC)	E'(30ºC)	E'(150ºC)	Tanδ (β)	Tβ (ºC)	Tanδ (α)	Tα (ºC)	T(B) (ºC)
1	16	-	$1.9\ 10^9$	$1.2\ 10^9$	$1.1\ 10^8$	0.126	34	0.210	116	165
2	16	PFTOS	$2.0\ 10^9$	$1.2\ 10^9$	$1.3\ 10^8$	0.121	32	0.206	116	203
3	23	-	$2.3\ 10^9$	$1.5\ 10^9$	$1.4\ 10^8$	0.143	39	0.209	119	168
4	23	PTMS	$2.0\ 10^9$	$1.3\ 10^9$	$1.0\ 10^8$	0.165	37	0.215	114	198
5	23	PFTOS	$2.1\ 10^9$	$1.4\ 10^9$	-	0.144	38	0.215	118	134

Table III.2: Comparison of non-linear DMA results for samples filled with grafted and non-grafted Silica 1. Grafting the silica did not prevent the breaking in the testing.

3.1.5 Conclusion

In conclusion, the grafting efficiency could only be observed indirectly, through the increase in crystalline content. Grafted samples with a filling rate of 16 vol% (sample 4 and 5) have a crystalline content higher by more than 5% than a non-grafted silica filled sample (sample 3).

The effect on the linear response and mechanical properties was very minimal and non-constructive. Linear viscoelastic results did not show any influence on the transition temperatures nor the damping factors. The same result was observed with non-linear DMA testing. The amelioration of these tests will be discussed in the next chapters.

When observing those results, it can be deduced that the grafting of the silica was insufficient to modify the mechanical properties of the composites.

3.2 Influence of the filler sieving before mixing

3.2.1 Introduction

Preventing the agglomeration of the silica in the blends is a hypothesis that may help avoiding breaking in the DMA tests by avoiding the dispersion inhomogeneity and weak areas in the samples. Thus, when modifying the surface of the silica, after the drying step the silica was sieved before incorporated to the mix. It can be visually noticed that the final material is more homogeneous (see figure III.3). Compared to blends made with unmodified silica, there were two changed parameters: the surface modification and the sieving. Thus, unmodified Silica 1 was sieved in a 0.125 mm mesh before adding it to the PEEK/PTFE mixer and the influence on microstructure and mechanical properties was tested to determine the role of the sieving in the process.

Samples with sieved unmodified silica had visually a better homogeneity. Figure III.5 shows two samples, with and without sieving unmodified silica, mixed with PTFE and PEEK. Clearly, the sample with sieved silica shows a homogeneous and smooth surface indicating a better dispersion and the absence of agglomerates.

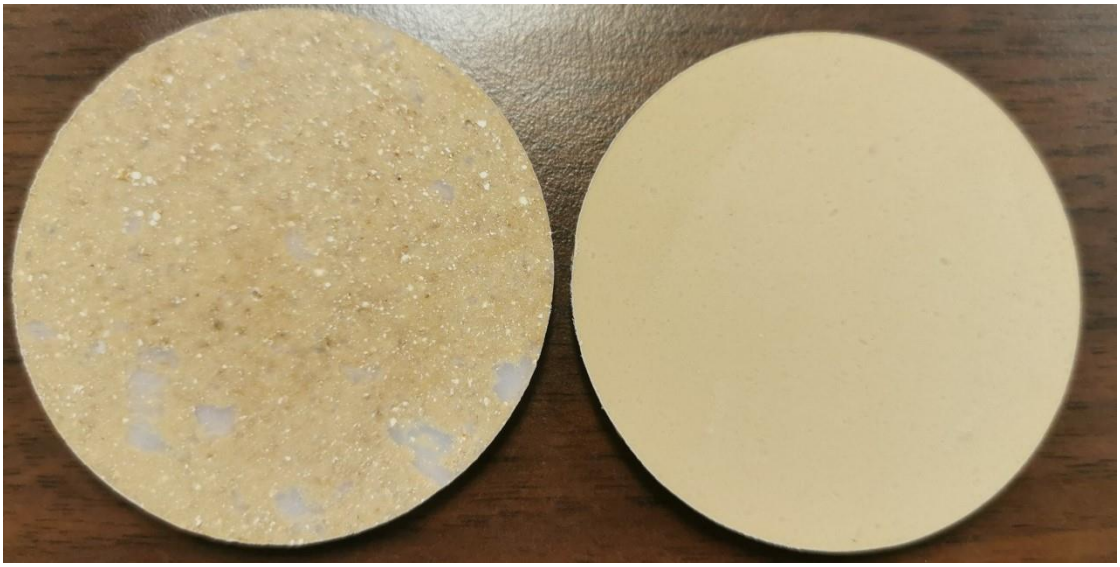

Figure III.5: PEEK/Silica (non-modified) filled PTFE samples. On the left non-sieved silica, on the right sieved silica.

3.2.2 Sieving effect on microstructure and mechanical proprieties

According to DSC analysis, sieved samples have a slightly higher crystalline content, while almost no effect was noticed on the linear response and DMA testing.

It is clear that sieving the silica before mixing influences the visual homogeneity of the material, but did not directly prevent the breaking of the sample in the dynamic mechanical testing. Therefore, in the following chapters for PEEK – PTFE – Silica samples, a sieving of the Silica was applied before the mixing.

				Rectangular torsion oscillation				DMA							
Sample	**PEEK content (vol%)**	**Silica 1 content (vol%)**	**Xc (%)**	**Tβ**	**Tanδ (β)**	**Tα**	**Tanδ (α)**	**E' (-50°C)**	**E'(30°C)**	**E'(150°C)**	**Tanδ (β)**	**Tβ**	**Tα**	**Tanδ (α)**	**T(B)**
I	21	15	32	22	0.135	112	0.080	$1.75\ 10^9$	$1.07\ 10^9$	$1.28\ 10^8$	0.113	34	117	0.187	170
II	21	21	31	20	0.119	112	0.071	$1.87\ 10^9$	$1.22\ 10^9$	$2.80\ 10^8$	0.094	31	127	0.144	180
I - S	21	15	38	22	0.132	113	0.087	$1.84\ 10^9$	$1.18\ 10^9$	$1.7\ 10^8$	0.105	32	119	0.173	220
II - S	21	21	40	22	0.138	112	0.085	$1.96\ 10^9$	$1.32\ 10^9$	$2.47\ 10^8$	0.096	33	123	0.154	170

Table III.3: DSC, linear DMA testing and non-linear DMA results of sieved and non-sieved silica filled samples. The results focus on the crystalline content, the transition temperatures their damping factors and the storage modulus E'. A part from a higher crystalline content noticed for sieved samples, sieving has very minor effects on the linear and non-linear mechanical properties.

3.3 Blending

Mixing of the fillers with the PTFE is a challenge as they are both powders. In the following sections, the chosen methods to properly disperse the filler in the PTFE powder will be described.

3.3.1 Internal mixer

A first attempt to mix the PTFE with the fillers was in an internal mixer with roller rotors (Figure III.6). Several tests were led varying the mixing parameters such as temperature, mixing time, mixing speed; but all the attempts failed in having a proper blend. The problem mainly came from the PTFE. As mentioned in the chapter II, literature review, PTFE has a fragile structure[5,10,15]. While mixing, even when maintaining low temperature of the internal mixer, with the lowest possible rotation speed, and a minimum loading of the mixer, it was not possible to avoid the heating up of the PTFE powder (up to 30 - 35ºC). This temperature is not recommended for PTFE low flow powder handling and mixing which directly impacted the quality of the blend and the samples[5,12,115]. When looking at the microstructure behavior, around this temperature occurs the β transition that determines a new crystalline conformation of the chains. When handling the PTFE at this temperature the probability of modifying the particle structure is high.

In addition, the thin gap zone in the mixer chamber brought a high shearing and stretching on the powder which has generated fibrillation on the particles. This fibrillation pre-sintering prevents the proper cohesion of the powder in the temperature cycle[5,59,85,145]. Figure III.10, shows a blend resulting from an internal mixer, Figure III.11 is a blend from pale mixing (see 3.3.2), and Figure III.12 shows a sample made of a blend from Figure III.10.

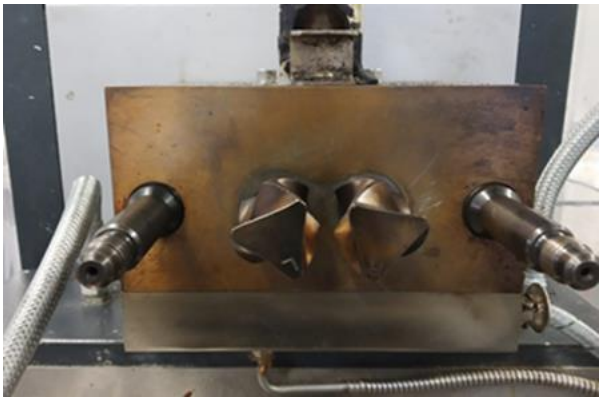

Figure III.6: internal mixer equipped with roller rotors.

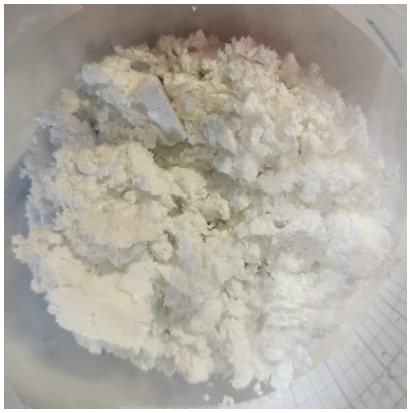

Figure III.7: PTFE/Silica produced with an internal mixer equipped with the roller rotors

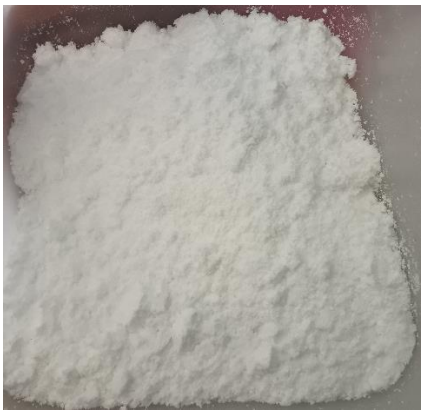

Figure III.8: PTFE/Silica produced with pale mixing

Figure III.9 : sample produced with PTFE mixed in the internal mixer equipped with the roller rotors.

Kitamura et al.[146], illustrated the effect of the heating and the shear on the morphology of PTFE particles. In some processes, such as paste extrusion of the PTFE, heating and shearing are necessary but controlled in order to create PTFE films that present a certain porosity rate. Figure III.10 illustrates the fibrillation phenomenon described by Kitamura et al[146]. This is a non-reversable phenomenon. Even if PTFE powder/particle are melted again, the fibrillated particle will not retrieve its original shape because of its high viscosity, which prevents complete chain relaxation.

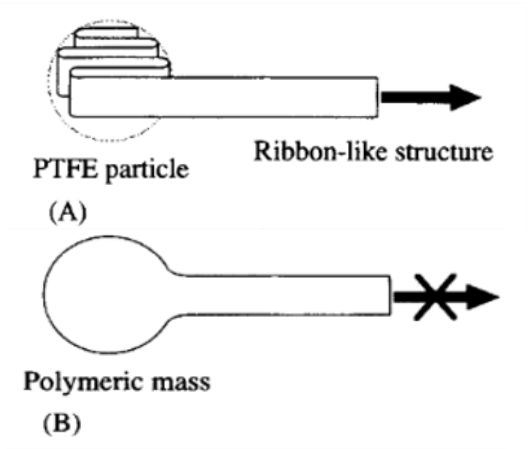

Figure III.10 : Deformation of the Ribbon-like structure of the PTFE due to heating and stretching[146]. (A) before deformation. (B) after deformation.

Ariwan et al[59] also discussed the morphology of PTFE particle subjected to heating and stretching. Figure III.11 illustrates the particle fibrillation due to heating and stretching of the PTFE.

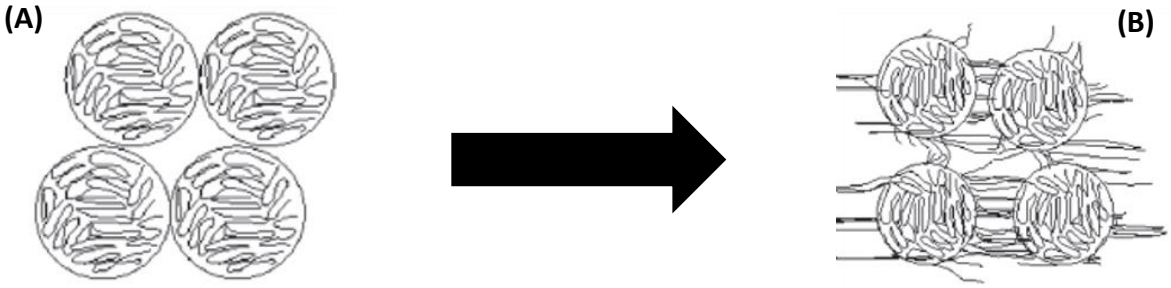

Figure III.11: Particle fibrillation before (A) and after (B) stretching and heating. The fibrils present in (B) create porosity after melting and avoid the complete fusion of the particles.

In our case, this fibrillation should be avoided before melting in order to prevent the porosity and voids in the produced samples.

3.3.2 Pale and turbula mixing

Powder blends were finally mixed with a pale attached to a motor with a high speed (1500 rpm). The powder container (50g capacity) was placed in a bowl of ice in order to keep the mixing at low temperature (<28°C).

At first PTFE was added into the container and mixed alone so that the agglomerates would break. Afterwards, the filler or PEEK were added progressively while mixing. The time between

each filler addition was respected (2 minutes) in order to have a repeated homogeneity. Finally, the blend was emptied in a sealed container before the last mixing step.

Figure III.12: Pale to be attached to a motor for high-speed mixing of PTFE, fillers and PEEK.

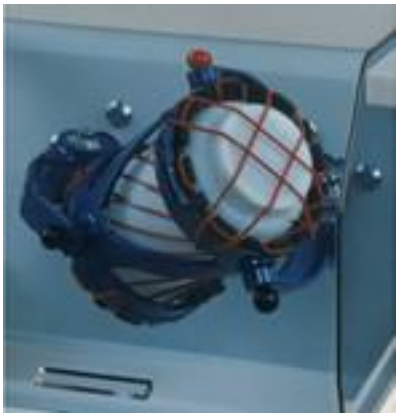

Figure III.13: Turbula mixer chamber. Used to homogenize the mix after the high-speed mixing without shearing.

After pale mixing, the sealed container was placed between rubber elastics in a turbula mixer and shaked for 10 minutes. This step is usually applied by industries to make sure of the homogeneity of the powder mix. Finally, the mix was stored in a dry space with a temperature between 21 and 25°C.

Note that for security reasons and the proper handling of Nano-silica particles, pale mixing was not possible. Therefore, nano-silica (Silica 3) was added to the PTFE under a fume cupboard in a sealed cup then mixed with the turbula mixer.

3.4 Molding parameters

3.4.1 Compression

Compression is the first step of the transformation process. Controlling this step is very important for the final material properties. The main parameter to focus on is the pressure applied to the powder. Indeed, the applied pressure gives the powder the strength needed for the handling step; in addition, it defines the final shape of the product. Furthermore, the pressure applied contributes in filling the voids in the powder. Depending on the PTFE grade, type and granule size, literature and processing guidelines recommend a corresponding applied pressure on the material. The optimum pressure applied insures the void closure and most of the final properties (Dielectric ones especially). Ebnesajad[5] recommended in his book a maximum pressure of 50 Mpa for unfilled PTFE and 100 Mpa for filled PTFE. This study also exposed testing results from Dupont

Co which show the best dielectric and mechanical properties (for unfilled PTFE) between 30 and 40 Mpa and best mold shrinkage result (void closure) for pressures around 40 and 45 Mpa. Beyond these pressures, a serious loss in the performances was noticed.

In our case, the pre-sintered samples were discs of 2 mm thick and 25 mm of diameter or discs of 4 mm thick and 60 mm of diameter. Samples of virgin PTFE and PTFE blended with PEEK were pressed at 40 Mpa, while filled PTFE with carbon black and silica were pressed at 60 Mpa with a dwell time of 5 minutes. This 60 MPa pressure was chosen according the supplier recommendations for the material, literature[5] and visual evaluation of the material. Indeed 40 Mpa was not enough to bring together the PTFE granule of the filled PTFE blends, especially for a filling higher than 10 vol%. The preform was easily cracked and for higher filling rates, the preform was thicker than it should be because of unfilled voids.

The dwell time is the necessary time in order to obtain an even compaction in the preform and avoid an "hourglass" shape. According to Ebnesajjad[5], the rule of thumb is 2 - 5 min of dwell per 10 mm of final height for billets inferior to 100 mm in diameter, explaining the choice of 5 min per sample. No matter the pressure and dwell time applied, it is recommended to compress at a temperature between 21-28°C[5].

3.4.2 Temperature cycle

a) Introduction

The final and most important step in the process is the temperature sintering cycle. The temperature profile influences all of the final properties, from the crystalline content to the mechanical properties, density, void content etc… It is therefore necessary to have a well-controlled profile in order to have the desired properties. Maximum temperature, cooling rate and residence time at maximum temperature are the key parameters that define the microstructure and crystalline properties. At first, based on the literature[5,29,53,147] and some laboratory tests, for virgin PTFE samples and filled PTFE samples we chose (the cycle 1 Figure III.14) a maximum temperature of 380°C, a cooling rate at 0.8°C/min ± 0.2 and a plateau of two hours at 300°C that allows a homogeneity in the sample while controlling the crystallization. The heating temperature up to 325ºC was at 0.8°C/min ± 0.2 with a plateau at 325ºC for 2 hours in order to have a homogeneous temperature in the sample and a heating rate of 0.2ºC/min between 325ºC and 380ºC.

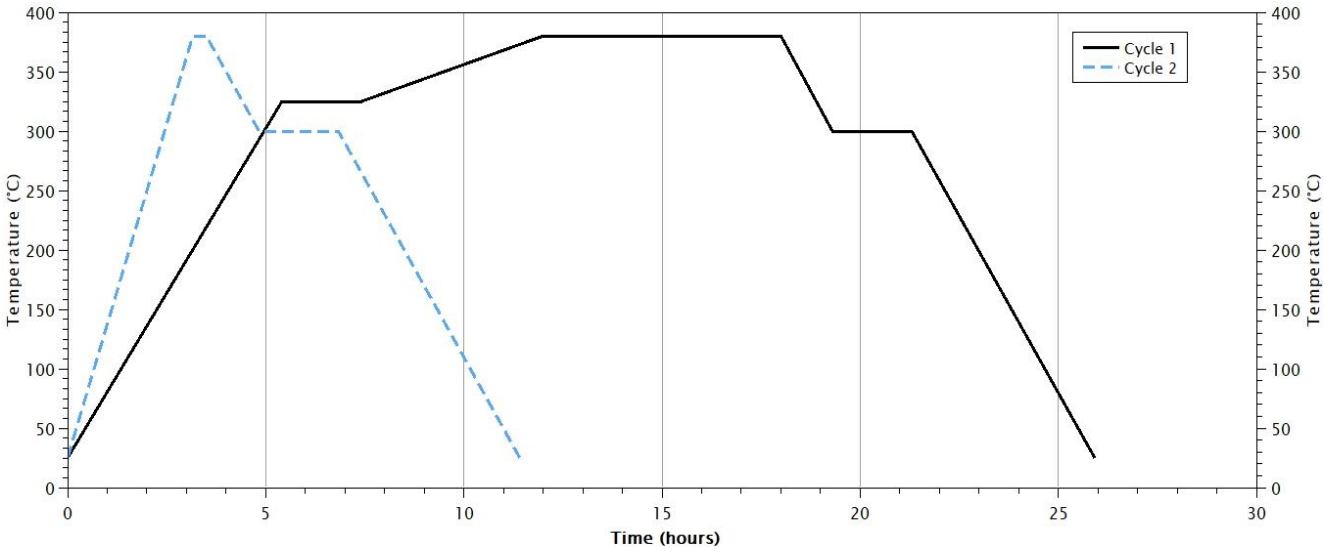

Figure III.14: Cycle 1 (black curve) and Cycle 2 (blue-dashed curve) of the sintering process. Cycle 1 is applied for neat PTFE and filled PTFE while cycle 2 is applied when PEEK is added to the mixtures PEEK could not handle the six-hours stay at maximum temperature and degraded in the process.

The process for PTFE filled with PEEK/silica blends (cycle2 Figure III.14) was different from the one used forthe composites PTFE + filler. It was complicated to apply the same temperature cycle due to degradation of the PEEK (Figure III.15) through the temperature cycle 1. Therefore, the time at the maximum temperature was reduced from 6 hours to 20 min and the heating rate increased from 1ºC/min to 2ºC/min without any plateau. However, the cooling rate and the plateau at 300°C were maintained so that the cooling conditions would remain the same as the blends without PEEK.

Figure III.15: PEEK-PTFE sample made with Cycle 1. The black-brown color indicated the degradation occurred in the process.

b) Microstructure influence

For comparison, virgin PTFE and some silica filled PTFE were also tested in the cycle 2 to study potential differences arising from the two temperature cycles.

The influence of cycles 1 and 2 on the microstructure were studied via DSC measurement and linear response in torsion on rectangular samples. A summary of the results is shown in the Table III.4 below:

Sample	Polymer	Filler	Filler content (vol%)	Cycle	Xc (%)	Tβ (°C)	S1	Tanδ (β)	Tα (°C)	S2	Tanδ (α)
A_1	PTFE	-	-	1	34	20	1.9	0.184	112	2.0	0.104
A_2	PTFE	-	-	2	39	22	1.9	0.193	113	2.3	0.110
B_1	PTFE	Silica 1	8	1	35	22	1.4	0.198	112	1.4	0.097
B_2	PTFE	Silica 1	8	2	41	23	2.0	0.184	113	1.9	0.108
C_1	PTFE	Silica 1	16	1	45	25	1.8	0.179	112	1.2	0.085
C_2	PTFE	Silica 1	16	2	41	23	0.9	0.187	111	1.6	0.110
D_1	PTFE	Silica 1	24	1	55	25	1.4	0.170	112	0.8	0.074
D_2	PTFE	Silica 1	24	2	48	23	1.3	0.186	113	1.1	0.096

Table III.4 DSC and linear viscoelasticity results on samples made with cycle 1 and cycle 2 sintering cycles. Cycle 2 shows an increase in the S2 indicator.

The difference between those two cycles is the holding time at the maximum temperature (380°C). Both cycles have the same cooling rate and plateau. The influence of the silica content on the microstructure of PTFE will be discussed in the following chapter.

An interesting difference between the two cycles is the increase in the S2 factor when using the cycle 2. The S2 indicator reflects the intensity of the drop in the storage modulus G' on the α transition (details of this indicator will be exposed in the following chapters). The smaller the number the less the influence of the α transition on the storage modulus.

This difference is illustrated in the graph of the Figure III.16, S2 indicator is always higher when processing by the cycle 2.

The main influence of reducing the dwell time at maximum temperature is giving less time for the polymer to relax from internal stresses generated from the melting. This influence is noticed after the α transition (after the amorphous phases get transformed to a rubbery phase). Therefore, when producing samples with the cycle 2, PTFE has less time to relax and cools while having internal stresses. These stresses appeal at the α transition where the mobile amorphous phase passes from the glassy to its rubbery state. At this point the chains relaxes completely and a sharp drop occurs on the storage modulus.

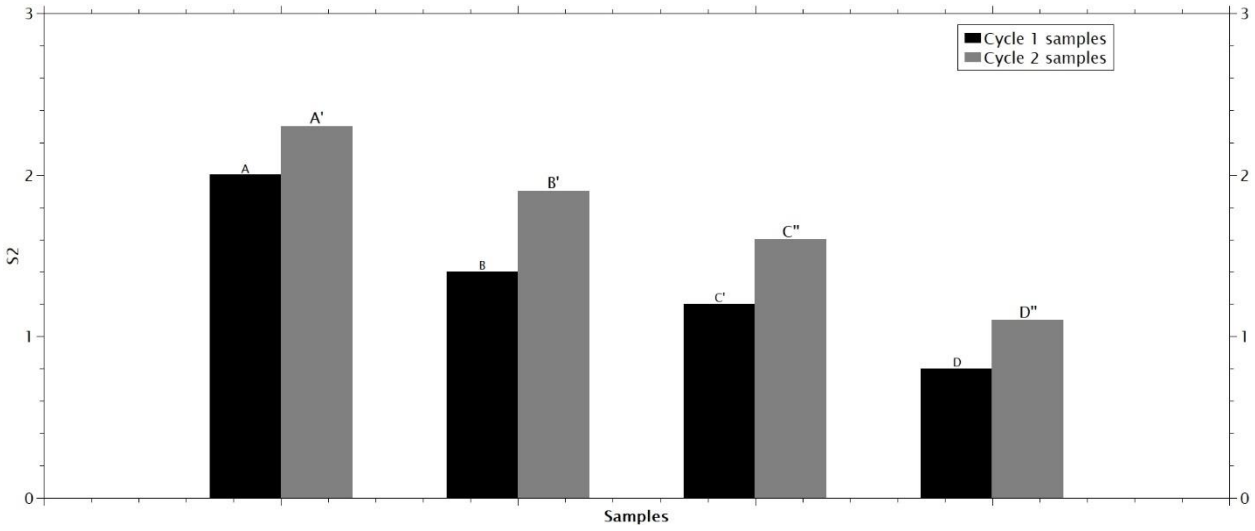

Figure III.16: Comparison of the damping factor tan δ at the α transition of samples made with cycle 1 and cycle 2 temperature cycles

c) Influence on mechanical properties

The influence of cycle 1 and 2 on non-linear traction compression oscillations tests are shown in the table below (Table III.5):

Sample	Filler	Filler content (vol%)	E'(-50°C)	E'(30°C)	E'(150ºC)	Tβ (°C)	Tanδ (β)	Tα (°C)	Tanδ (α)	T(B) (°C)
A_1	-	-	$1.29\ 10^9$	$6.72\ 10^8$	$3.91\ 10^7$	34	0.16	99	0.29	-
A_2	-	-	$1.40\ 10^9$	$6.12\ 10^8$	$3.69\ 10^7$	29	0.16	93	0.31	-
B_1	Silica 1	8	$1.74\ 10^9$	$1.11\ 10^9$	$8.63\ 10^7$	40	0.15	114	0.23	-
B_2	Silica 1	8	$1.89\ 10^9$	$1.18\ 10^9$	$1.08\ 10^8$	34	0.13	116	0.21	-
D_1	Silica 1	24	$2.58\ 10^9$	$1.69\ 10^9$	-	39	0.14	126	0.18	140
D_2	Silica 1	24	$1.58\ 10^9$	$8.59\ 10^8$	$6.17\ 10^7$	32	0.14	107	0.26	165

Table III.5: non-linear DMA results of samples produced with cycle 1 and cycle 2 sintering cycles. β transition temperature decreased when applying the cycle 2.

In the case of the non-linear DMA tests minor effects were observed on the storage modulus, and on the damping factors. The main effect can be seen for the β transition temperature where the transition occurs at lower temperatures for samples made with temperature cycle 2.

4 Conclusion

In this chapter the process steps to produce filled PTFE samples were described. Several parameters were tested at each step of the process and the influence on the crystallinity and the mechanical properties. Some modification did not affect the final properties such as the

modification of the silica surface. Others like the temperature cycle showed and influence on the mechanical properties.

An adaption of the mixing phase had to be done in order to avoid the fibrillation of the PTFE particles and to have proper samples. Instead of mixing with an internal mixer, the mixing had to be done with a pale followed by turbula mixing.

Likewise, the sintering temperature cycle had to be adapted so the degradation of the PEEK polymer can be avoided.

In the following chapter several fillers with different nature, type and size will be used to prepare the composites. The influence of these fillers on the crystalline and mechanical structure will be analyzed in order to find the best formula that enhances the dynamic mechanical properties.

Résumé chapitre III

Le chapitre suivant discute le choix des matériaux et les moyens de transformations. Le PTFE est un polymère haute performance avec des propriétés chimique et thermique remarquables. Cependant il présente une viscosité assez élevée (10^{10} – 10^{12} Pa) ce qui empêche les utilisateurs de le transformer avec les procédés de plasturgie classique tels l'injection ou l'extrusion.

Pour cette étude, quatre charges différentes ont été choisies : 3 silices de tailles différentes (0.2µm, 4µm et 200-300µm) et un noir de carbone d'un diamètre moyen de 25µm. Le PTFE choisi est un PTFEE modifié avec une quantité de PPVE inférieure à 1% afin que le PTFE soit soudable, il présente une taille de particule d'environ 25µm. Finalement, le PEEK a une taille de 50µm et une viscosité autour de 350 Pa.s.

Le procédé de transformation passe par plusieurs étapes et afin de l'optimiser pour avoir les meilleures propriétés, différents tests ont été fait. A partir de ces tests, les paramètres ont été choisis de manière à obtenir les meilleures propriétés pour chaque formulation.

La première étape du procédé est celle du mélangeage, celle-ci a été faite avec une pale rotatif liée à un moteur ou les poudres de matériaux ont été disposées dans un conteneur adéquat afin d'homogénéiser le mélange sans fibriller les particules de PTFE.

La deuxième étape du procédé est la mise en forme, celle-ci consiste à mettre en forme l'échantillon dans un moule en acier, et le compresser à différentes pressions selon que le PTFE est mélangé avec du PEEK ou avec des charges.

Après l'étape de la compression vient le cycle de température, l'échantillon est libéré du moule et soumis à un cycle de température défini, celui-ci était différent pour les échantillons contenant du PEEK afin d'éviter la dégradation de l'échantillon.

Une fois le cycle de température terminé, les échantillons pouvaient être caractérisés. Différents types de tests ont été mis en place pour analyser les propriétés mécaniques, thermiques ainsi que la microstructure ou encore la dispersion des charges dans la matrice PTFE. Les tests de DSC ont été utilisés pour quantifier le taux de cristallinité, des observations microscopiques pour analyser la morphologie, des tests rhéologiques dans le domaine linéaire pour définir les propriétés viscoélastiques des échantillons et enfin des tests d'analyse dynamique en tension-compression hors du domaine linéaire afin d'évaluer les propriétés mécaniques du composite. Tous ces tests ont permis d'étudier l'influence de la quantité et la taille des charges sur les propriétés du PTFE.

IV. Influence of the filler content size and chemical nature on PTFE.

1 Introduction

In order to counterbalance the lack in the creep and wear behavior of PTFE, adding a filler can be one of the solutions. For this, many studies were conducted to study the tribological and wear behavior of PTFE filled with several types of fillers such as glass fiber, carbon fiber[148], bronze, graphite[5] etc. Yet, in the literature studies of the influence of the fillers on the microstructure and its influence on the mechanical behavior are rare[58,143]. Due to the complicated and exceptional crystallization phenomenon of the PTFE, studies on mechanical behavior or microstructure are mainly based on virgin PTFE and its transition temperatures[11,15,21].

In this chapter, filler's chemical nature and size were studied. In order to study the influence of the nature two types of filler were tested: carbon black and silica. The effect of size was observed with silica fillers of three different sizes: Silica 1 is of 4 µm, silica 2 of 200 µm and silica 3 is a nano-silica and has a size of 200 nm (Silica 3 was on only applied to compare the effect of the size of the filler). In addition, in all cases the filler content was considered. The goal is to understand the influence of the filler on the crystalline structure (content, lamellae size), on the morphology of the composite, on the viscoelastic behavior of the material (storage modulus, damping factor…) and the mechanical response in traction-compression oscillations.

2 Filled polymer

The filler content influence was studied through four filler types: Silica 1, Silica 2, Silica 3 and carbon black. Each filler was mixed with the PTFE at different volume rate. As mentioned in the literature review previously, in order to be efficient, a filling must be at least at a 5 vol% and a maximum of 40 vol%[5]. Samples were prepared according to the process described in the chapter material and methods by following the temperature cycle 1.

Filler volume content is calculated according to the formula (IV.1) below:

$$\%V = \frac{w_f(\%)}{w_f(\%) + \frac{\rho_f}{\rho_m}\left(1 - w_f(\%)\right)} \qquad (\text{IV.1})$$

Where w_f, ρ_m and ρ_f, are respectively filler mass content, PTFE density and filler density.

A list of all the samples prepared is presented in the Table IV.1:

Polymer	Filler	Filler content (vol%)	Xc (%)
PTFE	-	0	34
PTFE	Silica 1	8	36
PTFE	Silica 1	16	45
PTFE	Silica 1	23	55
PTFE	Silica 1	40	68
PTFE	Silica 2	9	45
PTFE	Silica 2	13	42
PTFE	Silica 2	19	41
PTFE	Silica 2	22	44
PTFE	Silica 2	30	45
PTFE	Carbon black	10	40
PTFE	Carbon black	14	39
PTFE	Carbon black	27	38
PTFE	Silica 3	6 ± 2	37
PTFE	Silica 3	14 ± 5	34
PTFE	Silica 3	24 ± 7	40

Table IV.1: List of the blends with PTFE and filler and their crystalline content.

Silica 3 is a nano-sized silica and its density is hard to determine because of its fractal structure (high dispersibility silica). In addition, in our case, the mixing phase happens before the melting temperature and the melting occurs in a static phase. Therefore, it is hard to predict how the silica 3 will be structured (i.e., as agglomerates, or as particles) in the PTFE matrix. Thus, in our study the density value of the Silica 3 was estimated with an error on the value represented in Table IV.1.

Note: Considering that all the samples include PTFE, unfilled samples will be designated as PTFE_T1 or PTFE_T2 (T1 and T2 correspond to cycle Temperature 1 (T1) and cycle temperature 2 (T2). For filled samples a designation of 8%_Si1_T1 indicates a sample of PTFE filled with 8 vol% of silica 1 and made with temperature cycle 1.

3 Influence of the filler content

3.1 Microstructure characterization

The influence of the filler content was studied through the evolution of the microstructure while increasing the filler content. The microstructure was analyzed through the determination of the crystalline content by DSC measurements and the sample viscoelastic behavior via linear DMA characterizations.

The first step of analyzing the microstructure of the composite was to observe the morphology and the adhesion between the filler and the matrix using a scanning electron microscope.

Samples were cryo-fractured after soaking for a minute in liquid nitrogen, and then observed with a mini-SEM with different magnifications. Each filler had its own effect on the morphology depending on the content and size of the filler. Virgin PTFE was also observed in order to compare the crystalline orientation and the morphology aspect evolution. SEM micrographs are presented in Figure IV.1 through Figure IV.3 below

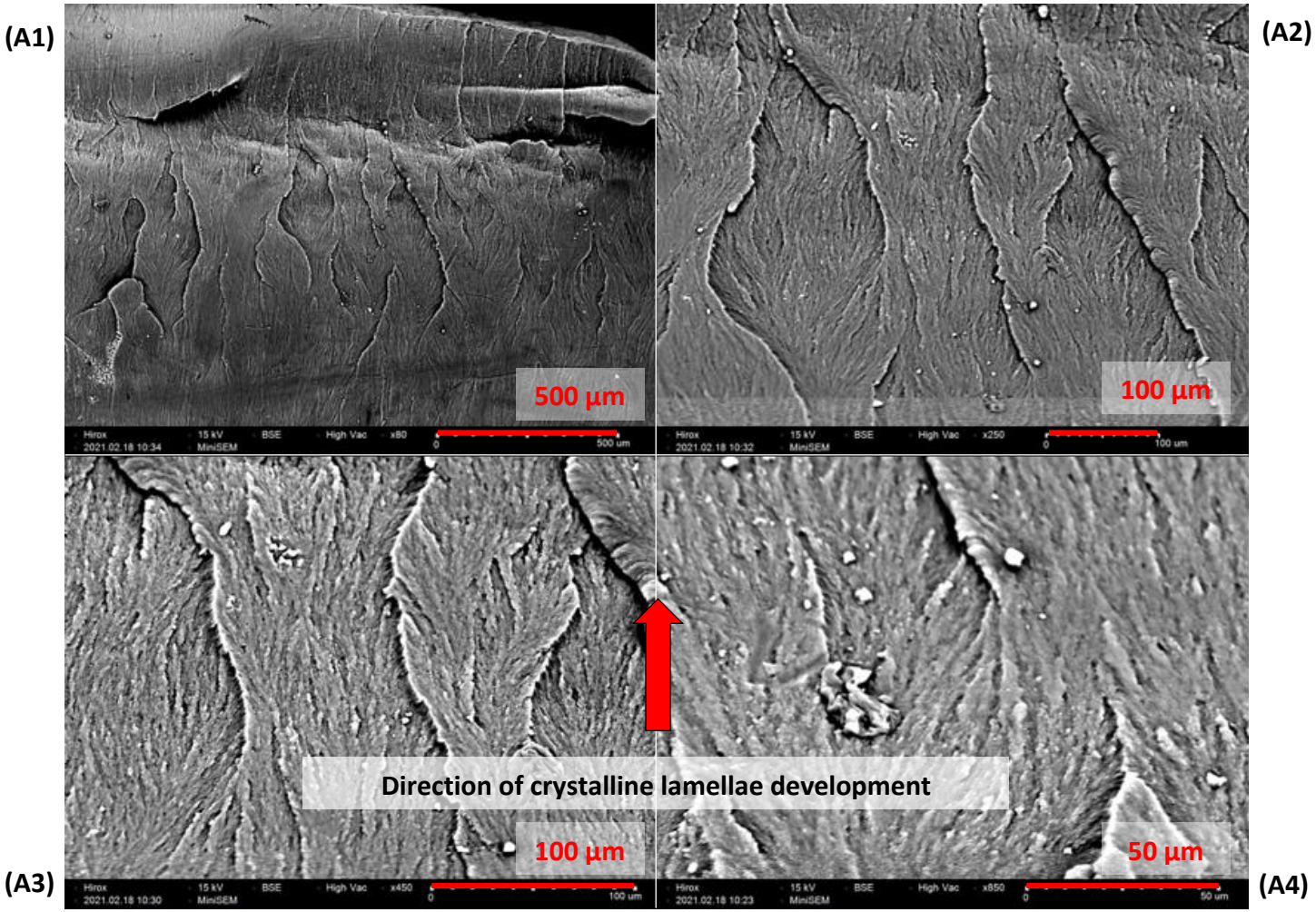

Figure IV.1: Virgin PTFE morphology and crystalline orientation at different magnitudes. (A1) x80 (A2) x250 (A3) x450 (A4) x850.The crystalline structure is vertically oriented (red arrow). Crystalline lamellae have the same orientation of the pressing direction

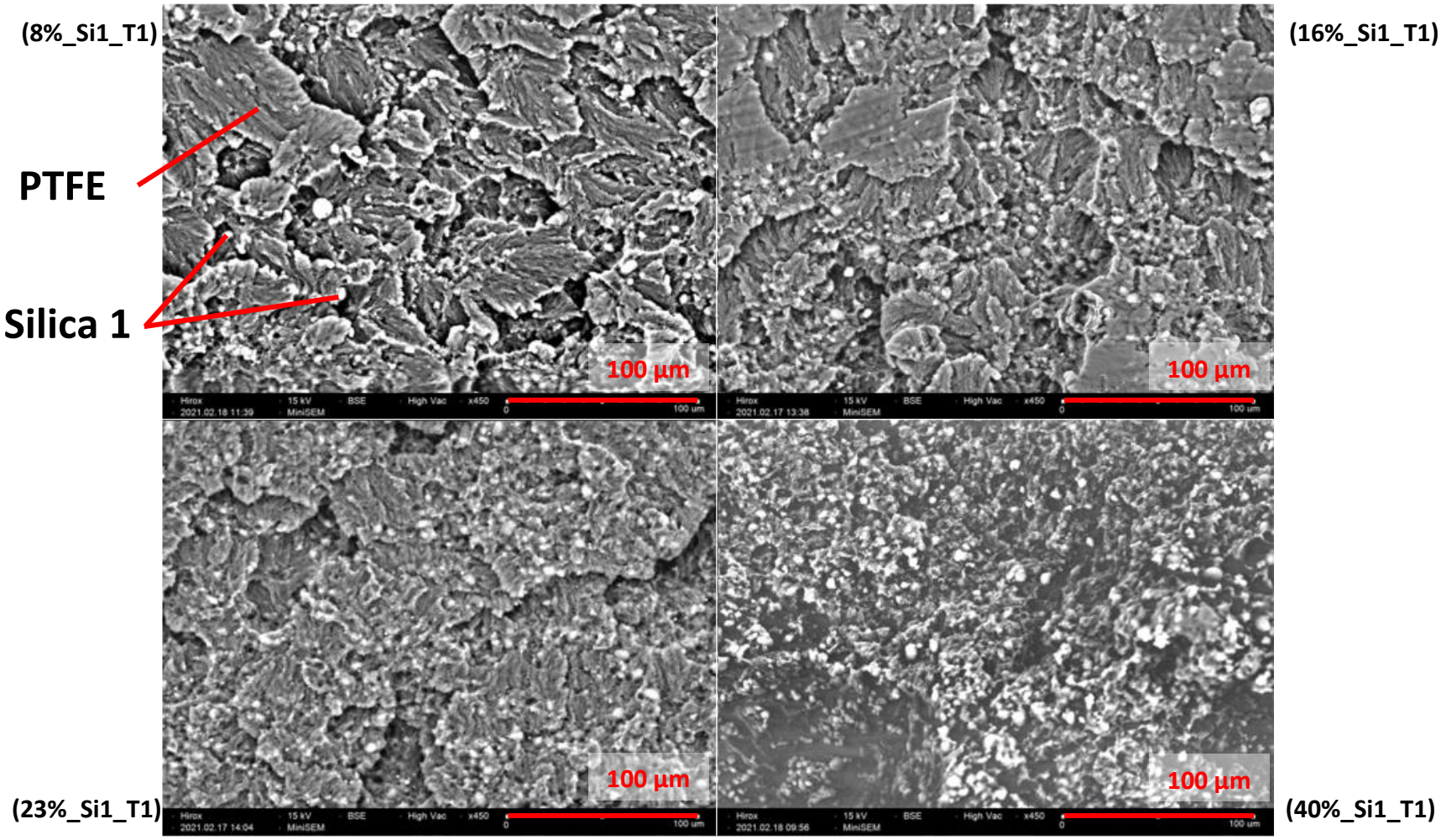

Figure IV.2: Samples filled with Silica 1 at different filling content 8, 16, 23 and 40 vol%.

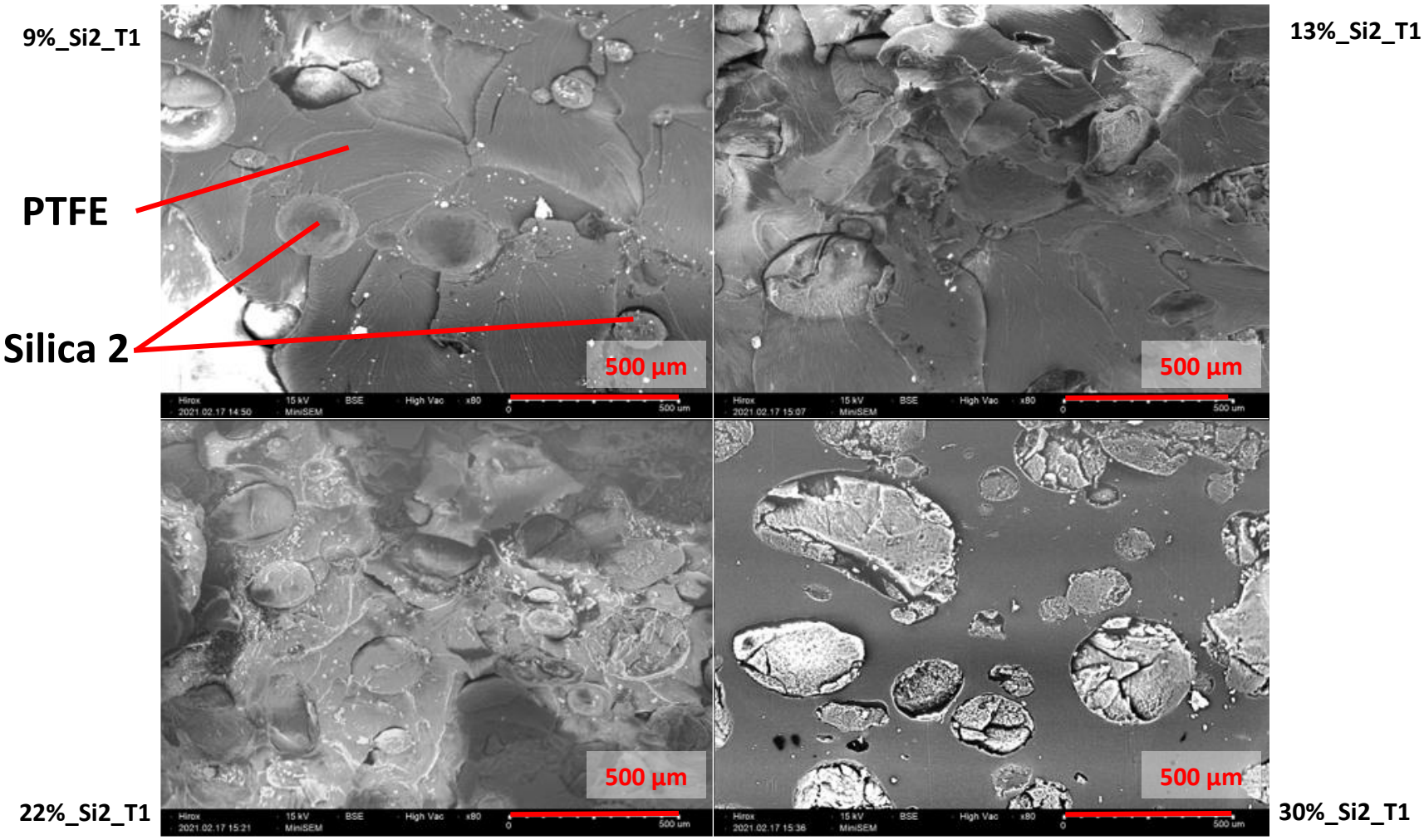

Figure IV.3: Samples filled with Silica 2 at different filling content 9, 13, 22 and 30 vol%.

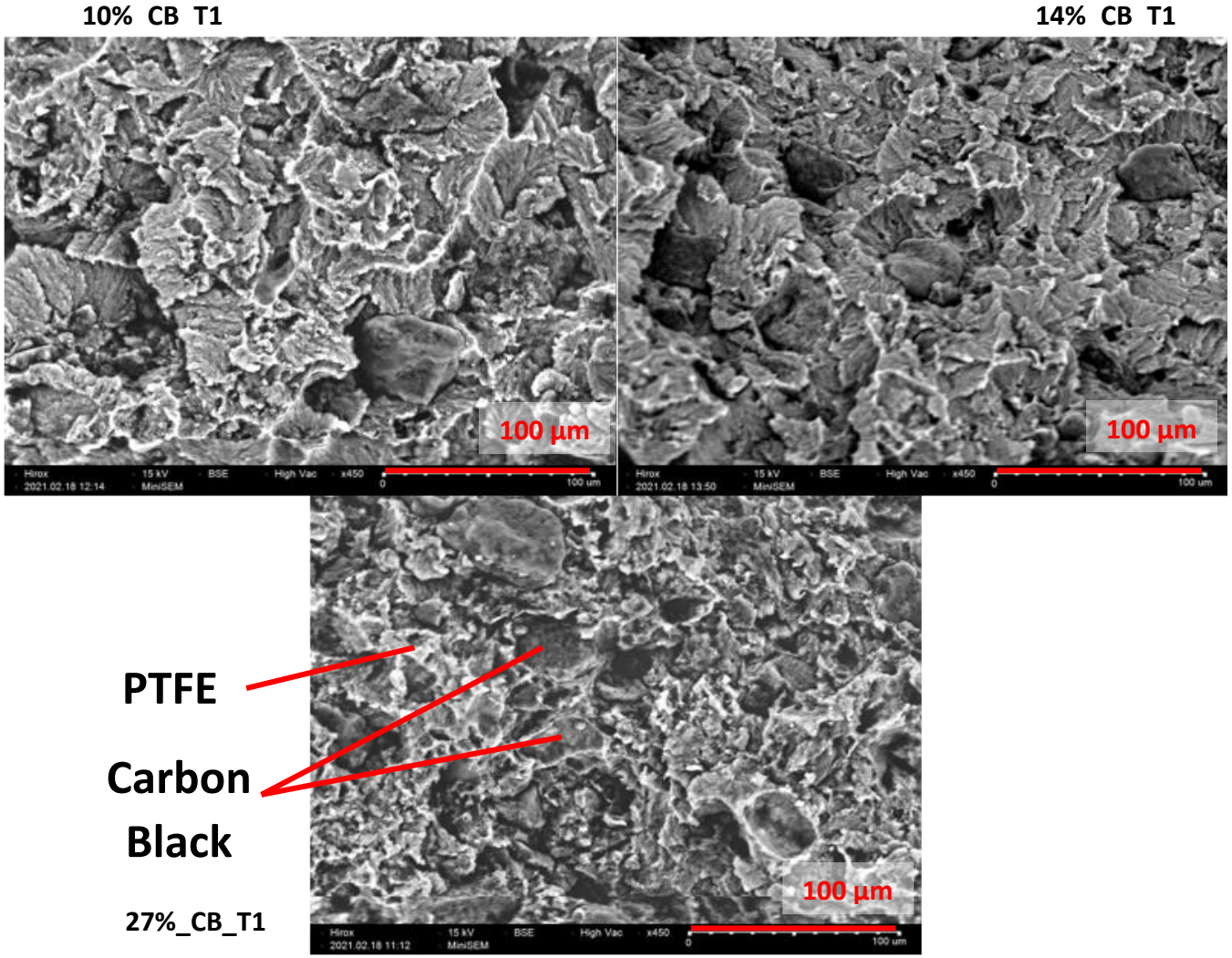

Figure IV.4: Samples filled with carbon black at different filling content 10, 14 and 27 vol%.

Figure IV.2, Figure IV.3 and illustrate the influence of the filler on the morphology of the PTFE. Because Silica 2 has a larger diameter than silica 1 and carbon black, photos were taken at smaller magnitude.

The observations taken from those figures are that the adhesion between all the fillers and the PTFE matrix is almost inexistent as a void around the fillers can be seen. However, the figures also show that all the fillers are well distributed in the matrix.

Silica 2 did not affect the crystalline morphology of the virgin PTFE compared at the same magnification, but the size and nature of the silica created visible porosity between the silica particles and the PTFE. Knowing that this silica is based on fragile agglomerates of small silica aggregates it was evident that in the shaping step, some of the particles broke thus creating inhomogeneity in the samples.

As said previously, carbon black as all fillers is well distributed in the matrix. The higher the filler content the better the distribution in the matrix; however, it is more likely to find agglomerates (poorly dispersed fillers) in the sample. It is complicated to judge the porosity level in the samples via microscopic observations. For this reason, density measurements of these samples are necessary to estimate the void content.

For silica 1, the higher the filler content the higher the chance to find agglomerated particles, as can be observed for carbon black as well. A kind of embedment of the silica1 in the PTFE matrix was also noticed at higher magnification, as shown in the Figure IV.5 below:

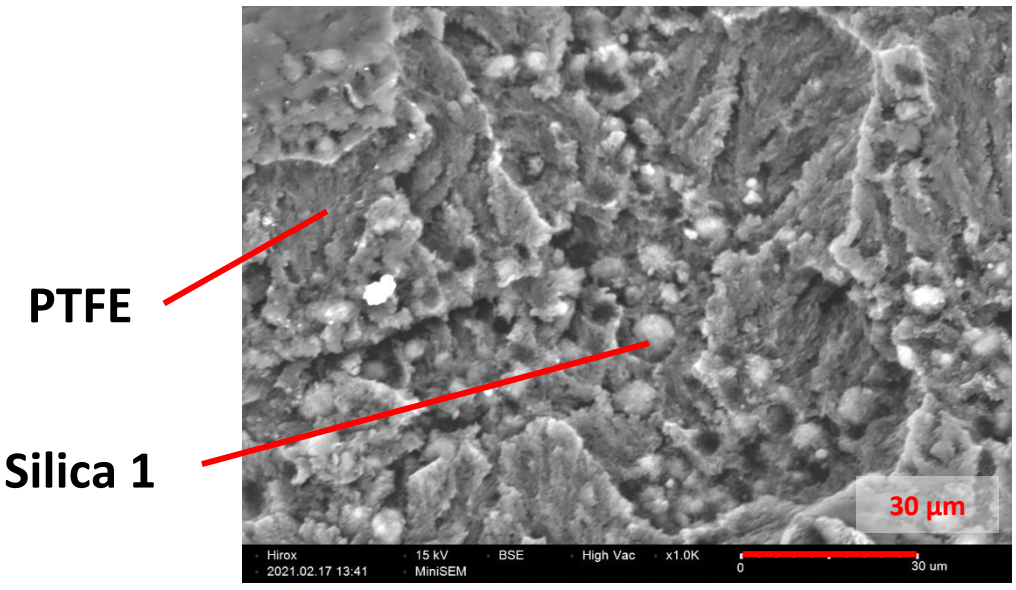

Figure IV.5: Sample 16%_Si1_T1 at 1.0K magnitude. Silica 1 ingrained in the PTFE matrix

At a same magnification compared with the virgin PTFE sample, the same lamellae crystalline structure is observed, however, a different orientation is noticed. For the virgin PTFE (Figure IV.1), crystal lamellae were formed in the pressing direction, while for the silica 1 and carbon black filled samples (Figure IV.2, Figure IV.3) the crystals were initiated from the filler towards any direction. Figure IV.6 illustrates schematically the influence of silica 1 and carbon black on the formation of the crystalline lamellae (the illustration does not respect the real scale)

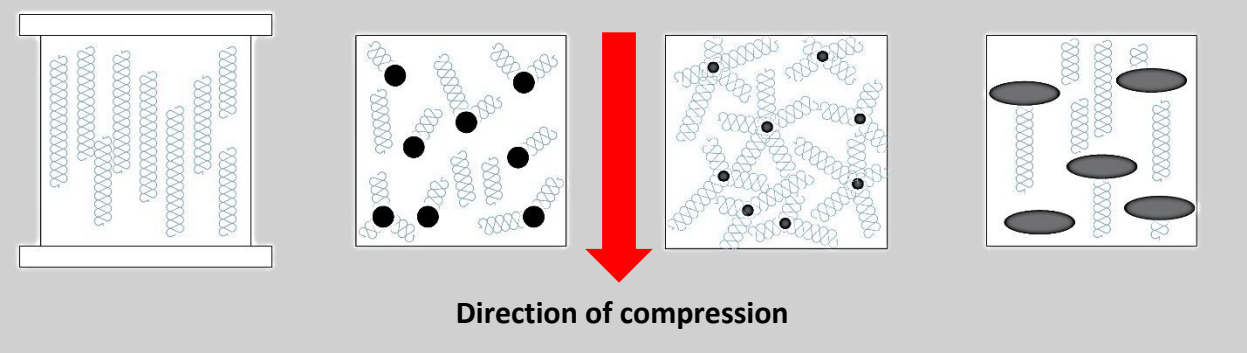

Figure IV.6: schematic illustration of the crystalline lamellae (in blue) formation for neat PTFE (a), carbon black filled (b), silica 1 filled (c) and Silica 2 filled (d) PTFE. Virgin PTFE and silica 2 PTFE crystalline lamellae formed in the pressing direction, while Silica 1 and carbon black filled PTFE changed the crystalline lamellae formation direction.

It is certain from the literature that the adhesion between PTFE and non-modified fillers is not existent due to the chemical structure of the PTFE[5,143,149] yet Carbon black and silica 1 modified the crystalline structure of the PTFE.

DSC tests gave an indication on the crystalline content in the sample by measuring the mass melt enthalpy. Results obtained for each sample are given in Table IV.1

It is remarkable that adding any type of filler to the PTFE matrix influences directly the crystalline content by increasing it from 34% for virgin PTFE to 68% for PTFE filled at 40 vol% of silica 1, 45% for PTFE filled at 19 vol% of Silica 2 and 38% for PTFE filled at 27 vol% of Carbon black. Graph IV.1 shows the evolution of the crystalline content of PTFE for each filler content of each filler type.

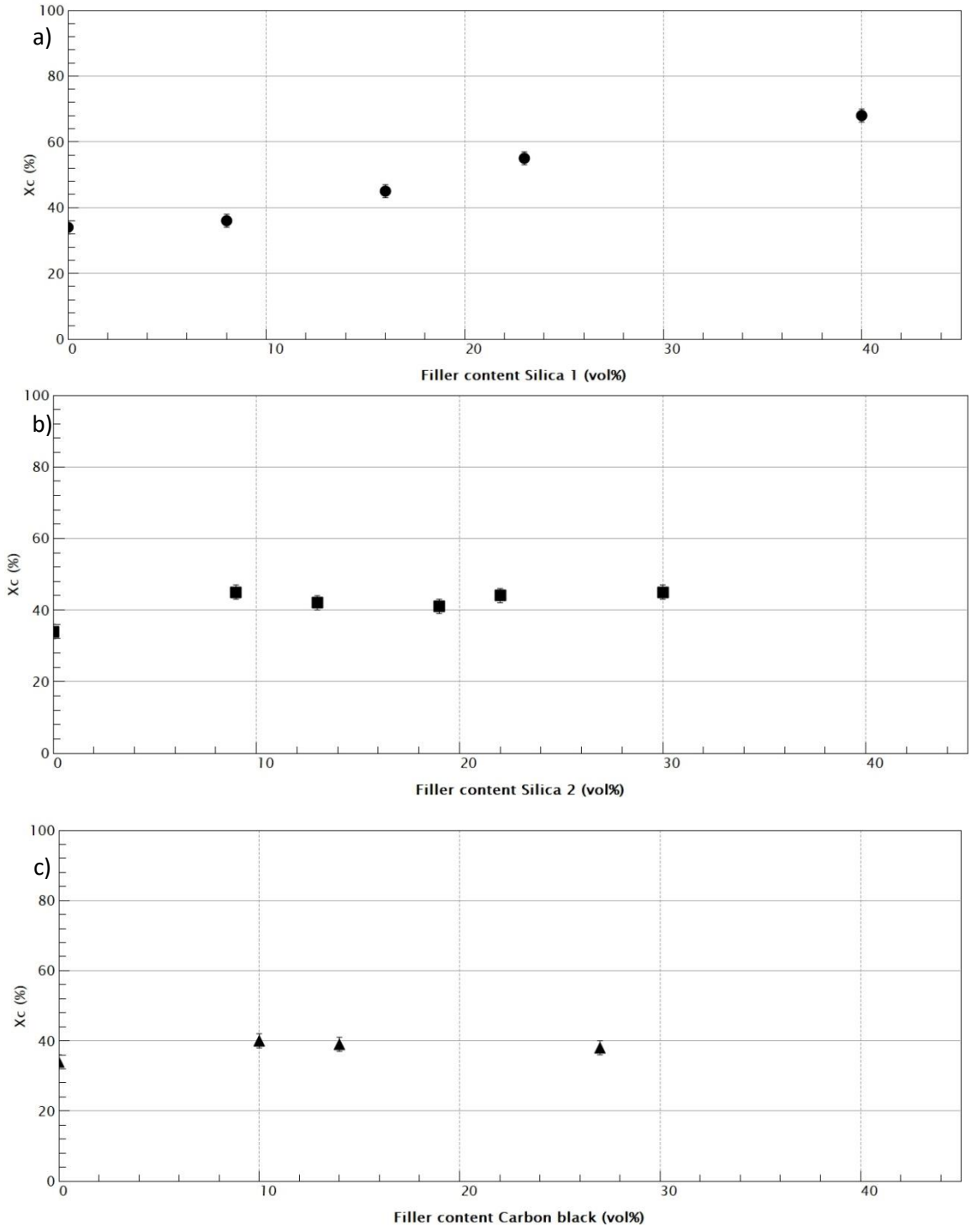

Graph IV.1: Crystalline content according to filler type and content. (a): Silica 1 (4µm) (b): Silica 2 (250µm) (c): Carbon black(25µm). Silica 1 showed a constant increase in the crystalline content when increasing the Silica 1 content

Even though the crystalline rate increases when adding a filler to the PTFE matrix, Carbon black and Silica 2 reached a constant level of crystallinity when increasing their content in the blend. Meanwhile, when increasing the content of Silica 1 the crystalline content increased constantly in the PTFE matrix.

In addition to the crystalline content measurement, density of samples was determined by means of liquid immersion in order to determine the void content in the samples after process (see materials and methods part III.2.1.3).

Density and void content results are summarized in Table IV.2 :

Polymer	Filler	Filler content (vol%)	Measured Density	Theoretical density	Void content
PTFE	-	0	2.11	2.13	1%
PTFE	Silica 1	8	2.09	2.09	0%
PTFE	Silica 1	16	2.08	2.07	0%
PTFE	Silica 1	24	2.05	2.05	0%
PTFE	Silica 1	40	1.88	1.95	3%
PTFE	Silica 2	9	2.08	2.11	2%
PTFE	Silica 2	13	2.00	2.10	4%
PTFE	Silica 2	22	1.91	2.06	7%
PTFE	Silica 2	30	1.85	2.01	8%
PTFE	Carbon black	10	2.14	2.14	0%
PTFE	Carbon black	14	2.10	2.12	1%
PTFE	Carbon black	27	2.08	2.12	2%

Table IV.2: Density results and void content in virgin PTFE and filled PTFE with silica 1 silica 2 and carbon black. PTFE/Silica 2 composite has the higher void content among the samples.

Void content is the difference between the theoretical and measured density. As observed in the Table IV.2 above, Silica 1 and Carbon black have minor effect on the void content, while silica 2 with a filling content above 13 volume percent has a void content around 7-8%, which is considerably high compared to the rest of the samples and may have an influence on the mechanical properties. Besides the poor adhesion between the filler and PTFE, compacted pure silica phase and the specific surface of the Silica 2 may be a reason for the increase in the void content.

Knowing that the microstructure of the PTFE not only depends on the crystalline content but also on its conformation and amorphous phases, the study was also carried out by evaluating the linear response of rectangular specimens in torsion oscillations. As mentioned in the literature study, McCrum et al[71,76] evaluated the crystalline amorphous transitions by the means of this test. In addition, Calleja et al[21] also qualified the temperature transitions and PTFE phases by a

linear DMA rheology testing. This test helps recognize the influence of the filler on the different amorphous and crystalline phases mentioned in the chapter I. An example of the result of the rectangular torsion test is given in the Graph IV.2:

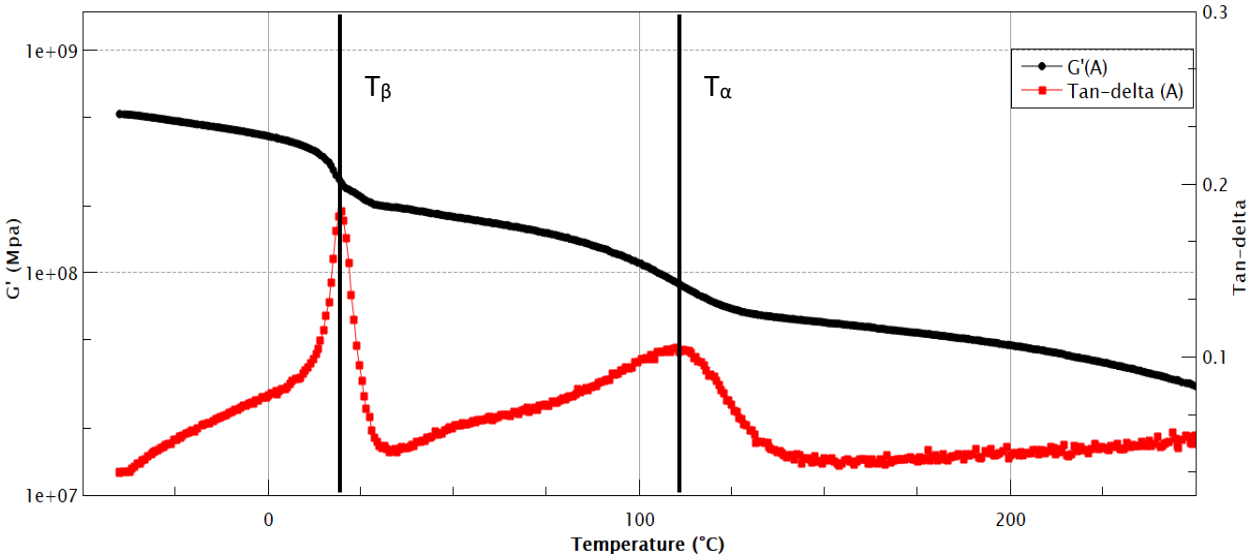

Graph IV.2: An example of the linear DMA results for a neat PTFE sample. The test allows a visualization of the α and β transition through the damping factor (peaks) and the drops in the storage modulus G'.

A drop in the storage modulus or a peak in the damping factors marks the phase transitions. In this test and in the case of the PTFE, two transitions are identified: one around 20°C, namely the β transition, indicating the crystalline conformation change, the second one around 110°C marking the disappearance of the rigid amorphous phase, also known as the α transition. The temperature of those transitions and the intensity[71,143,150] of the damping factor peak are indicators of the influence of the filler on the PTFE microstructure. Two additional indicators were used to identify this influence: S1 and S2 inspired by Mccrum's[71,150] work and defined by:

S1: The strength of the relaxation at Tβ.

S2: The strength of the relaxation at Tα.

$$S_1 = \frac{G'(-40ºC) - G'(50ºC)}{G'(-40ºC)} \qquad (IV.2)$$

$$S_2 = \frac{G'(50ºC) - G'(150ºC)}{G'(150ºC)} \qquad (IV.3)$$

These indicators translate the strength of the drop around the β and α transitions. In other words, the intensity of the ratio of decrease in the storage modulus.

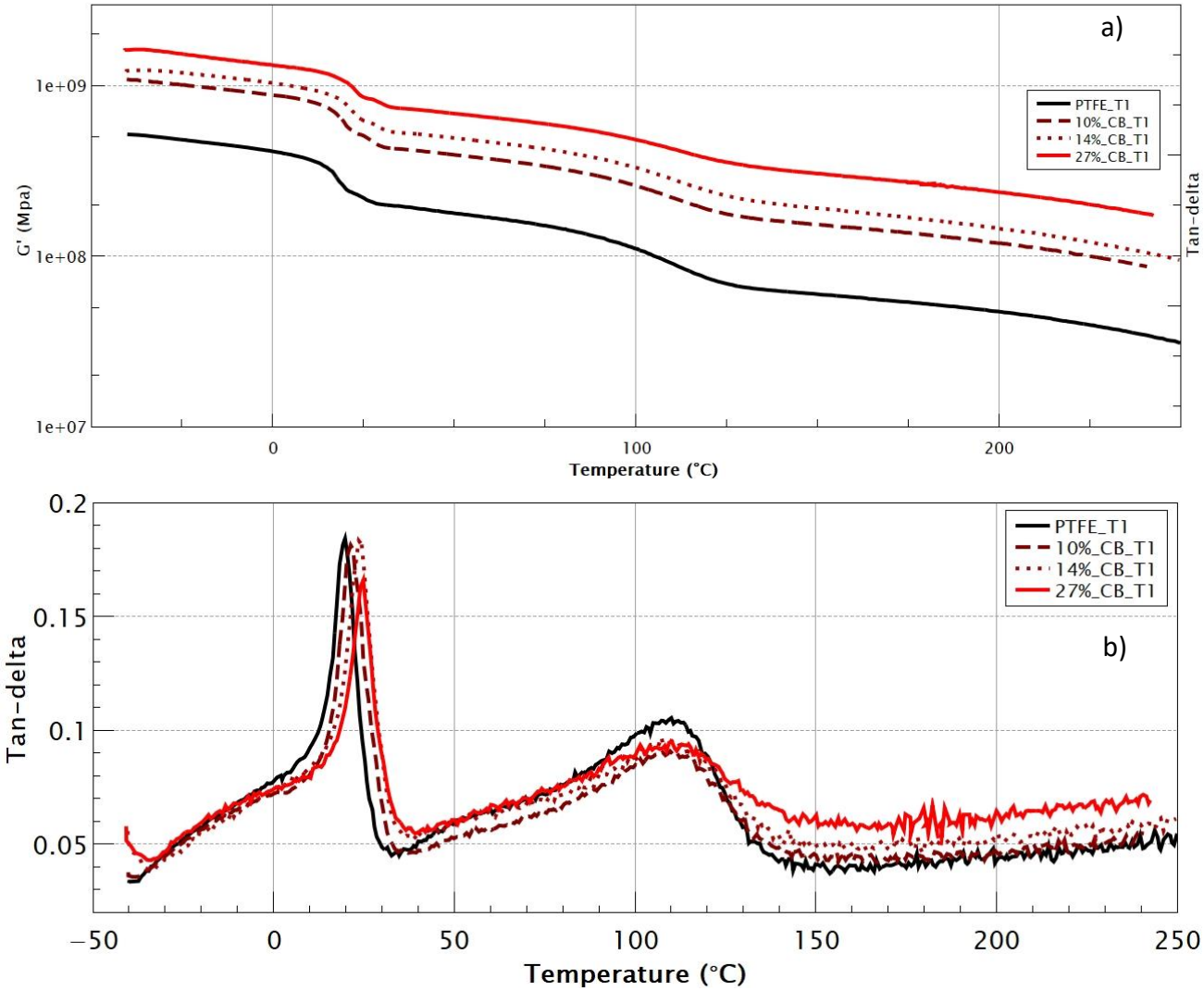

Graph IV.3: Storage modulus (a) and Tan-delta (b) curves of Carbon black filled PTFE at different content.

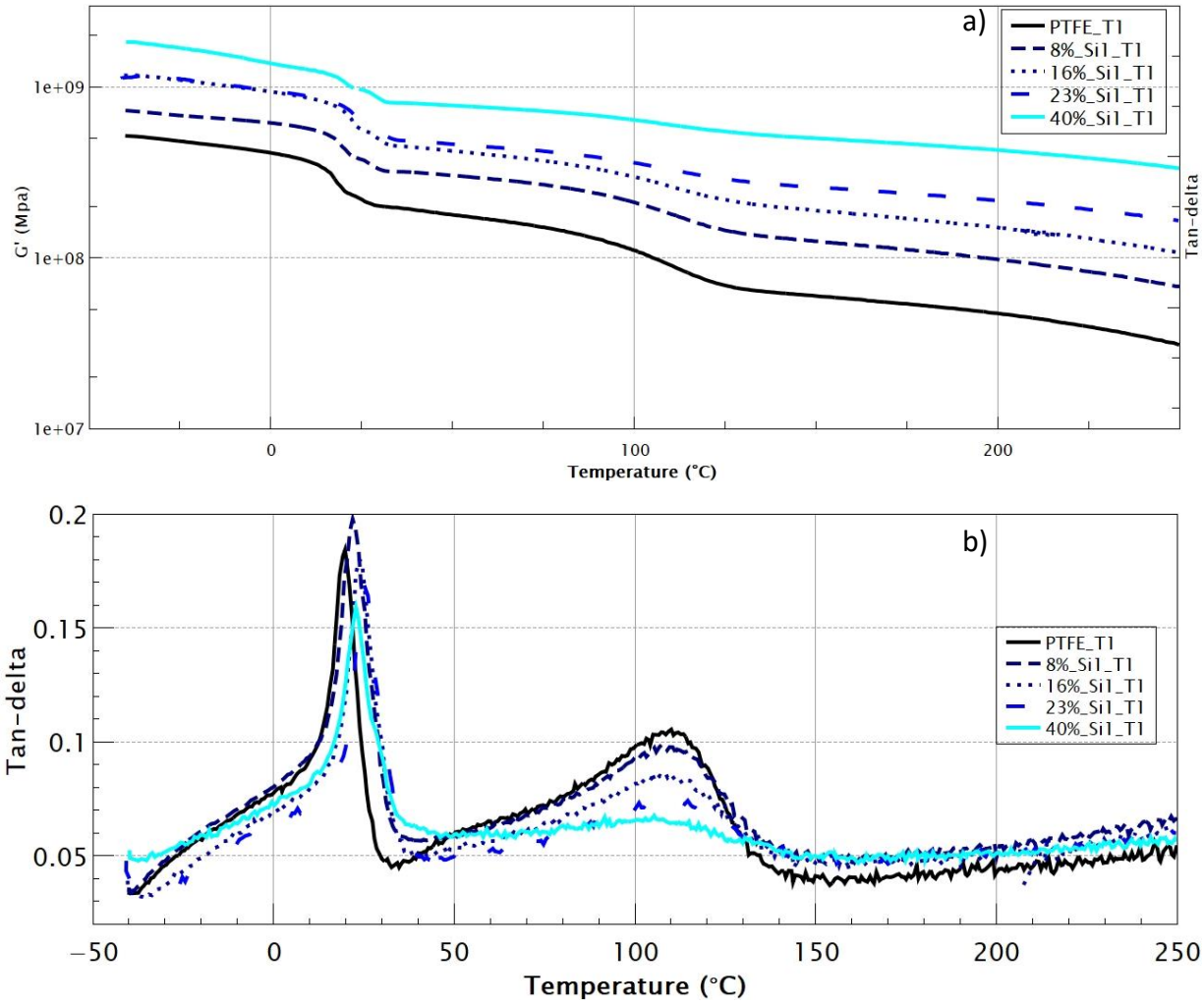

Graph IV.4: Storage modulus (a) and Tan-delta (b) curves of Silica 1 filled PTFE at different content. The graph reflects the reinforcement of the silica 1 at different temperatures.

Graph IV.3 and Graph IV.4 represent the storage modulus G' and tan-delta value for carbon black and Silica 1 filled samples respectively. Both samples show and increase in the storage modulus when increasing the filling content. This increase is mainly controlled by the crystalline content and the filler contribution. Depending on the temperature each filler influenced differently the storage modulus. In other words, each filler reinforced in a different way the properties of the PTFE; perhaps the reinforcement was not only hydrodynamical but accompanied a structure modification. This difference is expressed with S1 and S2 indicators in Table IV.3 that summarizes the indicators for all the samples.

Polymer	Filler	Filler content (vol %)	Tβ	S1	Tanδ (β)	Tα	S2	Tanδ (α)
PTFE	-	0	20	1.9	0.184	112	2.0	0.104
PTFE	Silica 1	8	22	1.4	0.198	112	1.4	0.097
PTFE	Silica 1	16	24	1.8	0.179	112	1.2	0.085
PTFE	Silica 1	23	25	1.4	0.170	112	0.8	0.074
PTFE	Silica 1	40	23	1.2	0.159	112	0.4	0.065
PTFE	Silica 2	9	22	1.9	0.202	112	1.7	0.099
PTFE	Silica 2	13	21	1.6	0.181	113	1.5	0.094
PTFE	Silica 2	19	24	1.7	0.164	112	1.5	0.091
PTFE	Silica 2	22	23	1.6	0.178	112	1.6	0.094
PTFE	Silica 2	30	23	1.7	0.194	111	1.4	0.096
PTFE	Carbon black	10	21	1.8	0.181	111	1.6	0.091
PTFE	Carbon black	14	24	1.5	0.182	112	1.6	0.093
PTFE	Carbon black	27	25	1.4	0.166	112	1.2	0.094

Table IV.3: Linear DMA tests results showing the influence of Silica 1, silica 2 and carbon black on PTFE. The test focused on the transition temperatures α and β in addition to the damping factors and the indicators S1 and S2.

Knowing that the alpha transition occurs in the amorphous phase, it is normal and already proven that it is inversely proportional to the crystalline rate[10,71,76,151] and the relaxation strength. At first sight, this is clearly the case of the Silica 1 where the crystalline content increases with the filler content, therefore the tan δ (at Tα) decreases and the strength of the relaxation S2 decreases. It is not that obvious for the carbon black and the Silica 2 where the crystalline content is almost constant with increasing the filler content and therefore the variation in the tan δ (α) and S2 are minimal.

The temperature at the α transition is not modified or only slightly by the filler content, while this is not the case for the temperature at the β transition. All three fillers show an increase in the temperature of the β transition when increasing the filler content. The β transition is considered as a first order transition, identified as an order-disorder transition by the authors[28]. Therefore, an increase in this temperature reflects a perturbation of the filler on the PTFE segments leading to a higher transition temperature.

It is now clear from DSC and rheological measurements that adding a filler to the PTFE matrix has a direct influence on the crystalline microstructure. This tendency may have many reasons: Bosq[143] showed a difference in the crystalline microstructure when adding nano-silica to PTFE matrix and hypothesized that the addition of the silica leads to a nucleation effect.

The size of the lamellae (l) is another important parameter to study when trying to understand microstructure modification. According to Ferry's work[19], it is possible to estimate the size of the lamellae by applying the Gibbs-Thomson theory.

$$T_m = T_m^{\infty}\left[1 - \frac{2\gamma}{\Delta H_m^{\infty} l}\right] \qquad (\text{IV.4})$$

Where T_m is the melt temperature, T_m^{∞} is the equilibrium melting temperature of an infinitely large and flat crystal, l the lamellae size and γ the crystal/liquid interfacial energy.

In order to eliminate the possible superheating phenomenon[19,152] on the melting temperature value (T_m), each sample has been tested at different heating rates (2, 5 and 10°C/min) and extrapolated the melting temperature values to zero heating rate. The work of Ferry et al[19]. showed that the equilibrium melting temperature (T_m^{∞}) of an infinitely large and flat crystal of virgin PTFE is 334°C. Graph IV.5 shows an example graph of the extrapolation to zero heating rate of the sample 16%_Si1_T1.

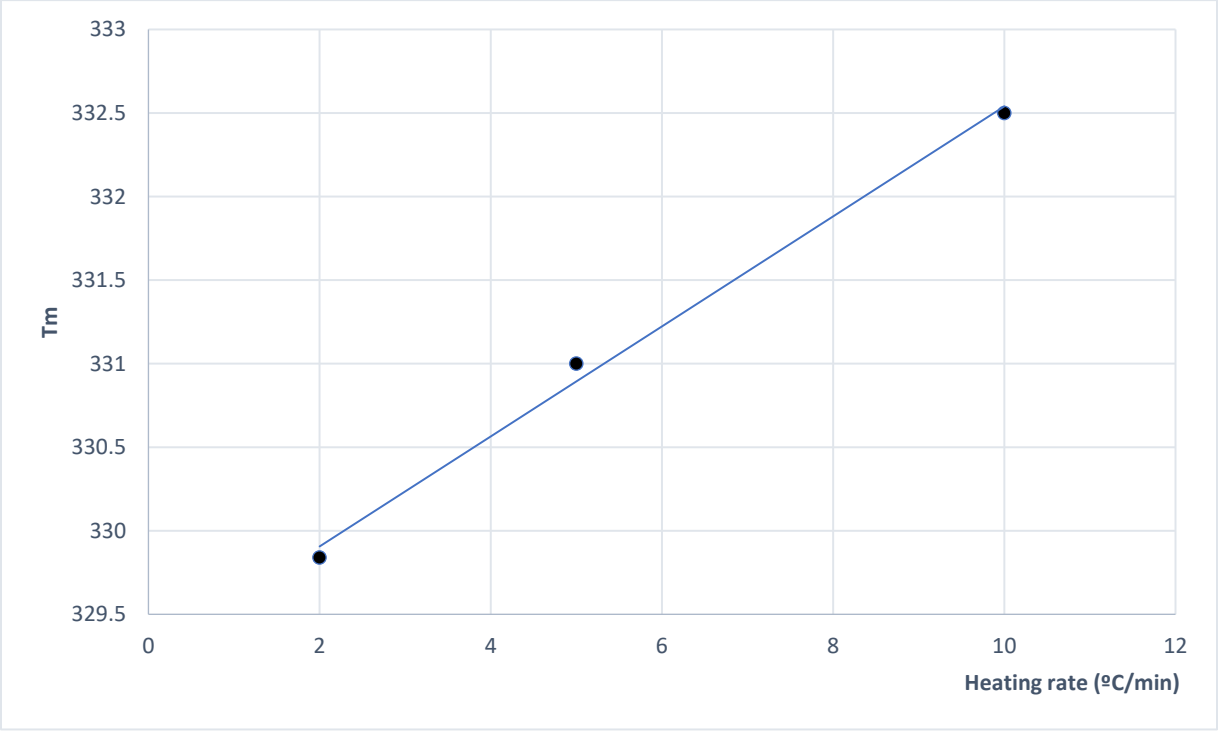

Graph IV.5: Melting temperature extrapolation method (Sample 16%_Si1_T1)

After fitting linearly, the curve and extrapolating to zero, we find a value of 329°C for Tm. This value applied to the equation (IV.4) gives a lamellae size l of 820 Å in accordance with values

reported in the literature (between 500-1500Å depending on the temperature cycle conditions[5,15,17,19]). Table IV.4 summarizes the values of the crystalline lamellae for each sample using their crystallinity rate and melt temperature extrapolation.

Filler	Filler content (vol%)	Crystalline content (%)	Tm	l
-	0	34	326	495
Silica 1	9	35	326	487
Silica 1	18	45	329	820
Silica 1	26	55	330	989
Silica 1	43	68	330.5	1113
Silica 2	9	45	327.5	599
Silica 2	13	42	327.5	599
Silica 2	22	44	328	649
Carbon black	10	40	327	557
Carbon black	14	39	327.5	599
Carbon black	27	38	328	649

Table IV.4: Lamellae size and melting temperature values of PTFE and PTFE filled with Silica 1, Silica 2 and carbon black at different volume rate.

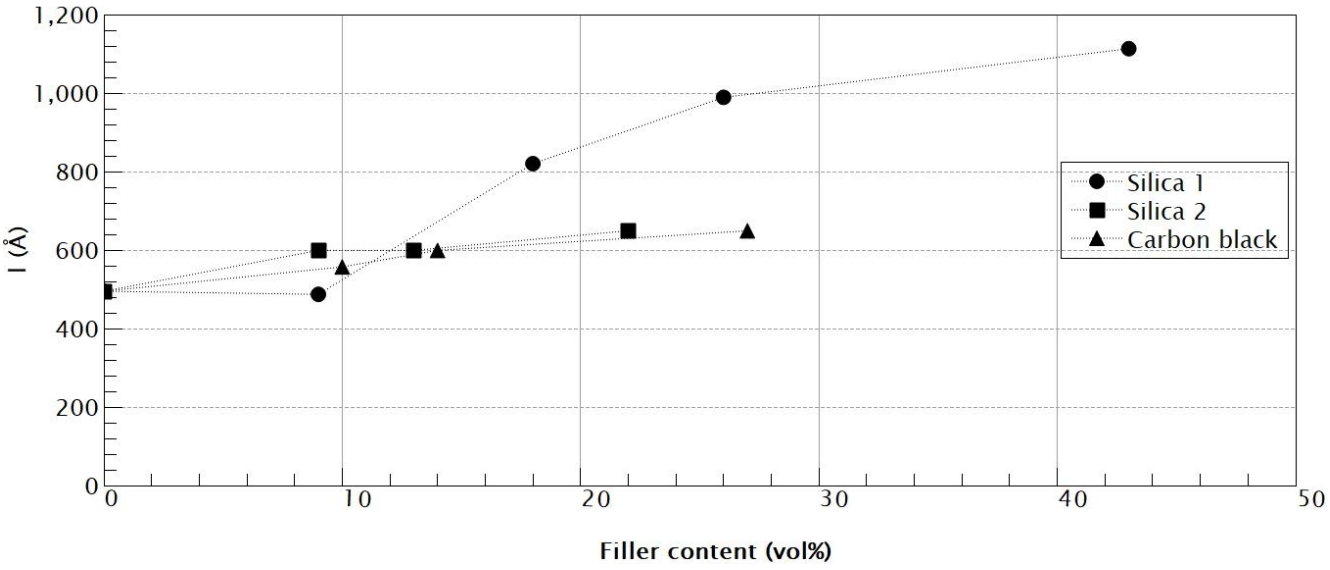

Graph IV.6: lamellae size values for neat PTFE and PTFE filled with silica 1 (•), Silica 2 (■) and carbon black (▲) at different volume rate. Lines are given to guide the eye.

A first observation of Table IV.4 is that for the silica 1 lamellae size and crystallinity both increase with the filler content. As for silica 2 and carbon black the lamellae size is stable whatever the filler content showing a similar behavior to that of the crystalline content.

To sum up, filling PTFE influences directly the microstructure of the PTFE, depending on the nature/size of the filler. Indeed, as it has been shown, crystallinity increases with the presence of a filler regardless of its nature. However, depending on the size of the filler results are different; silica 2 and carbon black show stable crystalline content and lamellae size for all filler contents. On the other hand, silica 1 displayed a constant increase of crystallinity rate and lamellae size with increasing volume fractions of filler.

3.2 Non-linear dynamic mechanical characterization

Non-linear dynamic mechanical analysis (non-linear DMA) testing evaluates the mechanical response of the material outside its linear domain. The samples undergo a temperature ramp from -60ºC to 250ºC under a traction compression oscillation of 0.5 Hz. Studies showed a particular behavior of PTFE in tension compression, especially at low temperatures and at room temperature[8,9]. In Rae et al's study[8,9], PTFE turned out to have a different poisson ratio when solicited in tension or compression. Further details can be found in II.1.4. Although these studies showed an interesting behavior of PTFE, very few experiments have been carried out with non-linear DMA.

The main indicators focused on, were the damping factor tan δ at the transitions α and β, as well as the transition temperatures and storage modulus at -50ºC, 30ºC and 150ºC. These values are summarized in the Table IV.5 below:

Filler	E' (-50°C)	E'(30°C)	E'(150°C)	Tβ(°C)	Tanδ (β)	Tα(°C)	Tanδ (α)	T(B) (°C)
-	1.29 10^9	6.72 10^8	3.91 10^7	33	0.16	99	0.29	-
Silica 1	1.74 10^9	1.11 10^9	8.63 10^7	40	0.15	114	0.23	-
Silica 1	2.32 10^9	1.49 10^9	1.42 10^8	39	0.14	119	0.21	168
Silica 1	2.58 10^9	1.69 10^9	-	39	0.14	126	0.18	140
Silica 1	2.24 10^9	-	-	-	-	-	-	47
Silica 2	1.25 10^9	7.24 10^8	3.37 10^7	35	0.17	97	0.29	-
Silica 2	1.18 10^9	6.97 10^8	3.11 10^7	35	0.15	99	0.28	-
Silica2	1.01 10^9	5.87E 10^8	-	36	0.16	-	-	62
Carbon black	1.57E+09	9.91E+08	6.11E+07	35	0.15	109	0.26	-
Carbon black	1.78E+09	1.16E+09	9.62E+07	37	0.15	114	0.23	-
Carbon black	2.45E+09	1.60E+09	2.49E+08	38	0.16	118	0.2	-

Table IV.5: Non-linear DMA results for neat PTFE and filled samples. The results present the transition temperatures α and β in addition to their damping factors, the storage modulus at different temperatures (-50°C, 30°C and 150°C) and the temperature of breaking if applicable.

Unfortunately, some samples did not resist this test and broke before the end of it (T (B) is the temperature at which the samples broke). Many reasons could be responsible for the samples

breaking, such as the nature of the filler (knowing that only Silica-filled samples broke), the inhomogeneity of the mixes or the lack of adhesion between the filler and the PTFE creating high porosity and weaknesses in the sample. However, this last hypothesis seems unlikely when considering the void content measurements (Table IV.2). Therefore, the breaking may be caused either by the strain amplification theory or by the chemical surface of the filler.

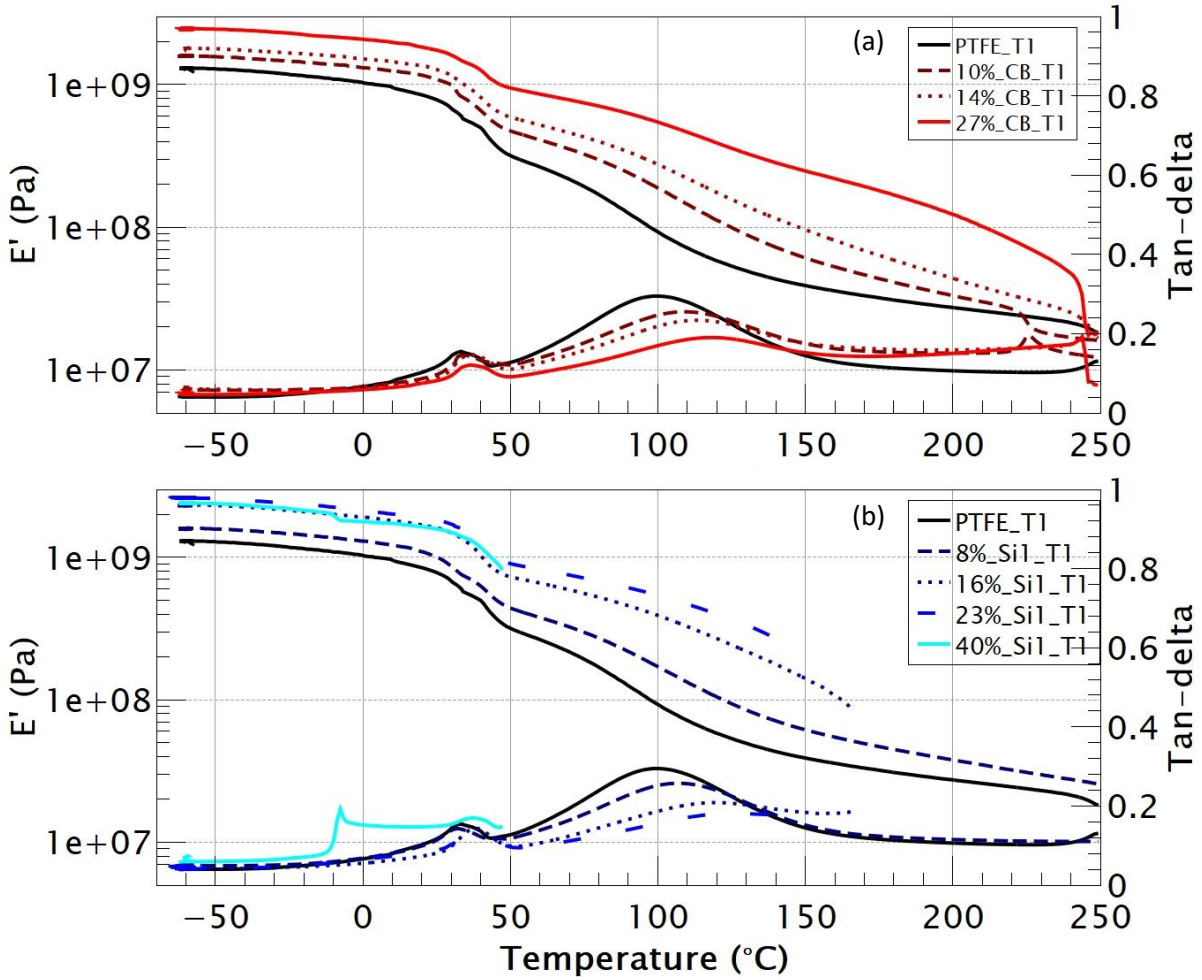

Graph IV.7: non-linear Dynamic mechanical analysis of carbon black (a) and silica 1 (b) filled PTFE at different contents.

Depending on the filler type and size, filler content affected differently the mechanical properties. When adding Silica 1, storage modulus and transition temperatures increased significantly and the damping factor at the transition temperature decreases. It is also remarkable that increasing the Silica 1 content contributed in breaking the sample at a lower temperature. Adding carbon black also increased the storage modulus and the transition temperatures but had minor influence on the damping factor at the transition temperatures and no breaking among

the samples can be observed. On the other hand, no significant changes were noticed in the mechanical properties of virgin PTFE when adding Silica 2, hence the results are not presented here.

3.3 Conclusion

To summarize this section, adding fillers to a PTFE matrix has a direct influence on its microstructure, crystalline shape, content, morphology and conformation transition temperature (Tβ). The fillers also affect the behavior of the sample in dynamic analysis. The addition of the filler increases the storage modulus and the rigid amorphous region transition temperature (Tα).

It is worth noting that each filler has a different impact on the PTFE. This difference may be a consequence of the size and/or the surface nature of the filler. This is why in the following two sections we will be discussing the influence of the size and the surface nature of the filler.

4 Influence of nature of the filler surface

4.1 Microstructure characterization

Another characteristic that may influence the microstructure of PTFE is the nature of the filler surface. Whether it is carbon-filled or silica-filled PTFE, the microstructure of PTFE and the blends might be impacted differently because of their chemical surface.

A comparison of silica 1, carbon black filled PTFE and the 25µm silica from Chen et al's study[117] is represented in the Graph IV.8.

A first observation of the graph shows that similar crystallinity rates are obtained with the Silica 25 µm (Chen et al.) and carbon black. Higher crystallinity rates can be observed with the smaller silica (Silica 1).

Linear response of these samples is given in the following table (Table IV.6):

Silica 1 shows a more significant effect on the linear response than carbon black, especially on the α transition strength and damping factor. S2 indicator decreased significantly in the presence of the Silica 1. The surface nature is an important parameter in the preparation of composite; in the studied samples, PTFE has no chemical adhesion or attraction with the fillers. Hence, the reinforcement of the PTFE with carbon black and Silica is assimilated to hydrodynamic reinforcement, the parameters that influences the microstructure linear testing are mainly the size and the filler content. Therefore, these parameters will be in the focus of the following paragraphs.

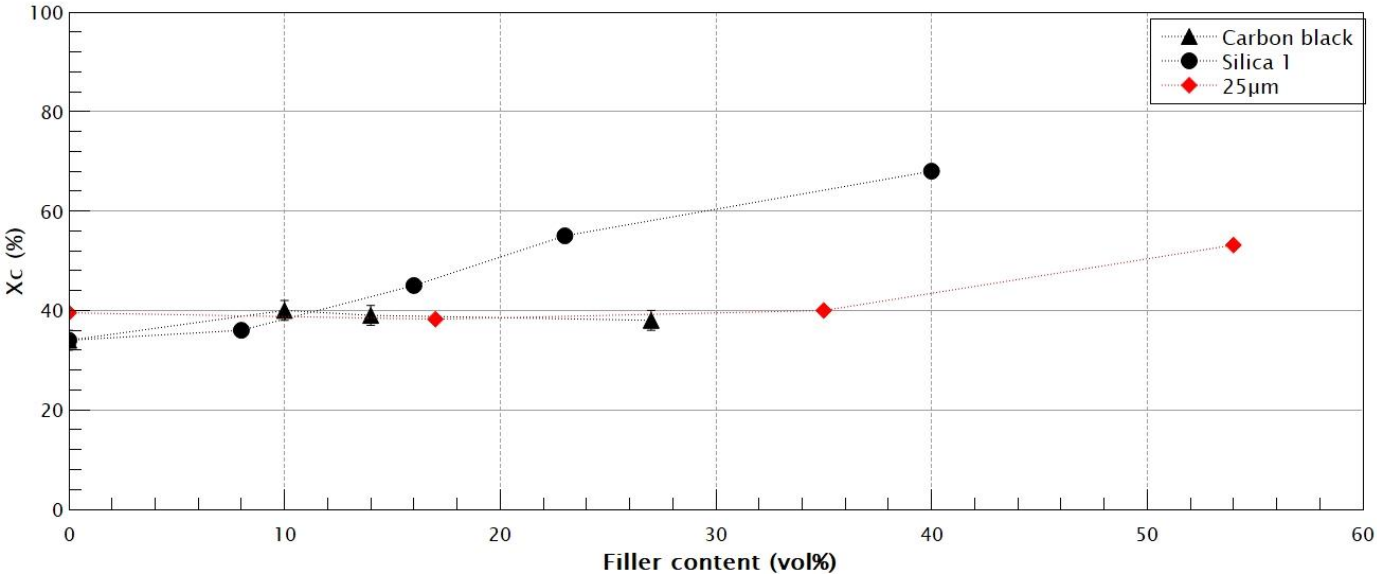

Graph IV.8: Crystalline content for different filler types The red curve represents the Silica from Chen et al's study[117]. Lines are given to guide the eye.

Polymer	Filler	Filler content (vol%)	Xc (%)	Tβ	S1	Tanδ (β)	Tα	S2	Tanδ (α)
PTFE	-	0	34	20	1.9	0.184	112	2.0	0.104
PTFE	Silica 1	9	35	22	1.4	0.198	112	1.4	0.097
PTFE	Silica 1	18	45	25	1.8	0.179	112	1.2	0.085
PTFE	Silica 1	26	55	25	1.4	0.170	112	0.8	0.074
PTFE	Silica 1	43	68	23	1.2	0.159	112	0.4	0.065
PTFE	Carbon black	10	40	21	1.8	0.181	111	1.6	0.091
PTFE	Carbon black	14	39	24	1.5	0.182	112	1.6	0.093
PTFE	Carbon black	27	38	25	1.4	0.166	112	1.2	0.094

Table IV.6: Linear response of different fillers nature.

4.2 Dynamic mechanical characterization

Table IV.7 summarizes the results of the dynamic mechanical testing for samples filled with carbon black and silica 1:

Filler	E' (-50ºC)	E'(30ºC)	E'(150ºC)	Tβ	Tanδ (β)	Tα	Tanδ (α)	T(B)
-	1.29 10^9	6.72 10^8	3.91 10^7	33	0.16	99	0.29	-
Silica 1	1.74 10^9	1.11 10^9	8.63 10^7	40	0.15	114	0.23	-
Silica 1	2.32 10^9	1.49 10^9	1.42 10^8	39	0.14	119	0.21	168
Silica 1	2.58 10^9	1.69 10^9	-	39	0.14	126	0.18	140
Silica 1	2.24 10^9	-	-	-	-	-	-	47
Carbon Black	1.57 10^9	9.91 10^8	6.11 10^7	35	0.15	109	0.26	-
Carbon Black	1.78 10^9	1.16 10^9	9.62 10^7	37	0.15	114	0.23	-
Carbon Black	2.45 10^9	1.60 10^9	2.49 10^8	38	0.16	118	0.20	-

Table IV.7: DMA results for fillers with different surface natures.

In the dynamic mechanical testing, none of the carbon black samples broke during the tests (10%_CB_T1, 14%_CB_T1 and 27%_CB_T1) as opposed to the silica 1 samples (12%_Si1_T1, 23%_Si1_T1, 40%_Si1_T1). Nevertheless, the influence on the temperature of α transition is clear, and the reinforcement of the storage modulus is present.

Both Carbon black and silica 1 have the same reinforcement tendency when considering filler content, in both cases the storage modulus increases linearly with the filler content. However, the storage modulus of PTFE filled with silica 1 is always higher thus indicating a higher reinforcement. An exception is noticed in the case of PTFE filled with 40vol% silica 1 at which the storage modulus is lower due to the fragilization of the composite by the over-blending.

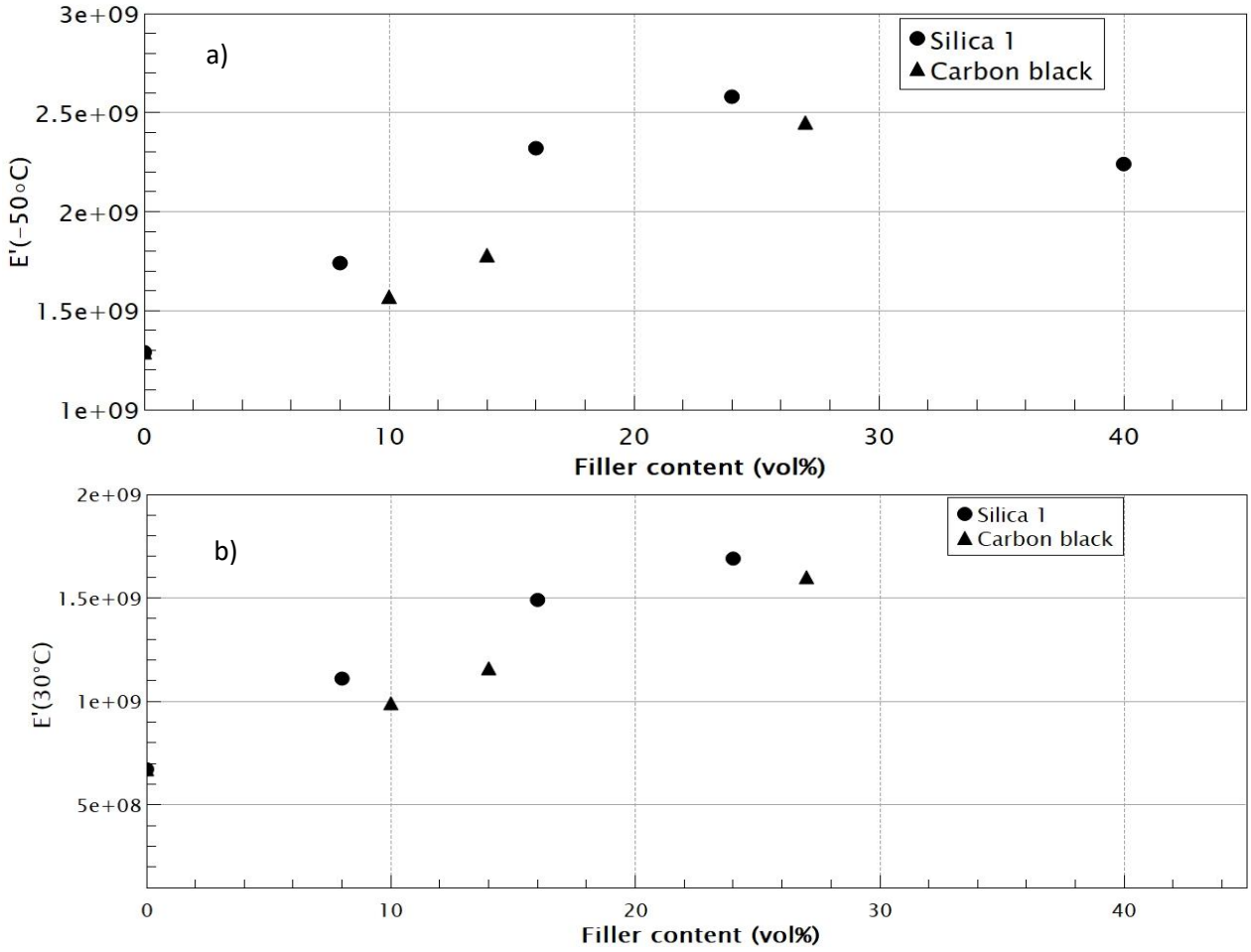

Graph IV.9: Storage modulus E' at (a) -50ºC and (b) 30 ºC of carbon black.

4.3 Conclusion

In this section the influence of the surface nature of the filler on the PTFE was evaluated. Silica 1 showed a higher impact on the crystalline microstructure (an increase from 35 to 68% for sample 40%_Si1_T1) and a higher reinforcement of the storage modulus. It was also remarkable that the silica 1 contributed in decreasing the S2 indicator more than the carbon black at similar filler content (i.e., sample 23%_Si1_T1 and sample 27%_CB_T1). Yet when comparing to literature, a Silica of the same size as the carbon black (25µm[117]) had the same influence on the crystalline content as the carbon black. In linear testing, the size and content of the filler are the main parameters affecting the results. However, for non-linear testing, it would have been interesting to test a carbon black with a similar size to that of the silica 1 (4µm).

5 Influence of the filler size

5.1 Microstructure characterization

Besides the influence of the filler content, section 3 highlighted a difference in the microstructure with the filler size. PTFE showed a different behavior on both microscopic and macroscopic level when changing the silica size. It is essential not only to mention the size of the silica but also to compare it with the size of the PTFE particles. In this part, the focus is on the influence of the size of the silica on the crystallization and morphology of PTFE particles.

Nano hydrophilic fumed silica (Silica 3) was also added to the PTFE in different volume content. The prepared samples along with the filler size and content are presented Table IV.8.

Filler	Filler size (µm)	Filler content (vol%)	Crystalline content (%)
-	-	0	34
Silica 1	4	9	38
Silica 1	4	18	45
Silica 1	4	26	55
Silica 1	4	43	68
Silica 2	250	9	45
Silica 2	250	13	42
Silica 2	250	19	41
Silica 2	250	22	44
Silica 2	250	30	45
Silica 3	0.25	6 ± 2	37
Silica 3	0.25	14 ± 5	34
Silica 3	0.25	24 ± 7	40

Table IV.8: List of samples with different silica sizes and their crystalline content.

As for Silica 1 Silica 2 and carbon black, Silica 3 filled blends were observed with a scanning electron microscope (SEM). However, the capacity of the used microscope was limited and could not provide good quality photos to analyze the morphology of the blends.

The crystalline content was calculated for all samples using the method described in III.2.1.1. Results can be seen in Graph IV.10 and were compared to the results obtained in Chen's study[117] in red.

Graph IV.10 shows the influence of the silica size on the crystalline content of PTFE. At low volume content (under 20 vol%) the silica size has little influence on crystalline content, while after 20 volume percent it is evident that Silica 1 has a higher impact on the crystalline content compared to silica 2 and 3.

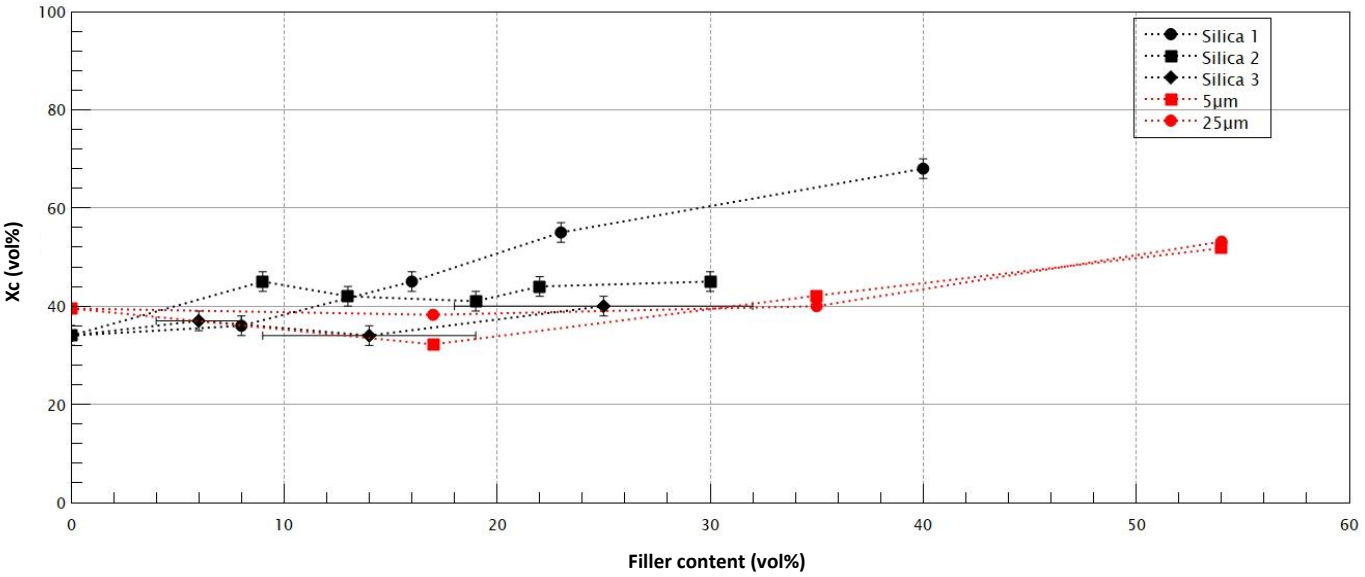

Graph IV.10: Filler size effect on crystalline content compared with Chen et al.'s study[117]. Silica 1 4µm Silica 2 200-300µ Silica 3 0.2µm. Red square and circles represent respectively the two sizes (5 and 25 µm) of Silica that Chen et al. used in their study.

The red curves represent the two silica types (5µm and 25µm) from Chen et al's study[117]. Both curves show little influence on the PTFE crystalline content for samples under 40 vol%.

In Graph IV.10, only Silica 1 has a constant effect on the crystalline content where it increases almost linearly with increasing the silica volume content. It is important to notice that although Silica 1 (4µm) and the 5µm Silica from literature are similar in size they do not have the same influence on the PTFE. This shows that it is not only the size of the filler but rather the ratio filler size/PTFE particle size (seen in Table IV.9) which is of importance.

Filler	Filler size (µm)	PTFE size (µm)	Ratio Filler/PTFE
Silica 1	4	25	0.16
Silica 2	250	25	10
Silica 3	0.25	25	0.01
5µm	5	0.25	20
25µm	25	0.25	100

Table IV.9: Ratio Filler/PTFE comparison with literature[117].

A schematic illustration of those ratios is represented in Figure IV.7:

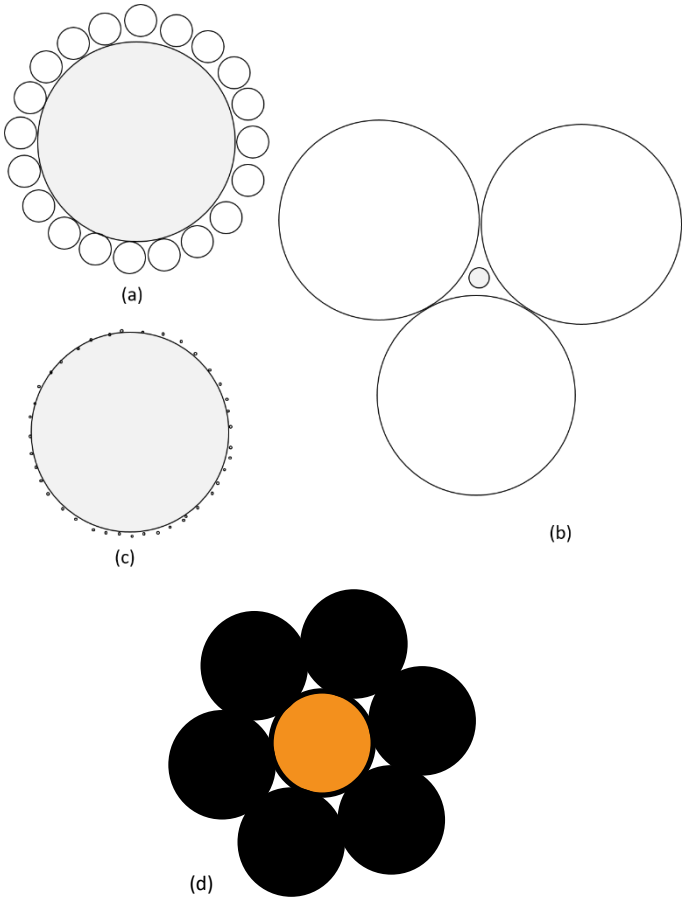

Figure IV.7: Illustration of the ratio between Filler and PTFE size. The grey circles represent the PTFE and the white one's represented the filler. (a): Silica 1 (b): Silica 2 (c): Silica 3 (d): 5µm Silica from literature[117].

Of course, those schematic representations do not take into consideration the agglomerations of Silica or PTFE particles. They intend to illustrate the magnitude of difference between the PTFE and silica particle sizes. This illustration can show the impact that the filler size could have on the PTFE microstructure (crystalline phase).

For a better comprehension of the influence of the particle size, the evaluation of the linear response of rectangular specimens in torsion oscillations is necessary.

Results are illustrated in Table IV.10 below:

Filler	Filler content (vol%)	Xc (%)	Tβ	S1	Tanδ (β)	Tα	S2	Tanδ (α)
-	0	34	20	1.9	0.184	112	2.0	0.104
Silica 1	8	35	22	1.4	0.198	112	1.4	0.097
Silica 1	16	45	25	1.8	0.179	112	1.2	0.085
Silica 1	23	55	25	1.4	0.170	112	0.8	0.074
Silica 1	40	68	23	1.2	0.159	112	0.4	0.065
Silica 2	9	45	22	1.9	0.202	112	1.7	0.099
Silica 2	13	42	21	1.6	0.181	113	1.5	0.094
Silica 2	19	41	24	1.7	0.164	112	1.5	0.091
Silica 2	22	44	23	1.6	0.178	112	1.6	0.094
Silica 2	30	45	23	1.7	0.194	111	1.4	0.096
Silica 3	6 ± 2	37	21	2.0	0.186	110	1.8	0.104
Silica 3	14 ± 5	34	21	1.2	0.126	109	1.1	0.073
Silica 3	24 ± 7	40	23	1.0	0.106	110	0.9	0.070

Table IV.10: Linear DMA test results comparing PTFE filled with different Silica sizes.

According to literature[21,71], the α transition occurs in the amorphous phase and is related to the rigid amorphous phase. It is written that the damping factor tan δ decreases with an increase in crystalline content for virgin PTFE[5]. As it can be seen from the Table IV.10, virgin PTFE and 14%_Si3_T1 sample have the same crystalline content (34%), yet their damping factor at the α transition is not the same (0.104 to virgin PTFE sample and 0.073 for sample 14%_Si3_T1). The difference between those two samples is in the case of the 14%_Si_T1 sample the presence of a filler (Silica 3). In the same way sample 23%_Si1_T1 and sample 14%_Si3_T1 have the same damping factor (0.074) at the α transition while their crystalline contents are different. The difference between those two samples is the size of the silica. Knowing that the damping factor is the ratio between the loss and the storage modulus, these results may imply two suggestions: either the filler has a direct influence on the RAF content, or the reinforcement of the filler varies according to the temperatures. Meanwhile, Silica 2 has minor effect on the indicators S2 and Tan δ (α).

An illustration of the variation of the strength of the α transition (S2) is represented in the Graph IV.11:

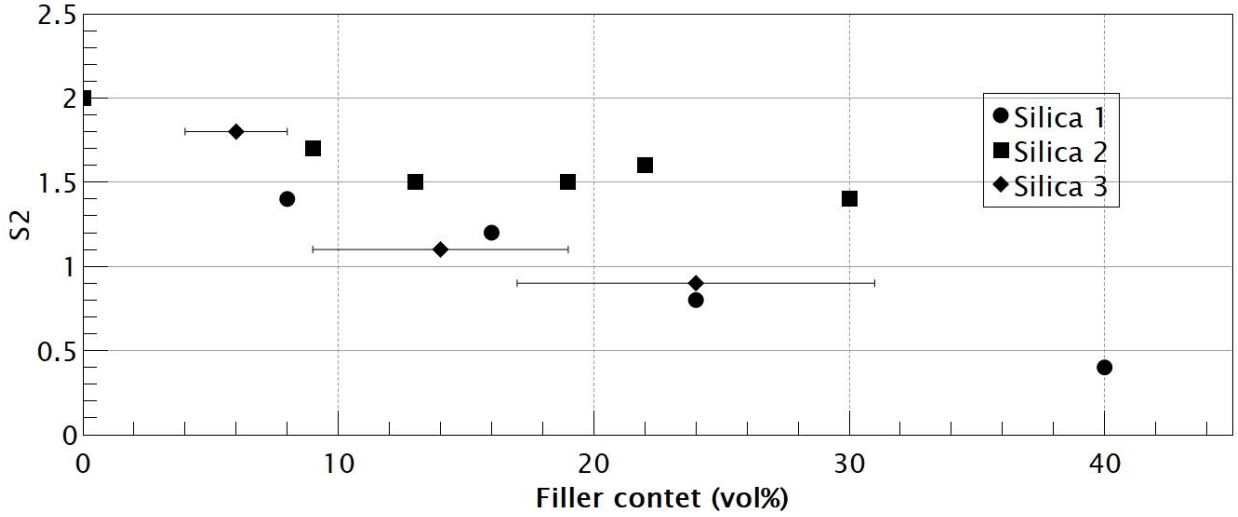

Graph IV.11: S2 variation according to filler size and content. Silica 1 and Silica 3 show the most influence on the PTFE S2 indicator.

All three Silica types contributed in reducing the strength of the transition at the α transition as compared to virgin PTFE. However, Silica 2 presents a value of S2 indicator independent of the filler content whereas Silica 1 and Silica 3 show a more remarkable decrease in this indicator. This drop in the S2 highlights the facts that the size of the filler has an important role in influencing the microstructure.

As a reminder of what it is discussed in the literature, PTFE has three phases below -100°C, two of them in the amorphous region called mobile amorphous fraction (MAF) and the other one is rigid amorphous fraction (RAF), the third phase is the crystalline one. The schematic representation can be seen in the figure below (Figure IV.8):

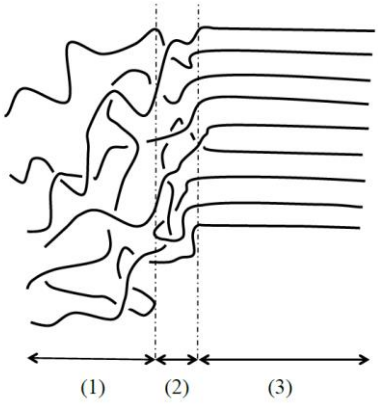

Figure IV.8: Illustration of PTFE phases[21]. (1) MAF; (2) RAF;(3) crystalline phase.

The linear test performed on the samples started after the transition of the mobile fraction transition temperature (1) therefore this phase is already in its rubbery state and the strength of its transition cannot be detected. On the other hand, the transition of the rigid amorphous phase (2) occurs in the test (α transition around 110°C). These results show that the strength of the transition seems mostly affected by the size of the filler rather than directly linked to the crystalline content. In the next part, the effect of size on mechanical properties in nonlinear domain will be studied through non-linear DMA tests.

5.2 Non-linear Dynamic mechanical characterization

The influence of the filler size was also studied in non-linear DMA, results are represented in the Table IV.11 below:

Filler	Content (vol%)	E' (-50ºC)	E'(30ºC)	E'(150ºC)	Tβ	Tanδ (β)	Tα	Tanδ (α)	T(B)
-	-	$1.29\ 10^9$	$6.72\ 10^8$	$3.91\ 10^7$	33	0.16	99	0.29	-
Silica 1	8	$1.74\ 10^9$	$1.11\ 10^9$	$8.63\ 10^7$	40	0.15	114	0.23	-
Silica 1	16	$2.32\ 10^9$	$1.49\ 10^9$	$1.42\ 10^8$	39	0.14	119	0.21	168
Silica 1	24	$2.58\ 10^9$	$1.69\ 10^9$	-	39	0.14	126	0.18	140
Silica 1	40	$2.24\ 10^9$	-	-	-	-	-	-	47
Silica 2	9	$1.25\ 10^9$	$7.24\ 10^8$	$3.37\ 10^7$	35	0.17	97	0.29	-
Silica 2	13	$1.18\ 10^9$	$6.97\ 10^8$	$3.11\ 10^7$	35	0.15	99	0.28	-
Silica 2	22	$1.01\ 10^9$	$5.87\ 10^8$	-	36	0.16	-	-	62
Silica 3	6 ± 2	$1.09\ 10^9$	$1.11\ 10^9$	$6.20\ 10^8$	31	0.15	104	0.27	
Silica 3	14 ± 5	$1.28\ 10^9$	$7.34\ 10^8$	$8.04\ 10^7$	32	0.12	111	0.20	-
Silica 3	24 ± 7	$9.58\ 10^8$	$5.69\ 10^8$	-	-	-	-	-	43

Table IV.11: DMA results for different silica sizes. Samples for higher filler content than 15vol% broke during the test.

The first observation that can be made is that above a certain filler content all samples broke, regardless of filler size. Meanwhile, looking at the results of the storage modulus at different temperatures, not all the silica sizes reinforced the storage modulus in the same way.

Graph IV.12 shows the storage modulus at -50°C. It is settled that silica 1 samples show the higher storage moduli indicating a better reinforcement of the PTFE as opposed to silica 2 and 3. Moreover, the higher the silica 1 content, the higher the reinforcement. However, Silica 2 and 3 did not bring any additional reinforcement to the PTFE matrix.

Although Silica 1 and Silica 3 had an effect in increasing the α transition temperature, Silica 2 did not have any influence on any parameter.

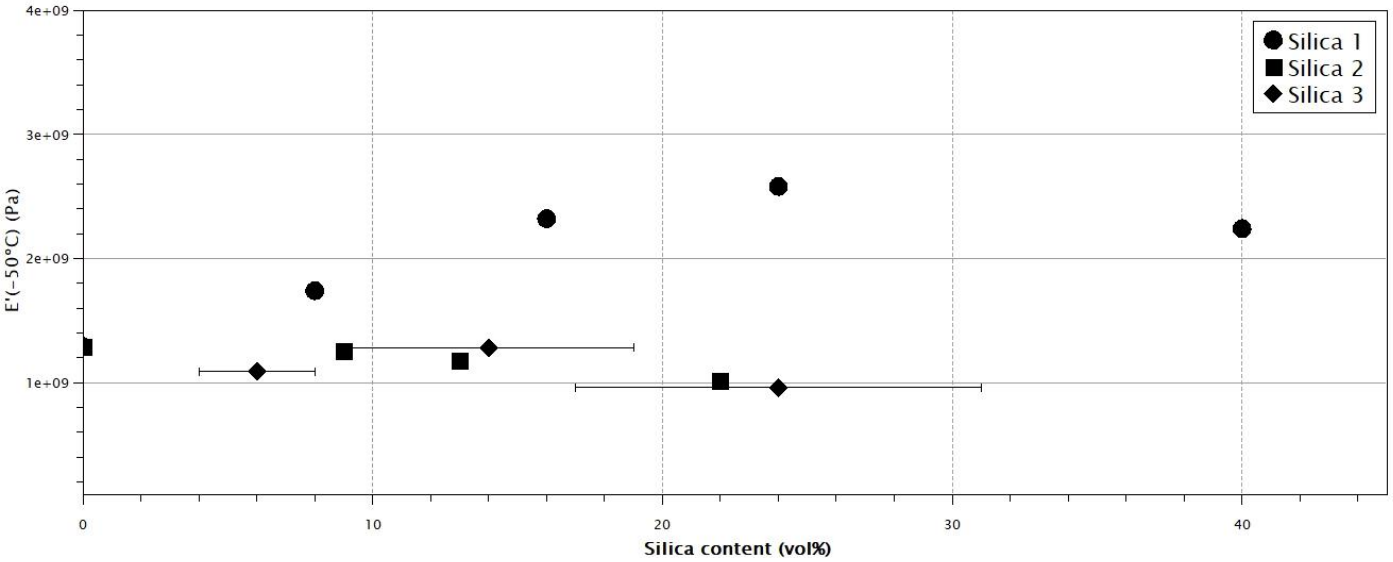

Graph IV.12: Storage modulus at -50ºC.

5.3 Conclusion

When using a filler of same chemical nature, the microstructure and mechanical response of PTFE vary with the size of the added fillers, this variation is mostly noticed on the crystalline content, α transition temperature and damping factor.

6 Discussion

In this section, the results seen in the previous sections will be discussed. Several questions could be asked concerning the influence of the filler on the PTFE matrix. As mentioned before, very few studies were done on filled PTFE regarding the microstructure and mechanical properties. Therefore, some phenomena observed are hard to compare with literature. Two essential results will be discussed: first, the reason of the increase in crystallinity when filling the PTFE, especially in the case of silica 1 and second, the reason of the failing in the dynamic mechanical testing for most of the samples filled with Silica. In addition, we will try to explain the influence of the filler on the rheological behavior around the α transition.

6.1 Crystallinity results

As it can be noticed from the results, there is an increase in the crystalline content of PTFE once filled with any type of filler. This increase is punctual for Silica 2, 3 and carbon black and becomes

constant with increasing the filler content, while for silica 1 the crystalline content keeps increasing when increasing the filler content. A first hypothesis is to consider that the filler has a nucleating effect on the PTFE matrix[143,153] however in such a case Silica 3 should have the higher nucleation effect due to its small size. Although the nucleation effect is not an impossible phenomenon, it does not explain the difference in crystalline content observed specifically for silica 1.

The processing of the PTFE relies on two essential steps: cold compression and free sintering. The compression step contributes in the void closure and giving strength to the material to support the free sintering. An optimal pressure has to be applied in order to prevent fibrillation, cracks and voids[5,147]. The free sintering cycle determines the crystalline content and microstructure properties. As mentioned in the literature, the crystals formed in the PTFE after melt are different from the ones formed in the native PTFE[45,154,155]. The as-polymerized PTFE crystallization is an irreversible phenomenon[10,15,156]. Therefore, the majority of the crystalline microstructure is defined in the free sintering step. The effect of the fillers on the crystallization from melt of PTFE matrix is almost inexistent in the literature, except for Bosq et al.[143] that studied the influence of nano-silica with a modified surface on the PTFE crystallization. The conclusion of the work is that silica promotes crystallization and acts as a nucleating agent at slow cooling rates while it hinders crystallization at high cooling rates. This observation might be effective in Bosq's work where the influence of the filler is noticeable at slow cooling rates. Yet, in our case the increase of crystallinity with increasing filler content (case of Silica 1) cannot be explained by a nucleating effect. The nucleation allows an increase in the nuclei quantity but does not modify the crystallinity rate.

Thus, even if the filler could act as a nucleating agent in some cases, it would not be the only reason for the change in the crystalline content when increasing the filler content. For a better understanding of the reason behind influence of Silica 1 on the crystallinity rate, a schematic representation morphology of the blends in the melt state is represented (*Figure IV.9*)

Step 1 represents the blends after mixing, step 2 the blends at the compression phase and step 3 the blends at the melting phase where the PTFE particles coalesce.

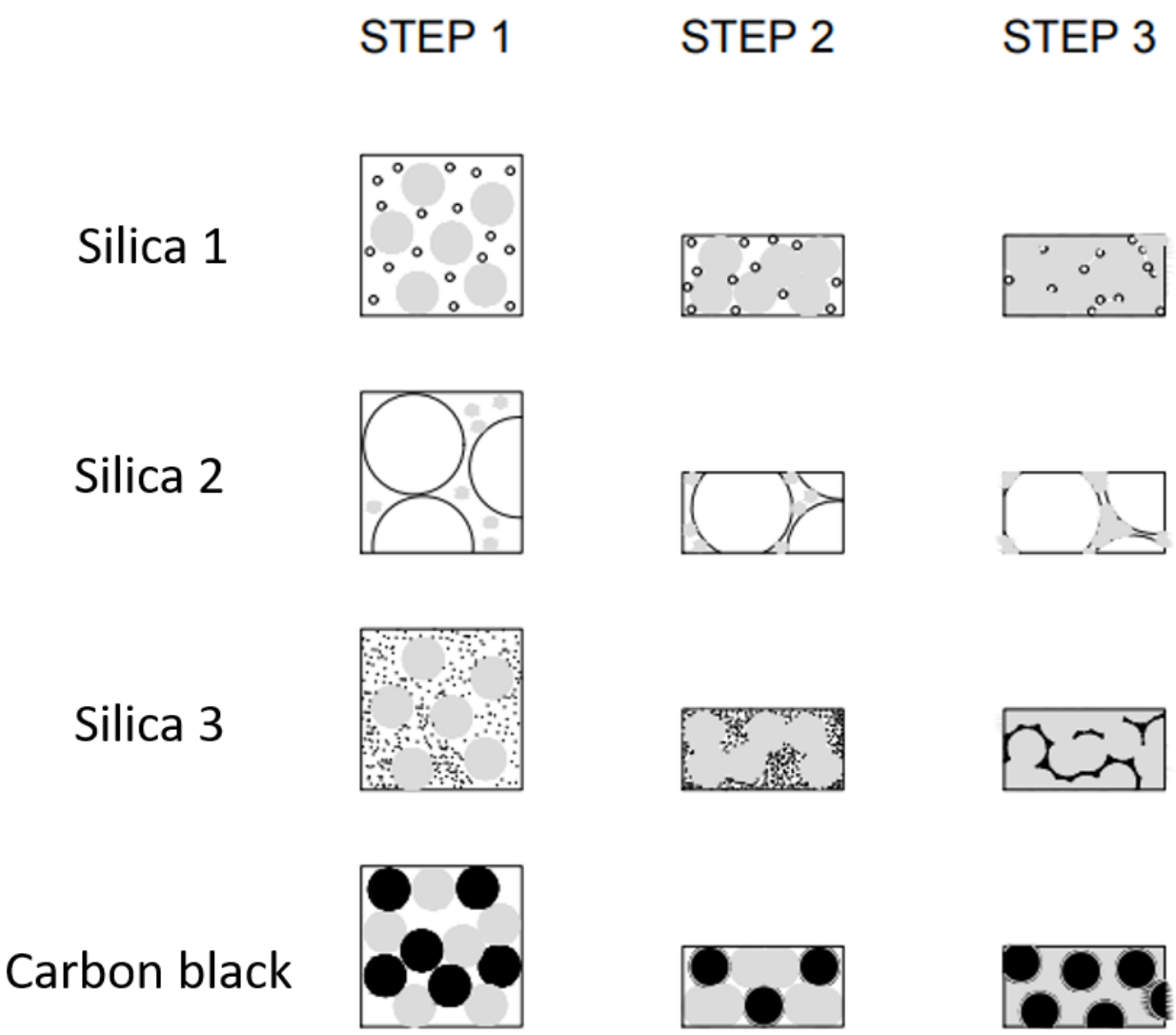

Figure IV.9: schematic presentation of the processing steps and the morphology of each blend. Step 1: mixing, step 2: compression and step 3: melting/coalescence. PTFE is represented by grey particles, silica 1 and 2 are represented by white particles and carbon black and silica 3 by black particles. The scale in the representation respects the ratio of the sizes between the PTFE particle and the filler particle but does not represent the same content of filler between each other).

This figure allows to identify the morphology of each blend according the ratio size between the PTFE and the filler. Even though the adhesion between the PTFE and the filler is inexistent, the compression phase allows the filler (relatively rigid compared to the fragile structure of PTFE[5]) to modify or not the surface of the PTFE particle depending on the size of the filler. This is the case when Silica 1 and Silica 3 are added, the size of the filler allows a penetration of the particles in

the PTFE creating a spherical indentation. This is not the case when working with the carbon black and the silica 2. The size of those fillers, equal or greater to a PTFE particle, prevents the particles of entering the PTFE granule. The interaction is between an agglomeration of PTFE particles and a filler particle, therefore the contact surface between those fillers and the PTFE is minimal compared to the one with smaller filling particles.

In the melting phase, when PTFE particles coalesce, PTFE filled with small particles (Silica 1, Silica 3) melt and then recrystallize in contact with the fillers indenting the PTFE particles. In the case of larger fillers, the coalescence of the PTFE agglomerate is not disturbed by the fillers and occurs in between the agglomerates without an indentation.

It is worth reminding that PTFE has a high viscosity (around $10^{10} – 10^{12}$Pa.s)[5] so its melting phase resembles more a rubbery polymer than a classical thermoplastic. In the cold compression step, the PTFE particles warp in order to take the imposed shape of the mold. The free sintering state allows the fusion and the coalescence of the particles. For unfilled PTFE, once at the melting temperatures all the particles coalesce into each other, producing a homogenous final material (supposing that the sintering cycle is well adapted). This is not the case of filled PTFE where two kinds of interphases exist, the coalescence of two PTFE particles into each other, and the melting of a PTFE particle against a spherical filler. Even if there is no adhesion between the PTFE and the filler, depending on the nature and size of the filler, a force is generated from the contact of the filler with the melted PTFE particle. This force generates stresses in the melted PTFE particles, therefore, in the cooling phase PTFE crystallization from melt is different for unfilled and filled and PTFE. This phenomenon could be explained by the contact mechanics theories.

In non-adhesive elastic contact, the contact between the fillers and PTFE can be assimilated to a contact between a sphere and a half space. The filler can be considered as the indenter. Since 1881, Hertz studied the stresses arising from the contact of two bodies. More specifically the stresses generated by a spherical indenter.

Figure IV.10 shows a schematic illustration of the spherical indentation analysis by Hertz[157].

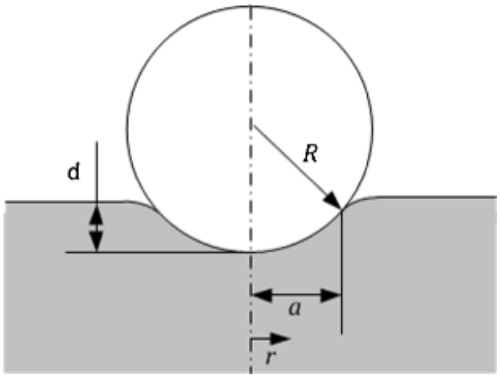

Figure IV.10: Hertzian contact analysis. Spherical indentation[157]

The contact between the sphere and the half space (that could represent a larger sphere) generates a deformation. The deformation generated depends on the pressure applied by the sphere and the radius of the sphere. When the sphere of radius R indents an elastic half space, it generates a deformation d which causes a contact area of a radius **a**.

$$\boldsymbol{a} = \sqrt{R * d} \qquad (IV.5)$$

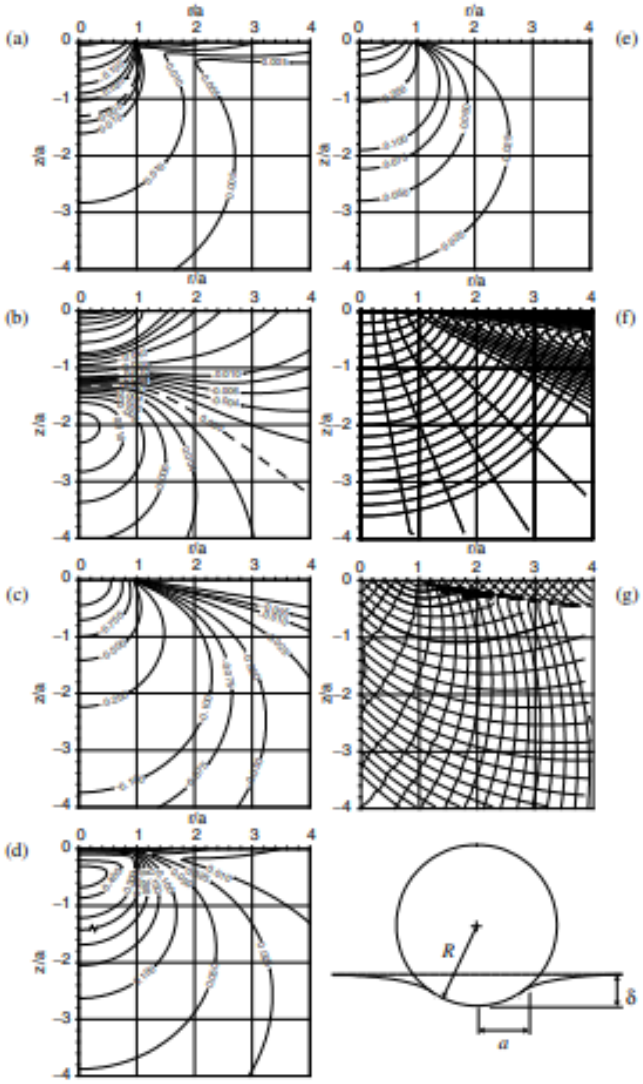

Figure IV.11: "Stress trajectories and contours of equal stress for spherical indenter calculated for Poisson's ratio v = 0.26. Distances r and z normalized to the contact radius a and stresses expressed in terms of the mean contact pressure pm. (a) σ_1, (b) σ_2, (c) σ_3, (d) τ_{max}, (e) σ_H, (f) σ1 and σ_3 trajectories, (g) τ_{max} trajectories."[158]

Figure IV.11[158] is a simulation example of the stress trajectories in the case of a spherical indenter. The figure considers a half space with a Poisson ratio of 0.26. The different graphs present the stresses σ_1 σ_2 and σ_3 in the r z plane ((a) (b) and (c)), the maximum shear stress τ_{max} (d) the trajectories of the stresses 1 and 3 and the trajectory of the maximum shear stress τ_{max}.

The repercussion of the pressure applied by the indenter on the half space spreads up to four times the diameter of the indenter.

In the case of this study, the indenter is the silica spheres (Silica 1; 4µm or Silica 3 0.2µm). Both Silica's have a small diameter compared to the PTFE particles (25µm), therefore, the indentation could be compared to the situation of a spherical indenter versus a half space (PTFE). Silica 2 has a diameter 10 times larger than that of the PTFE, hence the indentation is inexistant. As for the carbon black its radius is in the same range of the PTFE's therefore it is in the case of a contact between two spheres. The indentation in this case is assimilated to a circle and the maximum shear stress is minimal.

When PTFE is unfilled, the stress is equal to zero. Both in the compression step and in the melting phase, the filler exercises an indentation phenomenon on the PTFE surface. This effect creates a radius pressure in the PTFE matrix, creating stresses.

Considering the Hertzian theory for a contact between a sphere and a half sphere[158], the stresses within the indented specimen are expressed by the following equations:

$$\frac{\sigma_r}{P_m} = \frac{3}{2}\left\{\frac{1-2\nu}{3}\frac{a^2}{r^2}\left[1-\left(\frac{z}{u^{0.5}}\right)^3\right]+\left(\frac{z}{u^{0.5}}\right)^3\frac{a^2u}{u^2+a^2z^2} + \frac{z}{u^{0.5}}\left[u\frac{1-\nu}{a^2+u}+(1+\nu)\frac{u^{0.5}}{a}\tan^{-1}\left(\frac{a}{u^{0.5}}\right)-2\right]\right\} \quad (IV.6)$$

$$\frac{\sigma_\theta}{P_m} = \frac{3}{2}\left\{\frac{1-2\nu}{3}\frac{a^2}{r^2}\left[1-\left(\frac{z}{u^{0.5}}\right)^3\right] + \frac{z}{u^{0.5}}\left[2\nu+u\frac{1-\nu}{a^2+u}-(1+\nu)\frac{u^{0.5}}{a}\tan^{-1}\left(\frac{a}{u^{0.5}}\right)\right]\right\} \quad (IV.7)$$

$$\frac{\sigma_z}{P_m} = -\frac{3}{2}\left(\frac{z}{u^{0.5}}\right)^3\left(\frac{a^2u}{u^2+a^2z^2}\right) \quad (IV.8)$$

$$\frac{\tau_{rz}}{P_m} = -\frac{3}{2}\left(\frac{rz^2}{u^2 + a^2z^2}\right)\left(\frac{a^2u^{0.5}}{a^2 + u}\right) \quad (IV.9)$$

Where u is given as:

$$u = \frac{1}{2}[(r^2 + z^2 - a^2) + [(r^2 + z^2 - a^2)^2 + 4a^2z^2]^{0.5}] \quad (IV.10)$$

The principal stresses in the r z plane are given by:

$$\sigma_{1,3} = \frac{\sigma_r - \sigma_z}{2} \pm \sqrt{\left(\frac{(\sigma_r - \sigma_z)}{2}\right)^2 + {\tau_{rz}}^2}$$

$$\sigma_2 = \sigma_\theta \quad (IV.11)$$

$$\tau_{max} = \frac{1}{2}[\sigma_1 - \sigma_3]$$

The Poisson ratio is 0.46 of PTFE. When distances r and z normalized to the contact radius a and stresses expressed in terms of the mean contact pressure P_m, the τ_{max} is presented as follows:

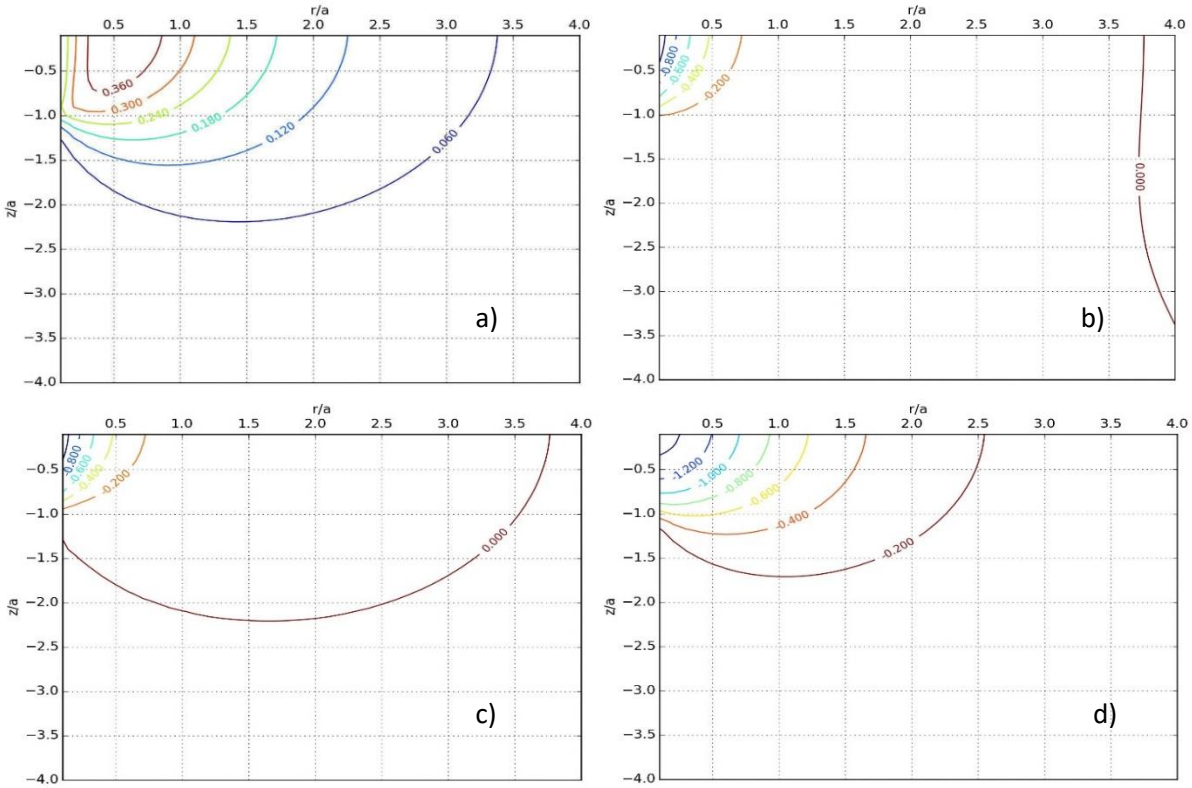

Figure IV.12: Stress σ1 (a) σ2 (b) σ3 (c) and τmax (d).

The data presented in Figure IV.12 expresses the stresses in the directions 1 2 and 3 and the maximum shear occurred in the specimen. For a depth equal to 3.3 times the diameter of the indenter the shear stress equals 5% of the applied pressure; 3 Mpa (60 Mpa is the applied pressure for filled samples III.3.4.1). When it comes to Silica 1 (4µm), 3.3 times its diameter is 6.6 µm which represents 50% of the PTFE diameter. Therefore, the indentation on the PTFE due to the silica 1 reaches a quarter of the PTFE particle. This is a theoretical demonstration for one direction, in reality the trajectories are in all the direction, and most of the time overlap with the trajectories of indentation created by another silica sphere on the same PTFE particle, thus creating an even higher impact on the PTFE chains. As for Silica 3 (0.2µm), 3.3 times the diameter is equivalent to 0.33µm and represents 2% of the PTFE diameter, therefore the influence on the PTFE particles is minimal.

According to Tobolsky et al[159]. the relaxation time is linearly related to the molecular weight of PTFE: the higher the molecular weight, the longer the relaxation time. In our case, molecular weight of PTFE was estimated by Suwa et al.[160] who showed a relationship between the melting temperature and molecular weight. The melting temperature of the native PTFE in our case is around 342°C which corresponds to an average molecular weight Mn = 10^7, this average molecular weight in Tobolsky et al's[159] study requires a relaxation time of 5.10^4 seconds at 380°C. Which is equivalent to 13 hours while the temperature cycle applied in our study is 6 hours at 380°C. Therefore, crystallization of PTFE in the sintering process occurs while the PTFE chains have not been completely relaxed. This relaxation time is determined for an unfilled PTFE, but as mentioned previously when filled with a spherical filler, it acts as an indenter and generates additional stresses in the polymer. The indentation action of the filler explains the differences in internal stresses that the PTFE is submitted to during the cooling phase and hence the difference in the crystalline rate.

The indentation phenomenon might be the explanation for the crystallinity rise when adding a filler. On the other hand, this rise is different when varying the filler size. Although it is common for Silica 1, Silica 2, Silica 3 and carbon black to increase crystallinity compared to unfilled PTFE, only samples containing Silica 1 showed a constant increasing in its crystallinity rate; . This is most probably caused by the size of the Silica 1. As showed in the morphology representation and SEM photos, Silica 1 is capable to form a network between all its particles covering a high surface of PTFE particles. While carbon black and Silica 2 form a "droplet – matrix" kind of morphology. As for Silica 3, the radius of the filler is very small compared the Silica 1 (0.25 µm for Silica 3 and 4µm for Silica 1) thus, the stresses generated in the PTFE particles are minimal compared to those generated by Silica 1.

6.2 Reinforcement of the filler in linear DMA testing

Torsion oscillation of rectangular samples showed different behavior of the PTFE according to the filler type, content and size. The influence of those fillers was mainly observed on the storage modulus, and the damping factor at the α transition. The fillers played a significant role on the variation of the damping factor, especially around the α transition. The storage modulus of PTFE is relatively high at low temperatures (around 1.10^9 Mpa); this value decreases progressively when increasing the temperature as large sections of the macromolecule start to relax. The PTFE changes state throughout the test. Significant drops of this modulus are observed at the transition phases β and α. Once the α transition temperature is reached, the rigid amorphous phase passes to its rubbery phase. At this stage of the test, the contribution of the filler is more or less significant depending on the added filler. The filler shows its contribution in maintaining the storage modulus value and reinforcing the PTFE. This contribution is very well observed when adding Silica 1 and Silica 2 (cf. S2 values from Table IV.3, Table IV.6 and Table IV.10). Graph IV.13 shows a comparison between the storage modulus and the damping factor results for unfilled PTFE and PTFE filled at around 20 %vol of Silica 1, Silica 2, Silica 3, and carbon black.

In part (a), i.e. $-50^oC < T < T\beta$, the storage modulus is determined by the PTFE its RAF and its crystallinity, as well as the filler. For $T\beta < T < T\alpha$ (b) the conformation of the crystalline chains has changed but the same factors influence the storage modulus. Part (c) $T > T\alpha$, the rigid amorphous phase has become rubbery and the storage modulus is a reflection of the contribution of the crystalline phase and the fillers. It would have been interesting to explore the contribution of the filler after the melting of the PTFE crystallites, but the test conditions were difficult to put in place.

In these results, blends filled with silica 2 silica 3 and carbon black have the same crystalline content (around 40%), therefore, after Tα only the filler's reinforcement makes the difference. Graph IV.13 highlights the difference between the reinforcement of each filler, Silica 1 and Silica 2 show the same reinforcing effect below Tα; above that temperature however, the difference between the 2 samples is remarkable. This can be explained by a higher crystallinity rate of the PTFE with Silica 1. When it comes to Silica 3, it is remarkable that the reinforcement of the storage modulus is almost inexistent before the β transition, and lower than all the other fillers before the α transition.

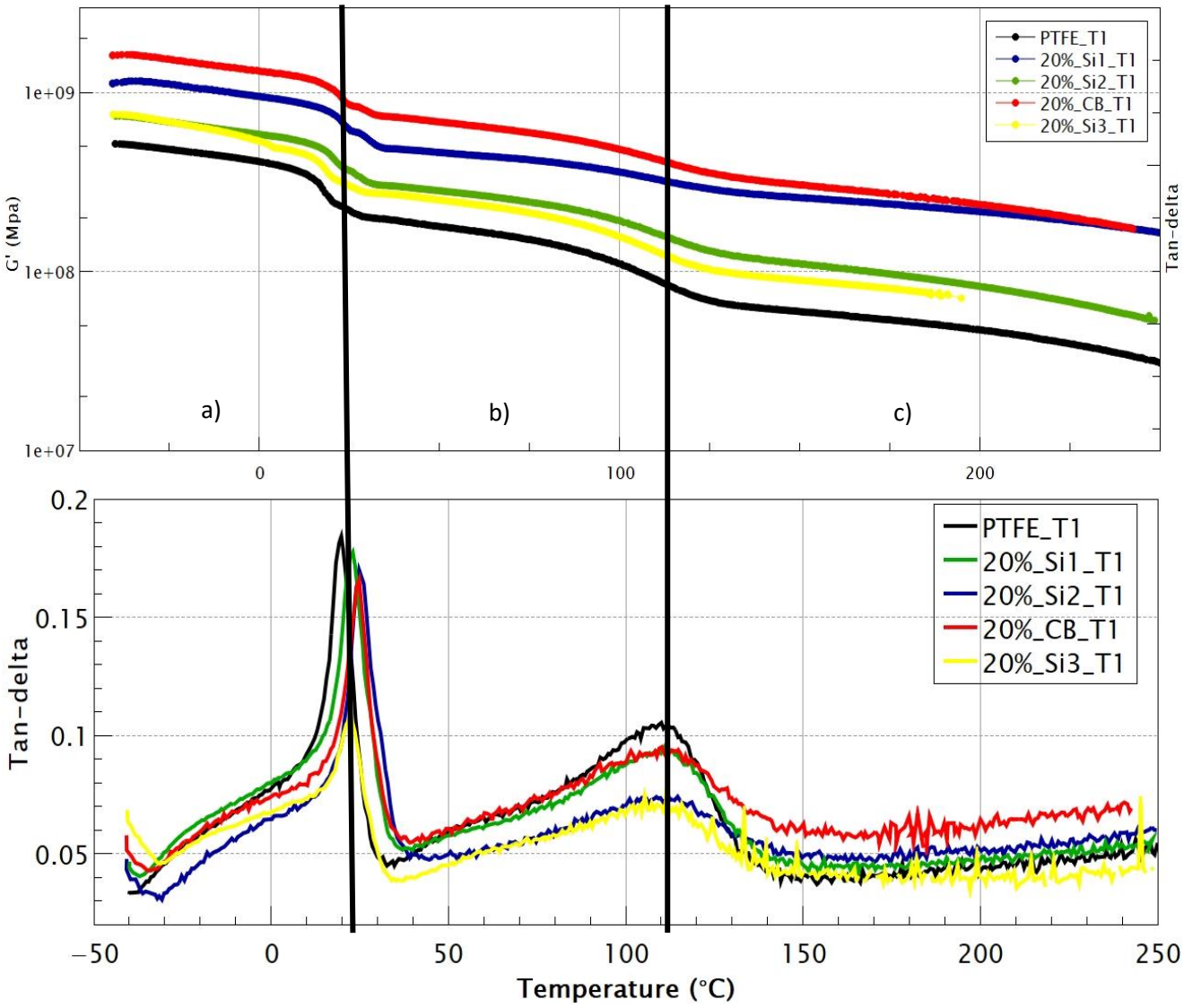

Graph IV.13: Linear DMA test results for unfilled PTFE (black curve) and PTFE filled of 20 vol% of Silica 1 (blue curve), Silica 2 (green curve), Silica 3 (yellow curve) and carbon black (red curve).

Silica 3 is a nano-silica that forms a network between the PTFE particles as shown in the adjacent illustration extract from the Figure IV.9

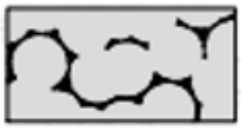

Because of the non-adhesion between the silica and the PTFE and their low mechanical contrast, the network reinforcement of Silica 3 is not remarkable at the storage modulus values. Yet, the damping factor at the α transition is at its lowest indicating a higher contribution of the filler in the reinforcement.

As for the carbon black, in this case, it represents the filler with the most reinforcement at all temperatures of the test and chain conformations of the PTFE. However, the silica 1 shows a better capacity of reinforcing after the α transition as shown by S2 (see Table IV.3).

Despite the higher storage modulus obtained with of carbon black, Silica 1 is an interesting filler considering its reinforcement capacity after the α transition. Indeed, one of the goals of the study is to improve the properties of PTFE around the alpha transition. More specifically, limit the drop of the storage modulus around this transition, and obtain a more stable material no matter the temperature applied.

6.3 Failure in the non-linear DMA testing

As seen previously, failure in the mechanical testing occurred in several samples. This failing came mainly in silica filled blends. More specifically, the failing occurred at a filling rate higher than 15 volume percent. Several reasons could be behind this failing:

Silica 2 is made of agglomerates of silica aggregates that are fragile and break under shear. In the process, silica 2 was not broken after the temperature cycle and mostly found with its initial size in the samples (around 300 µm) after the process. But, in the non-linear DMA testing, the stress applied is 5 Mpa. The stress needed to break the micro-pearls is around 0.2 MPa[161], therefore, eventual breaking in the micro-pearls through the testing should be expected. Thus, most of the silica 2 might be broken in the sample and create pores and instability in the samples leading to a propagation of the fracture in the matrix.

Concerning the Silica 3, the fracture for samples occurred at a filling content higher than 20 vol% (Sample 24%_Si3_T1). At this filling rate, Silica 3 with its high surface area (200 m^2/g) covers almost all the PTFE particles and prevent the fusion of the PTFE particles between each other. Therefore, the sample after the temperature cycle has a low cohesion between its particles and tends to break, even at low temperatures. This explanation is also valid for sample 40%_Si1_T1 (filled at 40 vol % of silica 1).

As for Silica 1 filled samples (excluding sample 40%_Si1_T1), the addition of the Silica 1 contributed in increasing the crystalline content through the indentation phenomenon explained in the section 6.1. As viewed in the literature study, the mechanical properties of the PTFE are highly affected by the crystalline content. Brown et al[162]. and Joyce et al.[34,35,64] studied the influence of the crystalline content on the fracture propagation in the PTFE and concluded a limited toughness and a higher propagation of the fracture when having a higher crystalline degree. In addition of increasing the crystalline content, Silica 1 has no adhesion with the PTFE matrix and creates micro-voids that promotes the forming of cracks under load. Therefore,

adding silica 1 to the PTFE matrix contributed in fragilizing the structure in non-linear DMA testing.

Finally, a final hypothesis is that the dispersion of the silica plays an important role. Indeed, the creation of agglomerates in the matrix creates inhomogeneity in the blend which in turn could lead to failure.

7 Conclusion

As a conclusion, different behaviors of the PTFE were observed depending on the filling rate, type and size. The size of the filler had the most influence on the PTFE matrix, as it had a direct influence on the crystalline content. In addition, depending on the size of the filler the reinforcement in the mechanical testing was different. Large sizes of silica are not capable of penetrating the PTFE particles, thus leading to a small impact on crystallization and microstructure. Smaller sizes of silica penetrate the PTFE particle but not sufficiently to induce a major change. To this day, the main problem with the Silica 1 is the failure occurring in the mechanical testing due to the poor adhesion between the PTFE and the silica and the increase in the crystalline content t induced by this size of silica. In order to remedy to this problem, a polymer with a lower viscosity (PEEK) was added in the blend in order to limit the indentation phenomenon and decrease the crystalline content. Ideally, PEEK would also fill in the voids between the PTFE and the silica and hence limit the propagation of the crack in the blend while preserving the interesting properties of the composite.

Résumé Chapitre IV

Le chapitre suivant étudie l'influence du rajout de charges organiques et organo-minérales à une matrice de PTFE. Le but des charges est d'améliorer le comportement du PTFE vis-à-vis de l'usure et du fluage. Plusieurs auteurs ont étudié l'influence des charges sur les propriétés tribologiques[100,128] mais rares sont ceux qui ont intégrés dans leurs études leur influence sur la microstructure et les propriétés mécaniques du PTFE[46,115].

Plusieurs formulations ont été élaborées afin d'évaluer l'influence des charges. Le premier paramètre étudié est la fraction volumique de la charge au sein du composite. Chaque charge a été ajouté à différents taux dans la matrice de PTFE. Le changement de taux de charge a eu un effet direct sur la microstructure, le taux de cristallinité, la taille des cristaux ainsi que la morphologie et la température de transition Tβ. Les charges ont également eu un effet sur le comportement en analyse dynamique linéaire et non-linéaire. Un renforcement a été observé sur le module de conservation ainsi que la température de transition Tα. Cependant, chaque charge a influencé dans des proportions différentes la microstructure et le comportement mécaniques. Ceci peut être à cause de la nature chimique ou la taille de la charge.

L'effet de la nature chimique de la charge (Noir de carbone ou Silice) sur les propriétés finales du composite a donc été mise en évidence. La silice 1 (4µm) a eu une influence plus prononcée sur le taux de cristallinité du PTFE (une augmentation de 35 à 68% pour certains échantillons) en plus d'un meilleur renforcement du module de conservation G'. Ces résultats semblent indiquer qu'il y a un effet de la nature chimique de la charge. Toutefois, la taille de la charge ici n'est pas prise en compte et une étude par Chen et al. [119] a montré qu'une charge de noir de carbone de taille équivalente à la silice 1 augmente elle aussi significativement le taux de cristallinité, indiquant ainsi que la taille de la charge est un paramètre important dans les composites de PTFE.

Ainsi, l'influence de la taille de chaque charge sur le comportement du PTFE a été observé de plus près. En comparant les charges de même nature avec différentes tailles (silice 1, silice 2 et silice 3), l'influence de ce paramètre sur la microstructure, plus précisément sur le taux de cristallinité et la température de transition Tα a pu être observée.

Les résultats ont montré une forte influence de la taille de la charge par rapport à la taille de particule du PTFE. Une petite charge (0,2 µm) et une grosse charge (taille équivalente ou supérieure à celle de la particule de PTFE) n'auront que peu d'influence sur la cristallinité et la microstructure des composites. A contrario, les charges de 4 µm ont montré une influence significative sur la cristallinité du PTFE. Cette augmentation peut être imputée à un phénomène d'indentation de la charge, créant un champ de contraintes qui n'ont pas le temps de se relaxer au cours du cycle de température.

L'augmentation de la cristallinité et des propriétés mécanique en torsion n'est pas observée en non linéaire. Cela peut s'expliquer par une faible adhésion entre la charge et le PTFE ou l'augmentation de la cristallinité.

Bien que le comportement intéressant que représentait le composite de PTFE chargé de Silice1, il a présenté un défaut durant le test non-linéaire de DMA, l'échantillon cassait avant la fin du test. Plus le taux de cristallinité était élevé plus la casse se produisait plus tôt. Ceci peut être causé par la faible adhésion entre le PTFE et la silice, ainsi que l'augmentation particulière du taux de cristallinité du PTFE.

V. PTFE/PEEK blends filled with Silica

1 Introduction

As seen in the previous chapter, fillers are capable of enhancing the mechanical properties of the PTFE. According to the filler size and content the microstructure of the PTFE was influenced differently.

Although Silica showed a better reinforcement of the mechanical properties of PTFE in the linear DMA testing after the α transition than the carbon black, some samples failed the non-linear DMA tests. Several reasons could be behind this failure. The addition of a micro-sized silica (silica 1) emphasized the stresses in the PTFE matrix that crystallized under stress and had higher crystalline rates, causing the failure. Another reason would be the lack of adhesion between the fillers and the PTFE matrix.

For this reason, one of the proposed solutions to improve the blend and prevent the cracking is to add PEEK polymer into the blend.

PEEK is a semi-crystalline polymer, usually blended with PTFE to enhance its tribological properties[129,134]. PEEK is known for its high mechanical resistance at temperatures exceeding 300°C. In addition, it has a low viscosity (10^2-10^3 Pa.s)[163] compared to PTFE. All these properties explain the introduction of PEEK in the PTFE/ Silica blends.

The idea is to achieve a blend of PTFE/Silica connected with PEEK polymer with a good distribution and dispersion of all the elements. The role of the PEEK will be to guide the silica with its low viscosity between the pores of the PTFE in order to reduce the indentation phenomenon, improve the mechanical properties and reduce the crystalline content of the blend.

An illustration of theoretical purpose of these blends is presented in the Figure V.1 :

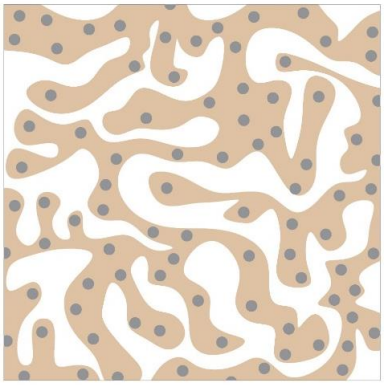

Figure V.1:Theoretical illustration of a PTFE/PEEK/filler blend. PTFE(white phase) PEEK(camel phase) filler (black dots)

2 Blends

Several samples were prepared according to the temperature cycle 2 mentioned in the Chapter II. Blends of PTFE/PEEK and blends of PTFE/PEEK/Silica 1 at different volume rates were prepared.

Polymer1	**polymer2**	**Polymer 2** (vol%)	**Filler**	**Filler content** (vol%)	**Xc** (± 2%)
PTFE	-	-	-	-	39
PTFE	-	-	Silica 1	9	41
PTFE	PEEK	6	-	0	40
PTFE	PEEK	8	-	0	40
PTFE	PEEK	14	-	0	39
PTFE	PEEK	23	-	0	34
PTFE	PEEK	22	Silica 1	9	29
PTFE	PEEK	21	Silica 1	16	37
PTFE	PEEK	20	Silica 1	24	40
PTFE	PEEK	28	Silica 1	8	35
PTFE	PEEK	28	Silica 1	16	36
PTFE	PEEK	22	Silica 1*	8	39
PTFE	PEEK	28	Silica 1*	8	29
PTFE	PEEK	34	Silica 1*	8	29
PTFE	-	-	Silica 1*	9	43
PTFE	-	-	Silica 1	18	41
PTFE	-	-	Silica 1	26	48

Table V.1: List of the blends prepared with PEEK added to the PTFE matrix and their crystalline content.

Note: Like the previous chapter, the designation of the samples will be as follows: 6%_PEEK_T2 for a sample with 6 vol% of PEEK and made with the cycle temperature 2, 22%_PEEK_9%_Si1_T2 is sample of 22 vol% of PEEK 9 vol% of silica and made with the temperature cycle 2. Grafted silica is designated as gSi.

* The silica 1 presented in the samples 22%_PEEK_9%_gSi1_T2, 28%_PEEK_8%_gSi1_T2, 34%_PEEK_8%_gSi1_T2 and 9%_gSi1_T2 is the Silica 1 grafted with a 3wt% of PFTOS. In chapter II, the grafting had no effect on PTFE filled with silica 1. In addition, around 7 vol % Silica 1 had no influence on the crystalline content and did not fail in the non-linear DMA testing. **However, the comparison will be established between samples that underwent the same processes and same silica treatment to observe the microstructure and mechanical evolution in the same conditions.**

Two attempts of blends failed:

1- Blend of 32 vol% of PEEK and 20 vol% of Silica 1
2- 47 vol% of PEEK

Those samples did not handle the temperature cycle and the sintering process. Therefore, the filling was limited with a weight fraction of PTFE higher than 70wt%.

***Note: in the subsequent sections (4 and 5), a fixed Silica or PEEK content is equivalent to an identic weight percent, but for confidentiality reasons the work is presented in a volume percent. Therefore, some minor volume percentage may vary while talking about a fixed silica or peek content*.**

Volume contents are calculated according to the equations (V.1) and (V.2):

$$\%V_{peek} = \frac{\%w_{peek} * \rho_{peek}}{\%W_{peek} * \rho_{peek} + \%W_{PTFE} * \rho_{PTFE} + \%W_{silica1} * \rho_{Silica}} \quad (V.1)$$

$$\%V_{silica} = \frac{\%w_{silica} * \rho_{silica}}{\%W_{peek} * \rho_{peek} + \%W_{PTFE} * \rho_{PTFE} + \%W_{silica1} * \rho_{Silica}} \quad (V.2)$$

3 PTFE/PEEK blends

3.1 Microstructure characterization

The crystalline content is calculated for the pure PTFE weight. The fusion temperature of the PTFE and the PEEK were very close ~330°C and ~ 340°C respectively. In addition, the amount of PEEK is small in the blend and therefore, its fusion peak was modest compared to that of the PTFE. An example of the DSC curve of PTFE/PEEK blend (Sample 14%_PEEK_T2) is represented afterwards.

The DSC curve shows the fusion temperature of the PTFE (black curve marked at ~ 330°C) and the small peak just afterwards (~340°C) is the fusion temperature of the PEEK. A better distinction between the two polymers is the crystalline temperature where the two temperatures are well separated.

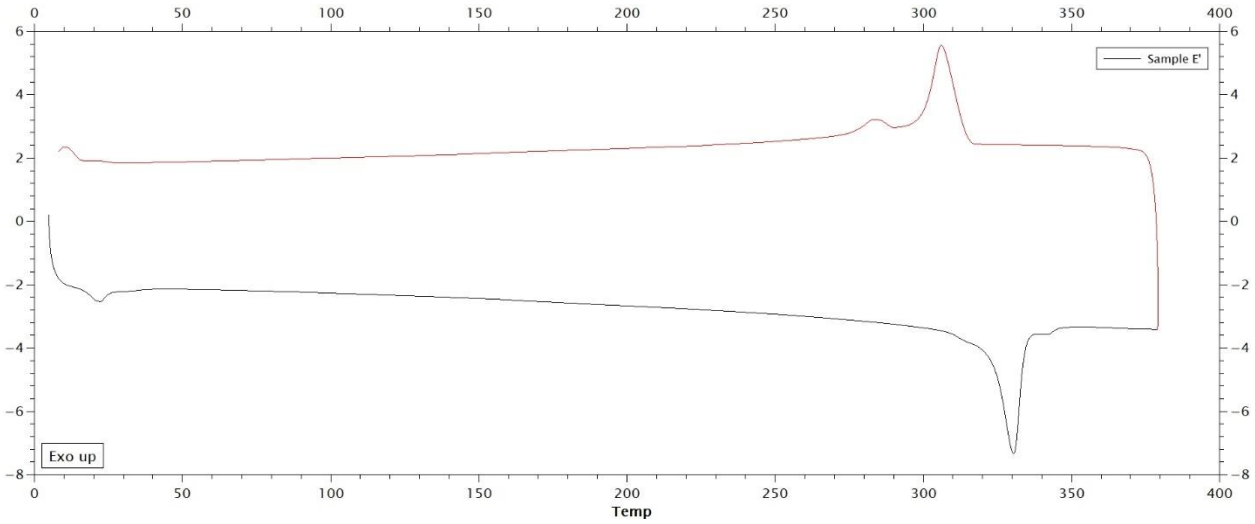

Graph V.1: DSC result for sample 14%_PEEK_T2

As shown in Graph V.2, for PTFE/PEEK blends with a PEEK content inferior to 23 vol%, the crystalline content is almost constant.

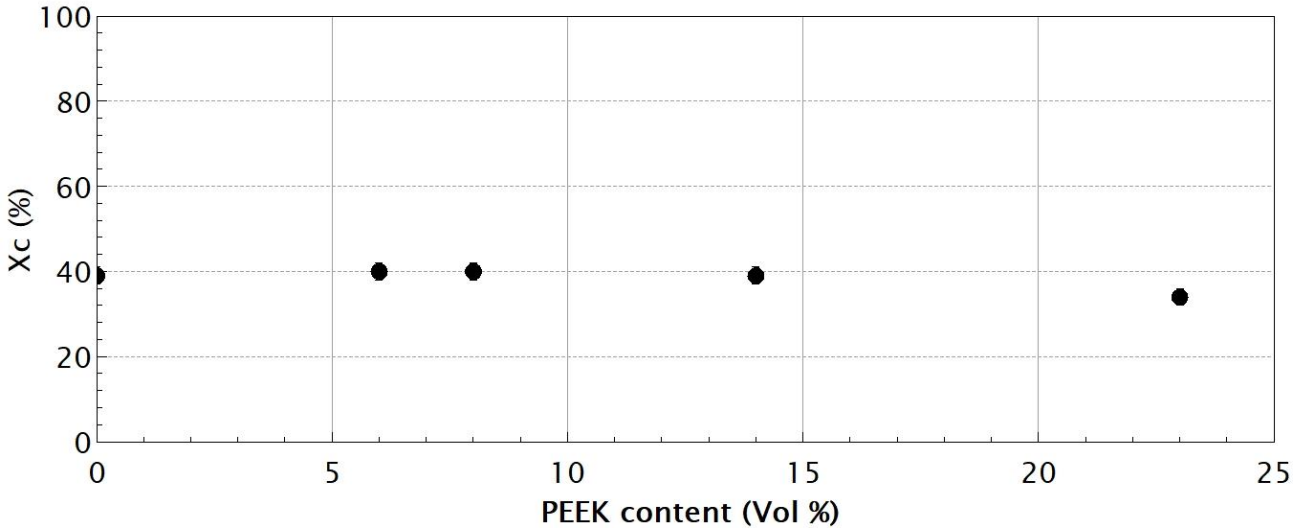

Graph V.2: crystalline content of PTFE mixed with different PEEK rates: 6, 8, 14, 23 volume percent

Samples were observed with SEM in order to identify the morphology of the composites and the miscibility between the two polymers (PEEK and PTFE). The following SEM photos show the morphology of the blends:

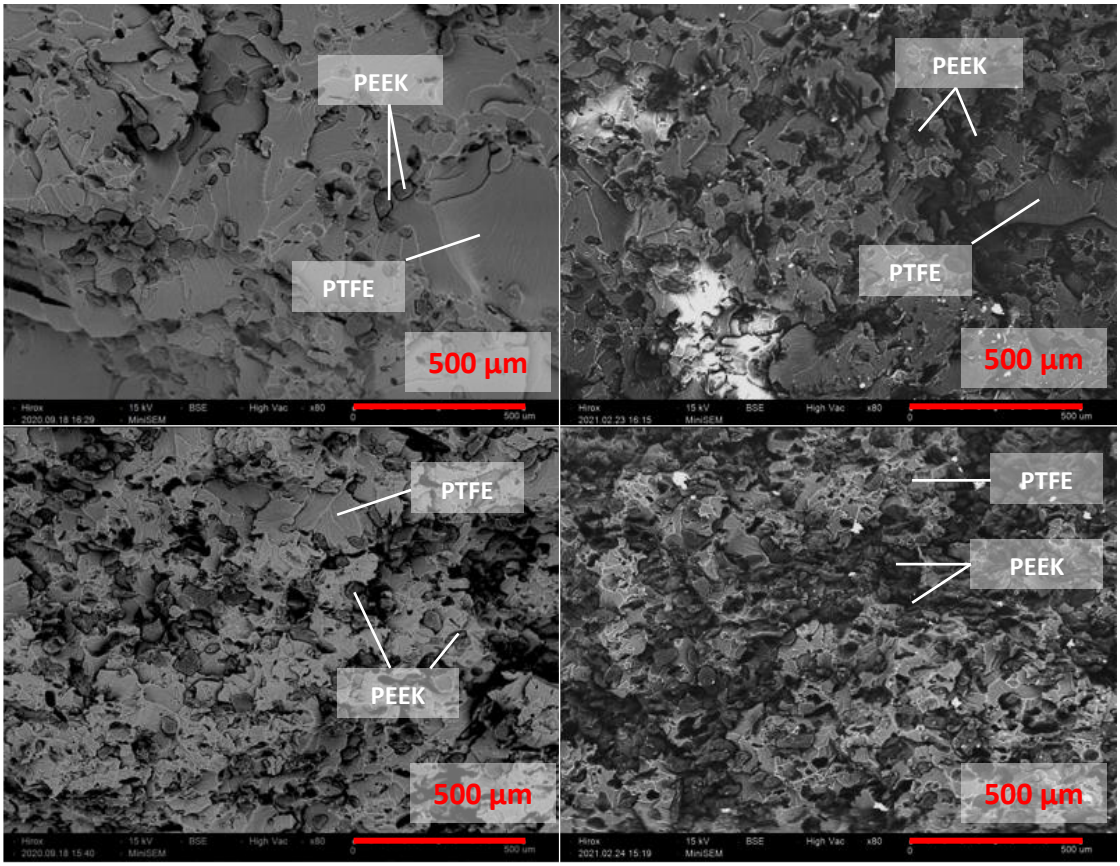

Figure V.2: SEM photos of PTFE/PEEK blends at different PEEK content: 6vol%, 8vol%, 14 vol% and 23 vol%. A 'droplet-matrix' morphology is observed.

Figure V.2 presents the morphology of PTFE/PEEK blends. The observations show a 'droplet – matrix' morphology no matter the PEEK content which seems logical considering that the amount of PEEK is well below a theoretical value of 50 vol% for which co-continuity could be expected[164]. A lack in the adhesion of the PEEK and PTFE can also be noticed, the two polymers at this stage are immiscible.

The linear response of rectangular specimens in torsion oscillations was also tested according to the method described in chapter II. Results are summarized in the Table V.2:

Polymer 1	Polymer 2	PEEK content (vol%)	Xc (%)	Tβ	S1	Tanδ (β)	Tα	S2	Tanδ (α)
PTFE	-	-	39	22	1.9	0.193	113	2.3	0.110
PTFE	PEEK	6	40	21	1.9	0.196	113	2.3	0.106
PTFE	PEEK	8	40	22	1.9	0.180	112	2.3	0.106
PTFE	PEEK	14	39	20	1.4	0.180	112	2.2	0.103
PTFE	PEEK	23	34	23	1.5	0.165	112	1.9	0.101

Table V.2: Linear viscoelasticity test results of PEEK/PTFE samples. A comparison between the crystalline content, damping factors, transition temperatures and S1, S2 indicators.

Adding PEEK to the PTFE (until 23 vol%) has minor effects on the linear viscoelasticity test when looking at the transition temperatures, damping factor or S1 and S2 indicators. At 23vol% of PEEK, the blend shows a drop in the S1 and S2 indicators accompanied by a light drop in the crystalline content.

Graph V.3 represents the evolution of the storage modulus and damping factor of the blends at several PEEK content. Before the β temperature transition ($T < 30^oC$), no evolution is noticed on the storage modulus. Meanwhile, after the β temperature transition, increasing the PEEK content contributes in increasing the storage modulus. A shy drop in the damping factor peaks (at the α transition) occurs when increasing the PEEK content.

An additional transition appears around 150^oC, this transition corresponds to the glass transition of the PEEK[163]. Therefore, on the damping factor curves the peak of this transition increases when increasing the PEEK content. The presence of two distinct transitions shows the immiscibility between the PTFE and the PEEK.

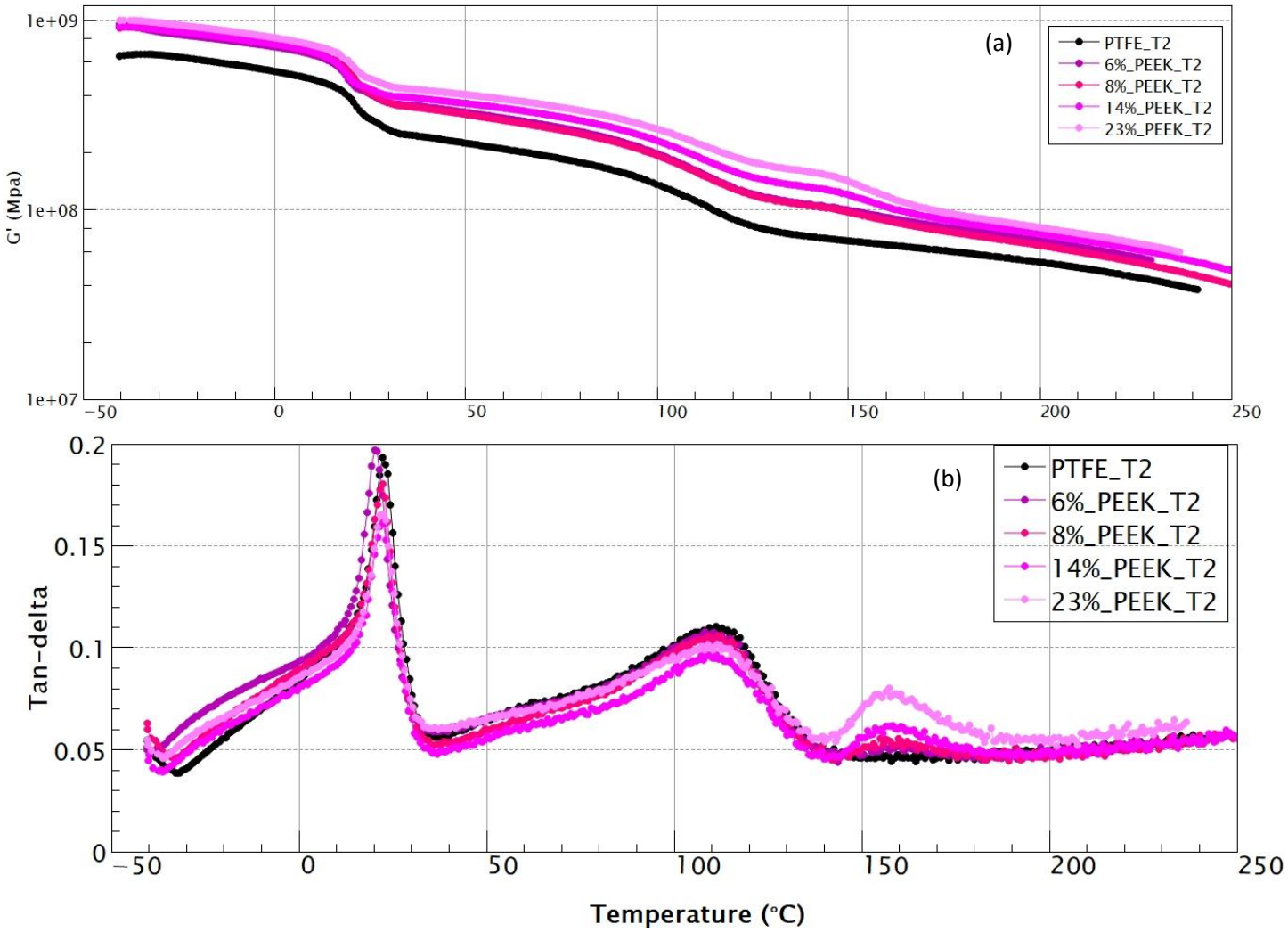

Graph V.3: Rectangular torsion testing on PTFE/PEEK samples. (a) Storage modulus and (b) damping factor)

3.2 DMA characterization

PTFE/PEEK blends were tested in the non-linear DMA, results are presented in the Table V.3:

PEEK content (vol%)	E' (-50ºC)	E'(30ºC)	E'(150ºC)	Tanδ (β)	T(β)	Tanδ (α)	T(α)
0	$1.40\ 10^9$	$6.12\ 10^8$	$3.69\ 10^7$	0.16	29	0.31	93
6	$1.41\ 10^9$	$6.78\ 10^8$	$4.00\ 10^7$	0.15	30	0.29	97
8	$1.47\ 10^9$	$6.83\ 10^8$	$4.05\ 10^7$	0.15	30	0.28	97
14	$1.46\ 10^9$	$7.43\ 10^8$	$4.44\ 10^7$	0.14	30	0.26	103
23	$1.44\ 10^9$	$7.93\ 10^8$	$4.02\ 10^7$	0.13	31	0.24	105

Table V.3: non-linear DMA results for PTFE/PEEK samples.

All PEEK/PTFE blends resisted to the non-linear DMA testing without breaking. Increasing the PEEK content contributed in increasing the temperature at the α transition (+12°C for sample 23%_PEEK_T2), meanwhile the temperature at the β transition remained around 30°C.

Both damping factors at α and β transitions decreased when increasing the PEEK content. On the other hand, the glass transition of the PEEK was not detected as seen in the Graph V.4.

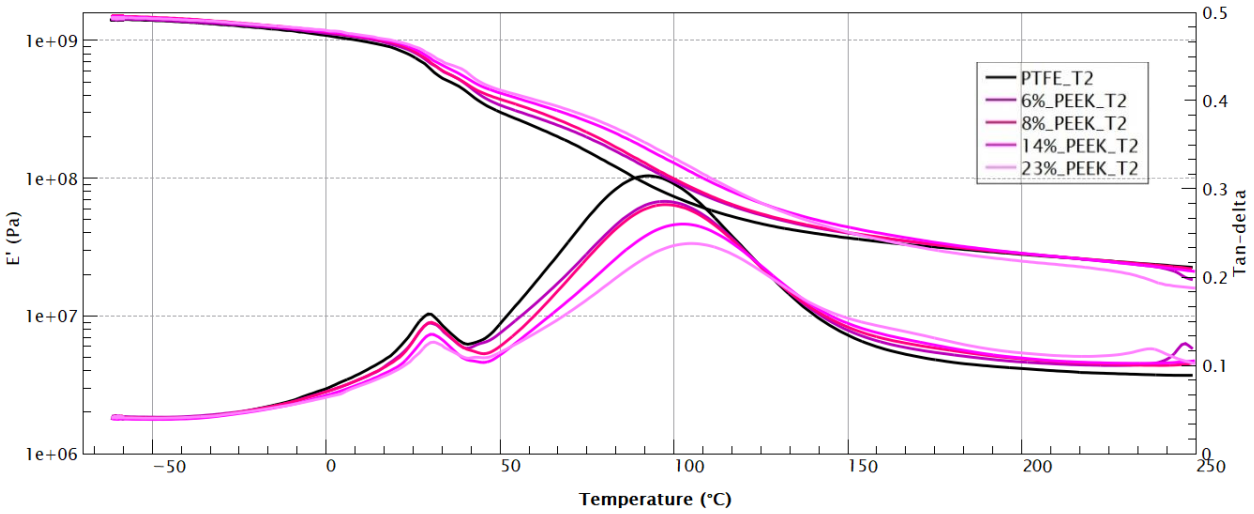

Graph V.4: DMA results for PTFE/PEEK samples.

The reinforcement of the PEEK is mainly observed between the β transition and the glass transition of the PEEK where the storage modulus is increased by the presence of PEEK.

3.3 Conclusion

In this section, the influence of the PEEK on the PTFE matrix was studied. Microscopic observations showed a drop-matrix morphology, with no adhesion between the peek and the PTFE. The crystalline content of the PTFE was not affected by the presence of the PEEK up to 23 vol % where a light drop was noticed. The linear viscoelasticity testing showed a constant storage modulus before the β transition and an increase after this transition when increasing the PEEK content.

Dynamic mechanical analysis testing did not show any breaking in the PTFE/PEEK blends and showed a noticeable increase in the α transition temperature when increasing the PEEK content. on the other hand, the glass transition of the PEEK was not detected in DMA, probably because of its low content in the blend.

4 Influence of PEEK content on PTFE/Silica blends

4.1 Microstructure characterization

After studying the influence of the PEEK content on the PTFE matrix, the influence of the PEEK on the PTFE/Silica 1 blends was studied.

As seen in the previous chapter, adding silica 1 to PTFE matrix increased the crystalline content. Around a filling of 8 vol% of silica, the crystallinity of PTFE was not affected. Meanwhile the addition of PEEK up to 23vol% did not change the crystallinity. Thus, at first, the influence of the PEEK content on the blend was studied with a fixed Silica 1 content of 8 vol%. This comparison has for goal to compare the influence of the PEEK content on PTFE/Silica blends without having an influence of the silica 1 on the PTFE.

Silica 1 content was fixed around 8 vol% and PEEK varied between 0 and 34 volume percent (comparison between samples 22%_PEEK_8%_gSi1_T2, 28%_PEEK_8%_gSi1_T2, 34%_PEEK_8%_gSi1_T2 and 8%_gSi1_T2. The variation of the crystalline content is illustrated in the Graph V.5.

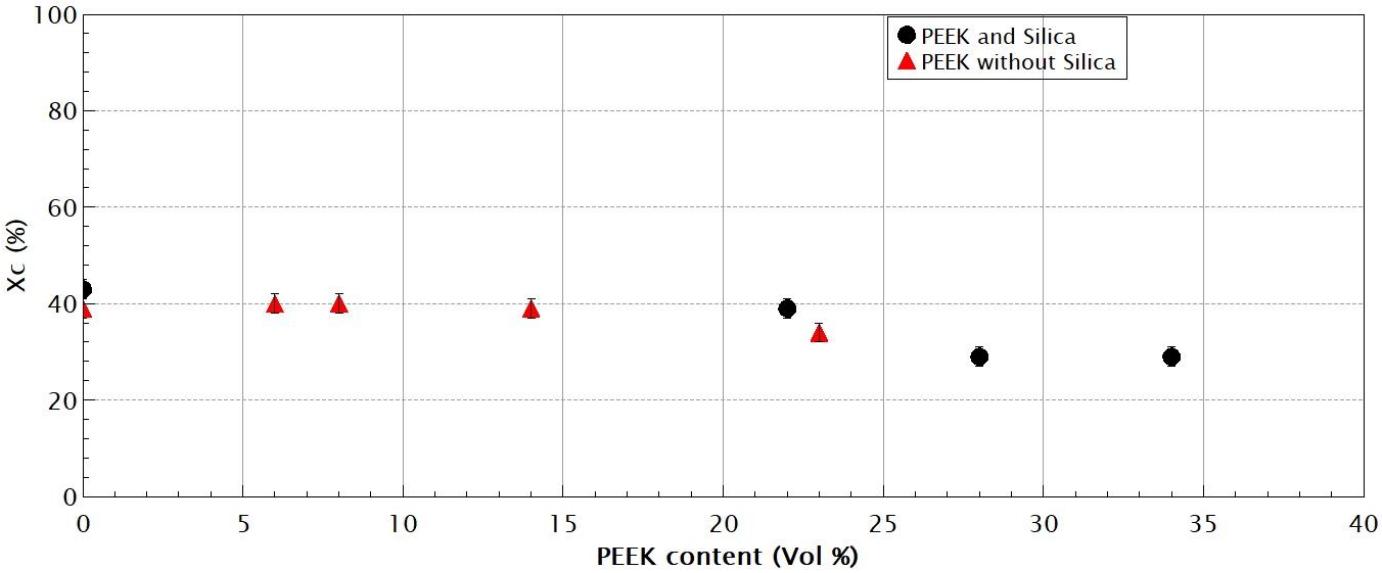

Graph V.5: Crystallinity content in PTFE/PEEK samples (triangle) vs. PTFE/PEEK/ 8 vol% Silica 1 (dots)

The red triangles represent the Samples PTFE_T2, 6%_PEEK_T2, 8%_PEEK_T2, 14%_PEEK_T2 and 23%_PEEK_T2 without silica. Black dots are samples with silica 1 at 8 vol% content.

Above 28 vol% of PEEK in the composite, the crystalline rate decreased by ~30 % (from 43 to 29%).

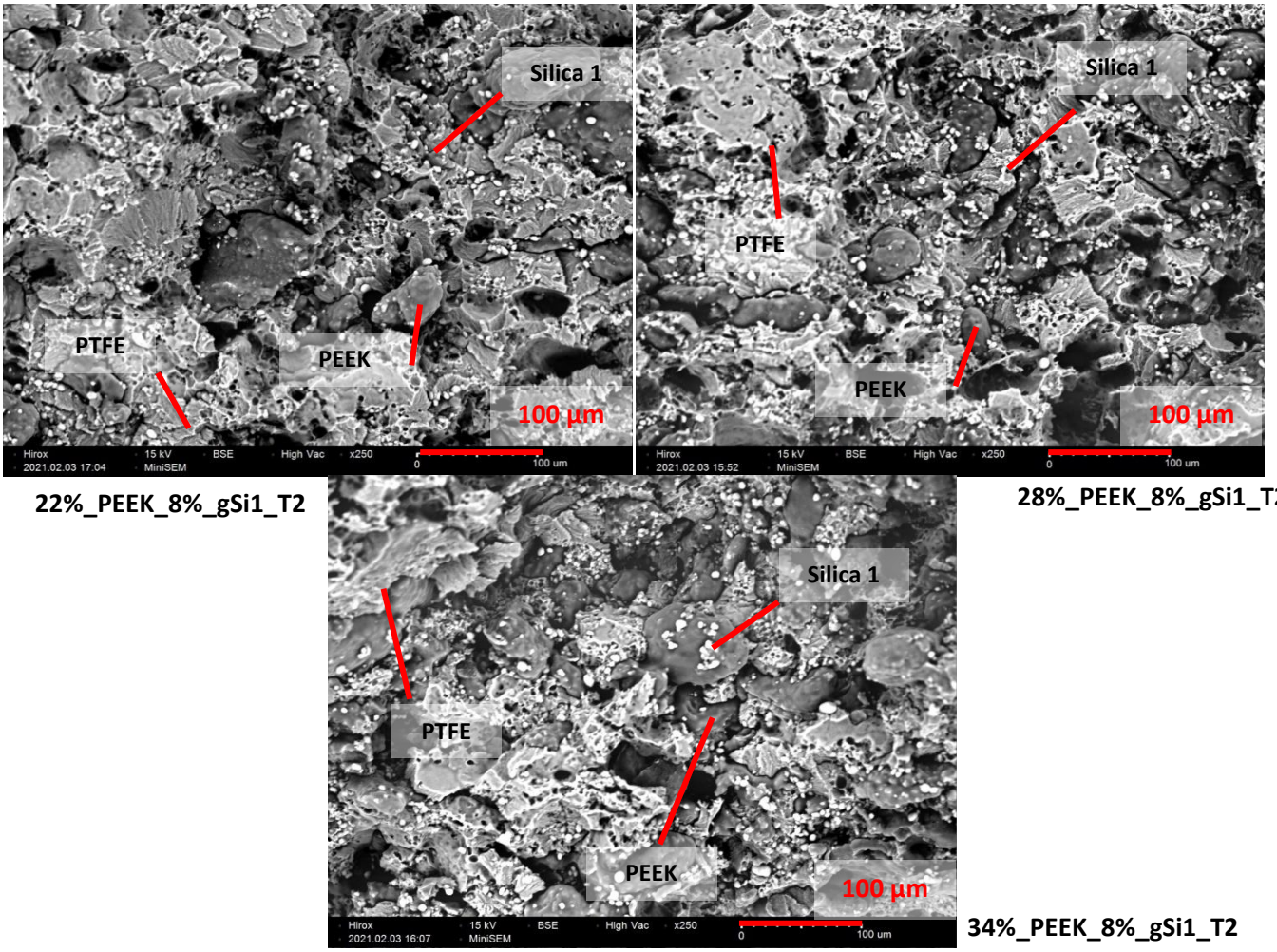

Figure V.3: Microscopic observations of samples L' M' and N' at 250x.

Microscopic observations show the evolution of the morphology of the blends when peek content increases. The photos confirm the presence of the Silica 1 distributed in both phases of the sample, i.e., both in the PEEK and the PTFE. The adhesion is still inexistent between all the components as demonstrated by the presence of voids between all phases.

The results of the linear viscoelasticity response of rectangular specimens in torsion oscillations of the samples 22%_PEEK_8%_gSi1_T2, 28%_PEEK_8%_gSi1_T2, 34%_PEEK_8%_gSi1_T2 and 8%_gSi1_T2 are represented in Table V.4:

Polymer 1	Polymer 2	PEEK Content (vol%)	Filler	Silica 1 Content (vol%)	Xc (%)	Tβ	S1	Tanδ (β)	Tα	S2	Tanδ (α)
PTFE	-	-	Silica 1*	8	43	21	1.6	0.190	112	1.9	0.107
PTFE	PEEK	22	Silica 1*	7	39	21	1.1	0.152	111	1.4	0.091
PTFE	PEEK	28	Silica 1*	7	29	23	0.9	0.135	111	1.3	0.089
PTFE	PEEK	34	Silica 1*	7	29	21	0.7	0.115	109	1.0	0.072

Table V.4: Linear viscoelasticity test results for samples 22%_PEEK_8%_gSi1_T2, 28%_PEEK_8%_gSi1_T2, 34%_PEEK_8%_gSi1_T2 and 8%_gSi1_T2.

S1 and S2 indicators show a decrease in the intensity of the PTFE transitions while the β and α transition temperature remained the same.

Graph V.6 presents the curves of the storage modulus and the damping factor of the samples 22%_PEEK_8%_gSi1_T2, 28%_PEEK_8%_gSi1_T2, 34%_PEEK_8%_gSi1_T2 and 8%_gSi1_T2.

These results show a marked reinforcement of the PEEK to the PTFE/Silica 1 blend after the β transition for all the samples and a reinforcement before the β transition when adding more than 22 vol % of PEEK. The reinforcement is mostly obvious between the α transition and the glass transition of the PEEK.

When comparing the storage modulus of the samples with PEEK to the sample without PEEK, the ratio of the storage modulus of samples with peek at 130°C over the storage modulus of the one without PEEK: $\frac{G'_{\text{samples with peek}}}{G'_{\text{sample without peek}}}$ shows a reinforcement by three times for the sample 34%_PEEK_8%_gSi1_T2.

Sample	G' (130ºC)	Ratio
22%_PEEK_8%_gSi1_T2	2.22 10^8	1.7
28%_PEEK_8%_gSi1_T2	3.10 10^8	2.4
34%_PEEK_8%_gSi1_T2	3.87 10^8	3.0

Table V.5: Storage modulus ratio between the sample 22%_PEEK_8%_gSi1_T2, 28%_PEEK_8%_gSi1_T2, 34%_PEEK_8%_gSi1_T2 and 8%_gSi1_T2 at 130°C.

Adding PEEK to the blend had an influence in increasing the storage modulus, the higher the PEEK content the more the reinforcement of G'.

For unfilled PTFE, the crystalline rate is inversely proportional with the damping factor around the α transition. When adding PEEK to the blend, results show a mutual decrease between the crystalline rate and the intensity of the damping factor. The reason behind this decrease in the damping factor is simply the decrease of the PTFE content in the blend.

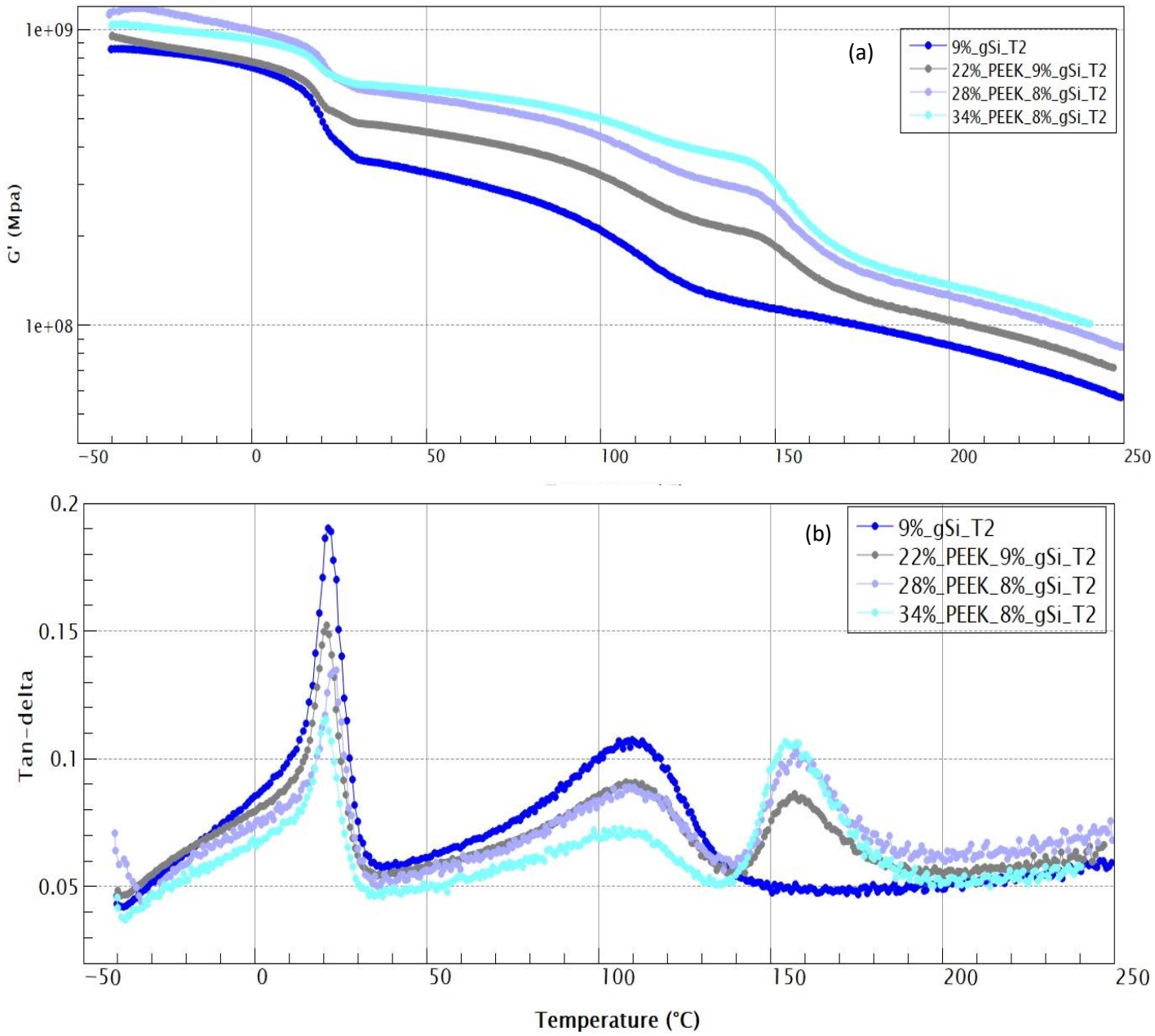

Graph V.6: (a) Storage modulus and (b) damping factor of samples 22%_PEEK_8%_gSi1_T2, 28%_PEEK_8%_gSi1_T2, 34%_PEEK_8%_gSi1_T2 and 8%_gSi1_T2.

4.2 Non-linear DMA characterization

Traction compression oscillation tests results are summarized in the Table V.6:

Sample	E' (-50ºC)	E'(30ºC)	E'(150ºC)	Tanδ (β)	T(β)	Tanδ (α)	T(α)
22%_PEEK_8%_gSi1_T2	$1.60\ 10^9$	$9.55\ 10^8$	$7.19\ 10^7$	0.117	31	0.216	112
28%_PEEK_8%_gSi1_T2	$1.73\ 10^9$	$1.12\ 10^9$	$1.55\ 10^8$	0.104	31	0.174	116
34%_PEEK_8%_gSi1_T2	$1.66\ 10^9$	$1.13\ 10^9$	$2.66\ 10^8$	0.098	31	0.140	119
8%_gSi1_T2	$1.65\ 10^9$	$8.53\ 10^8$	$5.03\ 10^7$	0.151	32	0.283	102

Table V.6: non-linear DMA results for 22%_PEEK_8%_gSi1_T2, 28%_PEEK_8%_gSi1_T2, 34%_PEEK_8%_gSi1_T2 and 8%_gSi1_T2 samples. The table represents the transition temperatures, the damping factors and the storage modulus at different temperatures.

Graph V.7 presents the non-linear DMA curves for 22%_PEEK_8%_gSi1_T2, 28%_PEEK_8%_gSi1_T2, 34%_PEEK_8%_gSi1_T2 and 8%_gSi1_T2:

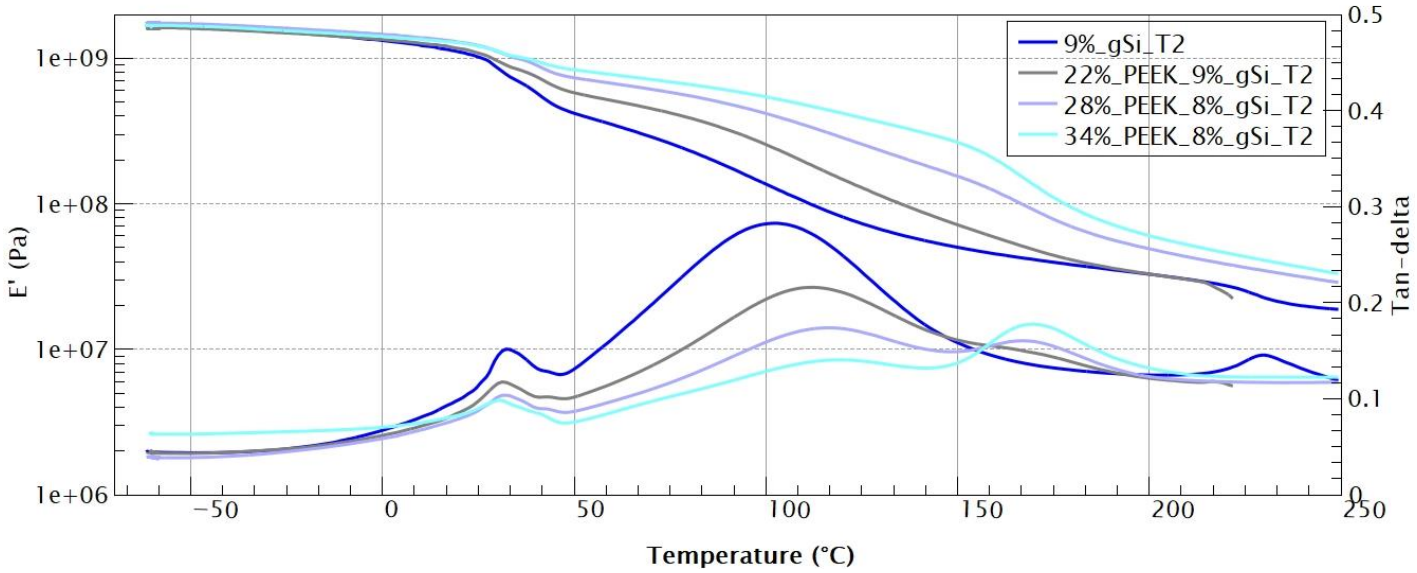

Graph V.7: non-linear DMA curves for samples22%_PEEK_9%_gSi1_T2, 28%_PEEK_8%_gSi1_T2, 34%_PEEK_8%_gSi1_T2 and 9%_gSi1_T2. The graph shows the storage modulus (E') and the damping factor Tan-delta.

Adding Silica to the PEEK/PTFE blend increased further the transition temperature at the α transition (17ºC for the sample 28%_PEEK_8%_gSi_T2). Meanwhile the temperature at the β transition remained the same. As for the damping factors there is a slight decrease in the value due to the increase of the PEEK content.

As it was also the case in the linear viscoelasticity testing, non-linear DMA testing results show an increase in the storage modulus only after the β transition. This enhancement is proportional to the PEEK content in the blend. The higher the PEEK content the higher the reinforcement of the storage modulus E'. It can also be noticed that the PEEK transition can be detected in DMA testing after 28 vol% content.

4.3 Conclusion

In this section the influence of the PEEK content on PTFE/8 vol% Silica 1 was studied. On a microstructure level, the addition of PEEK to the PTFE/Silica 1 blend decreased the crystalline content when adding more than 28 vol% of PEEK, this decrease was accompanied by an increase of the torsion storage modulus G' mostly after the β transition of the PTFE.

In the non-linear DMA testing, the same tendencies as the linear DMA response were noticed, i.e., a reinforcement of the torsion storage modulus E' after the β Transition.

5 Influence of Silica content on PTFE/PEEK blends

5.1 Microstructure characterization

After seeing the influence of the PEEK content on the microstructure and mechanical properties of the PTFE and PTFE/Silica 1 (8 vol%) blends, in this section, the content of PEEK is fixed and the content of silica varies. The purpose is to evaluate the influence of the Silica 1 on the PTFE/PEEK blends through the microstructure and the mechanical testing. The goal is also to observe the limits of filling the PTFE with silica and PEEK before breaking in non-linear testing.

In this section, the content of PEEK was fixed at ± 22 vol% and the silica content varied between ±9 and ±24 vol%. **All samples are produced with the temperature cycle 2**. (c.f. III.3.4.2).

Crystallinity of blends filled with PEEK and Silica were compared to the samples filled with only Silica (prepared with the same temperature cycle 2). The results can be seen in the Graph V.8 below:

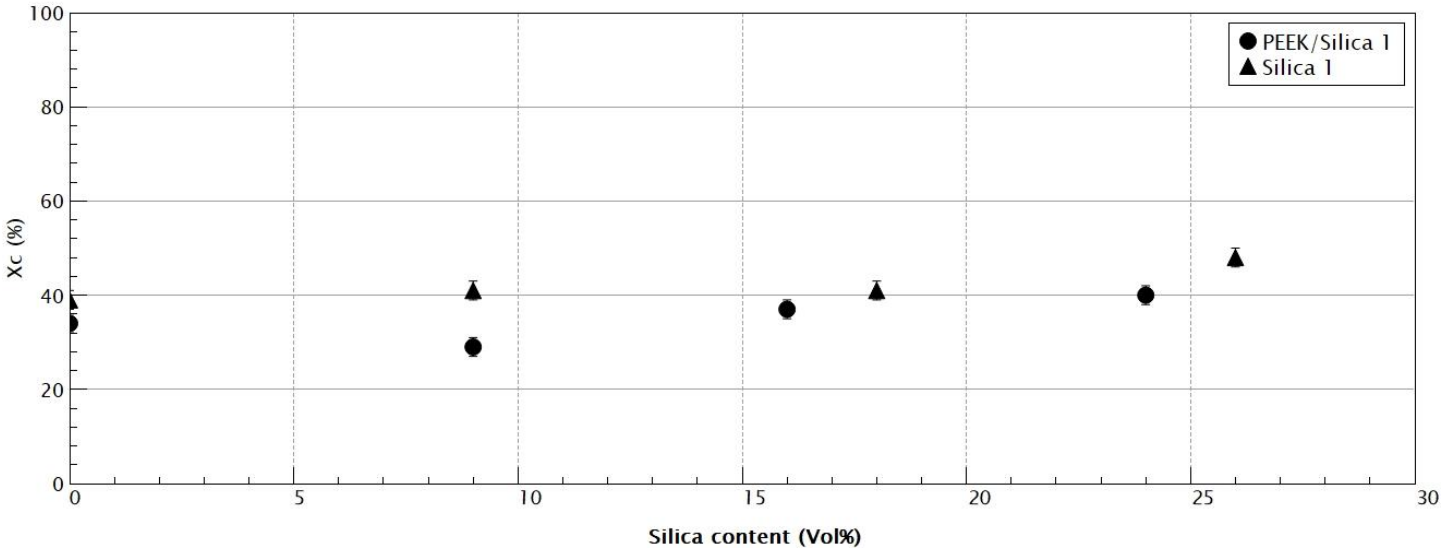

Graph V.8: Crystalline content of PTFE samples filled with silica 1 at different contents (triangles) and PTFE samples filled with silica 1 at different contents and PEEK at 22 vol% (dots)

The values of the crystalline content when adding PEEK to the PTFE/Silica 1 blends is inferior to those without PEEK. This could indicate a decrease in the indentation phenomenon in the PTFE matrix. However, even for a fixed PEEK content (22 vol%), the same trend of increasing the crystalline content when increasing the Silica 1 content is observed, i.e., an increase from 34 to 40 % in the crystalline content between sample 23%_PEEK_T2 and samples 20%_PEEK_24%_Si1_T2.

Linear response of the rectangular specimens in torsion results are shown in Table V.7:

PEEK content (vol%)	Silica 1 content (vol%)	Xc (%)	Tβ	S1	Tanδ (β)	Tα	S2	Tanδ (α)
0	0	39	22	1.9	0.193	113	2.3	0.110
0	8	41	23	2.0	0.184	113	1.9	0.108
23	0	34	23	1.5	0.165	112	1.9	0.101
22	7	29	23	0.7	0.129	112	1.2	0.082
21	14	37	22	1.1	0.132	113	1.3	0.087
20	20	40	22	0.9	0.138	112	1.1	0.085
0	15	41	23	0.9	0.187	111	1.6	0.11
0	22	48	23	1.3	0.186	112	1.1	0.097

Table V.7: Linear viscoelasticity test results of PTFE samples filled with different silica 1 content with or without ±22vol% PEEK.

The addition of Silica 1 to the PTFE and PTFE/PEEK blends contributed in decreasing the S2 indicator, the same trend seen in chapter IV. The temperature of the α and β transitions remained the same.

Samples 23%_PEEK_T2, 22%_PEEK_9%_Si1_T2, 21%_PEEK_16%_Si1_T2 and 20%_PEEK_24%_Si1_T2 are PTFE filled with different silica content and a ±22 vol% of PEEK. The storage modulus curve and its damping factor are presented in the Graph V.9:

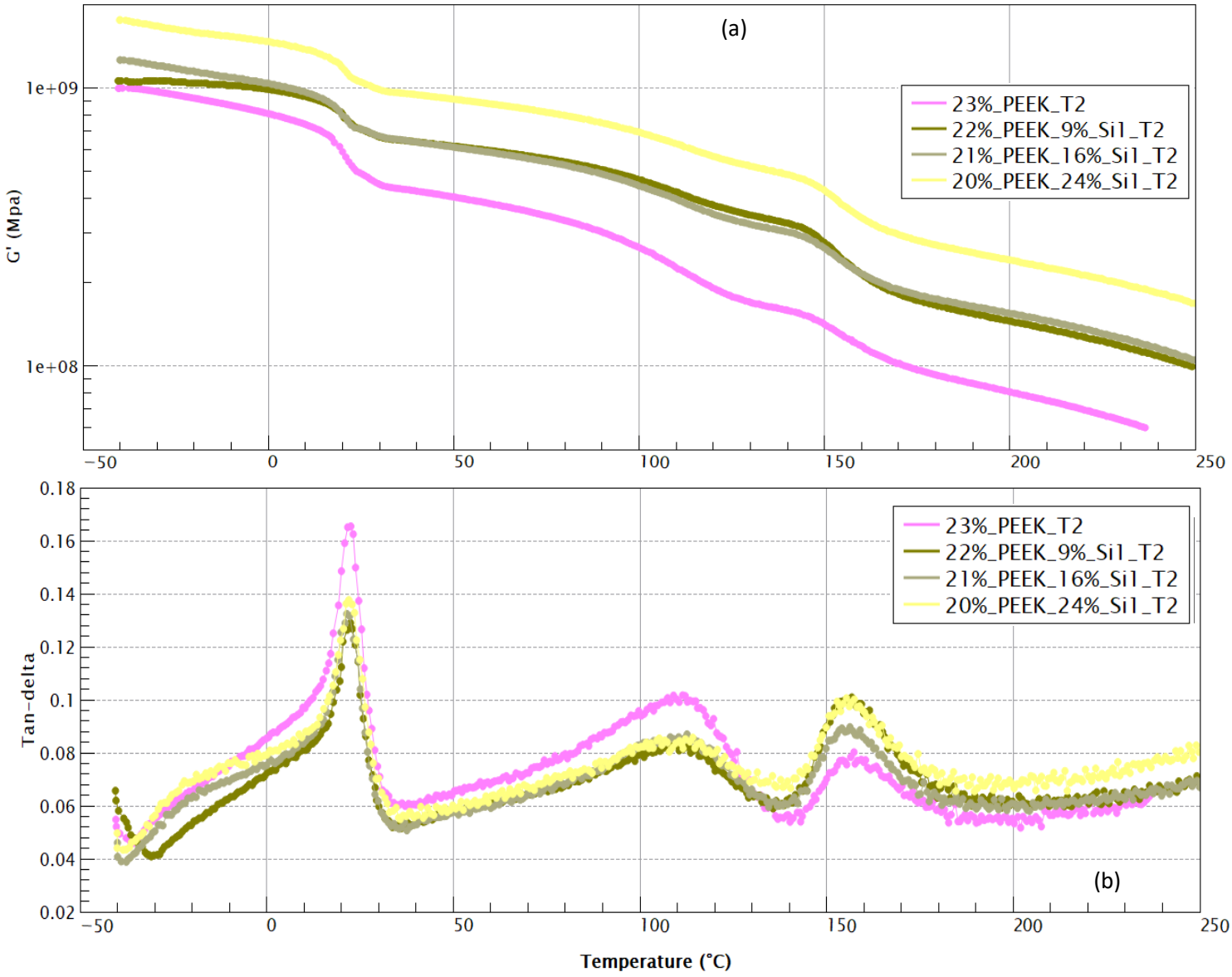

Graph V.9:(a) Storage modulus and (b) damping factor of samples 23%_PEEK_T2, 22%_PEEK_9%_Si1_T2, 21%_PEEK_16%_Si1_T2 and 20%_PEEK_24%_Si1_T2 (with 22vol% PEEK).

With no surprise, the storage modulus value increased when adding silica 1 to the blends. This is a trend already seen with samples containing no PEEK. In the same way the damping factor at the α and β transitions decreased when adding the Silica 1.

Comparing the damping factor at the α transition and its S2 indicator with samples without PEEK is presented in the Graph V.10.

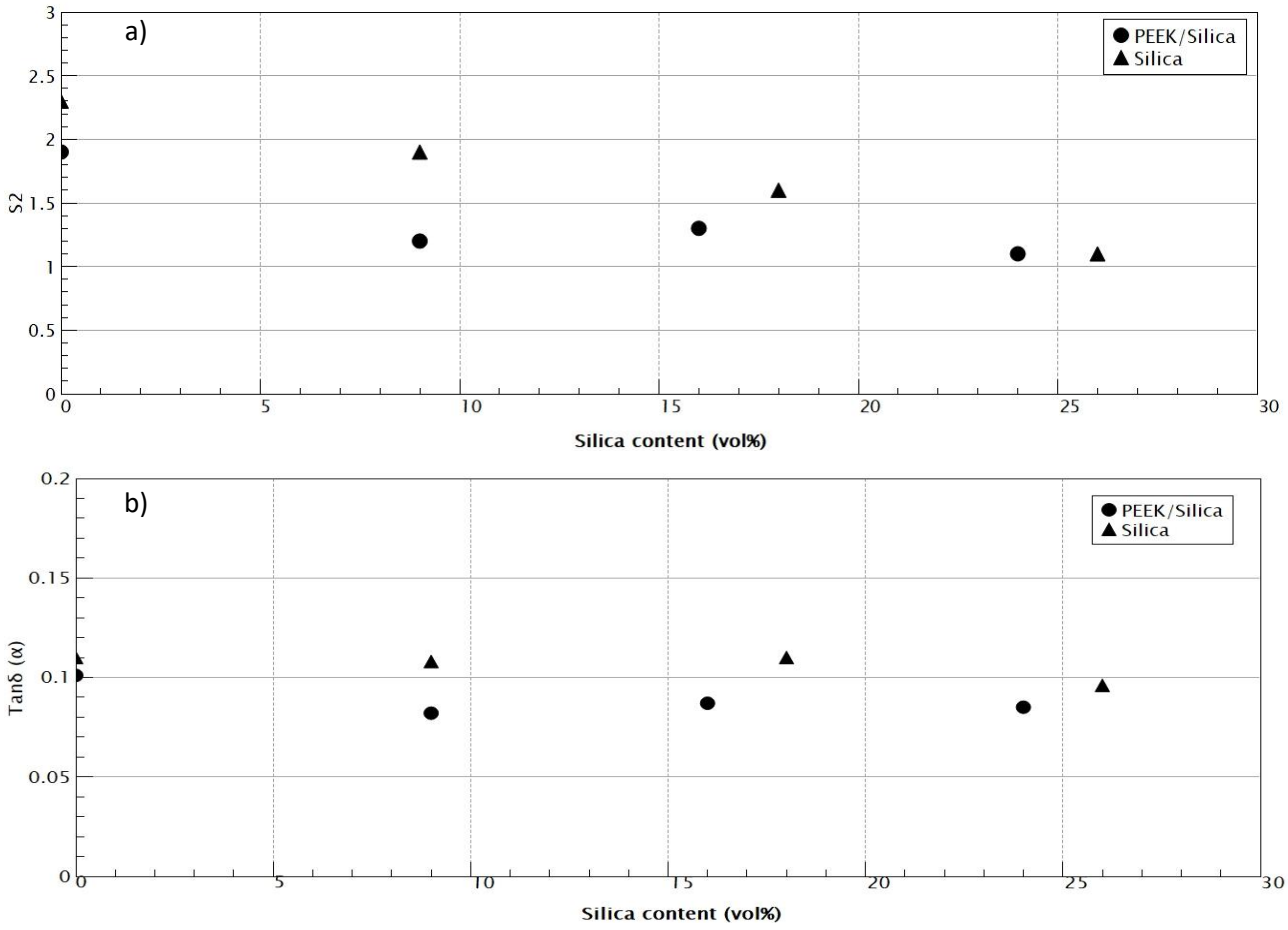

Graph V.10: S2 indicators (a) and damping factors intensity (b) for PTFE filled with silica 1 (triangle) and PTFE filled with silica 1 and PEEK (dot).

Despite the lower values of S2 at the α transition when adding PEEK to the blend caused by the lower crystalline content, both sample groups have the same tendency of decreasing when increasing the silica 1 content. For the damping factor, when adding PEEK to the blend values are lower than samples without PEEK.

5.2 Non-linear DMA characterization

The influence of silica 1 content on PTFE/PEEK blends was also tested in non-linear dynamic mechanical analysis.

The results are presented in the Table V.8:

Sample	E' (-50ºC)	E'(30ºC)	E'(150ºC)	Tanδ (β)	Tβ (ºC)	Tα (ºC)	Tanδ (α)	T(B) (ºC)
PTFE_T2	$1.4\ 10^9$	$6.1\ 10^8$	$3.7\ 10^7$	0.16	29	93	0.31	-
9%_Si1_T2	$1.6\ 10^9$	$8.6\ 10^8$	$6.2\ 10^7$	0.14	32	107	0.26	-
23%_PEEK_T2	$1.4\ 10^9$	$7.9\ 10^8$	$4.0\ 10^7$	0.13	31	105	0.24	-
22%_PEEK_9%_Si1_T2	$1.7\ 10^9$	$1.0\ 10^9$	$9.5\ 10^7$	0.11	30	114	0.20	-
21%_PEEK_16%_Si1_T2	$1.8\ 10^9$	$1.2\ 10^9$	$1.7\ 10^8$	0.10	32	119	0.17	219
20%_PEEK_24%_Si1_T2	$2.0\ 10^9$	$1.3\ 10^9$	$2.5\ 10^8$	0.10	33	123	0.15	170
26%_Si1_T2	$1.89\ 10^9$	$1.18\ 10^9$	$1.08\ 10^8$	0.13	34	116	0.21	165

Table V.8: non-linear DMA results for PTFE filled with Silica 1 with and without PEEK at 22vol%. All the samples with a silica content higher than 14 vol% broke during the test. The higher the silica content the lower the temperature at break.

All samples with a silica 1 content above 14 vol% broke during the DMA testing. The higher the silica 1 content the lower the temperature for which breaking occurred in the test.

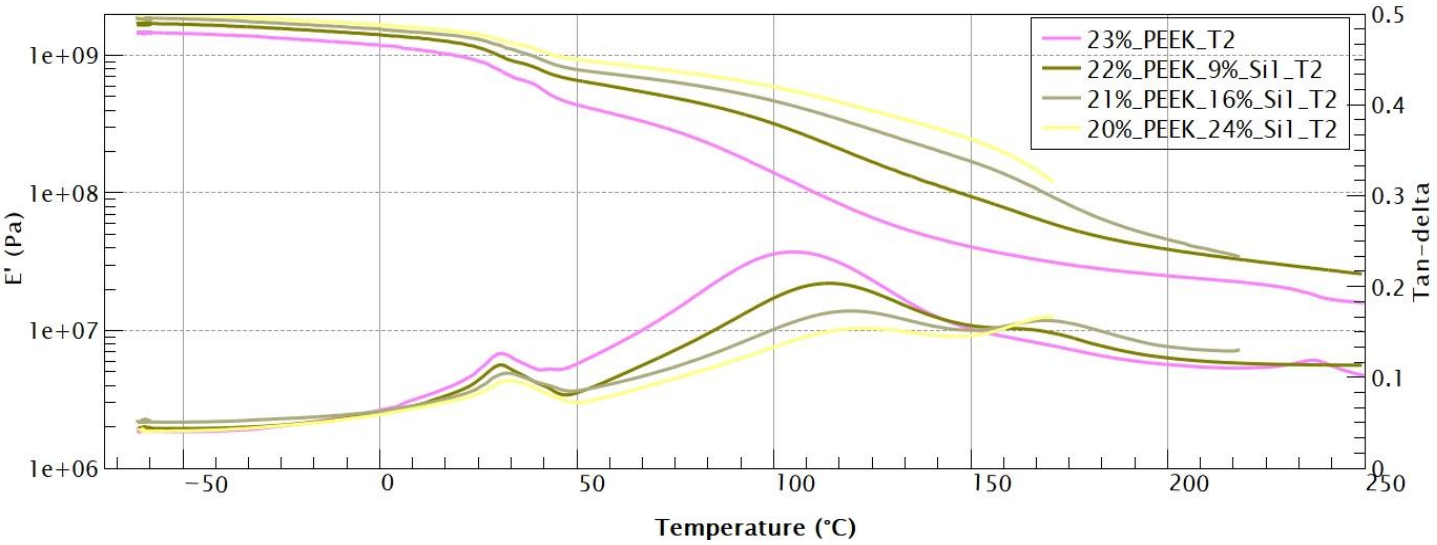

Graph V.11: non-linear DMA curves of samples filled with Silica 1 at different content and 21 vol% of PEEK.

The addition of the PEEK to the PTFE/Silica blend contributed in a further increase in the α transition temperature.

This increase is illustrated in Graph V.12. The increase in the alpha transition temperature is observed when increasing the silica content. This is also seen for samples filled with only silica.

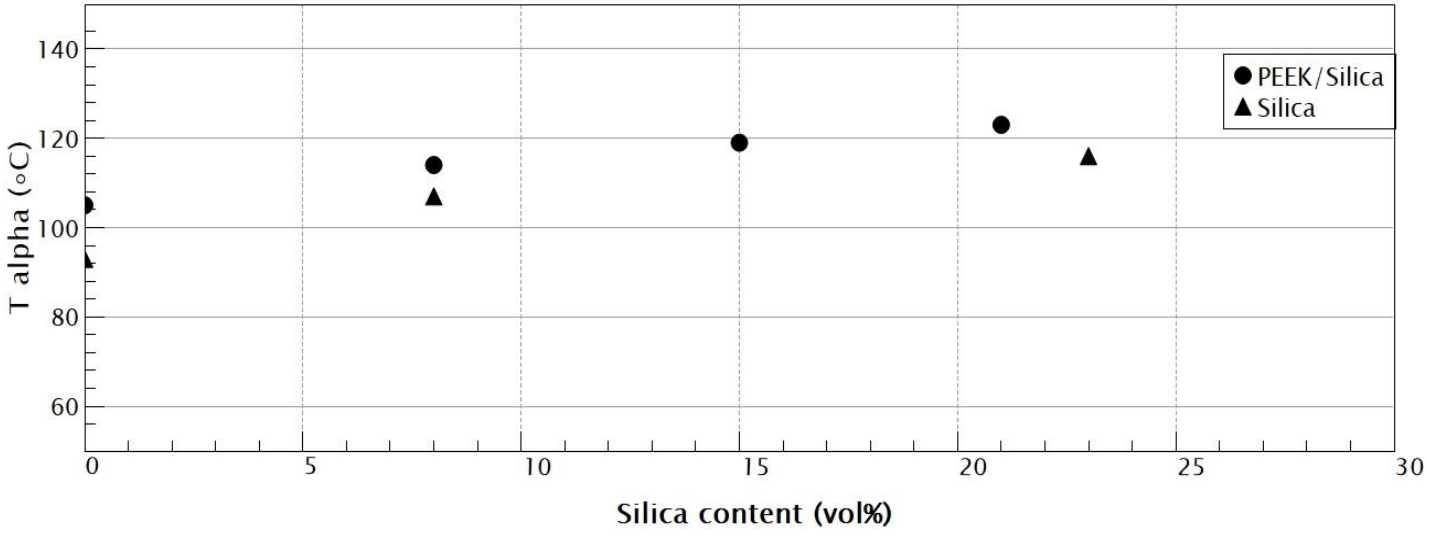

Graph V.12: comparison of the α transition temperature for PTFE filled with Silica 1 at different content and Silica 1/PEEK at 22 vol%.

The highest value of the α temperature transition is obtained with PEEK (± 22 vol%) added to the blend with the highest silica 1 content, i.e., sample 20%_PEEK_24%_Si1_T2; for this particular blend the α transition occurred at 123°C.

5.3 Conclusion

At this stage, adding PEEK to the PTFE/Silica 1 blends showed a better reinforcement of the storage modulus, an increase in the temperature transitions and a decrease in the crystalline content. Yet, adding PEEK to the silica blend for a silica 1 content higher than 14 vol% did not prevent the breaking in the DMA testing.

6 Discussion

In this section, the results presented in the previous sections will be discussed. The addition of the PEEK to PTFE matrix and PTFE/Silica 1 blends had an influence on the microstructure and on the mechanical properties in the DMA testing. Two essential results will be discussed: firstly, the influence of the PEEK on the crystalline content of PTFE/Silica 1 blends and secondly, the failing

in the DMA testing. In addition, an explanation of the influence of the filler on the rheological behavior around the α transition will be proposed.

6.1 Crystallinity results

The intended purpose of adding PEEK to the PTFE/Silica 1 blend is to decrease the crystalline content of the blend by limiting the indentation mechanism described in chapter IV. In other words, the role of the PEEK would be the reduction of the internal stresses caused by the filler to the PTFE matrix.

Looking at the PTFE/PEEK blends, PEEK has no effect on the PTFE crystallinity for a content lower than 23 vol%. This result is not chocking if considering the mechanism of polymer blends. Under a rate of 20 vol % of polymer B in a polymer A matrix the morphology tend to be a "droplet – matrix" morphology[164]. Between 20 vol% and 40 vol% the morphology of the blend is a partially continuous phase of polymer B in a polymer A matrix. Between 40 vol% and 60 vol% a continuous morphology is noticed[164]. The morphology of the blends was highly studied by many authors[164], the final morphology is influenced by several parameters such as the temperature, the mixing time, shear and the viscosities of the polymers.

In the case of this study, the mixing of the polymer powders occurred before the melting and melting was in a static phase. Therefore, the mechanisms for polymer blending in the melting phase do not fully apply. Nevertheless, it can be considered that one of the main parameters influencing morphology in dynamic and static blending is the content of each polymer phase. In addition, the difference in the viscosities of the two molten polymers could influence the morphology of the blend and its behavior in the dynamic analysis.

Generally, an extraction of the polymer B from the polymer A is made by dissolving the phase B and the continuity index is calculated by respecting the following equation:

$$\%\ continuity\ of A = \frac{m_{initial} - m_{final}}{m_{initial} * \phi_A} \qquad (V.3)$$

Where $m_{initial}$ is the mass before dissolving, m_{final} is the mass after dissolving and φ_A is the weight fraction of the polymer A in the blend.

Unfortunately, in this study, both polymers have a high chemical resistance and are therefore hard to dissolve. Hence, observation of the morphology of the blend through this technique cannot be achieved.

However, Burris et al.[134] studied the tribological properties of unfilled PEEK/PTFE blends at different rates of PEEK produced with compression molding. Their microscopic observations

showed a continuous phase of PEEK in the PTFE blend around 20 wt% of PEEK content, an equivalent of ~30 vol% of PEEK.

Therefore, for unfilled blends, a blending around 30 vol% of PEEK is needed to obtain a partially continuous phase of PEEK in the PTFE matrix.

In this work, higher PEEK content led to a decrease in the crystalline content of the PTFE (Graph V.12, for filled and unfilled samples). Knowing that the expected start of the continuous phase of PEEK is expected around 23 vol%, it would be probable that the continuous phases of PEEK created in the composite contribute in reducing the stresses on the PTFE.

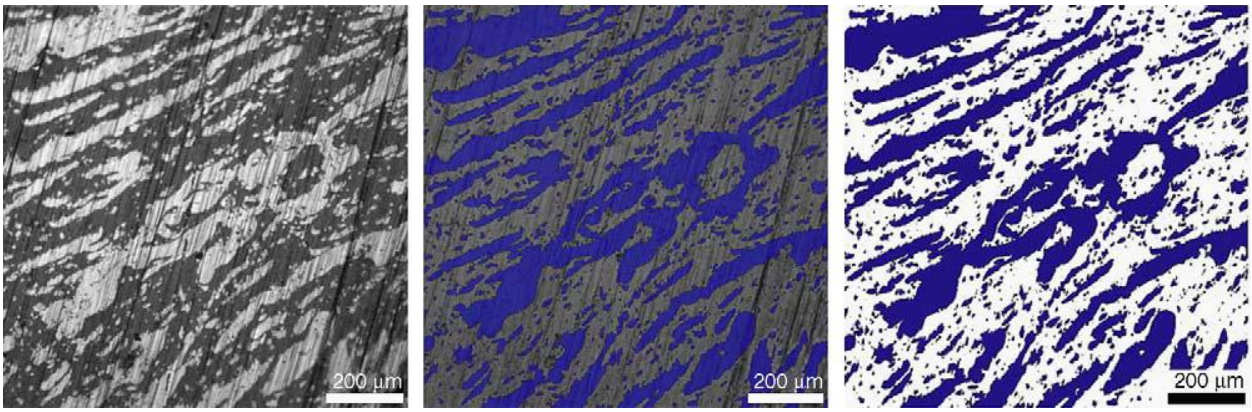

Figure V.4: SEM photos of Burris et al's[134] study showing a blend of PEEK filled PTFE at 20wt %. "Left: original image with PEEK at the light-colored phase; *center: PEEK is highlighted in blue*; *right: The background PTFE is removed for clarity. There is a clearly networked region of PEEK containing regions of PTFE in the center of the image".*

These results prove the contribution of the PEEK in limiting the indentation mechanism of the silica 1 on the PTFE. Microscopic observations showed the presence of the silica in the PTFE, the PEEK and the interphase PEEK/PTFE. So, on one hand having silica 1 in the PEEK phase reduces automatically the silica 1 content in the PTFE phase and therefore the amount of silica available for the indentation of the PTFE. On the other hand, the silica present at the PTFE/PEEK interphase can exercise indentation on both PTFE and PEEK. Knowing the low viscosity of the PEEK (10^2-10^3Pa.s) the silica would probably exercise this force and deform easily the PEEK particle leading to a decrease in the indentation on the PTFE phase. Once the stresses on the PTFE matrix are lowered, the crystallization of the PTFE occurs with less internal stresses and the crystalline content decreases. Figure V.5 illustrates the morphology obtained in this study: PEEK formed droplets or a start of a co-continuous phase in the PEEK and Silica 1 is present in both phases PEEK and PTFE.

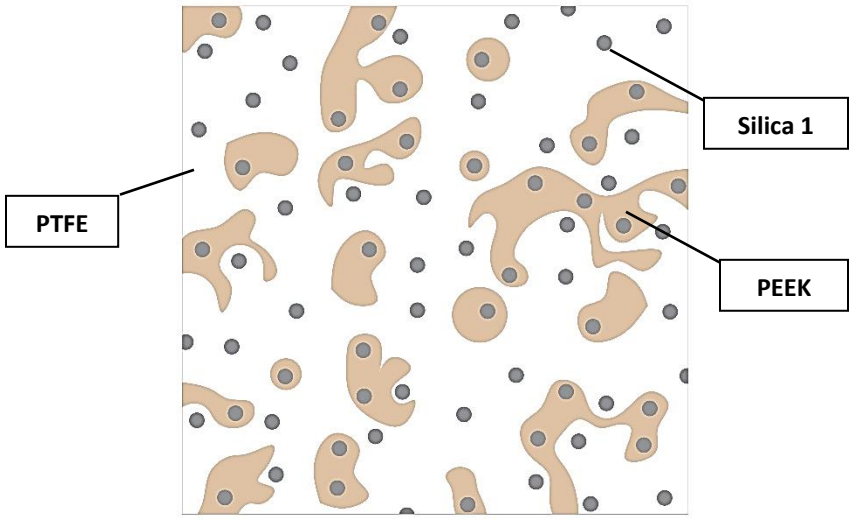

Figure V.5: Illustration of the morphology obtained in this study

6.2 Linear DMA response

Linear DMA testing on samples showed changes in the behavior when adding PEEK to the PTFE and PTFE filled with silica 1 blends (8 vol%). PEEK showed a reinforcement in the storage modulus G' even at low content (6 vol%). This reinforcement was accompanied with a decrease in the S2 indicator, therefore better stabilization of the drop in the storage modulus around the α transition. The reinforcement of the PEEK was observed mainly after the β transition where the conformity of the crystalline chain changes from phase IV to phase I. Around this transition the storage modulus experiences a drop in the storage modulus followed by another drop at the α transition assigned to the relaxation of the large sections of the macromolecules. On the other hand, PEEK in this temperature range has only one transition around 150°C[165], meaning that before this temperature, PEEK conserves its storage modulus. Therefore, between the β transition and the glass transition of the PEEK, the storage modulus is maintained thanks to the storage modulus of PEEK and its thermal stability.

PTFE filled with different Silica 1 contents showed a reinforcement in the storage modulus accompanied by a decrease in S2 and the damping factor around the α transition. The same behavior was observed when adding 22 vol% of PEEK to the blend, a reinforcement in the storage modulus accompanied by a decrease in S2 and the damping factor around the α transition. However, the values of the S2 indicator and the damping factor are lower in that last case. Thus, a combination of Silica 1 and PEEK contributes in the enhancement of the storage modulus and its stability through temperature.

6.3 Non-linear DMA

6.3.1 Storage modulus reinforcement

Dynamic mechanical testing for PEEK added to the PTFE samples showed a reinforcement of the PTFE matrix between the β transition and the glass transition of the PEEK. This reinforcement was evaluated by dividing the storage modulus E' of the blend with storage modulus E' of the PTFE samples.

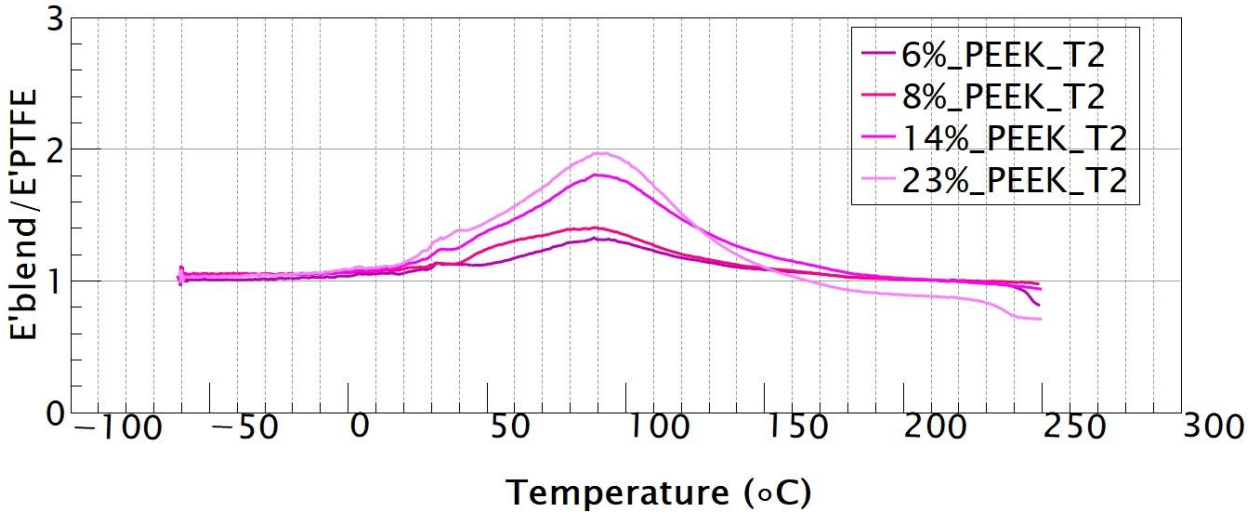

Graph V.13: Storage modulus ratio between the PTFE/PEEK blend and the pure PTFE sample.

The curves in the Graph V.13 highlights the reinforcement of the PEEK to the PTFE matrix. It is visible that the reinforcement occurs essentially between 20°C and 150°C. The value of the storage modulus in the sample 23%_PEEK_T2 is multiplied by 2. After 150°C, the value of the glass transition of the PEEK, the reinforcement is inexistent compared to virgin PTFE. Therefore, it can be noted that PEEK and PTFE have the same mechanical behavior in dynamic tension oscillation for temperatures lower than 30°C (Phase IV of the PTFE) and higher than 150°C (after the α transition of the PTFE and the glass transition of the PEEK). In between those 2 temperatures, PEEK shows a better stability to temperature compared to PTFE. This result is compatible with the linear response testing.

Adding Silica 1 in the PTFE blend also generated a reinforcement in storage modulus. In order to better compare this reinforcement with the one where PEEK was added to the PTFE/Silica 1 blend, the storage modulus of the PTFE/Silica 1 blends was divided with the neat PTFE storage modulus. The storage modulus of the blends containing both PEEK and silica 1 was divided with the storage modulus of the PTFE/PEEK (23vol%) blend (23%_PEEK_T2). The curves are presented in the Graph V.14 and Graph V.15.

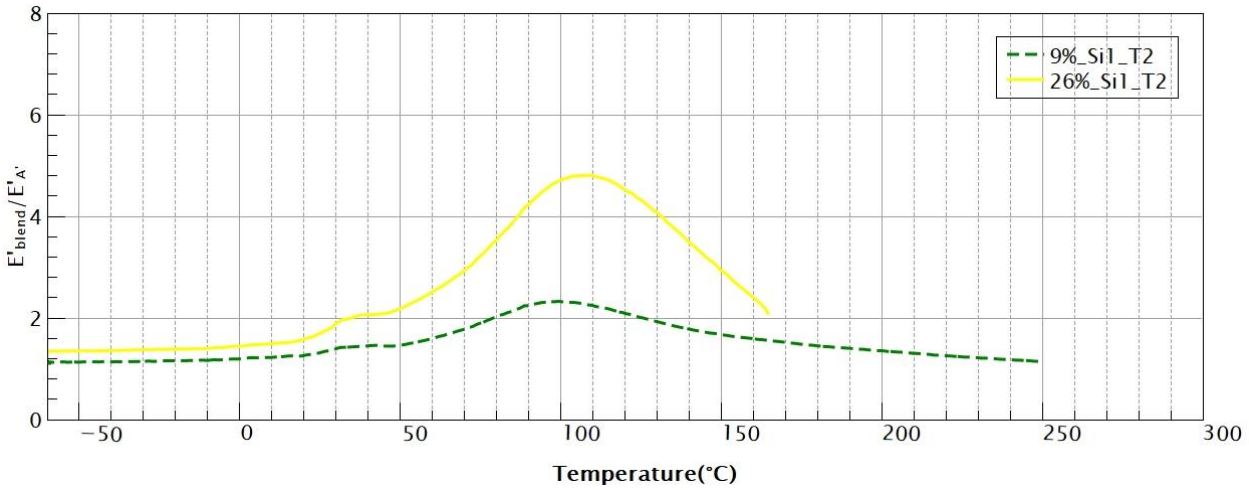

Graph V.14: Storage modulus ratio between the PTFE/Silica 1 blend and the pure PTFE sample (PTFE_T2).

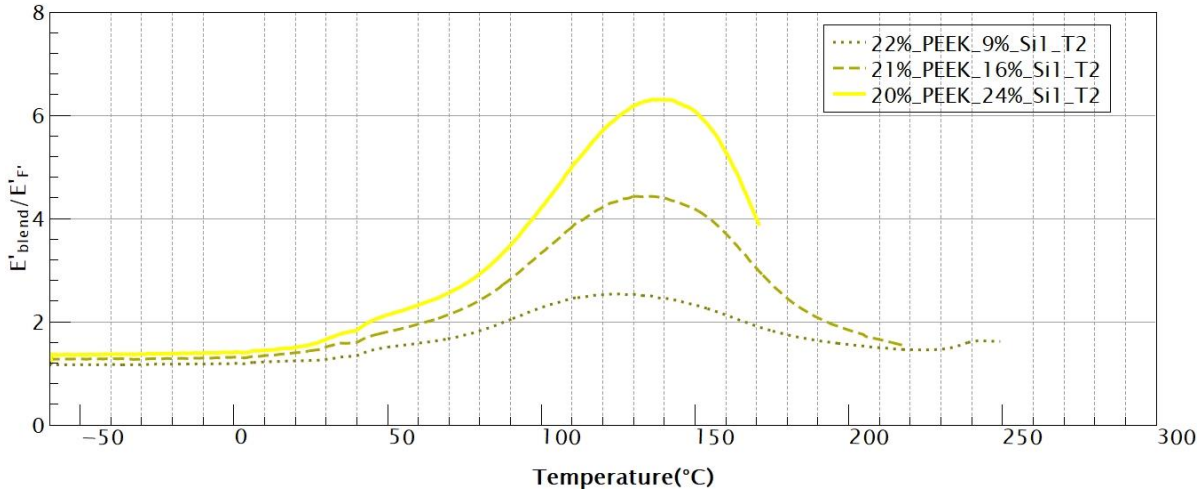

Graph V.15: Storage modulus ratio between the PTFE/PEEK/Silica 1 blend and the PTFE/PEEK (23vol%). samples contain respectively 9 16 and 24 vol% of silica 1

It is remarkable through these curves that the addition of silica 1 to the neat PTFE matrix (Graph V.14) reinforces the storage modulus by a factor of 2 for sample 9%_Si1_T2. Moreover, the PEEK added to these blends (by a 22 vol%) enhanced this reinforcement (Graph V.15) leading to factors of 2.5 for sample 22%_PEEK_9%_Si1_T2 and 6.4 for sample 20%_PEEK_24%_Si1_T2.

These results confirm that PEEK and Silica 1 are complementary in enhancing the storage modulus in non-linear DMA testing.

6.3.2 Transition temperature variation

A particular result is seen in Graph V.4 where the glass transition of the PEEK is undetected. Different explanations could be given to this. Knowing that the PTFE and the PEEK are immiscible polymers it could not be a merging of the glass transitions between the PTFE and the PEEK. In addition, this result was only seen on the non-linear testing and not on the linear one (Graph V.3).

Another remarkable phenomenon observed in the non-linear DMA testing is the evolution of the α transition temperature with the evolution of the blends. When considering the sample formed with only neat PTFE (PTFE_T2), its α transition temperature is around 93°C in the non-linear DMA testing. This transition is around 112°C in linear testing. Both tests have the same temperature range (from -50°C to 250°C with 3°C/min), the difference between those two tests is that the non-linear testing is based on a stress-control (5 Mpa in traction compression) while the linear testing is a strain-control test (0.1% strain in torsion). When working with stress-controlled testing the strain varies through the test; this causes a variation in the strain imposed to the sample and therefore influences the transition temperature such as the α transition. The higher the strain variation given to the system the lower is the transition temperature, explaining the difference of the transition temperature between the linear and non-linear tests (e.g.: sample PTFE_T2 where is α transition temperature in the non-linear testing is lower than the linear testing).

Adding fillers to the blend showed an increase in the α transition temperature exclusively in the non-linear testing. This increase reflects the absorption of the energy evolution in the testing by the filler. By adding the silica filler, the α transition temperature in the non-linear test increases to a value close to the one obtained in the linear testing. This evolution in the transition temperatures is studied by Salomko et al.[166] on Polystyrene and Polymethylmethacrylate filled blends where the strain-rate change has a high influence on the transition temperatures. Salomko et al. highlighted that depending on the polymer it could be influenced or not by the strain-rate change.

The results presented in this chapter highlighted the contribution of the PEEK in limiting the indentation phenomenon by limiting the increase of the crystalline content in the composite. However, this contribution has its limit when considering non-linear DMA testing, where samples broke through the test at filler content higher than 14 vol%. A combination of effects could explain this occurrence. Even though PEEK limited the indentation phenomenon by decreasing the crystalline content in the blend, it did not prevent an inhomogeneous dispersion of the filler in the composite. In addition, the α transition temperature increased remarkably between the neat PTFE (93°C) and filled PTFE, this creates a significant gap with the initial α transition (30°C between sample PTFE_T1 and 20%_PEEK_24%_Si_T2 for example). The modification of the α

transition and the presence of agglomerates in the samples could lead to a failing in the sample when strain-rate changes through the testing.

7 Conclusion

In this chapter PEEK powder was added to PTFE and PTFE/Silica 1 blends. PEEK is a semi-crystalline polymer with high glass transition temperature (150^{o}C) and a low viscosity (10^{2}-10^{3} Pa.s). Composites made of PTFE, PEEK and silica had a lower crystalline content compared to the ones without PEEK. This result proves the limitation of the indentation mechanism of the PTFE particles by the added silica 1. At the same time PEEK contributed in increasing the α transition temperature (by 13^{o}C for sample 23%_PEEK_T2 and 30^{o}C for sample 20%_PEEK_24%_Si_T2) and enhancing the storage modulus in DMA. Both PEEK and Silica 1 showed an interesting influence on the PTFE polymer when added to the blending.

Unfortunately, the addition of PEEK to PTFE/Silica 1 blend had its limit in non-linear testing where failure was observed for silica 1 content higher than 14 vol%. Further modifications have to be made to the blend in order to prevent the failure in the mechanical testing.

Résumé chapitre V

Le chapitre suivant présente l'effet du PEEK sur un mélange composé de PTFE et de la silice 1. Après avoir vu un effet intéressant de la silice 1 sur le PTFE (renforcement en propriétés mécaniques surtout après la température de transition Tα), ce chapitre aborde le défaut de rupture précoce en analyse de DMA non-linéaire.

L'ajout du PEEK dans le composite a pour but de guider la silice dans les pores du PTFE grâce à la faible viscosité du PEEK. Ceci diminuera l'effet de l'indentation créé par la silice sur les particules de PTFE (car moins de silice sera au contact du PTFE) et ainsi diminuera le taux de cristallinité. De cette façon, les propriétés mécaniques dans le domaine non-linéaire devraient être améliorées.

Plusieurs formulations de mélanges ont été choisies afin de mettre en évidence l'effet du PEEK sur le PTFE vierge dans un premier temps, ensuite sur le mélange PTFE/Silice 1 ainsi que l'effet de la silice sur un mélange de PEEK/PTFE.

Concernant l'influence du PEEK sur la matrice de PTFE, les observations microscopiques ont montré une morphologie « matrice-goutte » jusqu'à un taux de 23%vol de PEEK avec un manque d'adhésion entre les deux polymères. Les tests de DMA linéaire montre une stabilité dans le module de conservation jusqu'à la température de transition Tβ, température à partir de laquelle le renforcement s'améliore avec l'augmentation du taux de PEEK. Aucune rupture n'est observée durant les tests de DMA non-linéaire, cependant la température de transition α marque une augmentation significative.

En rajoutant un taux fixe de Silice 1 (8 vol%) au mélange PTFE/PEEK, une baisse du taux de cristallinité a été remarqué pour un taux de PEEK supérieure à 28 vol%. Cette baisse a été accompagnée par une augmentation des modules de conservations des échantillons en DMA linéaire surtout après la température de transition Tβ. En DMA non-linéaire la même tendance a été confirmée avec un renforcement du module de conservation E'. Malgré le renforcement des propriétés mécaniques et la diminution de taux de cristallinité qui démontre la réduction de l'effet de l'indentation sur les particules de PTFE, l'ajout du PEEK à la formulation n'a pas pu empêcher la rupture des échantillons pour des taux volumiques de charge supérieure à 14%.

VI. Blends with modified Silica

1 Introduction

In the previous chapter several points were raised concerning the influence of the PEEK on the PTFE/Silica blends. In chapter 2 the grafting of the silica was considered as insignificant for the enhancement of the mechanical properties of the composite. However, when filling PTFE with only silica, the indentation effect takes over and limits the capacity of the blends.

Therefore, after limiting the indentation effect, the distribution of the filler and the lack of adhesion between the PTFE and the filler constitute a threat to the mechanical properties of the composite. Improving the PTFE/Silica interface and reducing the formation of silica agglomerates can prevent failure in the non-linear DMA testing. This can be achieved by grafting the Silica for instance. Furthermore, choosing a fluorinated coupling agent may decrease the void in the interface between the PTFE and the fillers.

Therefore, in this chapter, the influence of grafting the silica 1 and adding the PEEK to PTFE/Silica blends will be studied.

2 Blends

Different samples were produced in order to study the influence of grafting the Silica 1 before adding it to the blends. Samples are presented in Table VI.1:

Polymer1	**polymer2**	**Polymer 2 (vol%)**	**Filler**	**Filler content (vol%)**	**Xc** (% ±2%)
PTFE	-	-	-	-	39
PTFE	PEEK	23	-	0	34
PTFE	PEEK	21	Silica 1	16	37
PTFE	PEEK	28	Silica 1	14	36
PTFE	PEEK	21	Silica 1*	15	33
PTFE	PEEK	28	Silica 1*	14	34

Table VI.1: List of blends prepared for testing and their crystalline content

Silica 1* is silica 1 grafted with 3 wt.% FTOS according to the method described in chapter 2 (III.3.1).

The goal behind this choice of samples is to study the influence of the grafting of the Silica 1 after the elimination of the indentation effect on the PTFE matrix. Therefore, blends containing PEEK and grafted silica 1 are compared to blends containing PEEK and non-grafted Silica 1 in addition to neat PTFE and PEEK/PTFE blends.

3 Microstructure

Crystalline content and linear DMA response of the samples were determined by means of DSC and linear DMA of rectangular specimens. The results are presented in the Table VI.2.

Polymer 1	Polymer 2	Content (vol%)	Filler	Content (vol%)	Xc (±2%)	Tβ	S1	Tanδ (β)	Tα	S2	Tanδ (α)
PTFE	PEEK	-	-	-	39	22	1.9	0.193	113	2.3	0.110
PTFE	PEEK	23	-	-	34	23	1.5	0.165	112	1.9	0.101
PTFE	PEEK	21	Silica 1	16	37	22	1.1	0.132	113	1.3	0.087
PTFE	PEEK	21	Silica 1*	15	33	21	0.9	0.128	113	1.4	0.081
PTFE	PEEK	28	Silica 1*	14	34	22	0.8	0.124	112	1.1	0.074
PTFE	PEEK	28	Silica 1	14	36	22	1.1	0.145	111	1.4	0.092

Table VI.2: Crystalline content and linear DMA test results. Results focusing on the damping factor and the transition temperatures α and β.

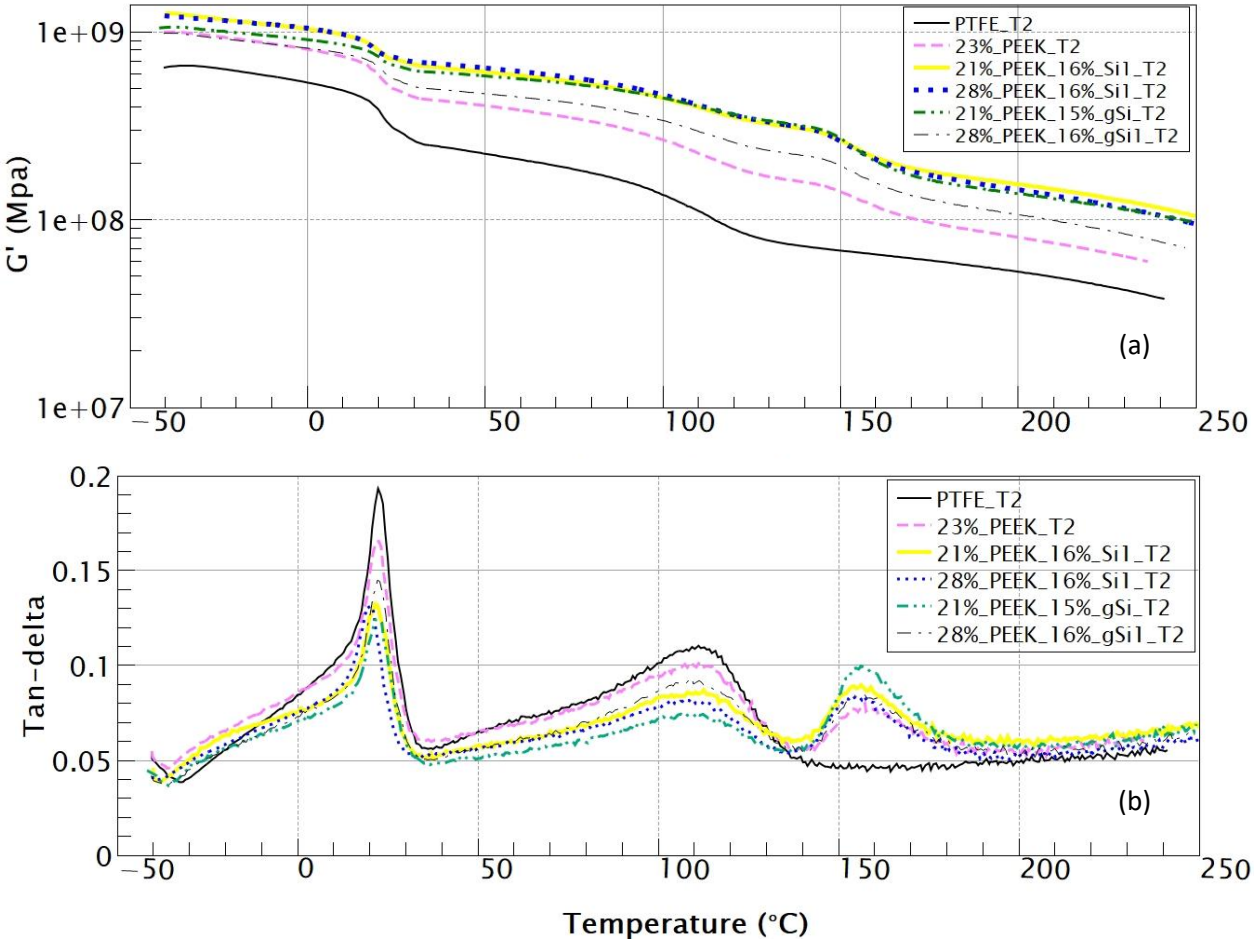

Graph VI.1: Storage modulus (a) and damping factor (b) curves for samples A', F', H', K', R' and S'.

Graph VI.1 shows the storage modulus and damping factor curves for samples PTFE_T2, 23%_PEEK_T2, 21%_PEEK_16%_Si_T2, 28%_PEEK_16%_Si_T2, 21%_PEEK_15%_gSi_T2 and 28%_PEEK_14%_gSi_T2. For samples with Silica 1 modified and non-modified, no changes are seen on the storage modulus. All Samples have the same storage modulus and the same crystalline content. This is contradictory of what it has been seen in the previous chapter 4 (IV.4) where the increase in the PEEK content decreased further the crystalline content and showed a higher reinforcement in the storage modulus. However, in this case the silica content is around 14 vol% while in chapter 4 the silica content was fixed at 8 vol% (a content at which the silica 1 has minor effect on the PTFE). Although in chapter III (III.3.1) grafting the silica showed a slight increase in the crystalline content, in this case on a microscopic level, the grafting of the silica did not show any influence on the linear DMA properties or the crystalline content.

4 Non-linear mechanical behavior

Samples were tested in non-linear DMA to observe the influence of the silica grafting on the PTFE/PEEK/Silica blends. Table VI.3 summarizes the results and Graph VI.2 presents the curves of the DMA.

Sample	E' (-50ºC)	E'(30ºC)	E'(150ºC)	Tanδ (β)	Tβ	Tα	Tanδ (α)	T(B)
PTFE_T2	$1.4\ 10^9$	$6.1\ 10^8$	$3.7\ 10^7$	0.16	29	93	0.31	-
23%_PEEK	$1.4\ 10^9$	$7.9\ 10^8$	$4.0\ 10^7$	0.13	31	105	0.24	-
21%_PEEK_16%_Si1_T2	$1.8\ 10^9$	$1.2\ 10^9$	$1.7\ 10^8$	0.10	32	119	0.17	219
21%_PEEK_15%_gSi1_T2	$1.7\ 10^9$	$1.1\ 10^9$	$1.6\ 10^8$	0.11	32	118	0.17	-
28%_PEEK_14%_gSi1_T2	$1.8\ 10^9$	$1.2\ 10^9$	$2.2\ 10^8$	0.10	31	120	0.16	-
28%_PEEK_14%_Si1_T2	$1.8\ 10^9$	$1.2\ 10^9$	$2.1\ 10^8$	0.10	31	121	0.16	202

Table VI.3: Dynamic mechanical analysis results

Samples 21%_PEEK_16%_Si_T2 and 21%_PEEK_15%_gSi_T2 have the same formulation except that the silica in sample 21%_PEEK_15%_gSi_T2 is grafted. In the same way, samples 28%_PEEK_14%_Si_T2 and 28%_PEEK_14%_gSi_T2 have the same formulation only the silica in the sample 28%_PEEK_14%_gSi_T2 is grafted. The four samples have exactly the same properties in term of transition temperatures and storage modulus. The difference between those samples is that samples with grafted Silica did not break during the test.

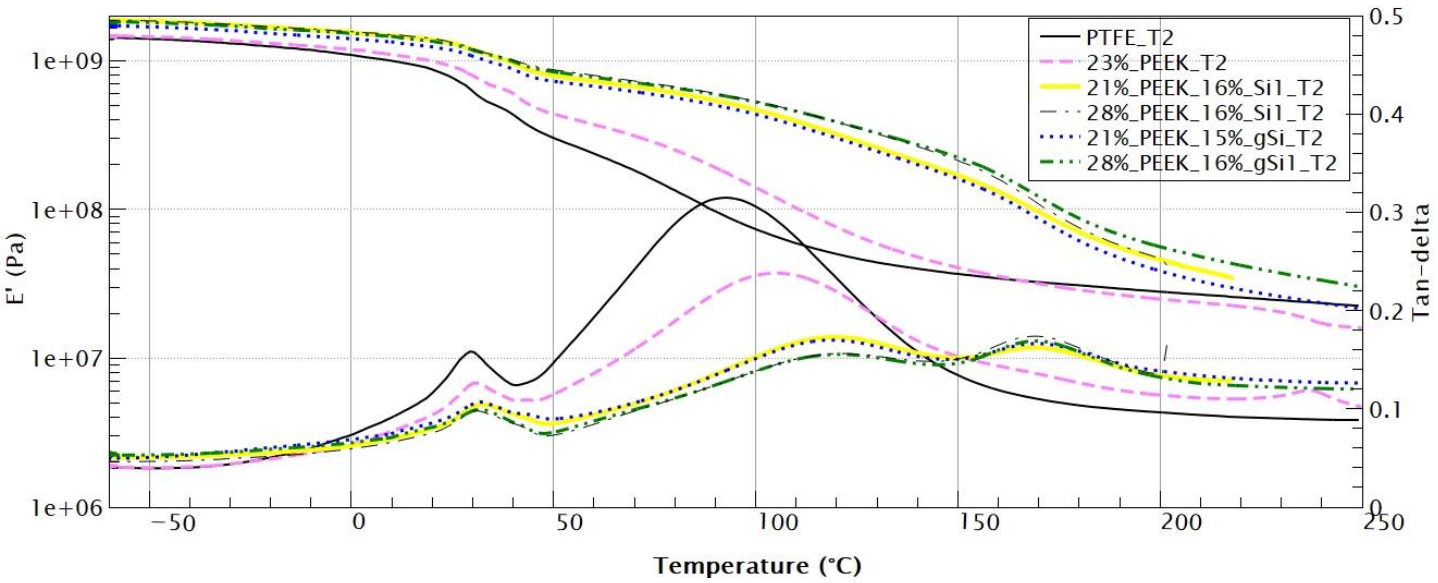

Graph VI.2: non-linear DMA results for samples PTFE_T2, 23%_PEEK_T2, 21%_PEEK_16%_Si_T2, 28%_PEEK_14%_Si_T2, 21%_PEEK_15%_gSi_T2 and 28%_PEEK_14%_gSi_T2.

5 Discussion

5.1 Microstructure

The four samples described above have the same crystalline content (around 35%). On one hand knowing that the four samples have the same filler content, it is normal to have the same crystalline content. However, in III.3.1.3, adding grafted silica 1 to PTFE matrix participated in increasing the crystalline content (with the temperature cycle 1). This increase is related to the fact that grafting the silica 1 limited the agglomeration of silica particles, thus promoting the indentation phenomenon on the PTFE particles. In the case of the blends formulated with PEEK and Silica 1, the additional polymer limited the indentation phenomenon on the PTFE particles (a part of the Silica 1 content was in the PEEK phase); therefore, the grafting did not have any influence on the crystalline content although there were fewer agglomerates.

As for the linear DMA tests, blends formulated with grafted silica or non-grafted silica did not have any difference in the behavior. The transition temperatures and the damping factors remained the same. This seems coherent since the filler content is the same in the four samples, and as seen in the previous chapters, the filler content is the main actor in the linear DMA properties.

5.2 Non-linear mechanical behavior

The only difference between grafted and non-grafted silica filled blends is the fact that samples with grafted silica did not break in the non-linear DMA testing. The presence of PEEK in the samples greatly reduced the indentation phenomenon that contributed in increasing the crystalline content in the samples. A high crystalline content has been correlated with a decrease in the mechanical properties in the non-linear regime[5]. The decrease of the indentation mechanism through addition of PEEK allowed for the reduction of crystalline content and thus increased the resistance to breaking in the non-linear test. However, from what has been discussed in the previous chapter, PEEK did not prevent the formation agglomerates in the composites.

When grafting the silica, the interactions between the silica particles is limited[144]. The choice of the grafting agent is very important. The size of the molecule and the amount of grafting agent play an important role in changing the interactions between the particles and/or creating interactions with the polymer matrix[144]. In the case of silica filled PTFE, several authors chose to graft the silica before mixing in the blend such as Bosq et al[143] and Chih chen et al[115,116]. Knowing that the silica applied in this study is a micrometric silica (particle size of 4µm) the grafting surface was less important than for nano-silicas. Nevertheless, the surface modification of the Silica 1 was sufficient to eliminate the weak points of the blend due to the agglomeration of the filler particles,thus, preventing the breaking in the non-linear DMA.

Concerning the α transition temperature, it is basically the same between composites with grafted and non-grafted Silica 1 (around 120°C). These temperatures are reached with the presence of both PEEK and Silica 1 in the composite, and observed for non-linear DMA testing as a response of the strain change through the test. However, it is seen through these results that the variation of the α transition did not have a direct effect on the failure in the non-linear DMA.

6 Conclusion

Grafting the silica 1 showed an enhancement in the behavior of the non-linear DMA testing, as samples filled with grafted silica did not break when tested. When looking closer, the ideal composite contained PEEK, and a surface grafted Silica 1. In other words, two weaknesses were limited; indentation mechanism by adding PEEK and agglomerate formation by grafting the surface of Silica 1.

However, it would have been ideal to focus more on the type and quantity of the grafted agent in order to have an even more effective grafting that could be detected easily.

Résumé chapitre VI

Dans le chapitre précédant plusieurs points ont été étudié sur l'influence du PEEK sur les mélanges PTFE/Silice. Dans le chapitre 2, la modification de surface de la silice n'a montré aucun effet sur le mélange PTFE/Silice. Cependant, le PTEF chargé avec la silice uniquement est emportée par l'effet de l'indentation de la silice qui limite les capacités du mélange.

Par conséquent, une fois l'effet de l'indentation limité, la formation d'agglomérats et le manque d'adhésion entre le PTFE et la charge constituent un risque sur les propriétés mécaniques du mélange. La modification de la surface de la silice pourrait contribuer à une meilleure distribution de la silice dans le mélange par le biais de la réduction des agglomérats. De plus, l'utilisation d'un agent de couplage fluoré pourrait améliorer l'interface entre la silice et le PTFE.

Ainsi, le greffage de la silice a montré un meilleur comportement en DMA non-linéaire. Les échantillons présentant de la silice greffée ont subi le test sans rupture. Cependant, il serait pertinent d'évaluer la quantité de greffage et ainsi adapter le mélange pour optimiser les propriétés.

VII. General conclusion

This work presented a study on composites based on Polytetrafluoroethylene (PTFE), a high-performance polymer with interesting thermal and chemical properties. Some of the mechanical properties of PTFE such as wear and creep need to be improved in order to answer challenging applications. In this aim, PTFE can be filled with organic fillers such as silica or carbon black.

The study discussed in this manuscript focused on the influence of the filler on the microstructure and mechanical properties (such as linear and non-linear DMA testing) of the PTFE.

Before studying the influence of the fillers, processing parameters had to be chosen in order to produce proper blends made out of PTFE and fillers or PTFE-PEEK blends and fillers. The process was composed of several steps. Step 1 the mixing phase where the powders (PTFE, filler or PEEK) were mixed by the mean of a pale until obtaining a homogeneous mixture. Step 2, shaping the mixture in a mold at a fixed pressure and ambient temperature. Step 3, mold-free sintering with a chosen temperature cycle. When choosing the process parameters, modifying the silica surface by grafting did not show any difference on the properties of only silica-filled composites.

After determining the process parameters, composites with fillers of different sizes, content and surface nature were tested. Three different silica sizes were tested (0.2µm, 4µm and 200-300µm), in addition one carbon black was tested with an average diameter size of 25µm. Although the filler content was important in defining the viscoelastic properties, and the crystalline content, filler size turned out to be a key parameter. Silica 1 (4µm) showed a critical diameter which probably induced an indentation on the PTFE particle resulting in a remarkable increase in the crystalline content. PTFE with a high crystalline content shows a mediocre behavior in the tension-compression and induces cracking in the testing. Therefore, in order to limit this phenomenon PEEK was introduced in the blends.

PEEK is a high performance semi-crystalline polymer with remarkable mechanical, chemical and thermal properties. Its viscosity is considerably lower than that of the PTFE's. Therefore, adding PEEK to the PTFE composite helped in limiting the indentation phenomenon and reduced the crystallinity rate. However, adding PEEK did not guarantee the homogeneity of the composite and did not prevent the formation of the agglomerates. These filler agglomerates constitute weak points in the sample that contributes in the failing in the non-linear testing.

This is where modifying the silica surface with a grafting agent was beneficial. When the indentation effect of the silica on the PTFE particle was limited, inhomogeneous dispersion generated weaknesses in the blends. Therefore, when modifying the silica surface the formation of agglomerates is limited. Silica can be better dispersed in the blend, preventing the break of the samples in non-linear DMA testing.

Certainly, more work can be done in order to understand and analyze the influence of the fillers on the PTFE.

First, the Silica with a size of 4µm showed an indentation effect on the PTFE, however it would have been interesting to add a filler with a different chemical nature such as the carbon black with the same size order as the silica 1 in order to compare the effect.

Second, it would be interesting to develop the grafting of the silica with several grafting content and to further improve the formulation in order to reach optimum properties.

In addition, implementing more testing techniques such as the AFM (atomic force microscope) could help in a better understanding of the blend composite. In this study the rheological characteristics of PTFE were tested in the solid state for linear and non-linear behavior, this testing allowed a comprehension of the influence of the filler combined to the crystalline state. Testing the PTFE in its molten state would be ideal to detect the contribution of the filler solely on the PTFE matrix after eliminating the crystalline phase.

Last but not least, in order to achieve the morphology defined in Figure V.1 another mixing option could be evaluated: making a silica/PEEK composite pre-blend before mixing it with PTFE. This way the silica could only be in the PEEK phase and prevent any fibrillation or indentation on the PTFE matrix.

VIII.References

1. The Editors of Encyclopaedia Britannica. Polymer definition. https://www.britannica.com/science/polymer.
2. Fox, M. Lube-Tech Polymer Tribology Lube-Tech. *Eur. Lubr. Ind. Mag.* **135**, 32–37 (2016).
3. Sperati, C. A. & Starkweather, H. W. Fluorine-containing polymers. II. Polytetrafluoroethylene. **5**, 465–495 (1961).
4. Mueller, M. B. Cold flow resistant homogeneoud copolymers of tetrafluoroethylene and hexafluoropropene and process for preparing them. (1972).
5. Ebnesajjad, S. *FLUOROPLASTICS Volume 1: Non-Melt Processible Fluoropolymers - The Definitive User's Guide and Data Book*. (2000).
6. Ebnesajjad, S. *Expanded PTFE applications handbook. Technology, manufacturing and applications*. (2016).
7. Brown, E. N., Dattelbaum, D. M., Brown, D. W., Rae, P. J. & Clausen, B. A new strain path to inducing phase transitions in semi-crystalline polymers. **48**, 2531–2536 (2007).
8. Rae, P. J. & Brown, E. N. The properties of poly(tetrafluoroethylene) (PTFE) in tension. *Polymer (Guildf).* **46**, 8128–8140 (2005).
9. Rae, P. J. & Dattelbaum, D. M. The properties of poly(tetrafluoroethylene) (PTFE) in compression. *Polymer (Guildf).* **45**, 7615–7625 (2004).
10. Bunn, C. W., Cobbold, A. J. & Palmer, R. P. The fine structure of polytetrafluoroethylene. *J. Polym. Sci.* **28**, 365–376 (1958).
11. Speerschneider, C. J. & Li, C. H. A correlation of mechanical properties and microstructure of polytetrafluoroethylene at various temperatures. *J. Appl. Phys.* **34**, 3004–3007 (1963).
12. Frick, A. *et al.* Relationship between structure and mechanical properties of melt processable PTFE: Influence of molecular weight and comonomer content. *Macromol. Mater. Eng.* **298**, 954–966 (2013).
13. Seo, Y. Nonisothermal crystallization kinetics of polytetrafluoroethylene. *Polym. Eng. Sci.* **40**, 1293–1297 (2000).
14. Wang, X. Q., Chen, D. R., Han, J. C. & Du, S. Y. Crystallization behavior of polytetrafluoroethylene (PTFE). *J. Appl. Polym. Sci.* **83**, 990–996 (2002).
15. Speerschneider, C. J. & Li, C. H. Some Observations on the Structure of Polytetrafluoroethylene. *J. Appl. Phys.* **33**, 1871–1875 (1962).
16. Pucciariello, R. & Villani, V. Phase behavior at low temperature of poly(tetrafluoroethylene) by temperature-modulated calorimetry. *J. Fluor. Chem.* **125**, 293–302 (2004).
17. Bassett, D. C. & Davitt, R. On crystallization phenomena in polytetrafluoroethylene. *Polymer (Guildf).* (1974).
18. Suwa, T., Seguchi, T. & Takehisa, M. Effect of Molecular Weight on the Crystalline Structure of Pol ytetrafluoroethylene As- Polymerized. **13**, 2183–2194 (1975).

19. Ferry, L., Vigier, G., Vassoille, R. & Bessede, J. . Study of polytetrafluoroethylene crystallization. 300–306 (1995).
20. Makinson, K. R. & Tabor, D. The friction and transfer of polytetrafluoroethylene. **281**, (1964).
21. Calleja, G., Jourdan, A., Ameduri, B. & Habas, J. P. Where is the glass transition temperature of poly(tetrafluoroethylene)? A new approach by dynamic rheometry and mechanical tests. *Eur. Polym. J.* **49**, 2214–2222 (2013).
22. Starkweather, H. W., Ferguson, R. C., Chase, D. B. & Minor, J. M. Infrared Spectra of Amorphous and Crystalline Poly(tetrafluoroethylene). *Macromolecules* **18**, 1684–1686 (1985).
23. Dlubek, G. *et al.* Glass transition and free volume in the mobile (MAF) and rigid (RAF) amorphous fractions of semicrystalline PTFE: A positron lifetime and PVT study. *Polymer (Guildf).* **46**, 6075–6089 (2005).
24. Gangal, S. & Brothers, P. *Perfluorinated polymers, polytetrafluoroethylene*.
25. Marega, C. *et al.* Relationship between the size of the latex beads and the solid-solid phase transitions in emulsion polymerized poly(tetrafluoroethylene). *Macromolecules* **37**, 5630–5637 (2004).
26. ARAKI, Y. Second-Order Transitions of Polytetrafluoroethylene at about -30" C. Measured by Several Methods. **9**, 3585–3596 (1965).
27. Quinn, F. A., Roberts, D. E. & Work, R. N. VolumeTemperature Relationships for the Room Temperature Transition in Teflon. **1085**, 22–24 (1951).
28. Marx, P. & Dole, M. Specific Heat of Synthetic High Polymers. V. A Study of the Order-Disorder Transition in Polytetrafluoroethylene. **20**, 1953–1956 (1955).
29. Villani, V. A study on the thermal behaviour and structural characteristics of polytetrafluoroethylene. *Thermochim. Acta* **162**, 189–193 (1990).
30. Brown, E. N., Rae, P. J., Dattelbaum, D. M., Clausen, B. & Brown, D. W. In-situ measurement of crystalline lattice strains in polytetrafluoroethylene. *Exp. Mech.* **48**, 119–131 (2008).
31. Suwa, T., Takehisa, M. & Machi, S. U. E. Melting and Crystallization Behavior of Poly (tetrafluoroethylene). New Method for Molecular Weight Measurement of Poly (tetrafluoroethylene) Using a Differential Scanning Calorimeter. **17**, 3253–3257 (1973).
32. Araki, Y., Industries, N. V. & City, A. Transitions of Polytetrafluoroethylene at About 90 and 130OC . Studied by X-Ray Diffraction and Infrared Spectra. **11**, 953–961 (1967).
33. Araki, Y., Valqwc, N. & City, A. First-Order and Second-Order Transitions of Polytetrafluoroethylene in the Temperature Range of 80-140 ° C . Measured by Several Methods. **9**, 3575–3584 (1965).
34. Brown, E. N. & Dattelbaum, D. M. The role of crystalline phase on fracture and microstructure evolution of polytetrafluoroethylene (PTFE). *Polymer (Guildf).* **46**, 3056–3068 (2005).
35. Brown, E. N., Rae, P. J., Bruce Orler, E., Gray, G. T. & Dattelbaum, D. M. The effect of crystallinity on the fracture of polytetrafluoroethylene (PTFE). *Mater. Sci. Eng. C* **26**, 1338–

1343 (2006).
36. Ryland, A. X-Ray Diffraction. **35**, (1958).
37. Moynihan, R. E. The Molecular Structure of Perfluorocarbon Polymers . **891**, (1959).
38. Lehnert, R. J., Hendra, P. J. & Everall, N. Crystallinity of poly(tetrafluoroethylene) using Raman spectroscopy. **36**, 2473–2476 (1995).
39. Rabolt, J. F. Characterization of Lattice Disorder in the Low- Temperature Phase of Irradiated PTFE by Vibrational Spectroscopy. **21**, 1797–1805 (1983).
40. Peacock, C. J., Hendra, P. J., Willis, H. A. & Cudby, M. E. A. Raman Spectrum and Vibrational Assignment for Poly(tetraf1uoro- ethylene). (1969).
41. Vega, A. & English, A. Multiple Pulse Nuclear Magnetic Resonance of Solid Polymers: Dynamics of Poly(tetrafluoroethylene). **12**, 353–354 (1979).
42. Vega, A. J. & English, A. D. Multiple-Pulse Nuclear Magnetic Resonance of Solid Polymers. Polymer Motions in Crystalline and Amorphous Poly(tetrafluoroethylene)t. *Macromolecules* **13**, 1635–1647 (1980).
43. Song, F., Wang, Q. & Wang, T. The effects of crystallinity on the mechanical properties and the limiting PV (pressure×velocity) value of PTFE. *Tribol. Int.* **93**, 1–10 (2016).
44. Starkweather, H. W., Zoller, P., Jones, G. A. & Vega, A. J. *The Heat of Fusion of Polytetrafluoroethylene*.
45. Pucciariello, R. & Villani, V. Melting and crystallization behavior of poly(tetrafluoroethylene) by temperature modulated calorimetry. *Polymer (Guildf).* **45**, 2031–2039 (2004).
46. Bosq, N., Guigo, N., Persello, J. & Sbirrazzuoli, N. Crystallization of polytetrafluoroethylene in awide range of cooling rates: Nucleation and diffiusion in the presence of nanosilica clusters. *Molecules* **24**, (2019).
47. Thomas, P. S. & Stuart, B. H. DSC Characaterisation of compression moulded PEEK-PTFE plaques. *J. Therm. Anal. Calorim.* **72**, 675–679 (2003).
48. Starkweather, H. W., Zoller, P. & Jones, G. A. Heat of Fusion of Copolymers of Tetrafluoroethylene and Hexafluoropropylene. *J. Polym. Sci. Part A-2, Polym. Phys.* **22**, 1431–1437 (1984).
49. Sciuti, V. F., Melo, C. C., Canto, L. B. & Canto, R. B. Influence of surface crystalline structures on DSC analysis of PTFE. *Mater. Res.* **20**, 1350–1359 (2017).
50. Lehnert, R. J., Hendra, P. J., Everall, N. & Clayden, N. J. Comparative quantitative study on the crystallinity of poly(tetrafluoroethylene) including Raman, infra-red and 19F nuclear magnetic resonance spectroscopy. *Polymer (Guildf).* **38**, 1521–1535 (1997).
51. Bigg, D. M. A Study of the on Effect of Pressure, Time, and Temperature High-pressure Powder Molding. *Polym. Eng. Sci.* **17**, 691–699 (1977).
52. Jog, J. P. Solid state processing of polymers: A review. *Adv. Polym. Technol.* **12**, 281–289 (1993).
53. Fredy, C. Modeling of the mechanical behavior of polytetrafluoroethylene (PTFE) compounds during their compaction at room temperature. (UPMC, 2016).

54. Guenoun, G., Schmitt, N. & Regnier, G. Thermal treatment influence on the crystalline microstructure of compacted Polytetrafluoroethylene. in (2017).
55. Lau, S. F., Suzuki, H. & Wunderlich, B. The Thermodynamic Properties of Polytetrafluoroethylene. *Polym. Sci.* **22**, 379–405 (1984).
56. Bertsil, B., Baker, J. & Kasprzak, D. J. Thermal degradation of commercial fluoropolymers in air. *Polym. Degrad. Stab.* **42**, 181–188 (1993).
57. Hanford, W. E. & Joyce, R. M. Polytetrafluoroethylene. *J. Am. Chem. Soc.* **68**, 2082–2085 (1946).
58. Yuan, Y. *et al.* Effect of sintering temperature on the crystallization behavior and properties of silica filled PTFE composites. *J. Mater. Sci. Mater. Electron.* **27**, 13288–13293 (2016).
59. Ariawan, A. B., Ebnesajjad, S. & Hatzikiriakos, S. G. S. G. Properties of polytetrafluoroethylene (PTFE) paste extrudates. *Polym. Eng. Sci.* **42**, 1247–1259 (2002).
60. Sun, H., Cooke, R. S., Bates, W. D. & Wynne, K. J. Supercritical CO2 processing and annealing of polytetrafluoroethylene (PTFE) and modified PTFE for enhancement of crystallinity and creep resistance. in *Polymer* vol. 46 8872–8882 (Elsevier BV, 2005).
61. Chen, X. & Hui, S. Ratcheting behavior of PTFE under cyclic compression. *Polym. Test.* **24**, 829–833 (2005).
62. Joyce, J. A. & Academy, U. S. N. Fracture Toughness Evaluation of Polytetrafluoroethylene. **43**, (2003).
63. Kisbenyi, M., Birch, M. W., Hodgkinson, J. M. & Williams, J. G. *Correlation of impact fracture toughness with loss peaks in PTFE*. (1979).
64. Joyce, P. J. & Joyce, J. A. Evaluation of the fracture toughness properties of polytetrafluoroethylene. *Int. J. Fract.* **127**, 361–385 (2004).
65. Brown, E. N., Trujillo, C. P., Gray, G. T., Rae, P. J. & Bourne, N. K. Soft recovery of polytetrafluoroethylene shocked through the crystalline phase II-III transition. *J. Appl. Phys.* (2007) doi:10.1063/1.2424536.
66. Rae, P. J. *et al.* The Taylor Impact Response of PTFE (Teflon) THE TAYLOR IMPACT RESPONSE OF PTFE (TEFLON). **671**, (2004).
67. Dyment, J. & Ziebland, H. The tensile properties of some plastics at low temperatures. (1958).
68. Fischer, S., Brown, N., Fischer, S. & Brown, N. Deformation of polytetrafluoroethylene from 78 to 298 ° K and the effects of environmental crazing Deformation of polytetrafluoroethylene from 78 to 298 0 K and the effects of environmental crazing. **4322**, (1973).
69. Wu, J. B. C. & Brown, E. N. The effect of specimen size on the mechanical behaviour associated with crazing. *J. Mater. Sci.* **12**, 1527–1534 (1977).
70. Koo, G. P. & Andrews, R. D. Mechanical Behavior of Polytetrafluoroethylene Around the Room-Temperature First-Order Transition :'. **9**, (1969).
71. McCrum, N. G. An Internal Friction Study of Polytetrafluoroethylene. *Polym. Sci.* **XXXIV**, 355–369 (1959).

72. Wortmann, F.-J. Analysing the relaxation behaviour of poly(tetrafluoroethylene) in the s-transition region by applying a two-component model*. *Polymer (Guildf).* **37**, 2471–2476 (1996).
73. Vincent, P. I. Impact strength and mechanical losses in thermoplastics. *Polymer (Guildf).* **15**, 111–116 (1974).
74. Ajroldi, G., Garbuglio, C. & Ragazzini, M. Some Rheological Properties of Molten Polytetrafluoroethylene. **14**, 79–88 (1970).
75. Frick, A., Sich, D., Heinrich, G., Stern, C. & Schlipf, M. Classification of New Melt-Processable PTFE : Comparison of Emulsion- and Suspension- Polymerized Materials. 329–341 (2012) doi:10.1002/mame.201100149.
76. McCrum, N. G. The low temperature in polytetrafluoroethylene. **XXVII**, 1–4 (1958).
77. Starkweather, H. W. & Nemours, E. I. De. A Comparison of the Rheological Properties of Polytetrafluoroethylene below Its Melting Point with Certain Low-Molecular Smectic States *. **17**, 73–79 (1979).
78. Tobolsky, A. V & Katz, D. Rheology of Polytetrafluoroethylene. *J. Polym. Sci. PART A* **1**, 483–489 (1963).
79. Tobolsky, A. V, Katz, D. & Eisenberg, A. Maximum relaxation times in Polytetrafluoroethylene. **7**, 469–474 (1963).
80. Wu, S. Characterization of Polymer Molecular Weight Distribution by Transient Viscoelasticity: Polytetrafluoroethylenes. *Polym. Degrad. Stab.* **28**, 538–543 (1988).
81. Levrett, G. F. Process for reducing filler loss. (1975).
82. Nakamura, Y. & Kawachi, S. Process for preparing filled polytetrafluoroethylene molding powder. (1983).
83. Asano, M. & Sukegawa, M. Filled granular polytetrafluoroethyelene powder. vol. 1 (2002).
84. Asano, M., Futatsugi, K. & Tsuji, M. Low-electrostatically-charging granular polytetrafluoroethyelene powder and preparation process of same. vol. 1 (2004).
85. Ebnesajjad, S. Introduction to Fluoropolymers. in *Applied Plastics Engineering Handbook: Processing, Materials, and Applications: Second Edition* 55–71 (Elsevier Inc., 2017). doi:10.1016/B978-0-323-39040-8.00003-1.
86. Chand, S. Carbon fibers for composites - Review. *Mater. Sci.* 1303–1313 (2000).
87. Fekete, J. R. & Hall, J. N. Design of auto body: Materials perspective. in *Automotive Steels: Design, Metallurgy, Processing and Applications* 1–18 (Elsevier Inc., 2017). doi:10.1016/B978-0-08-100638-2.00001-8.
88. Nguyen-tran, H., Hoang, V.-T., Do, V., Chun, D. & Yum, Y. Effect of Multiwalled Carbon Nanotubes on the Mechanical Properties of Carbon Fiber-Reinforced. (2018) doi:10.3390/ma11030429.
89. De Rosa, I. M., Sarasini, F., Sarto, M. S. & Member, S. EMC Impact of Advanced Carbon Fiber / Carbon Nanotube Reinforced Composites for Next-Generation Aerospace Applications. **50**, 556–563 (2008).
90. Sebok, E. . & Taylor, R. . Carbon Blacks. *materials science and technology* 902–906 (2001).

91. HUANG, J. Carbon Black Filled Conducting Polymers and Polymer Blends. **21**, 299–313 (2002).
92. Qayyum, M. M. & White, J. R. Effect of stabilizers on failure mechanisms in weathered polypropylene. *Polym. Degrad. Stab.* **41**, 163–172 (1993).
93. Park, S. & Ruoff, R. S. Chemical methods for the production of graphenes. *Nat. Nanotechnol.* **4**, 217–224 (2009).
94. Li, B. & Zhong, W. Review on polymer / graphite nanoplatelet nanocomposites. *Mater. Sci.* 5595–5614 (2011) doi:10.1007/s10853-011-5572-y.
95. Vodicka, R. Thermoplastics for Airframe Applications A Review of the Properties and Repair Methods for Thermoplastic Composites.
96. Shi, Y. J., Feng, X., Wang, H. Y., Liu, C. & Lu, X. H. Effects of filler crystal structure and shape on the tribological properties of PTFE composites. *Tribol. Int.* **40**, 1195–1203 (2007).
97. Friedrich, K., Zhang, Z. & Schlarb, A. K. Effects of various fillers on the sliding wear of polymer composites. *Compos. Sci. Technol.* **65**, 2329–2343 (2005).
98. Aderikha, V. N. & Shapovalov, V. A. Effect of filler surface properties on structure, mechanical and tribological behavior of PTFE-carbon black composites. *Wear* **268**, 1455–1464 (2010).
99. Shi, Y., Feng, X., Wang, H. & Lu, X. Tribological and mechanical properties of PTFE composites filled with the combination of short carbon fiber and carbon nano-fiber. **335**, 689–692 (2007).
100. Bijwe, J., Neje, S., Indumathi, J. & Fahim, M. Friction and Wear Performance Evaluation of Carbon Fibre Reinforced PTFE Composite. doi:10.1106/073168402025786.
101. Panda, A. *et al.* Manufacturing Technology of Composite Materials — Principles of Modification of Polymer Composite Materials Technology Based on Polytetrafluoroethylene. (2017) doi:10.3390/ma10040377.
102. Shi, Y., Feng, X. & Wang, H. Tribological properties of PTFE composites filled with surface-treated carbon fiber. 8465–8469 (2007) doi:10.1007/s10853-007-1767-7.
103. Ricaud, M. Les silices amorphes. vol. 1 (2007).
104. what is silica ?
105. Toquet, F. Study of the combined roles of the Silica / Oil / UHMWPE formulation and process parameters on morphological and electrical properties of battery. (2017).
106. Wang, H., Bai, Y., Liu, S., Wu, J. & Wong, C. P. *Combined effects of silica filler and its interface in epoxy resin*. *Acta Materialia* vol. 50 www.actamat-journals.com (2002).
107. Xu, G. C. *et al.* Synthesis and Characterization of Silica Nanocomposite In Situ Photopolymerization. *Appl. Polym. Sci.* **90**, 837–840 (2003).
108. Zhong, B., Jia, Z., Hu, D., Luo, Y. & Jia, D. Composites : Part A Reinforcement and reinforcing mechanism of styrene – butadiene rubber by antioxidant-modified silica. *Compos. PART A* **78**, 303–310 (2015).
109. Guneyisi, E., Turan, O. & Gesoglu, M. Properties of rubberized concretes containing silica fume. **34**, 2309–2317 (2004).

110. Kalfus, J., Jancar, J. & Kucera, J. Effect of Weakly Interacting Nanofiller on the Morphology and Viscoelastic Response of Polyolefins. **71**, 8–13 (2008).
111. Zhang, M. Q. I. U., Rong, M. I. N. Z. H. I., Zhang, H. A. I. B. O. & Rich, K. F. Mechanical Properties of Low Nano-Silica. **43**, (2003).
112. Garcia, A. L. Nano-silica production at low temperatures from the dissolution of olivine. (2014).
113. Singhon, R. Adsorption of Cu(II) and Ni(II) Ions on Functionalized Colloidal Silica Particles Model Studies for Wastewater Treatment. (UFC, 2014).
114. Basu, B. J. & Dinesh Kumar, V. Fabrication of Superhydrophobic Nanocomposite Coatings Using Polytetrafluoroethylene and Silica Nanoparticles. *ISRN Nanotechnol.* **2011**, 1–6 (2011).
115. Chen, Y. C., Lin, H. C. & Lee, Y. Der. The effects of phenyltrimethoxysilane coupling agents on the properties of PTFE/silica composites. *J. Polym. Res.* **11**, 1–7 (2004).
116. Chen, Y. C., Lin, H. C. & Lee, Y. Der. The Effects of Filler Content and Size on the Properties of PTFE/SiO 2 Composites. *J. Polym. Res.* **10**, 247–258 (2003).
117. Huang, S., Chen, T. H. & Chen, H. Study on the composites of two sized silica filled in PTFE. *J. Reinf. Plast. Compos.* **25**, 1053–1058 (2006).
118. Martins, S. A., Dias, F. W., Nunes, L. S., Borges, L. A. & D'Almeida, J. R. Mechanical characterization of silica Reinforced-PTFE matrix composites. in *Procedia Engineering* vol. 10 2651–2656 (Elsevier Ltd, 2011).
119. Martins, S. & Borges, L. Effects of Accelerated Ageing in a PTFE Matrix Polymer Composite. 92–98 (2011) doi:10.1002/masy.200900163.
120. Reitman, M., Jaekel, D., Siskey, R. & Kurtz, S. M. Morphology and Crystalline Architecture of Polyaryletherketones. in *PEEK Biomaterials Handbook* 49–60 (Elsevier Inc., 2012). doi:10.1016/B978-1-4377-4463-7.10004-1.
121. Victrex. Victrex materials properties guide.
122. Blundell, D. J. & Osborn, B. N. The morphology of poly (aryl-ether-ether- ketone). **24**, 953–958 (1983).
123. CHU, J.-N. & SCHULTZ, J. The influence of microstructure on the failure behaviour of PEEK. **25**, (1990).
124. Kemmish, D. J. & Hay, J. N. The effect of physical ageing on the properties of amorphous PEEK. *Polymer (Guildf).* **26**, 905–912 (1985).
125. Sobieraj, M. C. & Rimnac, C. M. Fracture, Fatigue, and Notch Behavior of PEEK. in *PEEK Biomaterials Handbook* 61–73 (Elsevier Inc., 2012). doi:10.1016/B978-1-4377-4463-7.10005-3.
126. Victrex. Injection molding.
127. Villoutreix, J. & Acetarin, J. Polyétheréthercétone Polyétheréthercétone (PEEK). **33**, (2020).
128. Aly, A. A., Zeidan, E.-S. B., Alshennawy, A. A., El-Masry, A. A. & Wasel, W. A. Friction and Wear of Polymer Composites Filled by Nano-Particles: A Review. *World J. Nano Sci. Eng.*

02, 32–39 (2012).
129. Rasheva, Z., Zhang, G. & Burkhart, T. A correlation between the tribological and mechanical properties of short carbon fibers reinforced PEEK materials with different fiber orientations. *Tribol. Int.* **43**, 1430–1437 (2010).
130. Lai, Y. H., Kuo, M. C., Huang, J. C. & Chen, M. On the PEEK composites reinforced by surface-modified nano-silica. *Mater. Sci. Eng. A* **458**, 158–169 (2007).
131. Kuo, M. C., Tsai, C. M., Huang, J. C. & Chen, M. PEEK composites reinforced by nano-sized SiO 2 and Al 2 O 3 particulates. **90**, 185–195 (2005).
132. Kuo, M. C., Huang, J. C. & Chen, M. Non-isothermal crystallization kinetic behavior of alumina nanoparticle filled poly (ether ether ketone). **99**, 258–268 (2006).
133. Mishra, T. K., Kumar, A., Verma, V., Pandey, K. N. & Kumar, V. PEEK composites reinforced with zirconia nanofiller. *Compos. Sci. Technol.* **72**, 1627–1631 (2012).
134. Burris, D. L. & Sawyer, W. G. A low friction and ultra low wear rate PEEK/PTFE composite. *Wear* **261**, 410–418 (2006).
135. Hufenbach, W. & Kunze, K. Sliding Wear Behaviour of PEEK-PTFE Blends. *Synth. Lubr.* **20**, 227–240 (2003).
136. Bijwe, J., Sen, S. & Ghosh, A. Influence of PTFE content in PEEK-PTFE blends on mechanical properties and tribo-performance in various wear modes. *Wear* **258**, 1536–1542 (2005).
137. Qu, S. & Wang, S. Elevated-Temperature Thermal and Mechanical Behavior of Carbon Fiber / Graphite / PTFE / PEEK Composite.
138. Gladson, T. S. F., Ramesh, R. & Kavitha, C. Experimental investigation of mechanical , tribological and dielectric properties of alumina nano wire-reinforced PEEK / PTFE composites Experimental investigation of mechanical , tribological and dielectric properties of alumina nano wire-reinforced PEEK. (2019).
139. Goyal, R. K. & Yadav, M. The wear and friction behavior of novel polytetrafluoroethylene/expanded graphite nanocomposites for tribology application. *J. Tribol.* **136**, (2014).
140. Takeichi, Y., Wibowo, A., Kawamura, M. & Uemura, M. Effect of morphology of carbon black fillers on the tribological properties of fibrillated PTFE. *Wear* **264**, 308–315 (2008).
141. Liu, P., Lu, R., Huang, T., Wang, H. & Li, T. A study on the mechanical and tribological properties of carbon fabric/PTFE composites. *J. Macromol. Sci. Part B Phys.* **51**, 786–797 (2012).
142. Yuan, Y. *et al.* Effects of perfluorooctyltriethoxysilane coupling agent on the properties of silica filled PTFE composites. *J. Mater. Sci. Mater. Electron.* **28**, 8810–8817 (2017).
143. Bosq, N. Nanocomposites à matrice polymère : influence de silices nanostructurées sur la cristallisation, la transition vitreuse et les propriétés thermomécaniques. (2014).
144. Yrieix, M. Impact du couplage charges / matrice sur les propriétés rhéologiques de nanocomposites silice / élastomère : application aux défauts volumiques d'extrusion. 167 (2016).
145. Gan, Y. X., Aglan, H., Faughnan, P. & Bryan, C. Fatigue fracture mechanisms of particle and

fiber filled PTFE composites. *J. Reinf. Plast. Compos.* **20**, 766–785 (2001).
146. Kitamura, T. *et al.* Morphology Change in Polytetrafluoroethylene (PTFE) Porous Membrane Caused by Heat Treatment. *Polym. Eng. Sci.* **40**, 809–817 (2000).
147. Guenoun, G. Frittage de pièces de Polytétrafluoroéthylène (PTFE) compacté : Mécanismes physiques et modèles.
148. Shi, Y. J., Feng, X., Wang, H. Y. & Lu, X. H. Tribological and Mechanical Properties of PTFE Composites Filled with the Combination of Short Carbon Fiber and Carbon Nanofiber. *Key Eng. Mater.* **334**–**335**, 689–692 (2007).
149. Shi, Y., Feng, X., Wang, H. & Lu, X. Tribological properties of PTFE composites filled with surface-treated carbon fiber. *J. Mater. Sci.* **42**, 8465–8469 (2007).
150. McCrum, N. G. The low temperature transition in polytetrafluoroethylene. *J. Polym. Sci.* 116–117 (1958) doi:10.1097/01241398-199212010-00020.
151. Hirakawa, S. & Takemura, T. Transitions and phases of polytetrafluoroethylene. (1969).
152. Minakov, A. A., Wurm, A. & Schick, C. Superheating in linear polymers studied by ultrafast nanocalorimetry. *Eur. Phys. J. E* **23**, 43–53 (2007).
153. Zinet, M. *Modélisation de la cristallisation des polymères dans les procédés de plasturgie : quantification des effets thermiques et rhéologiques*. https://tel.archives-ouvertes.fr/tel-00555771.
154. Suwa, T., Takehisa, M. & Machi, S. *Melting and Crystallization Behavior of Poly(tetrafluoroethylene). New Method for Molecular Weight Measurement of Poly (tetrafluoroethylene) Using a Differential Scanning Calorimeter*. *JOURNAL OF APPLIED POLYMER SCIENCE* vol. 17 (1973).
155. Khatipov, S. A., Serov, S. A., Sadovskaya, N. V. & Konova, E. M. Morphology of polytetrafluoroethylene before and after irradiation. *Radiat. Phys. Chem.* **81**, 256–263 (2012).
156. Ranjbarzadeh-Dibazar, A., Barzin, J. & Shokrollahi, P. Microstructure crystalline domains disorder critically controls formation of nano-porous/long fibrillar morphology of ePTFE membranes. *Polymer (Guildf).* (2017) doi:10.1016/j.polymer.2017.06.003.
157. Cheneler, D., Mehrban, N. & Bowen, J. Spherical indentation analysis of stress relaxation for thin film viscoelastic materials. *Rheol. Acta* **52**, 695–706 (2013).
158. *Chapter 5 Elastic Indentation Stress Fields*.
159. Tobolsky, A. V, Katz, D. & Eisenberg, A. *Maximum Relaxation Times in Polytetrafluoroethylene On leave from the Scientific Department, Israel Ministry of Defence*. *JOURNAL OF APPLIED POLYMER SCIENCE* vol. 7 (1963).
160. Suwa, T., Seguchi, T., Takehisa, M. & Machi, S. Effect of Molecular Weight on the Crystalline Structure of Pol yt e t r afluor oe t h ylene As-Polymerized. *J. Polym. Sci. Polym. Phys. Ed.* **13**, 2183–2194 (1975).
161. Boudimbou, I. *Mécanismes élémentaires de dispersion de charges de silice dans une matrice élastomère*. (2011).
162. Bourne, N. K., Brown, E. N., Millett, J. C. F. & Gray, G. T. Shock, release and Taylor impact

of the semicrystalline thermoplastic polytetrafluoroethylene. *J. Appl. Phys.* **103**, (2008).
163. Lei, M. *et al.* Thermomechanical behaviors of polyether ether ketone (PEEK) with stretch-induced anisotropy. *J. Mech. Phys. Solids* **148**, 104271 (2021).
164. Castro, M. & Prochazka, C. C. F. Morphologie co-continue dans un mélange de polymères incompatibles : POE / PVdF-HFP. (2003).
165. Candia, F. De, Michele, A. & Renzulli, A. Molecular motions in polyetheretherketone (peek): NMR analysis of the low- temperature relaxation mechanism. 37–41.
166. Solomko, V. P. & Semko, L. S. Effect of strain rate on the mechanical properties and transition temperatures of glass-reinforced polystyrene and polymethylmethacrylate. **4**, 373–375.
167. Ashish. what makes teflon cookware non-stick ? *Science ABC* https://www.scienceabc.com/pure-sciences/ptfe-teflon-cookware-non-stick-water-resistant-slippery-properties.html (2017).

IX.Table of figures

X. Table of graphs

XI.Table of tables